TRANSPORTATION RESEARCH RECORD 968

Asphalt Mixtures and Performance

TRB
TRANSPORTATION RESEARCH BOARD
NATIONAL RESEARCH COUNCIL

Transportation Research Record 968
Price $12.20
Editor: Scott C. Herman
Compositor: Harlow A. Bickford
Layout: Theresa L. Johnson

modes
1 highway transportation
4 air transportation

subject area
31 bituminous materials and mixes

Transportation Research Board publications are available by ordering directly from TRB. They may also be obtained on a regular basis through organizational or individual affiliation with TRB; affiliates or library subscribers are eligible for substantial discounts. For further information, write to the Transportation Research Board, National Research Council, 2101 Constitution Avenue, N.W., Washington, D.C. 20418.

Printed in the United States of America

Library of Congress Cataloging in Publication Data
National Research Council. Transportation Research Board.
Asphalt mixtures and performance.

(Transportation research record; 968)
1. Pavements, Asphalt–Addresses, essays, lectures. 2. Asphalt–Addresses, essays, lectures. I. National Research Council (U.S.). Transportation Research Board.

TE7.H5	no. 968	380.5 s	84-27352
[TE270]		[625.8'5]	
ISBN 0-309-03750-6		ISSN 0361-1981	

Notice: The Transportation Research Board does not endorse products or manufacturers. Trade and manufacturers' names appear in this Record because they are considered essential to its object.

Contents

Addresses of Authors

Abdulshafi, A., Resource International, 281 Enterprise Drive, Columbus, Ohio 43081; formerly with Ohio State University

Anderson, David A., Department of Civil Engineering, Pennsylvania State University, Research Building B, University Park, Pa. 16802

Bell, C. A., Department of Civil Engineering, Oregon State University, Corvallis, Oreg. 97331

Chrismer, Steven M., Association of American Railroads, 3140 S. Federal Street, Chicago, Ill. 60616

Engelbrecht, Johann C., Department of Civil Engineering, University of Stellenbosch, Stellenbosch, Republic of South Africa

Ezzat, F., Petroleum Research Institute, Cairo, Egypt

Gadallah, A. A., Faculty of Engineering, Cairo University, Giza, Egypt

Hicks, R. G., Department of Civil Engineering, Oregon State University, Corvallis, Oreg. 97331

Highter, William H., Department of Civil Engineering, University of Tennessee, 220 Perkins Hall, Knoxville, Tenn. 37996

Kennedy, Thomas W., Center for Transportation Research, Bureau of Engineering Research, University of Texas at Austin, ECJ 10.338, Austin, Tex. 78712

Keyser, Joseph Hode, Department of Civil Engineering, Ecole Polytechnique de Montreal, C.P. 6079, Succursale A, Montreal, Quebec H3C 3A7 Canada

Kietzman, J. H., Manville Service Corporation, Research and Development Center, Ken-Caryl Ranch, Denver, Colo. 80217

Kiggundu, Badru M., New Mexico Engineering Research Institute, University of New Mexico, Campus P.O. Box 25, Albuquerque, N.Mex. 87131

Kim, Ok-Kee, Department of Civil Engineering, Oregon State University, Corvallis, Oreg. 97331

Lee, Kang W., Department of Civil Engineering, King Saud University, Riyadh, Saudi Arabia; formerly with Center for Transportation Research, University of Texas at Austin

Majidzadeh, Kamran, Department of Civil Engineering, Ohio State University, 470 Hitchcock Hall, 2070 Neil Avenue, Columbus, Ohio 43210

Newcomb, David E., Department of Civil Engineering, University of Washington, 121 More Hall, FX-10, Seattle, Wash. 98195; formerly with New Mexico Engineering Research Institute

Noureldin, A. S., Faculty of Engineering, Cairo University, Giza, Egypt

Nusser, Betty J., New Mexico Engineering Research Institute, University of New Mexico, Campus P.O. Box 25, Albuquerque, N.Mex. 87131

Osman, A., Faculty of Engineering, Cairo University, Giza, Egypt

Roberts, Freddy L., Department of Civil Engineering, Texas A&M University, College Station, Tex. 77843; formerly with Center for Transportation Research, University of Texas at Austin

Rodier, C. E., Calgary Department of Streets, Engineering Department, P.O. Box 2100, Calgary, Alberta T2P 2M5 Canada

Ruth, Byron E., Department of Civil Engineering, University of Florida, 346 Weil Hall, Gainesville, Fla. 32611

Wall, Douglas J., Department of Civil Engineering, University of Tennessee, 220 Perkins Hall, Knoxville, Tenn. 37996

Zallen, Dennis M., New Mexico Engineering Research Institute, University of New Mexico, Campus P.O. Box 25, Albuquerque, N.Mex. 87131

Effect of Petroleum Coke on Certain Paraffinic-Waxy Asphalt Cement Characteristics

A. A. GADALLAH, A. S. NOURELDIN, F. EZZAT, and A. OSMAN

ABSTRACT

The findings of a laboratory investigation are reported. The investigation was performed to evaluate the effect of using petroleum coke (with different percentages and degrees of fineness) as an additive to paraffinic-waxy asphalt cement (AC 60/70) produced in Alexandria, Egypt, refineries. Also reported are its physical properties and the engineering properties of its asphalt concrete mixtures. One aggregate type and gradation and one asphalt cement type and grade were used in the study. Marshall and Hveem tests were used to evaluate the properties of the asphalt concrete mixture. The evaluation resulted in a number of significant results. The use of petroleum coke as an additive to Alexandria asphalt cement (AC 60/70) proved to be beneficial in improving its properties. The experiments also indicated that the degree of fineness of the petroleum coke plays a significant role in affecting the degree of improvement.

The production of asphalt cement in Egypt takes place in Suez and Alexandria. In Suez refineries asphalt cements are produced by a straight-run distillation process that uses crude oils recovered from the eastern region. These asphalt cements were successfully used in hot asphaltic mixtures and provided roads with satisfactory service records. In Alexandria refineries asphalt cements are produced by means of propane deasphalting and phenol extraction processes that use a mixture of crudes recovered from the western desert region. These asphalt cements caused serious performance and construction problems and were classified according to the base of its crude oil as paraffinic-waxy asphalts (1-3).

Previous work conducted in the area of improving asphalt cement or its mix characteristics indicated that one of the most successful methods followed is the use of additives. The most commonly used additives are resins, rubber, sulfur, and carbon black. The results of several studies on carbon black and sulfur (4) directed this study to the use of petroleum coke (which contains about 90 percent carbon and sulfur) as an additive to the western desert paraffinic-waxy asphalt cement.

Petroleum coke, which is a by-product of the coking process performed on heavy petroleum products to produce light fractions, has a crystal structure similar to carbon black but differs in the size of crystallites (5). Sachanen (6) defined petroleum coke as an ultimate condensation product of petroleum residues. He stated that petroleum coke has an intermediate structure between that of asphalt and metallurgical coke. Therefore, petroleum coke, when added to asphalts, may act as a bodying agent similar to asphaltenes and also as a reinforcing agent similar to carbon black (4).

Reported in this paper are the findings of a laboratory investigation to evaluate the effect of using petroleum coke with different percentages and degrees of fineness as an additive to paraffinic-waxy asphalt cement (AC 60/70) produced in Alexandria refineries. Also reported are its physical properties and the engineering properties of its asphalt concrete mixtures.

One aggregate type and gradation and one asphalt cement type and grade were used in the study. Marshall and Hveem tests were used to evaluate the properties of the asphalt concrete mixture.

EXPERIMENTAL DESIGN

A complete laboratory testing program that used two factors--the petroleum coke content and its degree of fineness--was conducted on Alexandria 60/70 asphalt cement (see Table 1) to evaluate the following items:

1. Effect of petroleum coke content and degree of fineness on the physical properties of asphalt cement (i.e., penetration, kinematic viscosity, absolute viscosity, and softening point), and
2. Effect of petroleum coke content and degree of fineness on engineering properties of the asphalt concrete mixture of the treated asphalt cement (i.e., Marshall stability and Hveem cohesion).

In addition, the same testing program was conducted on a Suez asphalt cement sample without additive for comparative study (Table 1).

TABLE 1 Experimental Program

Sample No.	Asphalt Cement Source		Petroleum Coke Content[a]				Degree of Fineness[b]		
	Alexandria	Suez	0%	7%	10%	15%	1	2	3
1		X	X						
2	X		X						
3	X			X			X		
4	X			X				X	
5	X			X					X
6	X				X		X		
7	X				X			X	
8	X				X				X
9	X					X	X		
10	X					X		X	
11	X					X			X

[a] Percent by weight of asphalt cement.
[b] See Table 4.

MATERIALS

Asphalt Cement

Two samples of asphalt cement (AC) 60/70 were secured--one from the production of an Alexandria refinery and the other from the production of a Suez refinery. The physical properties and the chemical constituents of these two samples are given in Table 2.

TABLE 2 Physical Properties and Chemical Constituents of AC 60/70

Asphalt Source	Physical Properties						Chemical Constituents			
	Pen. 0.1 mm.	Duct. cm	Soft. point °C	Kin. visc. c.st. 135°C	Abs. visc. pois- es. 60°C	Sp.Gr. 60°C	Wax[3] %	Oils %	Resins %	Asph-alte-ne. %
Alex.	66	100+	47	230	986	1.018	7.5	33	51	16
Suez	62	100+	52	358	2122	1.020	5.5	26	49	25
Spec. Limits[1]	60/70	90+	45/55	320[2]	-	-	-	-	-	-

(1) Egyptian Standard Specifications.

(2) Proposed.

(3) Determined by modified Hold's method (7).

Mineral Aggregate

Based on previous field experience, the severity of the performance problems of waxy asphalt appears to depend on two main factors related to mix components: the coarse aggregate type and the gradation of the aggregate mix.

The research work of the Cairo University/Massachusetts Institute of Technology (CU/MIT) Technological Planning Program (4) performed on the Alexandria asphalt cement hot mixtures indicated that the Asphalt Institute dense gradation (4-C) and crushed limestone are the best gradation and type of coarse aggregate to be used with the Alexandria waxy asphalt cement. Consequently, the experimental program in this study was designed to use crushed limestone as the coarse aggregate material in the asphalt cement hot mixtures. Silicious sand and limestone dust were used as the fine aggregate and mineral filler, respectively.

The data in Table 3 present test properties of the aggregate components used together with the percentages of each component to meet the midpoint gradation of the Asphalt Institute dense gradation 4-C.

TABLE 3 Physical Properties of the Mineral Aggregate

Properties	Aggregate Components			
	Crushed Lime-stone	Silicius Sand	Lime-stone Dust	Standard Specifi-cations
Bulk specific gravity	2.45	2.68	2.80	
Bulk specific gravity (SSD)	2.583			
Apparent specific gravity	2.663			
Percent absorption	1.88			5[a]
Percent wear (Los Angeles test)	31.8			40[a]
Percent in aggregate combination[b]	57.5	37	5.5	

[a] Maximum.
[b] Percentages of different components to meet the midpoint gradation of the AI gradation (4-C).

Petroleum Coke

Petroleum coke samples were secured from the production of the Suez Oil Processing Company. The analysis and constituents of the petroleum coke samples are given in the following table:

Constituents	Percent by Weight
Moisture content	0.40
Ash content	0.49
Volatile matter	9.8
Total carbon	83.4
Sulfur content	5.6
Total hydrogen	0.39

The existing price of Alexandria asphalt cement is about 20 £E per ton and the price of petroleum coke is about 100 £E per ton. Based on cost analyses and economic considerations, petroleum coke can be added to a content not more than 15 percent, thus making the price of the treated asphalt cement less than 32.5 £E per ton, which is approximately the price of the Suez asphalt cement.

Petroleum coke was ground to three different degrees of fineness (Table 4) and then mixed with Alexandria AC 60/70 at a temperature of 150°C and a mixing time of 30 min by using manganese stearate as a dispersing agent with a content of 0.1 percent by weight of asphalt.

ANALYSIS OF RESULTS

Physical Properties

Figures 1-3 illustrate the concentration effects of the three different degrees of fineness of petroleum

TABLE 4 Degrees of Fineness of Petroleum Coke

Degree of Fineness	Petroleum Coke (%)			
	Passing #100	Passing #140	Passing #200	Surface Area (ft^2/lb)
1	100	90	74	535
2	100	100	87	570
3	100	100	100	600

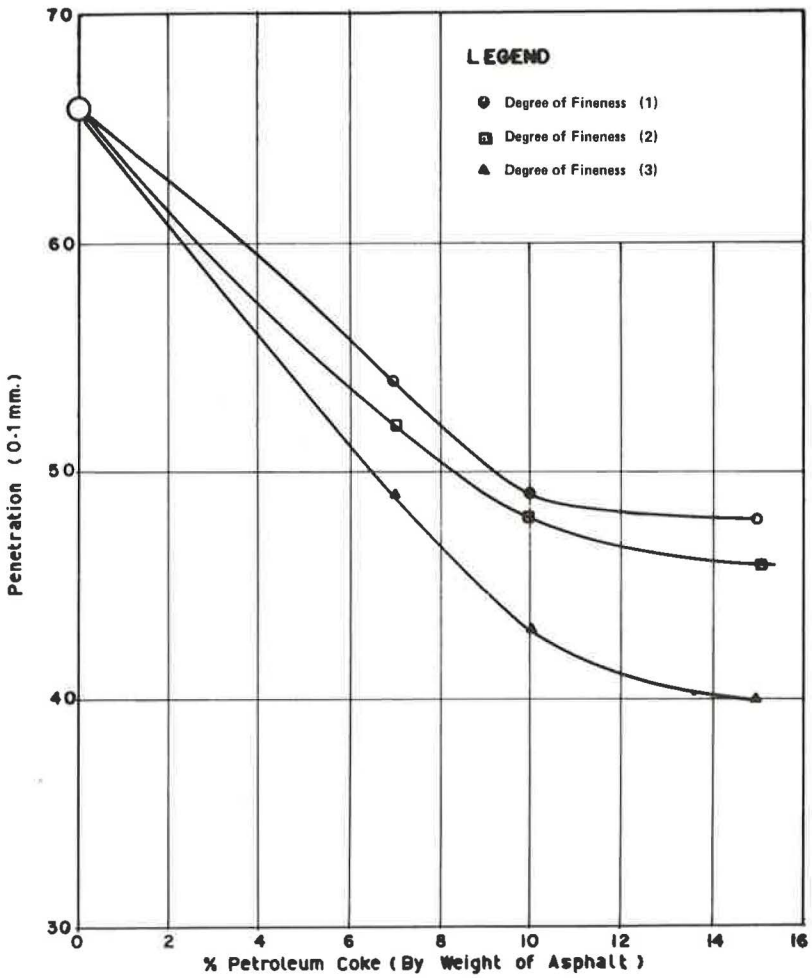

FIGURE 1 Effect of coke content and degree of fineness on penetration of coke-asphalt cement blends.

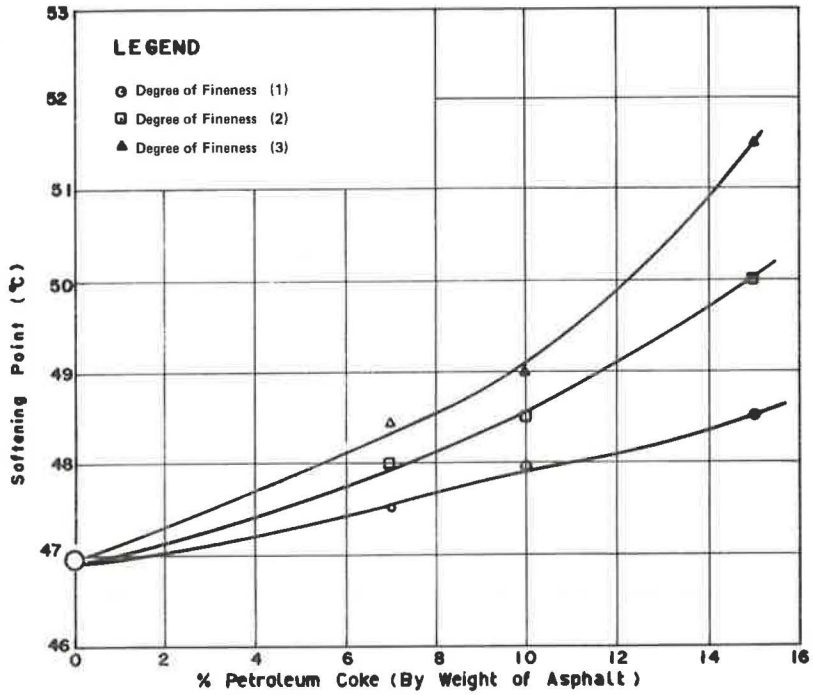

FIGURE 2 Effect of coke content and degree of fineness on softening point of coke-asphalt cement blends.

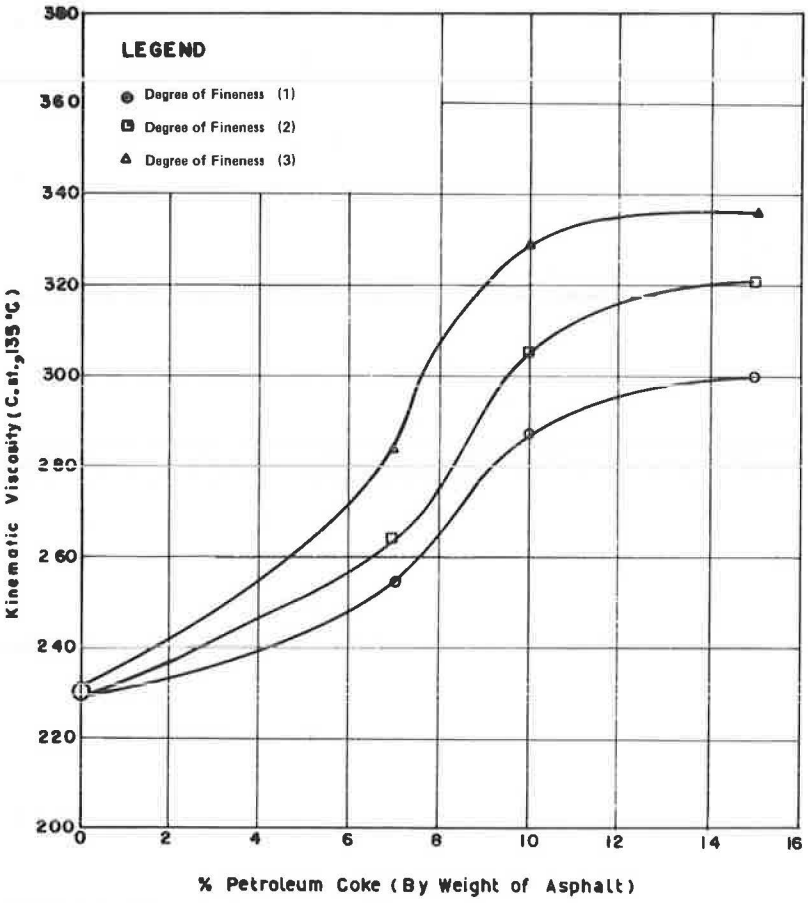

FIGURE 3 Effect of coke content and degree of fineness on kinematic viscosity of coke-asphalt cement blends.

coke on the penetration, softening point, and kinematic viscosity of coke-asphalt cement mixtures. The test results performed on coke-asphalt blends are as follows.

1. The increase of coke content consistently reduces the penetration of the mixture. In addition, the increase in the degree of fineness (i.e., increase in surface area) of the petroleum coke reduces the penetration of the coke-asphalt cement mixture. The effect of the degree of fineness is more pronounced at high concentrations of coke.
2. Softening point versus coke concentration trends indicate a slight increase in the softening point of the mixture with the increase of coke concentration. The effect of coke concentration is more pronounced when increasing the surface area of coke.
3. The increase of coke content consistently increases the kinematic viscosity of the mixture at 135°C. In addition, the increase in the degree of fineness of the petroleum coke increases the kinematic viscosity of the coke-asphalt cement mixtures. Again, the effect of the degree of fineness on kinematic viscosity is more pronounced at higher concentrations of coke.
4. The percentage increase in absolute viscosity values at 60°C were similar to viscosity changes at 135°C for the different concentrations and surface areas.
5. At the concentrations used, petroleum coke tends to harden the asphalt to a great extent. In addition, when the surface area of petroleum coke is higher there is an increase in the viscosity and the softening point and a decrease in the penetration. This could be attributed to the fact that the smaller the particle size of coke, the easier it is dispersed in asphalt and, hence, it strongly affects its physical properties.
6. The addition of coke to asphalt increases its kinematic viscosity to a limit that meets the proposed minimum value in the Egyptian standard specifications for this grade of asphalt (320 C.St. min). The addition of coke also reduces the gap between Alexandria and Suez asphalt cements. This result is obtained when using a coke content of 10 to 15 percent that has a surface area more than 570 ft^2/lb.
7. The results also indicate that the use of petroleum coke as an additive to Alexandria asphalt cement (AC 60/70) provides a product that is close in its characteristics to Alexandria asphalt cement (AC 40/50 grade). This suggests that the use of AC 40/50 grade could be a promising alternative for overcoming the reported problems that are associated with the use of Alexandria asphalt cement (AC 60/70 grade).

Temperature Sensitivity

Three asphalt cement samples were selected for the temperature sensitivity analysis. The first represented Alexandria asphalt cement (AC 60/70), the second was prepared by blending the original Alexandria asphalt cement (AC 60/70) with 10 percent coke that has a surface area of 600 ft^2/lb, and the third sample represented Suez asphalt cement (AC 60/70). The second sample was selected because the kinematic viscosity value (330 C.St.) of this sample

exceeds the minimum value proposed in the Egyptian standard specifications for AC 60/70 (320 C.St. min.), and because the sample complies with the economic requirements for the price of local asphalt cement produced in Egypt.

Figure 4 shows the bitumen test data chart suggested by Heukelom (8) to relate the consistency of asphalt with temperature. Results of the penetration tests conducted at 10°, 15°, and 25°C are plotted on the upper left part of the chart, and results of viscosity tests (in poises) at 60° and 135°C are plotted on the lower part of the chart.

It is clear from the chart that the penetration lines did not coincide with the viscosity lines. The observed shift for the Suez asphalt sample was the smallest shift reported for the three samples. This indicated that the paraffinic-waxy nature was more pronounced for Alexandria asphalt cement (refer also to Table 2). Furthermore, the observed shift for Alexandria asphalt cement was almost equal to that observed for the Alexandria asphalt blended with 10 percent coke. This also reflects that coke concentration does not affect the paraffinic-waxy nature of Alexandria asphalt cement, although it improves its viscosity.

Also, it is apparent from the data in Figure 4 that the slopes of the three viscosity-temperature lines are almost the same, which indicates that they have about the same temperature sensitivity. However, the slopes of lines 2 and 3 tend to be more flat than that of line 1. This indicates that the use of coke as an additive slightly affected the temperature sensitivity of Alexandria asphalt cement to a limit that is equal to that of Suez asphalt cement.

Engineering Properties of AC 60/70 Paving Mixtures

It was anticipated that the surface area and amount of petroleum coke would influence the behavior of the pavement during all phases of construction and service life. Consequently, the influence of coke on asphalt concrete mixture properties such as density, stability, and cohesion were evaluated by using Marshall tests together with the Hveem cohesion test.

The data in Table 5 present the engineering properties of coke-Alexandria asphalt concrete mixtures at optimum asphalt contents together with the properties of the original untreated Alexandria and Suez asphalt concrete mixtures. The aggregate type and gradation in all mixtures were the same, as previously discussed.

Study of test results presented in Table 5 and Figures 5 and 6 indicate that all measured properties were affected quite pronouncedly by the amount and surface area of petroleum coke. In addition, optimum asphalt contents for samples that had various coke concentrations were greater than those of the original samples without coke by about 0.5 percent. This increase could be attributed to the fact that the coke acted only as a filler in the asphaltic mix (it should also be noted that the concentration of coke in asphalt represented approximately 0.5 percent of the mix).

The density and Marshall flow of the asphalt concrete mix are not significantly affected by the amount of coke used. However, the addition of coke significantly increased the stability and cohesion of the asphalt concrete mix. At the three surface areas (535, 570, and 600 ft^2/lb), the coke concentration of 10 percent provided the optimum increase

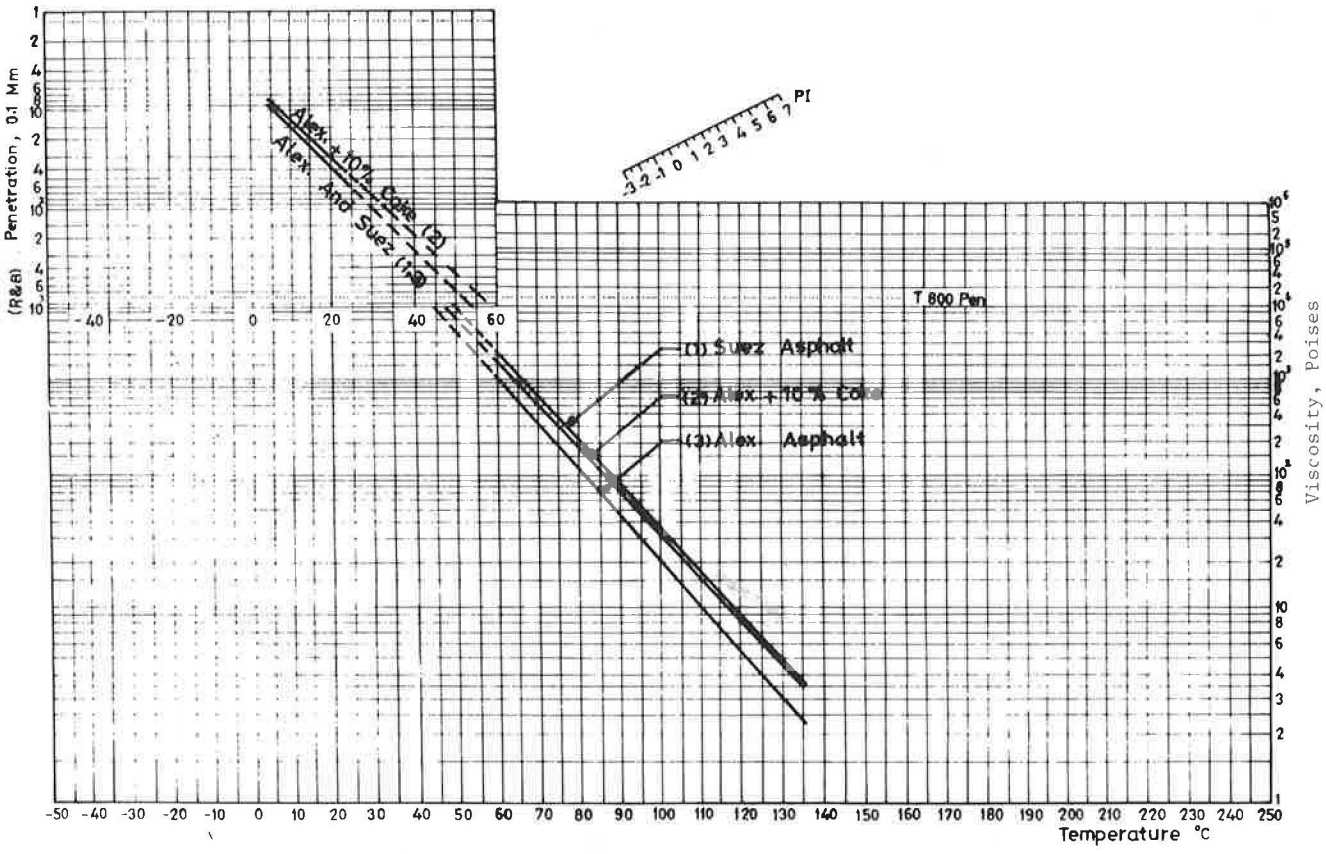

FIGURE 4 Heukelom bitumen test data chart.

TABLE 5 Investigation of Effects of Petroleum Coke on Mixture Properties at Optimum Asphalt Contents

Mix No.	Asphalt Source	Petroleum Coke(%*)	Coke Surface Area (ft^2/lb)	Optimum Asphalt Content (%**)	Marshall Stability (Lbs).	Unit Weight (pcf)	Air Voids (%)	Marshall Flow (0.01 in.)	Voids in Mineral Aggr.	Hveem cohesion (gm/in) at Optimum Asphalt cont.
1	Alex.	-	-	5.62	1420	147.2	3.1	10.5	15.5	193
2	Alex.	7	535	6.10	1620	146.8	3.8	11.3	15.5	245
3		10	"	6.15	1650	146.2	4.6	9.7	16.3	261
4		15	"	6.20	1630	146.6	3.9	9.6	16.2	250
5	Alex.	7	570	6.10	1910	145.3	4.7	9.5	15.5	255
6		10	"	6.20	2150	146.4	4.3	11.0	16.1	275
7		15	"	6.25	1960	146.0	3.8	10.8	15.6	265
8	Alex.	7	600	6.10	2200	146.4	3.8	9.7	15.5	290
9		10	"	6.25	2400	146.9	4.8	11.2	16.4	300
10		15	"	6.25	2280	147.0	4.4	11.5	16.2	290
11	Suez	-	-	5.60	2340	146.0	4.0	9.7	16.1	403

* Asphalt Weight Bases

** By Weight of Aggregates

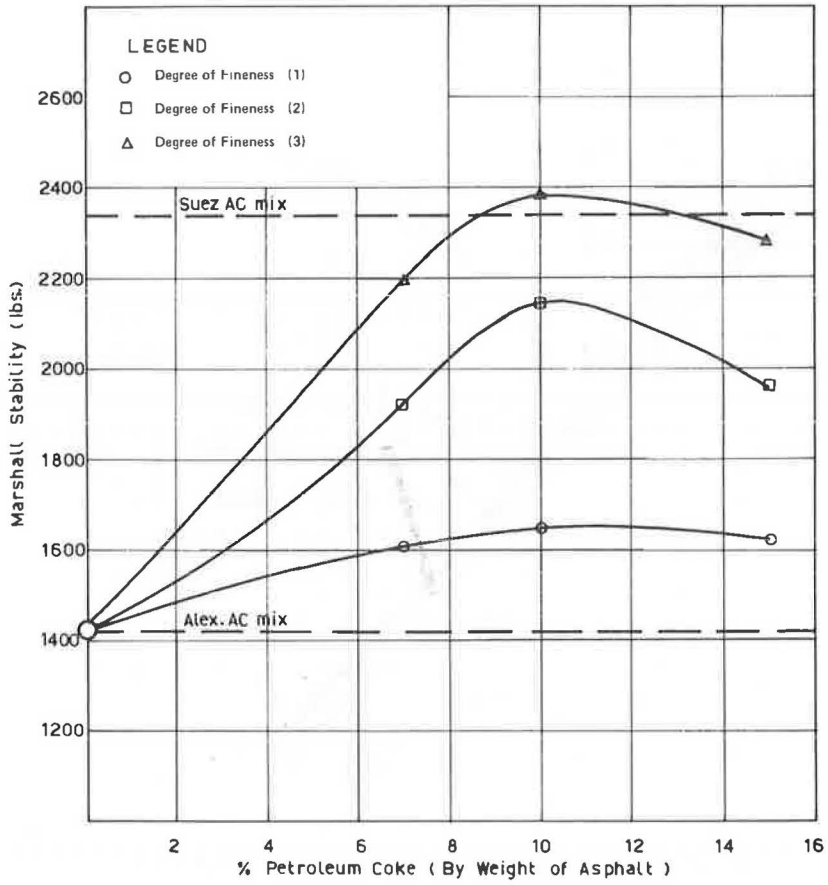

FIGURE 5 Effect of petroleum coke content and degree of fineness on Marshall stability.

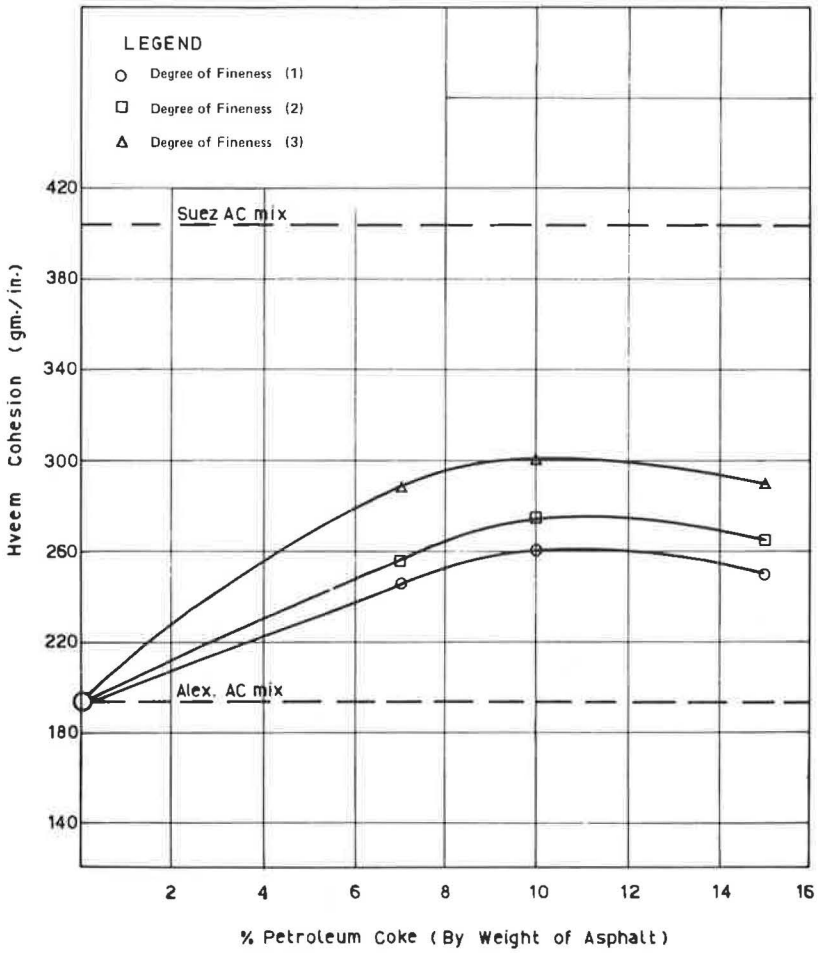

FIGURE 6 Effect of petroleum coke content and degree of fineness on Hveem cohesion.

in stability and cohesion (Figures 5 and 6). Furthermore, at all coke concentrations (7, 10, and 15 percent), the stability and cohesion of the asphaltic mix increased with the increase of surface area. However, cohesion values and most of the stability values of all samples treated by coke were still less than those of the original untreated Suez asphalt cement (Figures 5 and 6).

SUMMARY OF RESULTS

The analysis and evaluation of the test data revealed a number of significant results that pertain to the effect of petroleum coke concentration and degree of fineness of the physical properties of the local paraffinic-waxy asphalt cement (AC 60/70) and the engineering properties of its mixtures. The main results are as follows.

1. Petroleum coke tends to harden the asphalt to a great extent. The increase of coke content increases the viscosity and softening point and decreases the penetration. This effect was apparent for the three degrees of fineness used.
2. When the surface area of coke is high, there is an increase in viscosity and softening point and a decrease in the penetration of the coke-asphalt cement blend. This could be attributed to the fact that the smaller the particle size of coke, the easier it is dispersed in the asphalt and hence strongly affects its physical properties.
3. The use of petroleum coke with a surface area of more than 570 ft^2/lb and a concentration of 10 percent as an additive to Alexandria asphalt cement (AC 60/70) will result in an increase in its kinematic viscosity at 135°C to a limit that meets the minimum proposed value in the Egyptian standard specifications.
4. The addition of 10 percent petroleum coke to Alexandria asphalt cement (AC 60/70) slightly reduced its temperature sensitivity without causing any change in its paraffinic-waxy nature.
5. Petroleum coke significantly increased the stability and cohesion of the paving mixture. The use of 10 percent coke by weight of asphalt could be considered optimum. In addition, at all coke concentrations the stability and cohesion of the paving mixture increased with the increase of the surface area.
6. The use of petroleum coke as an additive to Alexandria asphalt cement (AC 60/70) acts as a filler and plays a dual role in paving mixtures. First, it forms with asphalt a high consistency binder and cements the aggregates. Second, it acts as a part of the mineral aggregates, fills the interstices, and provides contact points between particles, thereby strengthening the paving mixture.
7. Suez asphalt concrete mixtures still have better cohesion than the improved Alexandria asphalt concrete mixtures.
8. The use of petroleum coke as an additive to Alexandria asphalt cement (AC 60/70) provides a product that is close in its characteristics to

Alexandria asphalt cement (AC 40/50). This result suggests that the use of AC 40/50 grade could be a promising alternative for overcoming the reported performance problems that are associated with the use of Alexandria AC 60/70 grade.

ACKNOWLEDGMENT

This study is a part of a research project sponsored by the Development Research and Technological Planning Center, Cairo University, and the Technology Adaptation Program, Massachusetts Institute of Technology.

REFERENCES

1. Performance of Paraffinic-Waxy Asphalt Cements in Egyptian Road Construction--Volume I: Literature Review and Background of the Problem in Egypt. TAP Report 80-4. CU/MIT Technological Planning Program, Cairo University, Cairo, Egypt, 1980.
2. Performance of Paraffinic-Waxy Asphalt Cements in Egyptian Road Construction--Volume II: Chemical and Physical Properties of Western Desert Asphalt Cements. TAP Report 80-5. CU/MIT Technological Planning Program, Cairo University, Cairo, Egypt, 1980.
3. S.S. Metwally et al. Flexible Pavements, Paraffinic Asphalt Cements. Presented at XI World Road Congress, Mexico, Oct. 1975.
4. Performance of Paraffinic-Waxy Asphalt Cements in Egyptian Road Construction--Volume IV: Evaluation of Methods to Improve the Characteristics of Asphalt Cements and Mixtures. CU/MIT Technological Planning Program, Cairo University, Cairo, Egypt, 1983.
5. M.M. Khedr. Investigation in Petroleum Coke. M.Sc. thesis. Chemical Engineering Department, Cairo University, Cairo, Egypt, 1981.
6. A.N. Sachanen. The Chemical Constituents of Petroleum. Rinehart Publishing Corporation, New York, 1954.
7. D. Hold. Kohlen Wasserstaffe und Fette. Springer Verleg, Berlin, 1933.
8. W. Heukelom. An Improved Method of Characterizing Asphaltic Bitumens with the Aid of Their Mechanical Properties. Proc., Association of Asphalt Paving Technologists, Vol. 42, 1973.

Publication of this paper sponsored by Committee on Characteristics of Bituminous Materials.

Effect of Diatomite Filler on Performance of Asphalt Pavements

J. H. KIETZMAN and C. E. RODIER

ABSTRACT

Diatomite, a widely used industrial filler, has been evaluated in heavy-duty pavements in Houston, Calgary, and Los Angeles. These pavements typically have high density, extremely low permeability, and a low initial asphalt hardening rate, with or without an increase in asphalt content. After 2 and 3 years in Calgary and Houston, recovered asphalt shows penetration values of 88 and 90 percent of the original 164 and 104 asphalt penetration at 77°F, respectively. Resistance to rutting at low void contents and characteristic abrasion resistance of the mortar is attributed to microaggregate interlock of diatom particles within the mastic films. One percent diatomite appears capable of either stabilizing pavements or permitting a 15 percent increase in standard asphalt content. The primary value of diatomite appears to be that it allows the use of softer asphalt, which alone should greatly increase pavement life. The effect of increasing the cost per ton of mix (10 to 20 percent) on cost per square yard of pavement was eliminated recently in Los Angeles by reducing overlay thickness by 50 percent. Eight different grades, types, and sources of diatomite were also evaluated in small paving sheets under truck traffic at Denison, Texas, and Lompoc, California. Several types gave extremely unsatisfactory resistance to plastic flow. Tests are under way to correlate basic diatomite properties (shape, size, purity, and so forth) with pavement performance. The scope of the program to date has been limited to dense-graded city pavements. The results are reported here to generate interest in more trials needed to justify continuation of the program.

Diatomite products are amorphous silicas produced worldwide from natural sedimentary deposits of diatomaceous earth, which consist of microscopic skeletal remains of diatoms (see Figures 1 and 2). Commercial deposits contain different amounts of impurities, but all require processing for end use to remove clay, silt, silicates, and so forth; all require high temperature drying to remove water and organics; and all require reduction to effective particle-size distribution.

Perhaps the most well-known use of diatomite is for filtration (e.g., for food purification). Uses include hundreds of other products such as the flatting agent in paint (by imparting microtexture to the surface) and an abrasive in automobile polishes. Diatomite has been used for 25 years in hot-poured asphalt joint filling compounds to control flow. In 1928, 5 percent diatomite was used in an overlay for concrete warehouse floors (1).

In comprehensive laboratory evaluations of a variety of fillers, the Asphalt Institute reported that use of too much diatomite (7 percent in a sheet asphalt) caused water susceptibility, which was avoidable by cutting back to 3.5 percent diatomite (2,3).

Preliminary laboratory tests at Manville Research, before the recent field tests, confirmed that in large amounts (3 to 5 percent) diatomite created voids in asphalt concrete rather than filling voids because of the high absorptivity of diatom structures (Figures 1 and 2).

With this background of laboratory testing, a field test program was initiated in January 1981. The objectives were to determine the effectiveness of adding diatomite after premixing the hot aggregate with asphalt (instead of during the dry mix cycle) and to find out how diatomite might improve pavement durability. Laboratory strength tests on laboratory and plant mixes were included only to explain or confirm performance results.

The grade of diatomite used in the field trials described herein is a high grade (pure), high-bulk, natural type produced from marine deposits in Lompoc, California. In the future, this grade will be designated CAP (CELITE for asphalt pavement) to differentiate it from other grades and sources whose effect on pavement performance appears to be unsatisfactory or remains unproven.

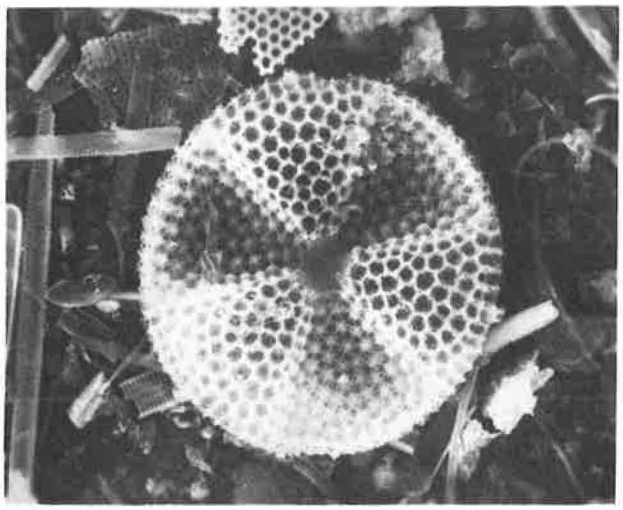

FIGURE 1 Diatomite micrograph (X563 magnification): marine diatom structures.

TEST SECTIONS AND MATERIALS

Field tests have included five sites: the cities of Houston, Calgary, and Los Angeles, and Manville Corporation plants in Denison, Texas, and Lompoc, California.

Materials used in the test pavements represent the best quality crushed stone, stone screenings, and sand available in each area, as described in Figure 3. For preformed paving sheets, stone screenings (dense, nonporous, quartz monzonite) were used with the same type of EXXON AC-10 (104 penetration) asphalt that was used in the Houston pavement trial.

It was discovered after placement that the diatomite-modified pavement in Houston was made with AC-10 asphalt and not the AC-20 asphalt used in the standard pavement. Although this precluded comparison of asphalt hardening, the mistake proved fortunate because performance results gave the first indication that diatomite made it possible to use a softer asphalt for heavy traffic pavements.

The same high bulk, natural grade of marine diatomite from Lompoc was used in the field tests to

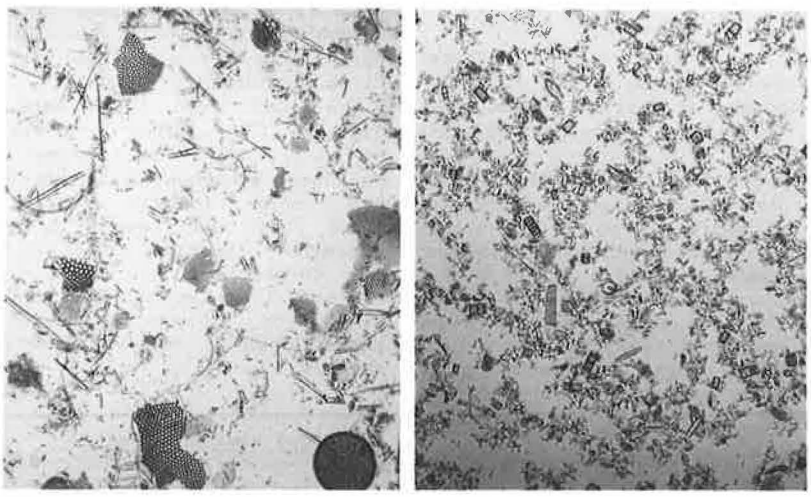

FIGURE 2 Diatomite micrographs (X150 magnification): high-bulk diatomite (left) and Nevada diatomite (right).

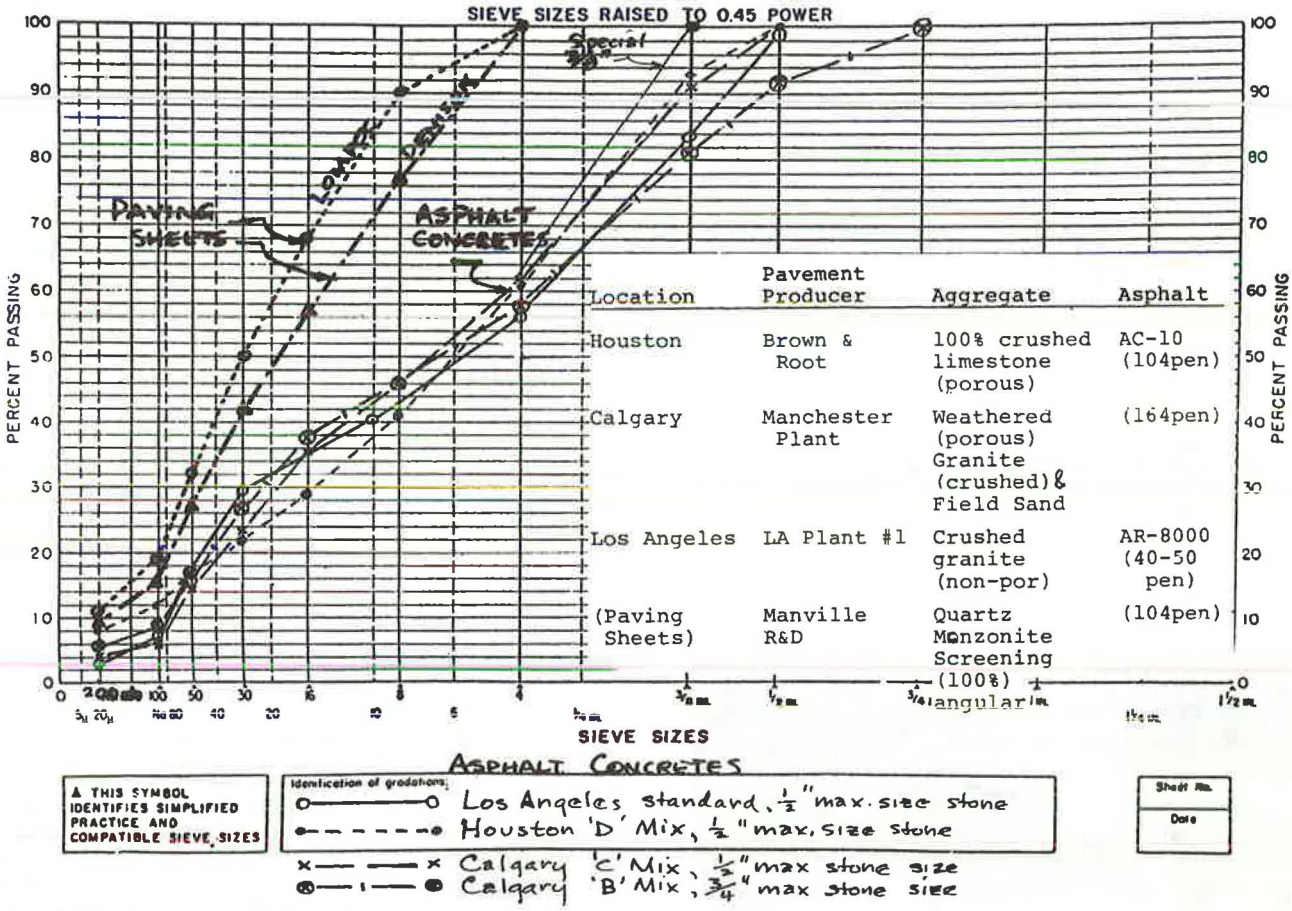

FIGURE 3 Aggregate gradation chart.

date. It has a surface area of approximately 250 000 cm^2/g. Other grades and sources of diatomite tested in the small paving sheets varied widely not only in particle-size distribution, shapes, purity, and so forth, but also in their ability to control plastic flow. Until current laboratory tests demonstrate which diatomite properties determine their effect on pavement performance, it appears advisable not to give identifying properties that could prove to be misleading.

TEST PROCEDURES

The performance evaluation includes visual surface effects such as rutting, cracking, mortar abrasion (exposure of coarse stone), surface friction, and internal effects such as density voids, permeability, and asphalt hardening.

Void contents of pavement cores were measured by the difference between underwater weights before and after vacuum saturation, expressed as a percentage of bulk volume. Vacuum saturation of the cores was done by using vacuum techniques similar to the standard ASTM test for measuring theoretical maximum density of uncompacted pavement mixes. Past correlations indicate that vacuum saturation of cores or compacted pavement samples gives void contents 1 percent total weight less than values obtained by using maximum theoretical density based on the standard Rice test.

Air permeability was measured by Soiltest's pavemeter, modified by reversing the position of tubing to apply negative pressure on pavement surfaces or cores. This allowed use of up to 12 in. of H_2O partial pressure and differentiation of tight pavements (e.g., in Calgary, where all were impermeable to water).

Special Laboratory Tests

The effect of saturation of laboratory cohesive strength of Los Angeles pavement mixes was determined by using a plate flexure test on 6-in.-diameter, 1.25-in.-thick pavement specimens compacted by gyratory shear to initial field density. Each pavement specimen was supported around its top periphery by a ring, with load applied at the bottom center through a rubber ball. Load is applied by using the Marshall tester with load and deflection taken at first visible crack (4).

Vertical shear tests were performed on 4-in.-diameter, 2-in.-thick pavement specimens compacted by 50 and 75 Marshall hammer blows on both sides. The shear equipment was mounted in a Universal testing machine with the specimen mounted horizontally as a fixed cantilevered beam, clamped along the centerline. Vertical load was applied at the overhang (centerline) at a rate of 200 lb/min, and the ultimate load was recorded. Shear strength in pounds per square inch was calculated by dividing the ultimate load by the vertical cross section of the specimen.

Preformed Pavement Sheets

Field tests on small paving sheets were conceived as an expedient way to compare stability (i.e., resistance to plastic flow) of a large number of paving

formulations under the same concentrated truck loading.

To make small paving sheets, sheet asphalt was mixed in 4000-g batches by using standard mixing equipment and adding the diatomite after premixing of hot aggregate with liquid asphalt. Each hot mix was rolled into sheets 0.375 in. thick, cooled to room temperature, and trimmed to a 12 x 18-in. size.

The paving sheets were tested on pavements at Manville plants in Denison (1982) and in Lompoc (1983). They were placed in rows in the wheel path for exposure to channelized truck traffic of up to 1,500 vehicles per month. A 2:1 water diluted SS-1 emulsion paint coat was used to bond the sheets to the pavements. Increase in width of the sheets (transverse to the direction of traffic) was measured monthly to show plastic flow, which is expressed as a percentage of the original width.

The sheets were exposed to warm weather traffic from June to October (4 months) at Denison and from April to September (5 months) at Lompoc. These tests compared the relative resistance to plastic deformation of different mix formulas. Only the high-quality, high-bulk diatomite was tested at Denison, with 2 to 4.8 percent diatomite and 11 to 15 percent asphalt (diatomite/asphalt ratios of 0.15 to 0.31). In subsequent tests at Lompoc, each type of diatomite was tested in three different formulations (sheets), 1 or 2 percent diatomite with 12.5, 13, and 14 percent asphalt (maximum diatomite/asphalt ratio of 0.15).

The paving sheets were placed in the wheel paths at the exit and entrance gates, where concentrated truck traffic decelerates and accelerates. The sheet asphalt formulations were intended to accentuate the effects of traffic on plastic flow (stability) by leaving out the stone fraction (50 to 60 percent of standard asphalt concrete) to test only the mortar phase and the effect of the diatomite on pavement cohesion (viscosity) and microaggregate interlock within the mastic.

The paving sheets at Lompoc were thoroughly wet with water once a week during the first 2 months.

PAVEMENT PRODUCTION METHOD

Adding diatomite after (or during) the normal wet mixing cycle (aggregate plus hot asphalt) proved to be an effective way to avoid the pulverizing of diatom particles that occurs when diatomite is added during the standard dry mix cycle. This was first demonstrated to be effective in the Houston trials in January 1981 by extracting asphalt from the plant mix in situ on glass slides. Microscopic examination indicated that the only significant effect on particle size during batch mixing was a 25 to 30 percent decrease in the length of spicules. Equally important, diatomite dispersion was good in the pavement mixes.

This simple change in batch plant procedure served a second vital purpose: it prevented loss of the lightweight, easily airborne diatom particles through the dust collector system that occurs when diatomite is added during the dry mix cycle.

In Houston the standard mixing time per batch was increased from 10 to 30 sec in proportion to the time required to pour the diatomite (0.6 to 2.4 percent total weight) into the pug mill by hand.

In Los Angeles diatomite was poured from 50-lb paper bags into the pug mill immediately after the asphalt was added in the standard wet mix cycle. This limited the total increase in batching time to 5 or 10 sec.

Supplying diatomite in heat-degradable plastic bags was first tried in Calgary in 1981 with success. The 25- to 50-lb bags were dropped into the pug mill by an automatic feed system after the normal wet mix cycle, with an additional, final 20 to 30 sec of mixing.

Placeability (paver speed) of the mixes was described by crews as superior in Los Angeles, normal in Calgary, and slower than normal in Houston for the high diatomite content mixes (perhaps because of the combined effect of angularity of the 100 percent limestone aggregate and high diatomite content in two of the Houston mixes).

FIELD TEST RESULTS

Houston

The four paving mixes produced to evaluate the new mixing sequence (four truckloads in all) were included in a city paving project on Franklin Street, a major downtown thoroughfare in Houston. After 1 year the superior resistance to traffic abrasion of the mortar phase was extremely noticeable in the test sections, as shown by the limited exposure of coarse stones compared with extensive surface exposure of stone in the connecting standard mix (Figure 4). After 3 years the coarse stone has become

FIGURE 4 Surface abrasion in Houston pavements after 1 year: 0.6 percent diatomite and 6.8 percent asphalt (top) and standard (bottom).

TABLE 1 Houston Core Analyses, Franklin Street Pavement

Aggregate	Texas Modified 'D' Mix: Diatomite-Modified 100% Limestone I	IV	II	III	STANDARD Limestone + 25% gravel Parker Bros.
Diatomite Content %	0.6	0.6	1.8	2.4	
Asphalt Content %	6.8	6.0	7.4	7.3	5.5
Density, gm/cc 1981 (1 yr)	2.31	2.33	2.28	2.35	2.28
1983 (3 yr)	2.384	2.397	2.358	2.398	2.363
Void Content, % 1981 (1 yr)	1.3	1.7	2.0	2.8	4.2
1983 (3 yr)	0.4	1.7	0.4	0.7	2.1
Air Perm. 1981 (1 yr) ml/min/in head 1983 (3 yr)	0.10	0.88	0.04	145.5	1.5
Thickness, inch	1.63	1.30	1.47	1.15	1.60
1981-Core Extract (1 yr)					
Asphalt Recovered, %	6.2	5.5	7.7	5.5	4.8
(% of original asphalt)	(91%)	(92%)	(100+%)	(75%)	(87%)
Penetration of Rec. Asph.	89	82	94	73	42
(% of original)	(86%)	(79%)	(90%)	(70%)	(--)
1983-Core Extract (3 yr)					
Asphalt Recovered, %	6.3	5.3	6.6	5.4	4.6
(% of original asphalt)	(93%)	(88%)	(89%)	(74%)	(84%)
Penetration of Rec. Asph.	94	83	85	90	44
(%of original)	(90%)	(80%)	(82%)	(87%)	(--)

NOTE: Test values above are the average of 3 cores in most instances.

exposed in the test sections, but it is less apparent in the standard mix, possibly because of pull-out of coarse stone.

More important are the results of core analyses (Table 1). Despite the range in diatomite content (0.6 to 2.4 percent and asphalt content from 6 to 7.4 percent), all four mixes show high density and low void contents, and after 3 years penetration of recovered asphalt remained as high as 90 percent of the original 104 penetration.

In Figure 5 recovered asphalt penetrations are plotted with data published in 1975 by the Pennsylvania Department of Transportation. The 1975 data

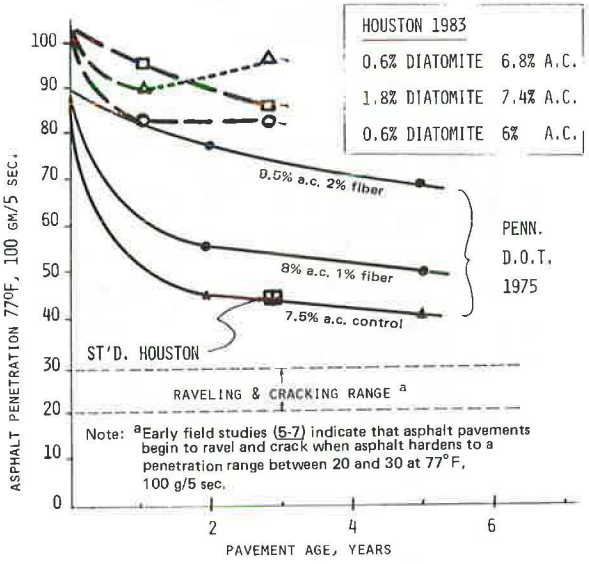

FIGURE 5 Resistance to asphalt hardening in Houston test pavements.

indicate that by increasing asphalt content 25 percent more than standard optimum, initial retained asphalt penetration could be increased from 45 to 87 percent of original penetration. In contrast, all of the Houston diatomite-modified mixes showed 80 to 90 percent of original asphalt penetration after 3 years, with or without an increase in asphalt content.

Rutting remains minimal at the Austin Street stoplight intersection, despite the extremely low diatomite content. Beyond the stoplight rutting is so slight as to be attributable to differential compaction or wear in the wheel path (Table 2).

Laboratory tests on Houston plant mixes indicated that adding 0.5 to 1 percent diatomite prevented the normal decrease in stabilometer values when asphalt content was increased 1 percent total weight more than standard optimum (Figure 6).

Calgary

Success of the simple batch plant mixing procedure at Houston laid the groundwork for further field tests. Starting in June 1981, test pavements were laid in Calgary to make a direct comparison with fiber-reinforced, high asphalt content pavements used for 20 years for all heavy traffic overlays to benefit durability in the cold climate.

The 1981 Calgary trials compared the effect of 1 and 2 percent diatomite with the standard 1 and 2 percent 7M asbestos fiber in pavement mixes made with the same 164 penetration asphalt and aggregate, produced and placed continuously from the city batch plant. The test pavements were located on the main north-south artery, MacLeod Trail, and a major east-west highway, Southland Drive.

In general, results in Calgary have been comparable to those in Houston, with diatomite imparting superior abrasion resistance (Figure 7) and resistance to initial asphalt hardening (Table 3). Most

TABLE 2 Pavement Surface Characteristics

Pavement (Age)	A.C.	Rut Depth, inch		Surface Friction
	%	Inside Wheelpath	Outside Wheelpath	BPN
I. TRANS-CANADA HIGHWAY (1yr.)				(65°F)
0.5% diatomite	7.0	.09	0.19	75
0.75% diatomite	7.5	.06	0	76
1.00% diatomite	7.5	0.13	0	80
Control (2% Fiber)	7.8	.06	.03	74
II. HOUSTON (3 yrs.)		At Stoplight	Beyond Stoplight	(79°F)
0.6% diatomite	6.0	-	0	60
0.6% diatomite	6.8	0.10	.05	61
1.8% diatomite	7.4	-	.03	68
Standard	5.5	0.20	.03	60

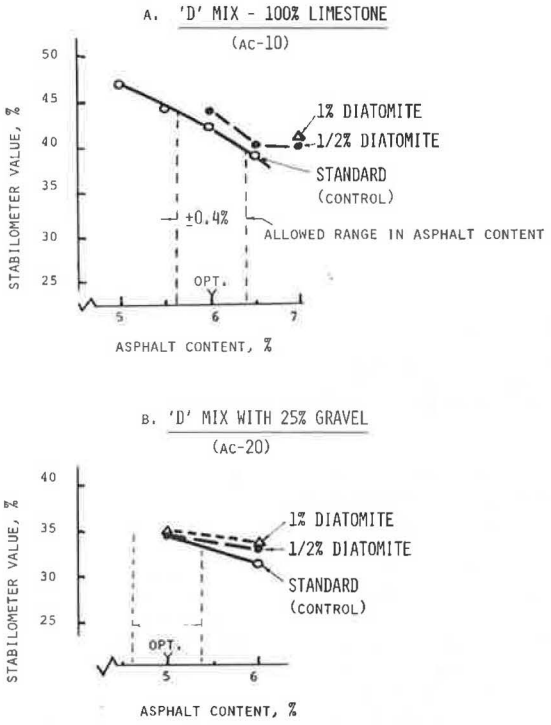

FIGURE 6 Stabilometer tests on Houston plant mixes.

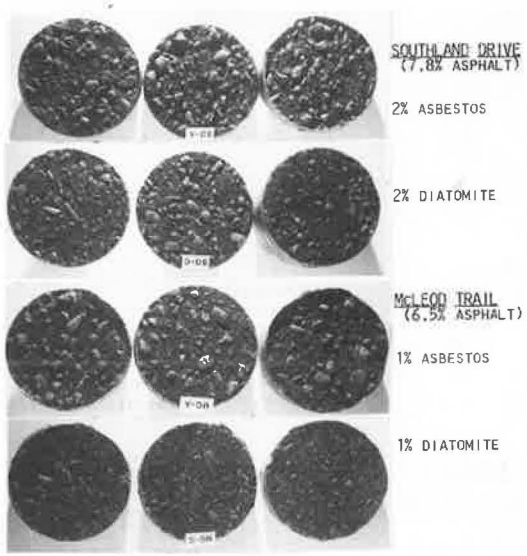

FIGURE 7 Abrasion resistance in Calgary after 1 year.

notable was pavement made with 1 percent diatomite, which after 2 years showed an asphalt penetration of 144, 88 percent of the original 164 penetration, after correction for ash content.

In 1982 more field tests in Calgary on the Trans-Canada Highway indicated that pavement mixes made with less than 0.75 percent diatomite plus an increase in asphalt did not compact to the desired high density and low permeability, and it showed measurable rutting (Table 2).

In another 1982 trial (MacLeod Trial north) a pavement mix was placed by using 1 percent diatomite with asphalt content lower than the connecting control mix with no additive. The surprising results from 1-year core analyses were higher retained asphalt penetration, much lower permeability, and higher density (see Table 4).

The data in Table 5 give the Marshall stability test data on Calgary plant mix samples.

Los Angeles

In the first large-scale field trial of diatomite-modified pavement, 1,000 tons were placed in Los Angeles in 1982 by city crews; 900 tons of the standard (1/2 in. maximum stone) resurfacing mix and 100 tons of a special 3/8 in. maximum stone mix, both with AR-8000 asphalt (about 35 penetration). Primary laboratory mix design objectives included low permeability and increased cohesive strength. The laboratory flex tests on mixes compacted to initial field density (Table 6) and shear tests on pavement mixes compacted to ultimate traffic compaction (Figure 8) both suggested that satisfactory results would be obtained by using 1 percent diatomite with approximately 6.5 percent asphalt. However, 0.5 percent

TABLE 3 Calgary Core Analyses, 1981 Pavements

	Macleod Trail		Southland Drive	
	Control		Control	
	1% Diatom	1% Fiber	2% Diatom	2% Fiber
Asphalt Content,[a] % wt	6.5	6.5	7.8	7.8
1982 Recovery* %	6.00	5.50	7.71	7.65
(% initial a.c.)	(92%)	(85%)	(99%)	(98%)
1983 Recovery* %	6.05	5.75	7.10	7.25
(% initial a.c.)	(93%)	(88%)	(91%)	(93%)
Density, gm/cc 1982 (1 yr)	2.327	2.324	2.368	2.354
1983 (2 yr)	2.394	2.379	2.336	2.337
Void Content, % 1982 (1 yr)	4.3	4.4	3.1	2.8
1983 (2 yr)	0.12	1.35	1.14	1.10
Permeability 1982 (1 yr) (ml/min/in. head)	7.0	52.0	0.90	18.0
1983 (2 yr)	0.02	0.17	0.47	0.07
Core Thickness, inch	1.88	1.71	0.84	1.20
Asphalt Penetration at 77°F				
1982 (1 yr)	111	70	100	92
% original	(68%)	(43%)	(61%)	(56%)
1983 (2 yr)	126	83	84	87
% original	(77%)	(51%)	(51%)	(53%)
Ash Content, % of asph. 1983	2.7	1.9	5.2	2.0
Asphalt Penetration Corrected for ASH				
1983	144		104	
% original[b]	(88%)		(63%)	

NOTE: (a) Original asphalt penetration was 164 at 77°F.

(b) A Canadian DPW report of 1973 indicated that increasing asphalt content from 6 to 7.5 percent total weight of mix increased penetration of recovered asphalt after 3 years from 62 to 93 (8).

TABLE 4 Calgary Core Analyses, 1982 Pavements

Additive	Asphalt Content	Density gm/cc	Air Permeability Max./Min. > Average ml/min/inch: Wheel Path	Air Permeability: Near Curb	Asphalt Hardening Penetration after 1 Year (% retained)
None (Control)	6.5%	2.345	28 / 15 > 22.0	-	106 (66%)
Standard 2% asbestos	7.8%	2.335	0.21 / 0.13 > 0.17	-	91 (57%)
1% CELITE	6.0%	2.371	0.15 / 0.11 > 0.13	2	113 (71%)

diatomite with 6 percent asphalt was also included in the field trials placed on Slauson Avenue between Estrella and Vermont. Placeability was satisfactory. The quick-setting properties of the diatomite mixes permitted traffic on the mat before completion of final rolling, despite the 104°F ambient (air) temperature.

Core analyses 1 year later confirmed the superiority of 1 percent diatomite with 6.5 percent AC, which showed extremely low permeability and averaged 75 percent higher retained penetration than the connecting control (Table 7). Pavements with 0.5 percent diatomite and 6 percent asphalt averaged 30 percent higher penetration of retained asphalt than the control. One beneficial surface effect already shows up, that is, resistance to dripline erosion (see Figure 9). [Note that in Figure 9 the top photograph shows the standard control eastbound at an intersection at Figueroa, and the bottom photograph shows the standard with 1 percent diatomite and 6.5 percent asphalt (one block west of Figueroa).] Although not often seen in Los Angeles' overlays, this kind of localized erosion appears to be a fairly common occurrence in some communities in southern California.

Slight rutting has occurred at only one point on Slauson Avenue, in the truck lane at the stoplight at the Hoover intersection, where the asphalt content exceeded 6.5 percent. Results of Hveem stabilometer tests on plant mixes sampled in 1982 revealed satisfactory values (36 to 38 percent) for the special 3/8 in. stone mixes with 0.5 percent and 1 percent diatomite, 6 and 6.5 percent asphalt content. In the standard 1/2 in. stone mix, 0.5 percent diatomite with 6 percent asphalt showed a 36 percent stabilometer value. But with 1 percent diatomite and 6.5 percent asphalt, the stabilometer value dropped to 16 percent, presumably because laboratory-compacted densities were much higher than the density of the pavement cores.

A second large-scale test pavement was placed on

TABLE 5 Marshall Stability Tests of Calgary Plant Mixes (trials placed 9/82)

		Marshall 50-blow Compaction			
Additive	Asphalt Content (165 pen) %	Density gm/cc	Air Voids % (Vac sat)	Stability (140F) Lbs	Flow .01 in
1% CELITE	6.0	2.351	2.1	3820	14.7
3/4% CELITE	7.5	2.348	1.8	2100	18.3
1% CELITE	7.5	2.344	1.6	2180	20.0
2% CELITE	7.8	2.335	1.2	2060	22.7
2% 7M Fiber	7.8	2.348	1.6	1715	19.7
None	6.5	2.365	3.0	2740	11.0

TABLE 6 Effect of Saturation on Cohesive Strength of Los Angeles Pavement Mixes

Standard L.A. Resurfacing Mix

				PLATE FLEXURE TESTS[a]					
							After Vacuum Saturation & 24 Hr. Immersion 140°F		
CELITE Content % Total Wt.	Asphalt Content	Density gm/cc	Water Permeability ml/min. (12" head)	Load at Crack 140°F lb.		Deflection at Crack inch	Load at Crack 140°F lb.		Deflection at Crack inch
0	5.2	2.20	670	25		.027	20		.033
1/2	5.2	2.16	154	45		.039	20		.033
1/2	5.7	2.20	120	35		.038	40		.038
1	6.2	--	20	--		--	40		.035
1	6.7	2.30	2.2	45		.028	50		.033
2.2	7.5	2.285	1.3	25		.027	55		.039

(a) Gyratory Compacted Samples (6" diam., 1 1/4" Thick)

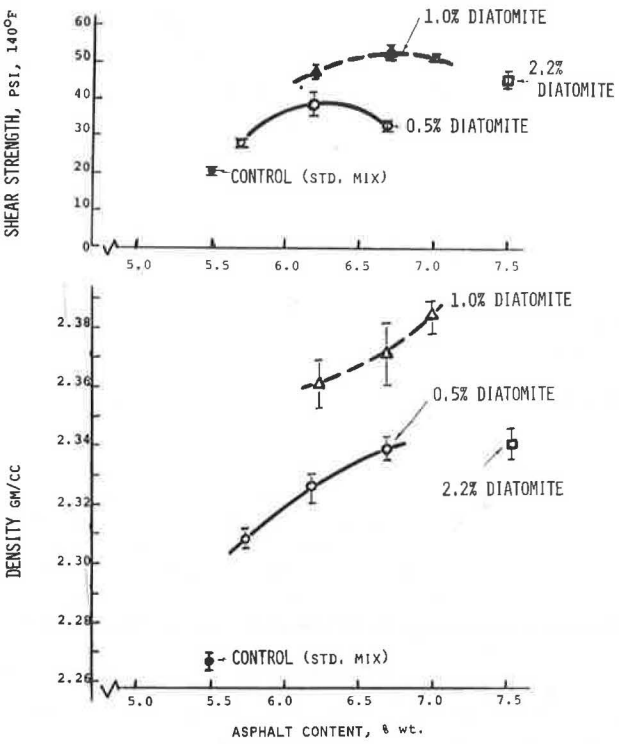

FIGURE 8 Los Angeles mix design.

FIGURE 9 Resistance to drip-line erosion, Slauson Avenue.

TABLE 7 Slauson Avenue Core Analyses After 1 Year

	Control (Std Mix) 5.2% a.c.	Diatomite-Modified ½% Diatom 6.0% a.c.	1% Diatom 6.5% a.c.
I. Std. Resurfacing:1/2"Max Stone			
Asphalt Recovery, %[a]	4.6	6.0	6.5
(Ash Content, % of asphalt)	0.12	1.38	1.93
Density gm/cc	2.255	2.270	2.346
Void Content, %	8.2	6.2	1.2
Permeability ml/min/in. head	106.1	45.4	1.40
Thickness, in.	1.49	1.46	1.46
Penetration of Recovery Asphalt at 77°F	10	15	21
II. Special Mix:3/8" Max Stone			
Asphalt Content, %[a]	5.2	6.0	6.5
Asphalt Recovery (1983) % wt	5.25	6.2	6.6
Ash Content, % of asphalt	(0.56)	(1.19)	(0.87)
Density, gm/cc	2.235	2.286	2.338
Void content, %	6.9	6.1	1.8
Air permeability ml/min/in. head	166	10.9	0.63
Thickness	1.21	1.22	1.11
Penetration of Recovered Asphalt at 77°F	15	16	21

(a)AR-8000 (30-40 pen)

Chatsworth Avenue in Los Angeles in August 1983. The purpose was to evaluate the special 3/8 in. stone mix made with 1 percent diatomite and 6.5 percent AR-2000 asphalt (70 penetration). This softer asphalt reportedly cannot normally be used for heavy traffic pavements because of slow setting properties. However, when placed in August, adding diatomite made the mix set up quickly like the standard pavement mix made with AR-8000 (hard) asphalt. Initial core analyses demonstrated the higher retained penetration (60 percent) in the diatomite-modified mixes, but all mixes showed considerable asphalt hardening.

Tests on these plant mixes also gave Hveem stabilometer values of 34 to 35 percent.

The diatomite-modified overlay on Chatsworth westbound lanes was placed and compacted to a 1-in. nominal thickness without problems. The standard 1/2 in. stone mix placed on the adjacent eastbound lanes was 1.5 in. nominal thickness.

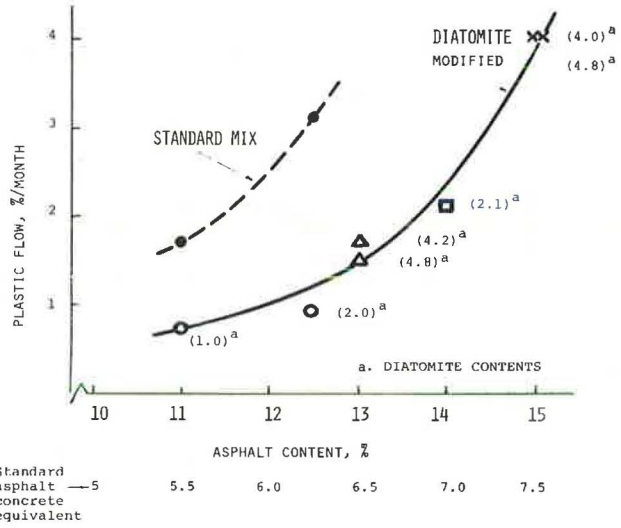

FIGURE 10 Resistance to plastic flow (Denison paving sheets).

Paving Sheets

The first tests on paving sheets exposed to concentrated truck traffic at Denison, Texas, in 1982 contained only the high-bulk, high-grade Lompoc diatomite and diatomite/asphalt ratios of 0.15 to 0.32 (2 to 4.8 percent diatomite, 11 to 15 percent asphalt). In Figure 10 the relation between plastic flow (increase in width) and asphalt content is apparent. Results imply that the minimum diatomite/asphalt ratio of 0.15 percent had optimum effect on stability and would permit approximately 2 percent total weight increase in asphalt content (1 percent in comparable asphalt concrete) without increasing the standard plastic flow.

A second and more extensive series of tests on paving sheets at Lompoc in 1983 included diatomite/asphalt ratios of 0.15 or lower. The data in Table 8 demonstrate the effect of the high-bulk Lompoc diatomite content on the control of plastic flow.

Other paving sheets at Lompoc compared the effect of other grades of diatomite and other types or sources on resistance to plastic flow. Results plotted in Figure 11 show that a finely pulverized diatomite failed to prevent excessive plastic flow. This confirms the necessity of adding diatomite to the pug mill after premixing the asphalt and hot aggregate to minimize crushing of diatom particles. Paving sheets that contain diatomite made from a low-

TABLE 8 Effect of Diatomite Content on Plastic Flow in Lompoc Paving Sheets

Asphalt Content % Total Wt. (equivalent to asphalt concrete)		PLASTIC FLOW (6 Wks.), % Diatomite Content,[a] %		
		0	1[a]	2[b]
11	(5.5%)	4.4	2.6	-
12.5	(6.25%)	8.2	4.7	-
13	(6.5%)	(12.0 est.)	(6.8)	5.0

(a) Equivalent to 1/2 % in asphalt concrete.

(b) Equivalent to 1% in asphalt concrete.

grade California crude also showed excessive plastic flow.

A diatomite from France was slightly less effective in controlling plastic flow than the high-bulk commercial grade from California (Figure 12). Diatomites from Spain and Mexico were one-third to one-half as effective. Results with paving sheets containing a Nevada diatomite stand out in Figure 12 because with 13 percent asphalt content, excessive plastic flow continued through July and August.

Other data from Lompoc (not reported here) indicate that (a) reducing aggregate fines from 14 to 7 percent in the sheet asphalt mix had little effect on plastic flow, and (b) with 164 penetration asphalt, a diatomite/asphalt ratio higher than 0.15 would be needed to control plastic flow in southern California.

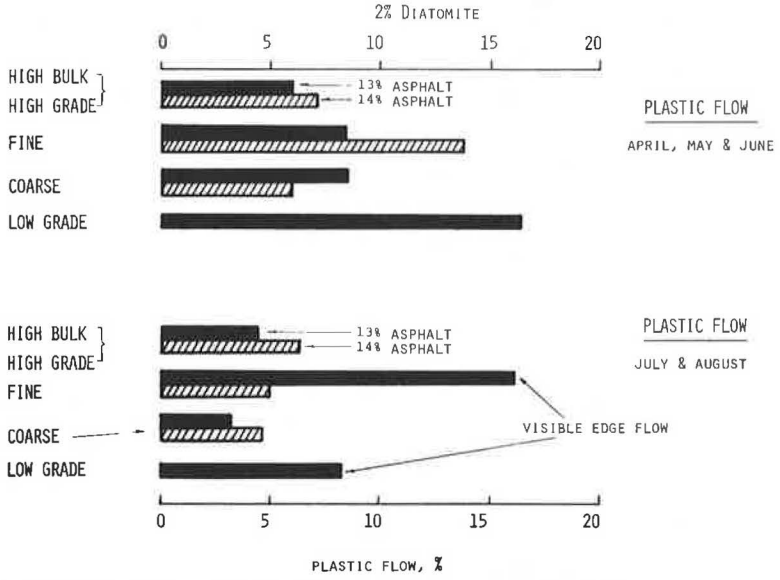

FIGURE 11 Effect of grade of diatomite (Lompoc) on plastic flow.

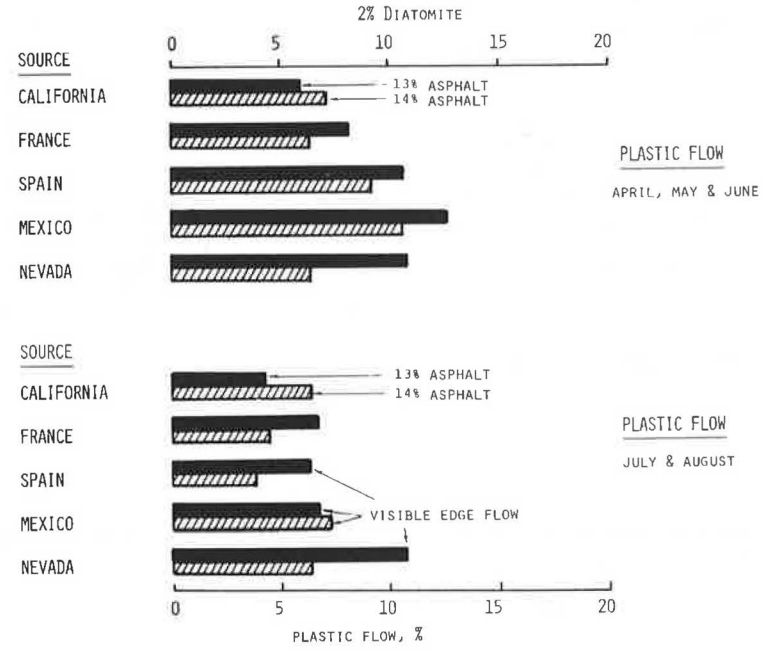

FIGURE 12 Effect of source of diatomite on plastic flow.

INTERPRETATION OF RESULTS

Compaction and Asphalt Hardening

Field tests have indicated that the high-grade Lompoc diatomite used in the field tests tends to promote pavement compaction. In Calgary, even with asphalt content below normal, adding 1 percent diatomite gave higher initial density and much lower permeability than the control mix. The test pavements in all three cities also demonstrate a marked resistance to initial asphalt hardening with or without a nominal increase in standard asphalt content. In both respects, the diatomite-modified pavements during mixing and placement act like high asphalt content pavements, as illustrated in Figure 5.

The best explanation for these effects to date is that the diatomite extends the volume of hot asphalt mastic. By out-gassing of adsorbed water (6 percent of diatomite weight), adsorption of asphalt is apparently delayed until the mix cools below about 200°F. The high-bulk diatomite has an absorption capacity equal to 3 times its weight of asphalt. One percent diatomite could theoretically extend the volume of 6 percent asphalt by 50 percent. Actually, the volumetric extension and delayed absorption is much less than theoretical maximum and depends on asphalt viscosity, aggregate fines, and so forth. This explanation could explain the observed effects of diatomite on pavement properties. Note that poor performance of some types or sources of diatomite (Figure 12) could be related to asphalt absorption.

Stability

Considering the twofold function of fillers (3), interparticle contact, and increase in asphalt consistency, the first term appears to describe the main effect of low diatomite contents. By using the term microaggregate for fine fillers, a term coined by Tons and Henault (9), a primary function of diatomite appears to be increasing microaggregate interlock. Because diatom structures are 85 to 90 percent voids after complete absorption, 1 percent diatomite with 6.5 percent asphalt may occupy up to 55 percent of the asphalt mastic (excluding rock dust). With rock dust included, the total point-to-point interparticle contact and internal friction within the mastic films must be greatly multiplied. Differences in physical properties of diatomites (e.g., effective absorption, particle size) help to explain the results shown in Figures 11 and 12.

The fact that diatomite increases asphalt mastic viscosity and cohesive strength of pavements is its second function. However, pavement performance to date shows little correlation between high diatomite contents (and resulting high cohesive strength) and pavement stability for mixes with diatomite/asphalt ratios greater than 0.15 and with AC-10 asphalt.

Use of too much diatomite content where absorptive capacity equals or exceeds the volume of asphalt present could possibly cause water susceptibility problems.

Crack Resistance

The standard pavement adjacent to the test sections in Houston shows very fine but extensive cracking, both longitudinal cracking in the wheel paths and short transverse cracks extending out from joints in the gutter. No fine cracking is visible in the diatomite-modified sections (made with softer asphalt). However, several coarse, random reflection cracks are visible in the test section with high diatomite content mix at the south end (intersection) and in the adjacent standard overlay.

There is no evidence from other test sections that adding diatomite to asphalt concrete will alone greatly affect reflection cracking. However, by permitting use of softer asphalt (e.g., AC-10), diatomite should give significant resistance to some types of reflection cracking, as it did, for instance, in Houston.

MIX FORMULATION

The criticality of the 0.15 minimum diatomite/asphalt ratio, based on the paving sheet results, was not recognized until after the 1982 test pavements had been placed. A typical asphalt concrete (e.g., one of those placed in Los Angeles) that would meet the stability criteria for heavy city traffic would include 1 percent diatomite (the high-bulk, high-quality Lompoc type) and 6.5 percent asphalt (AC-10). The aggregate recommended for thin surface overlays is 3/8 in. maximum size stone (e.g., the special 3/8 in. stone mix first placed in Los Angeles in 1982 and 1983). Note that both of these plant mix samples contained 6.5 percent asphalt and both met the California stabilometer criteria for stability. Use of diatomite with less than 5.7 percent asphalt is not recommended for general use, based on the data given in Table 6.

CONCLUSIONS

1. Adding diatomite during or after the normal wet mix cycle in batch plant production proved to be an effective way to avoid both pulverizing of diatomite when added in the dry mix cycle and loss of airborne diatomite particles by dust collection.
2. Core analyses consistently showed much less asphalt hardening in the diatomite-modified pavements than the standard or control pavements.
3. With the high-grade, high-bulk Lompoc diatomite, a minimum diatomite/asphalt ratio of 0.15 maintains stability of asphalt concrete with AC-10 (85 to 100 penetration) asphalt. Where stability of asphalt concrete is adequate, 1 percent diatomite should allow an increase in standard optimum asphalt content of 1 percent total weight of mix.
4. Adding diatomite consistently facilitated compaction of dense-graded pavement mixes, even without increasing asphalt content; after 2 or 3 years of heavy city traffic the pavements appear capable of maintaining stability despite low void contents.
5. Several other types and sources of diatomite did not control pavement stability under heavy traffic. Although none of the test pavements with high-bulk, high-grade Lompoc diatomite shows any evidence of water susceptibility, other types of diatomite (impure, low absorption, and so forth) may cause such problems.
6. The combined effects of the Lompoc high-bulk diatomite, such as compaction, abrasion resistance, and increased cohesive strength of asphalt hot mixes, suggests special benefit to thin pavement overlays.

Many dense-graded pavements, such as those used in these field tests, may require one of the surface treatment methods that create the macrotexture required for high traffic speeds, that is, open-graded friction courses (OFC), aggregate sprinkle treatments, or grooving. The impermeability typical of diatomite-modified dense-graded pavements could prove valuable, however, in binder courses used to support OFC surface overlays.

ACKNOWLEDGMENT

Field tests in the United States to date have been made possible by the interest of J.W. Deskins, Director, Street and Bridge Department and by E.D. Longley, Director of Street Maintenance in Los Angeles. Their interest and cooperation is gratefully acknowledged. The assistance of A.B. De Simon, Chief of Calgary's Plants Operation, and Paul Nemorin are appreciated. Milton F. Masters and Leo Davis of Industrial Asphalt Inc. have provided valuable help in coring and testing the initial Los Angeles test pavements.

Texas stabilometer tests were performed on Houston plant mixes by Southwestern Laboratories, Inc. LaBelle Consultants measured stability of the recent Los Angeles pavements by using standard California procedures. The Chicago Testing Laboratory ran Marshall stability tests on Calgary plant mixes and performed extraction-recovery tests on all pavement cores reported herein.

REFERENCES

1. H.W. Skidmore and J. Donohue. Special Sheet Asphalt Floors in Industrial Plant at Kohler, Wisconsin. Engineering and Contracting, March 1928.
2. B.F. Kallas and H.C. Krieger. Effects of Consistency of Asphalt Cements and Types of Mineral Fillers on the Compaction of Asphalt Concrete. Proc., Association of Asphalt Paving Technologists, Vol. 29, 1960, pp. 162-172.
3. B.F. Kallas and V.P. Puzinauskas. A Study of Mineral Fillers in Asphalt Paving Mixtures. Proc., Association of Asphalt Paving Technologists, Vol. 30, 1961, pp. 493-538.
4. D. Tamburo and J.H. Kietzman. The Effect of Asbestos Fibers on Structural Properties of Asphalt Pavement. Proc., Association of Asphalt Paving Technologists, Vol. 31, 1962.
5. F.L. Raschig and P.C. Doyal. An Extension of Asphalt Research as Reported in the 1937 Proceedings. Proc., Association of Asphalt Paving Technologists, Vol. 9, 1937.
6. P. Hubbard and E.H. Gollomb. The Hardening of Asphalt with Relation to Development of Cracks in Asphalt Pavements. Proc., Association of Asphalt Paving Technologists, Vol. 9, 1937.
7. V.A. Endersby, F.H. Stross, and T.K. Miles. The Durability of Road Asphalts. Proc., Association of Asphalt Paving Technologists, Vol. 14, 1942.
8. N.A. Huculak. Experience with Asbestos in Asphalt Pavement: 6 Year Performance. Canadian Department of Public Works, 1973.
9. E. Tons and G.G. Henault. Evaluation of Micro Aggregates by Smith Triaxial Test. Bull. 329. HRB, National Research Council, Washington, D.C., 1962, pp. 48-63.

Publication of this paper sponsored by Committee on Characteristics of Nonbituminous Components of Bituminous Paving Mixtures.

Combo Viscoelastic-Plastic Modeling and Rutting of Asphaltic Mixtures

A. ABDULSHAFI and KAMRAN MAJIDZADEH

ABSTRACT

Constitutive equations used in solving the boundary value problem of flexible pavements employ linear elastic or viscoelastic theory. Accordingly, permanent deformations are calculated based on elastic or viscoelastic deformation laws. Advances in the field of constitutive modeling of materials indicated the need to develop a constitutive relationship that better replicates asphaltic mixture responses under various loading and environmental conditions. In this paper a one-dimensional combo viscoelastic-plastic constitutive model composed of Burger-type mechanical elements connected in series with a friction slider is used. The friction slider is the mechanical representation of plasticity with a Drucker-Prager yield criterion. This model is solved under creep phase loading conditions, and the solution is used to develop a rutting model that incorporates a densification phase represented by a relaxing spring. Within the verification of the constitutive model a true yield line has been identified and used instead of the Mohr-Coloumb failure line. The two developed models are supplemented by appropriate experimentation phases to identify and numerically evaluate the relevant parameters. Experimentation is based on actual existing routine methods, with proper adjustments, modifications, or extensions to comply with proper evaluation of the model parameters, and kept as simple as possible to encourage wider user acceptance. An example using actual data is worked out and compared with results obtained from the VESYS III structural subsystem program.

Flexible pavements have traditionally been designed as multilayer elastic systems, in which each layer is assumed to be isotropic and homogeneous. Alternatively, the design could be based on an equivalent full-depth asphaltic concrete layer constructed by using layer equivalency concepts. Design techniques are based on analytical study of quasi-static algorithms with loading conditions of a slow-moving vehicle.

Design approaches based on performance were introduced in the early 1970s and are based on designing a flexible pavement to guard against functional or structural failures. Functional failures are more subjective in nature because they are associated with road user riding quality. Structural failures are dominantly caused by rutting (or permanent deformation) or fatigue cracking (1,2). These observed distress failures introduced a set of empirical laboratory-evaluated equations that were then raised to the phenomenological level by correlating their coefficients with the material constitutive system constants and loading conditions. In addition, mechanistic models have been proposed and applied to the design, thereby contributing to a better understanding of the damaging mechanisms involved, especially for fatigue cracking (3-5).

Advances in the fields of material characterization and fracture mechanics necessitated more research investigations in the area of flexible pavement structural failures, particularly the development of constitutive relationships that better replicate material responses such as viscoelasticity and viscoplasticity (i.e., viscous-elasic-plastic elements combined in any configuration) with and without yield surfaces, which describe cracking mechanisms such as elastoplastic fracture mechanics. Viscoelastic characterization of asphaltic materials has been investigated (6-9), and computer programs that input the creep compliance or relaxation modulus have been implemented (10,11). Viscoplasticity with yield surface as a constitutive relationship has been developed in the field of solid mechanics (12-15) and has recently been applied to soils (16).

Rutting and fatigue are major field problems. Rutting has been extensively studied at the empirical and phenomenological levels (2,11,17-19), with no attempt to characterize the asphalt mix as other than linear elastic or viscoelastic. Accumulations of permanent deformation were calculated by using elastic and viscous deformation laws. Thus it is not surprising that unsatisfactory correlations with actual field performance still exist; however, these correlations could be improved if concepts such as those previously cited were used.

The objective of this paper is to attempt to bridge part of the existing gap in correlation between laboratory and field performance by outlining and discussing the development of a viscoelastic-plastic constitutive relationship to characterize asphalt mixtures and to predict rutting. The fatigue problem will be addressed separately in a future paper.

VISCOELASTIC-PLASTIC MODELING OF ASPHALTIC MIXTURES

The total strain of asphaltic mixtures under a single impulse load can be decomposed into a recoverable part (elastic and viscoelastic) and a nonrecoverable part (viscous and plastic). By using vectorial notations, this is written as

$$\underset{\sim}{\epsilon}(t) = (\underset{\sim}{\epsilon}_E + \underset{\sim}{\epsilon}_{ve})_{recoverable} + (\underset{\sim}{\epsilon}_v + \underset{\sim}{\epsilon}_{PL})_{nonrecoverable} \quad (1)$$

where

$\underset{\sim}{\epsilon}(t)$ = total strain response vector;
$\underset{\sim}{\epsilon}_E$ = elastic strain vector (time independent), recoverable;
$\underset{\sim}{\epsilon}_{ve}(t)$ = viscoelastic strain vector (time dependent), recoverable;
$\underset{\sim}{\epsilon}_v(t)$ = viscous strain vector (time dependent), nonrecoverable; and
$\underset{\sim}{\epsilon}_{PL}$ = plastic strain vector (time independent), nonrecoverable.

Because plastic strains are preceded by elastic or viscoelastic response, it is instructive to rearrange the terms in Equation 1 as follows:

$$\underset{\sim}{\epsilon}(t) = (\underset{\sim}{\epsilon}_v + \underset{\sim}{\epsilon}_{ve}) + (\underset{\sim}{\epsilon}_E + \underset{\sim}{\epsilon}_{PL}) = \underset{\sim}{\epsilon}_{VE} + \underset{\sim}{\epsilon}_{EP} \quad (2)$$

where, in this equation, $\underset{\sim}{\epsilon}_{VE}$ represents both the recoverable and nonrecoverable parts of the viscoelastic strain response and $\underset{\sim}{\epsilon}_{EP}$ represents an elastic recoverable strain response associated with nonrecoverable plastic strain response. In fact, this arrangement lumps the time-dependent response in a viscoelastic element and the time-independent response in an elastoplastic element. In the following sections, a viscoelastic-plastic constitutive model will be developed based on this strain decomposition.

Elastic-Plastic Strain Response

It is generally assumed that plastic deformation (yielding) does not commence before the stress path reaches a surface in the stress space called the yield surface. The total elastic-plastic strain response for a stress state on the yield surface is made up from the contributions of an elastic response within the yield surface added to the plastic response. Mathematically stated,

$$\underset{\sim}{\epsilon}_{EP} = \underset{\sim}{\epsilon}_E + \underset{\sim}{\epsilon}_{PL} \quad (3)$$

Further, at any stress level, the total stress is related to the elastic strain through Hook's law as follows:

$$\underset{\sim}{\sigma} = \underset{\sim}{D}_E \cdot \underset{\sim}{\epsilon}_E \quad (4)$$

where $\underset{\sim}{\sigma}$ is the total stress vector and $\underset{\sim}{D}_E$ is the elastic constitutive matrix. By substituting Equation 4 into Equation 3, it can be rearranged to obtain

$$\underset{\sim}{\sigma} = \underset{\sim}{D}_E(\underset{\sim}{\epsilon}_{EP} - \underset{\sim}{\epsilon}_{PL}) \quad (5)$$

The next step is to eliminate the plastic strain response in a similar manner; however, this requires understanding the assumptions of the theory of plasticity. The four cornerstones of the classical theory of plasticity are based on the existence of a yield condition, a surface hardening condition, a flow rule, and a hardening rule, as discussed in the following list (1 through 4).

1. The yield condition is a scalar function to determine the onset of plastic deformation. It can be written in the form (20):

$$F(\underset{\sim}{\sigma}, \underset{\sim}{K}, \underset{\sim}{\epsilon}_{PL}, k) = f(\underset{\sim}{\sigma}, \underset{\sim}{K}, \underset{\sim}{\epsilon}_{PL}) - \langle k \rangle = \begin{cases} <0 \text{ no yielding} \\ 0 \text{ onset of yielding} \\ >0 \text{ unattainable} \end{cases} \quad (6)$$

where

$F(\underset{\sim}{\sigma}, \underset{\sim}{K}, \underset{\sim}{\epsilon}_{PL}, k)$ = yield condition,
$\underset{\sim}{\sigma}$ = any stress state on the yield surface,

$\underset{\sim}{K}$ = prestress state that generated the present yield surface,
$\underset{\sim}{\varepsilon}_{PL}$ = plastic strain,
$\underset{\sim}{k}$ = yield parameter,
$f(\underset{\sim}{\sigma},\underset{\sim}{K},\underset{\sim}{\varepsilon}_{PL})$ = loading function, and
<k> = yield parameter that can be a function of the plastic strain.

The loading function is usually chosen referenced to the invariant stress space. In multidimensional stress space, the vector argument of the loading function allows much freedom in choosing its form to suit the required material characteristics. For example, if plastic flow is not affected by hydrostatic stress, as in the case for most metals, then the loading function could be expressed in terms of the second invariant deviatoric stress, J_2. If, on the other hand, plastic flow is affected by both shear stress and hydrostatic stress, as is usually the case in soils and asphalt mixes, then the loading function would more appropriately be expressed in terms of both the first and second invariants of stress. Further, the loading function serves as a test for whether or not plastic deformation occurs. For F = 0, the current stress state is on the yield surface, and for an increment of stress $d\underset{\sim}{\sigma}$ (which could be in a direction different from that of the outward normal to the yield surface, $\hat{\underset{\sim}{n}}$), the equation is

$$(\partial f/\partial \underset{\sim}{\sigma})\cdot d\underset{\sim}{\sigma} = \begin{cases} >0 \text{ plastic loading} \\ 0 \text{ neutral loading} \\ <0 \text{ elastic (or viscoelastic) unloading} \end{cases} \tag{7}$$

where $\partial f/\partial \underset{\sim}{\sigma}$ is the gradient of the loading function; its direction is in the direction of the outward normal to the yield surface, $\hat{\underset{\sim}{n}}$.

2. The surface hardening condition is the law that describes the movement of the yield surface during plastic deformation in the stress space. The yield surface translating in space as a rigid body is kinematic hardening; if it dilates or contracts without either change in shape or translates in space, it is isotropic hardening. Various movements of the yield surface can also be described, such as anisotropic hardening (same as isotropic but with change in shape) or universal (mixed) mode hardening where both isotropic and kinematic hardening are in effect.

3. The flow rule is the relationship between the stress and strain during plastic yielding. The direction of the plastic strain can be normal to the yield surface (associated flow rule) or can be inclined to this surface (nonassociated flow rule). Because plastic strain is a vector in multidimensional space, then its inclination is hypothesized to be due to the fact that not all the loading function is effective in pulling the yield surface, but only a part of it. The acting stress is also a vector in multidimensional space that can be decomposed into effective and noneffective stress vectors. The effective stress vector can evidently have a unit normal in a direction different from that of the whole stress vector.

4. The hardening rule is the mathematical expression that provides the value of the hardening function or coefficient as a measure of thermodynamic state variable, namely, work hardening and strain hardening. The choice between the two is a matter of experimental or calculable convenience.

Because the onset of plastic deformation only needs an increment of stress on the yield surface, it is more sensible to deal with the incremental theory of plasticity. In fact, all of the preceding equations could be obtained in compliance with this theory by replacing $\underset{\sim}{\sigma}$, $\underset{\sim}{\varepsilon}$, t, and so forth by their corresponding increments $d\underset{\sim}{\sigma}$, $d\underset{\sim}{\varepsilon}$, dt, and so forth. The plastic strain increment could be written as

$$d\underset{\sim}{\varepsilon}_{PL} = \lambda \hat{\underset{\sim}{m}} \tag{8}$$

where λ is the magnitude of plastic strain increment, and $\hat{\underset{\sim}{m}}$ is the unit vector in the direction of the plastic strain increment. Based on Prager's assumption (21), the effective stress vector $(\hat{\underset{\sim}{n}} \cdot d\underset{\sim}{\sigma})$ is related to the magnitude of plastic strain increment by the following equation:

$$\lambda = (1/H)(\hat{\underset{\sim}{n}}^T \cdot d\underset{\sim}{\sigma}) \tag{9}$$

where $\hat{\underset{\sim}{n}}^T$ is the transpose of the yield surface outward normal and H is the hardening parameter that could be found experimentally, as will be shown later. Substituting Equation 9 into Equation 8 yields

$$d\underset{\sim}{\varepsilon}_{PL} = (1/H)(\hat{\underset{\sim}{n}}^T \cdot d\underset{\sim}{\sigma})\hat{\underset{\sim}{m}} \tag{10}$$

By some mathematical manipulations (22-24), the following can be obtained:

$$d\underset{\sim}{\sigma} = (\underset{\sim}{D}_E - \underset{\sim}{D}_{PL})d\underset{\sim}{\varepsilon} \tag{11}$$

where

$$\underset{\sim}{D}_{PL} = \underset{\sim}{D}_E\hat{\underset{\sim}{m}}\,\hat{\underset{\sim}{n}}\,\underset{\sim}{D}_E/(H + \hat{\underset{\sim}{n}}^T\underset{\sim}{D}_E\hat{\underset{\sim}{m}})$$

Equation 11 is the elastic-plastic constitutive equation in multidimensional stress space.

Model Development for Asphaltic Mixtures

To devise a simple test to obtain the required parameters that characterize the elastic-plastic response behavior of asphalt mixes, Equation 11 must be reduced to a one-dimensional equivalent. Figure 1

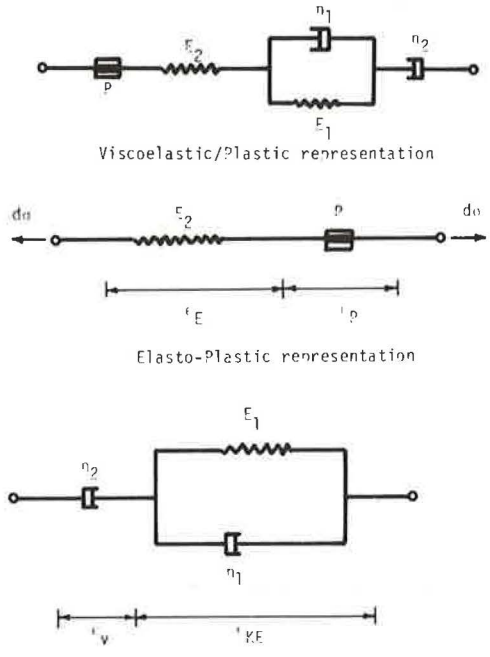

FIGURE 1 One-dimensional mechanical models.

shows a one-dimensional mechanical model representation. The following assumptions are made:

1. Yield condition: $F = F(\underset{\sim}{\sigma}, K) = F(\underset{\sim}{\sigma}) - K$
   (a) Yield parameter: isotropic hardening, $K = K_o + \Delta K$
   (b) Loading function:
      (i) Von Mises--$f(\underset{\sim}{\sigma}) = \sqrt{J_2'}$
      (ii) Drucker-Prager--$f(\sigma) = \alpha I_1 + \sqrt{J_2'}$
2. Associated flow rule: $\hat{n} = \hat{m}$
3. Hardening parameter is a function of the plastic work, $H = H(W_p)$,

where

K = yield parameter (measure the current cone or cylinder radius);
K_o = cone or cylinder radius at initial onset of plastic deformation;
ΔK = increment of increase in cone or cylinder radius due to plastic strain increment;
I_1 = octahedral normal stress = 1st stress invariant = $(1/3)(\sigma_1 + \sigma_2 + \sigma_3)$;
J_2' = 2nd reduced stress invariant = $(1/6)[(\sigma_1 - \sigma_2)^2 + (\sigma_2 - \sigma_3)^2 + (\sigma_3 - \sigma_1)^2]$;
$\sigma_1, \sigma_2, \sigma_3$ = principal stresses; and
α = scalar multiplier that measures the rate of increase of the cone radius along the hydrostatic stress line (the cone centerline).

Note that if $\alpha = 0$, the Drucker-Prager yield condition reduces to that of Von Mises. In conclusion, a Drucker-Prager yield condition is the general case, where α, K, and $H(W_p)$ must be found experimentally to uniquely define an asphalt mix constitutive equation. Cylinderical triaxial tests could be used for that purpose. The stress path of this test fixes a point on the yield surface where Von Mises, Tresca, Drucker-Prager, and Mohr-Coloumb yield surfaces intersect. Thus the use of the Mohr-Coloumb yield criterion to obtain parameters for any of the previous yield conditions is justified. Figure 2 shows a Mohr-Coloumb failure line that can be expressed mathematically as

$$\tau = C + \sigma \tan \phi \tag{12}$$

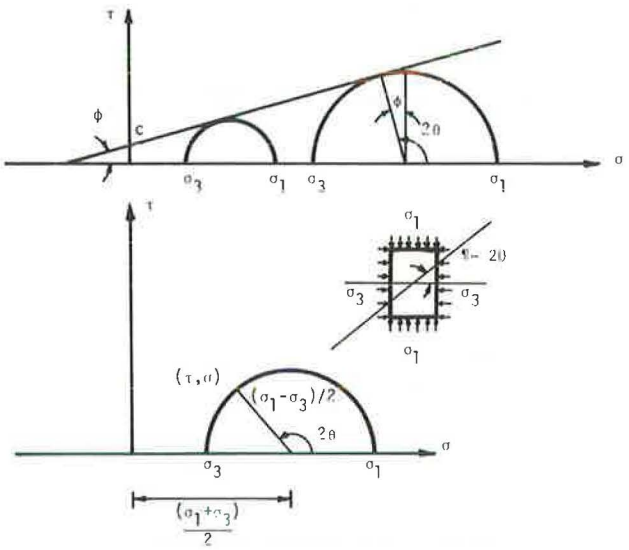

FIGURE 2 Mohr-Coloumb stress state graphical representation.

where

τ = shear stress at failure,
C = cohesion intercept,
σ = normal stress at failure, and
ϕ = angle of internal friction.

Because it is known that

$$\sigma = [(\sigma_1 + \sigma_3)/2] + [(\sigma_1 - \sigma_3)/2] \cos 2\theta \; ; \tau[(\sigma_1 - \sigma_3)/2] \sin 2\theta \tag{13}$$

and by substituting Equation 13 into Equation 12 and doing some rearranging,

$$\sigma_1 - [(1 - \cos 2\theta)/(1 + \cos 2\theta)]\sigma_3 - [(2C \sin 2\theta)/(1 + \cos 2\theta)] = 0 \tag{14}$$

For stress states typical of that found in triaxial tests, $\sigma_2 = \sigma_3$,

$$I_1 = (\sigma_1 + 2\sigma_3)/3 \text{ and } \sqrt{J_2'} = (\sigma_1 - \sigma_3)/3 \tag{15}$$

Substituting Equation 15 into assumption b-ii of the yield condition gives

$$F(\underset{\sim}{\sigma}, K) = (\alpha/3)(\sigma_1 + 2\sigma_3) + (|\sigma_1 - \sigma_3|/\sqrt{3}) - K = 0 \tag{16}$$

The triaxial test previously cited is not currently considered in routine asphalt testing. Thus it is desirable to find the two model parameters (α and K) from other independent tests that are routinely performed, such as direct compression and indirect tension tests. If it is assumed that asphalt mixes are a unimodular material, and by setting $\sigma_3 = 0$ and using some mathematical manipulations (22), then Equation 16 will be reduced to

$$\pm \sigma_1 = 3K_o/[\alpha + \sqrt{3}\ \text{sgn}(\sigma_1)] \tag{17}$$

where $-\sigma_1$ and $+\sigma_1$ are the compressive and tensile ultimate stresses, respectively, and $\text{sgn}(\sigma_1)$ denotes the sign of the major principal stress (uniaxial stress in this case). A major criticism of this scheme is using the Mohr-Coloumb failure line as a yielding line. Fortunately, actual yield points in tension and compression of asphalt mixes can be found by using creep test data. The third quantity to be determined is the hardening parameter, H. For a one-dimensional model, $d\underset{\sim}{\sigma} = d\sigma_1$; $d\underset{\sim}{\varepsilon}_{PL} = d\varepsilon_{PL}$; $\hat{n} = \hat{m} = n_1$. Hence by substituting these in Equation 10,

$$H = n_1^2(d\sigma_1/d\varepsilon_{PL}) \tag{18}$$

where $d\sigma_1/d\varepsilon_{PL}$ is the instantaneous slope of the stress-plastic strain curve, and

$$n_1 = 2[\alpha + \sqrt{3}\ \text{sgn}(\sigma_1)]/\sqrt{6(2\alpha^2 + 3)} \tag{19}$$

The procedure for determining the plasticity parameters α, K, and $H(W_p)$ is as follows:

1. The stress-plastic strain curve is established from appropriate tests by deducting all other strains from the total strains.
2. The slope of the curve is found at selected appropriate points, and these values are multiplied by n_1^2 to get H.
3. Values of the plastic work done ($W_p = {}_o\int^{\varepsilon} \sigma_1 d\varepsilon$ = area under the $\sigma - \varepsilon_{PL}$ curve) is found, and the curve-fitting H versus W_p is established.
4. This will give $H(W_p)$, which is the required hardening parameter.
5. The values of the α and K parameters could be obtained from creep test data (22) as well as indirect tension and uniaxial compressive strength tests.

Substitute Equation 18 into the incremental equivalents of Equations 3 and 4 to get

$$d\epsilon_{EP} = C_{EP} \cdot d\sigma_1 \tag{20}$$

where

C_{EP} = elastic-plastic compliance = $(1/E_2) + <n_1^2/H(W_p)>$

and

$$<n_1^2/H(W_p)> = \begin{cases} 0 \text{ if } \sigma < \sigma_{yield} \\ n_1^2/H(W_p) \text{ if } \sigma \geq \sigma_{yield} \end{cases}$$

Equation 20 is the governing equation for the response of the elastic-plastic element.

Viscoelastic Strain Responses

Figure 1 includes the one-dimensional viscoelastic element to be solved. The governing differential operator equation is easily found to be (22)

$$[E_1\eta_2(d/dt) + \eta_1\eta_2(d^2/dt^2)]\ \epsilon_{VE} = [E_1 + (\eta_1 + \eta_2)(d/dt)]\ \sigma_1 \tag{21}$$

where d/dt is the time derivative. Because creep tests will be used for model verification, then by imposing incremental creep phase loading conditions, $d\sigma_1 = d\sigma = \text{const.}$, Equation 21 will yield the following solution:

$$d\epsilon_{VE}(t) = C_{VE}\, d\sigma_1 \tag{22}$$

where

C_{VE} = viscoelastic compliance = $(t/\eta_2) + (1/E_1)\{1 - EXP[-(E_1/\eta_1)t]\}$,
t = time scale,
E_1 = uniaxial elastic spring coefficient, and
η_1, η_2 = viscous coefficients of the corresponding dashpots.

Equation 22 is in the form of the required viscoelastic strain response.

Viscoelastic-Plastic Strain Response

Substitute Equations 20 and 22 into Equation 2 to obtain

$$d\epsilon_1(t) = C_{VEP}\, d\sigma_1 \tag{23}$$

where C_{VEP} is the viscoelastic-plastic compliance, that is,

$$C_{VEP} = \left(\left\{(1/E_2) + (t/\eta_2) + (1/E_1)[1 - EXP(-E_1/\eta_1)t]\right\} + <[n_1^2/H(W_p)]>\right)$$

Equation 23 represents the mathematical relationship of the viscoelastic-plastic mechanical model for asphalt mixes, where the parameters E_1, E_2, η_1, η_2, α, K, n_1, and $H(W_p)$ could be found experimentally.

Rutting or Permanent Deformation Model

Rutting is defined as the accumulation of permanent deformation in the wheel path and is caused by one or more of the following mechanisms: densification, viscous flow, and plastic deformation. If no interaction is assumed among these mechanisms, then the one-dimensional mathematical relationship that describes the permanent deformation will be

$$\epsilon_p = \epsilon_{p_o} + \epsilon_v(t) + \epsilon_{PL} \tag{24}$$

where

ϵ_p = permanent total deformation;
ϵ_{p_o} = permanent deformation due to densification; it could be represented by an in-series mechanical relaxing spring with constant E_{p_o};
$\epsilon_v(t)$ = time-dependent viscous permanent deformation; and
ϵ_{PL} = time-independent plastic permanent deformation.

By using the relevant elements of the viscoelastic-plastic model, Equation 24 could be written as

$$\epsilon_p = C_p \cdot \sigma_1 \tag{25}$$

where

$C_p = \left\{(1/E_{p_o}) + (t/\eta_2) + <[n_1^2/H(W_p)]>\right\}$,
$\sigma_1 = \begin{cases} \sigma_c \text{ in uniaxial compression} \\ \sigma_t \text{ in uniaxial tension,} \end{cases}$
E_{p_o} = densification spring modulus, and
η_2 = coefficient of viscosity of the in-series dashpot.

Equation 25 represents permanent deformation caused by a constant stress-loading condition acting for an arbitrary time t. An immediate permanent deformation due to densification will occur and may or may not be accompanied by plastic deformation, depending on the magnitude and sign of the stress. Contrary to that, the permanent viscous deformation is effective only after a time step is defined. On the other hand, experimental testing for rutting establishes the relationship between the permanent deformation per cycle (ϵ_p) and the number of cycles (N) at the measured values of ϵ_p by procedures found elsewhere in the literature (11,19,25). The general form of this relationship is

$$\epsilon_{p_{acc}} = \epsilon'_{p_{acc}}/N = K_1 N^{-m} \tag{26}$$

where

$\epsilon_{p_{acc}}$ = average accumulated permanent deformation per cycle,
$\epsilon_{p_{acc}}'$ = accumulated permanent deformation,
K_1 = ϵ_p at N = 1,
N = number of cycles at measured permanent deformation, and
m = slope of the log ϵ_p - log N relationship.

By substituting $\epsilon_p' = \epsilon(t) - \epsilon_{VER}$, where $\epsilon(t)$ is the total deformation and ϵ_{VER} is the viscoelastic recoverable deformation, then

$$\epsilon(t) - \epsilon_{VER} = K_1 N^{1-m} \tag{27a}$$

Then substitute $\epsilon_{VER} = \sigma_1/E'$ in Equation 27a and rearrange terms to get

$$\sigma = E'[\epsilon(t) - K_1 N^{1-m}] \tag{27b}$$

Finally, substitute Equation 27b into Equation 25 to get

$$\epsilon_{p_{acc}} = K_2(\sigma,t)[\epsilon(t) - K_1 N^{1-m}] \tag{28}$$

where

$$K_2(\sigma,t) = \begin{cases} (E'/E_{p_o}) + (E'/\eta_2)t + n_1^2\,[E'/H(W_p)] & \text{if } \sigma > \sigma_{yield},\ t > 0 \\ (E'/E_{r_o}) + (E'/\eta_2)t & \text{if } \sigma < \sigma_{yield},\ t < 0 \\ E'/E_{p_o} & \text{if } \sigma < \sigma_{yield},\ t = 0 \\ (E'/E_{p_o}) + n_1^2\,[E'/H(W_p)] & \text{if } \sigma > \sigma_{yield},\ t = 0 \end{cases}$$

E' = retarded elastic creep modulus $= 1/\left\{(1/E_2) + (1/E_1)\left\{1 - \mathrm{EXP}\left[(-E_1/\eta_1)t\right]\right\}\right)$, and

N_D = design number of load repetitions.

Recalling the principle of exhaustion of ductility, then $\varepsilon(t)$ could be found from any monotonic stress-strain diagram such as those routinely used in asphalt mix testing. The important contribution here is that $K_2(\sigma,t)$ in Equation 28 reflects the effects of the different constitutive mechanisms to the accumulation of a rut depth that, in turn, rationalize decision alternatives. For example, if the contribution of densification is more dominant than that of the viscous and plastic deformations, then a decision on raising the compaction level of the asphalt mix pavement is rationalized. Similarly, if plastic deformation is dominant, then a decision to reduce contact stress or stiffen the mix with admixtures could be made. On the other hand, if viscous deformation is dominant, then consideration can be given to improving the asphalt cement (AC) viscosity by mixing grades or using additives. And if the ranges of K_1 and m can be established, then a design scheme for rutting could be implemented. In the next section an example is presented to show numerically how the procedure given in this section is used in calculating the laboratory-evaluated permanent deformation.

EXPERIMENTATION

Materials, Specimen Preparation, and Testing Program

This phase consisted of five laboratory-prepared recycled asphalt concrete mixes and their respective extracted field cores. Specific information on the mixes is given in Table 1.

The percentage of rejuvenator in the mix was selected on the basis of constructing viscosity design nomographs, which were used by targeting at a blend of 2000 poises absolute viscosity at 140°F to obtain the required percentage of rejuvenator (26). A total of 295 laboratory samples were prepared to conduct various tests, such as

1. Diametral modulus of resilience (MR) on Marshall-sized samples at 40°, 70°, and 100°F;
2. Indirect tensile strength (σ_{It}) using the same type samples and test temperatures as used for MR;
3. Unconfined compressive strength (q_u) on 4 x 4-in. cylinders at 70°F;
4. Incremental static compression rutting-creep test on 4 x 8-in. cylinders at 40°, 70°, and 100°F; modification is included (22) to account for determination of the friction element parameters in compression; and
5. Incremental static indirect tension rutting-creep test on cylinderical discs 4 in. in diameter by 2.5 in. in height at 70°F; modification is included (22) to account for determination of the friction element parameters in tension.

The test results from these series of tests are summarized in Tables 2 and 3.

MODEL VERIFICATIONS

Verification of Viscoelastic-Plastic Model

Elasto-Plastic Unit

Characterization of this model requires determining the yield condition parameters (α and K) and the hardening coefficient H. This is done as follows. First, the yield condition parameters are determined. The data in Table 1 summarize the results obtained on mixes 1 through 5 and give the MR, σ_{It}, and q_u values for the laboratory-fabricated samples and the two extracted field core assignments (1st assignment taken immediately after construction and 2nd assignment taken one year later). Tests were conducted at 40°, 70°, and 100°F for the MR and σ_{It}. The following example uses the Florida mix (mix 1).

Step 1: Direct Application of Classical Theory of Plasticity

Use Equation 17 to obtain

$$\pm\sigma_1 = 3K_o/[\alpha + \sqrt{3}\ \mathrm{sgn}(\sigma_1)] = \begin{cases} -802 \text{ psi compression} \\ +160 \text{ psi tension} \end{cases}$$

Then the following is obtained: $\alpha = 1.156$, $K_o = 154$ psi, and $\arctan\ \alpha = 49.1°$. Then substitute Equation 19 to get

$$n_1^2 = \begin{cases} 0.9802 \text{ in tension} \\ 0.039 \text{ in compression} \end{cases}$$

TABLE 1 Mix Information

Mix No.	Location	State	Mix Proportions		Rejuvenator
			Reclaimed %	New Agg. %	Type, % / %aged Asphalt
1	SR-91	Florida	65	35	AER, 38% / 62%
2	I-94	Michigan	85	15	AC-5, 81% / 19%
3	M-55(a)	Michigan	50	50	AC-20, 54% / 46%
4	M-55(b)	Michigan	50	50	AC-20, 45% Cyclogen, 10% / Aged Asphalt, 45%
5	M-55(c)	Michigan	50	50	Sulfur, 60% / 40%

TABLE 2 Test Results Summary (σ_{It}, MR, q_u, I)

		MIX No. 1			MIX No. 2			MIX No. 3			MIX No.4	MIX No.5
		LAB	FIELD 1st ass.	FIELD 2nd ass.	LAB	FIELD 1st ass.	FIELD 2nd ass.	LAB	FIELD 1st ass.	FIELD 2nd ass.	LAB	LAB
σ_{IT} psi	40°F	243.42	306.19	274.40	232.02	291.8		238.48	305.23	303.40	235.40	231.19
	70°F	160.71	62.58	58.83	109.98	57.25	55.95	113.97	61.93	56.50	104.65	229.75
	100°F	39.57	15.74	16.93	19.79	9.28	26.5	15.19	16.58	11.13	17.10	3.567
MR x 10^6 psi	40°F	1.352	2.61	2.27	1.304	2.97	2.82	1.146	3.74	3.33	0.418	3.567
	70°F	0.607	0.706	1.07	0.541	0.92	0.82	0.26	0.93	1.26	0.248	2.018
	100°F	0.203	0.303	0.193	0.061	0.123	0.104	0.033	0.145	0.168	0.037	1.256
Immersion Compress. psi	q_u	763	528	706	432	565	484	546		863	480	613
	q^*	802	585	719	539	564	700	470		657	438	1004
	I%	95	90	98	80	100	69	100		100	100	61

q_u = unconfined compressive strength after immersing in water

q^* = unconfined compressive strength

$I = q_u / q^*$ = index of retained strength

TABLE 3 Strain from Uniaxial Compression Creep Tests (x 10^{-3} in./in.)

Stress psi	t = 1.0 sec.			t = 3.0 sec.			t = 10.0 sec.			t = 30 sec.			t = 100 sec.			t = 1000 sec.			Aver. Value
	ϵ_t			ϵ_t			ϵ_t			ϵ_t			ϵ_t			ϵ_t			
	ϵ_c	ϵ_{Po}	ϵ_{PL}	ϵ_c	ϵ_{Po}	ϵ_{PL}	ϵ_c	ϵ_{Po}	ϵ_{PL}	ϵ_c	ϵ_{Po}	ϵ_{PL}	ϵ_c	ϵ_{Po}	ϵ_{PL}	ϵ_c	ϵ_{Po}	ϵ_{PL}	ϵ_{PL}
20	.563	1.14	0.0	.625	1.14	0.0	.813	1.14	0.0	.9	1.14	0.0	1.063	1.14	0.0	1.375	1.14	0.0	0.0
40	1.12	2.28	0.0	1.25	2.28	0.0	1.63	2.28	0.0	1.8	2.28	0.0	2.13	2.28	0.0	2.75	2.28	0.0	0.0
60	1.69	3.52	0.0	1.88	3.52	0.0	2.44	3.52	0.0	2.7	3.52	0.0	3.19	3.52	0.0	4.13	3.52	0.0	0.0
80	2.56	5.895	.31	2.81	5.895	.31	3.52	5.895	.27	3.89	5.895	.23	4.4	5.895	.15	5.6	5.895	.1	.22
120	4.68	6.0	1.31	5.01	6.0	1.26	6.08	6.0	1.2	6.35	6.0	.95	7.0	6.0	.82	9.0	6.0	.74	1.04
160	7.31	6.0	2.81	7.7	6.0	2.7	9.23	6.0	2.73	9.81	6.0	2.61	10.5	6.0	2.0	13.59	6.0	2.59	2.68

ϵ_{PL} = plastic strain = $\epsilon t - J(t) \times \sigma - \epsilon_{PO}$

$J(t) = \{\{64.25 + 0.00475t\} - \{9.73e^{-0.0185t} + 8.97 \times e^{-0.13658t} + 16e^{-0.4688t}\}\}$ microin./in/p.s.i.

Hence,

$$H = n_1^2 (d\sigma_1/d\epsilon_{PL}) \tag{29}$$

Step 2: Modification to Step 1

Step 1 assumes that yielding commences when $\sigma = \pm\sigma_1$ (maximum compressive or tensile strength of the material). Intuitively, however, yielding starts at some level of $\sigma < |\sigma_1|$. Consequently, a yield value of the material in both tension (σ_{ypt}) and compression (σ_{ypc}) should be obtained and substituted instead of $\pm\sigma_1$. These values for asphalt concrete are found by plotting the relationship between the steady-state creep rate ($\dot{\epsilon}_{ss}$) of the creep data under different stress levels versus the stress.

The rationale for using this method to find the yield point of asphalt mixes is based on the findings of many investigators regarding factors affecting creep. One of the simplest relationships between stress and steady-state strain rate, found to apply for certain metals and alloys, is of the form

$$\epsilon_{ss} = A\sigma^n \tag{30}$$

where $\dot{\varepsilon}_{ss}$ is the steady-state creep strain rate and A,n are the material constants that are stress dependent.

Values of n have been reported in the range of 1 to 10. Asphalt mixes at low stress and strain levels are considered linear viscoelastic, that is, n = 1 and Aσ = constant. However, at high stress levels it becomes nonlinearly stress dependent. For a viscoelastic-plastic system, the friction slider represents the element that possesses material nonlinearity. Consequently, a plot of $\dot{\varepsilon}_{ss}$ versus σ should reveal the stress at which nonlinearity occurs; that is, the friction slider element activated. This stress level is termed the yield point, σ_{yp}. Figure 3 shows the $\dot{\varepsilon}_{ss}$ - σ relationship; as expected, the coefficient of the in-series dashpot of the fitted Burger mechanical model does not change value up to a stress level of 60 psi. This substantiates the previous linear viscoelasticity hypothesis of asphalt mixes. The same plot is made for the indirect tension creep tests where this test was found to be sufficiently sensitive to the stress level, such that this finding could not be detected. Back extrapolation to $\dot{\varepsilon}_{ss} = 0$ gave the following values:

σ_{ypt} = 3 psi, σ_{ypc} = 75 psi.

Using these values instead of $\pm\sigma_1$ gives α = 1.599, K_o = 3.33 psi, arctan α = 57.9°, and

$$n_1^2 = \begin{cases} 0.9117 \text{ in tension} \\ 0.00145 \text{ in compression} \end{cases}$$

Such results are not compatible with those obtained under Mohr-Coloumb failure criteria. Determining the hardening coefficient will be done after determining the viscoelastic model parameters.

Determination of Viscoelastic Unit Parameters from Rutting-Creep Tests

Compression and tension rutting-creep tests were conducted on 4 x 8-in. (diameter x height) cylinders and 4 x 2.5-in. (diameter x height) discs, respectively. Test results are given in Table 3 and plotted in Figures 4 and 5, showing ε(t) versus t for different stress levels. A mechanical model for the 20-psi stress level is found by using the nonlinear SAS regression program. From these fittings, the relationship ε(t) versus t is found to be dependent on stress level. For stress levels of 20, 40, and 60 psi, the in-series dashpot and spring constants are identical, but Kelvin element constants vary. The SAS program was used to fit the creep data by an equation of the form

$$\epsilon(t) = \sigma\{\beta_0 + \beta_1 * t + \beta_2 [1 - EXP(-\beta_3 t)]\} \quad (31)$$

which corresponds to a Burger model type response under creep loading conditions. The SAS program gave the following result:

$$\epsilon(t) = (\sigma/10^6)\{29.55 + 0.00475\, t + 1.73\, [1 - EXP(-1949.6t)]\} \quad (32)$$

from which the mechanical Burger model coefficients are

$\eta_2 = 2.105 \times 10^8$ psi-sec, $E_2 = 3.384 \times 10^5$ psi.
$\eta_1 = 2.958 \times 10^8$ psi-sec, $E_1 = 5.767 \times 10^5$ psi.

To determine the hardening coefficient H from fitting creep data by a Burger model, the creep compliance in uniaxial compression J(t) is calculated at the lowest stress level (20 psi) and by the linearity assumption; this creep compliance is independent of stress level. At higher stress levels, plastic deformation occurs and can be calculated from Equation 33, although a slightly different approach was adopted in the calculations in Table 3:

$$\epsilon_{PL} = \epsilon_p - \epsilon_{p_o} = \epsilon(t) - J(t) \times \sigma - \epsilon_{p_o} \quad (33)$$

where

$\epsilon(t)$ = total deformation,
ϵ_p = permanent deformation,
ϵ_{PL} = plastic deformation,
ϵ_{p_o} = permanent deformation due to densification,
σ = stress level, and
J(t) = creep compliance evaluated at the lowest stress level below the yield point.

The stress-average plastic strain relationship is given in Table 3 and is shown in Figure 6. The hardening coefficient is calculated and the results are

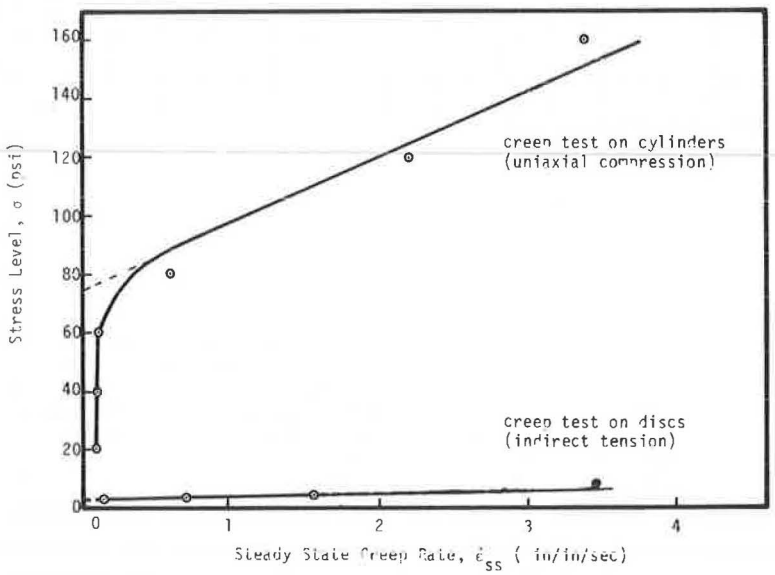

FIGURE 3 Steady-state deformation rate versus stress level curve.

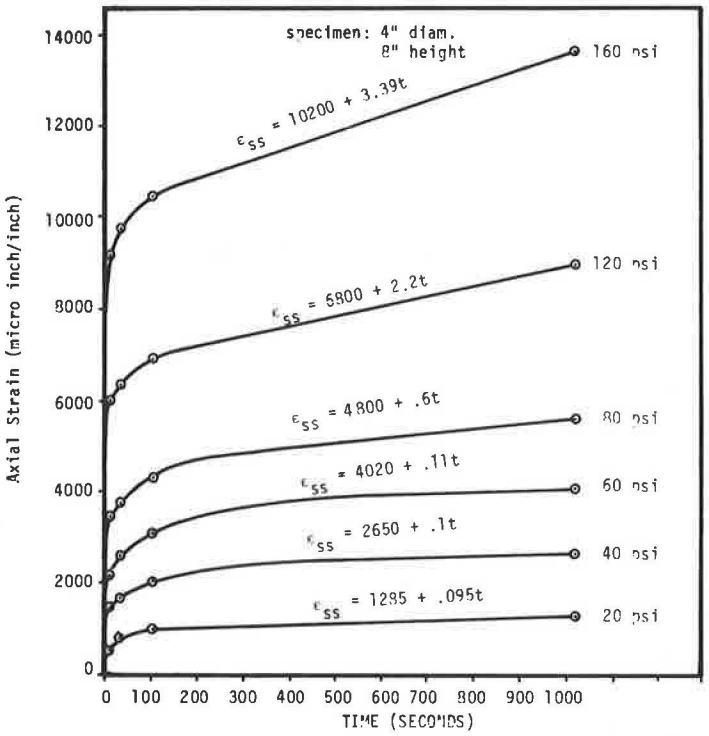

FIGURE 4 Compression rutting-creep.

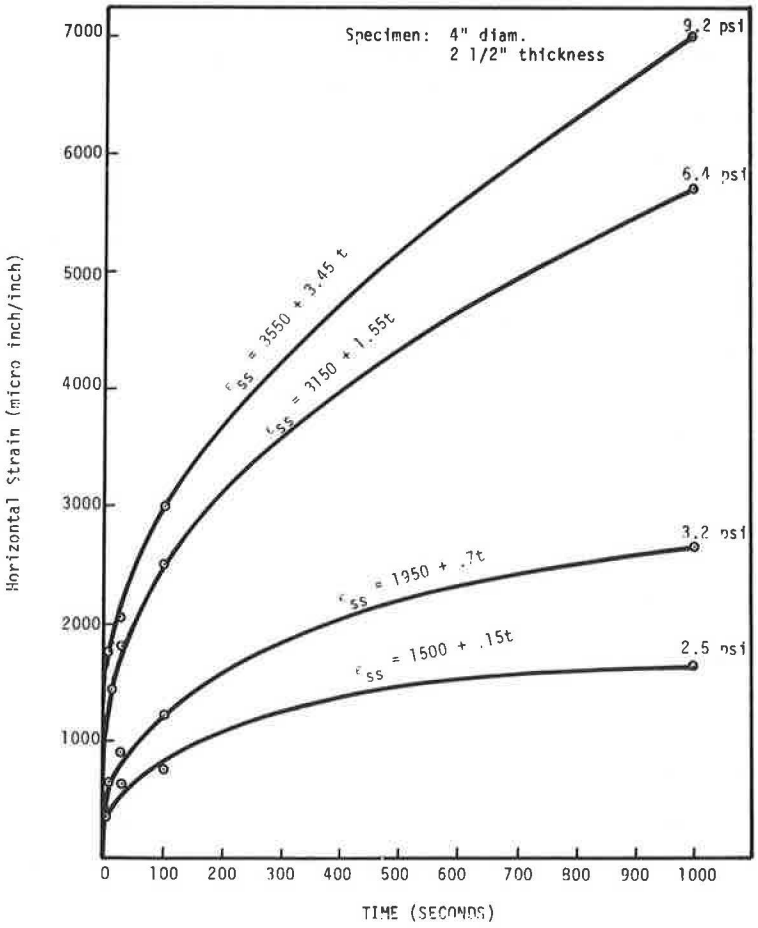

FIGURE 5 Indirect tension rutting-creep.

summarized in Table 4. The fitted equation is found by nonlinear SAS regression as

$$H(W_p) = 49.376 - 0.243W - 0.00043W^2 \quad (34)$$

This is plotted in Figure 7.

Summary of Example of Viscoelastic-Plastic Modeling

The model is summarized as follows:

$$\epsilon(t) = \sigma\{[1/(3.384 \times 10^5)] + [t/(2.105 \times 10^8)] + [1/(5.567 \times 10^5)](1 - e^{-1949.6t}) + <[n_1^2/H(W_p)]>\} \quad (35)$$

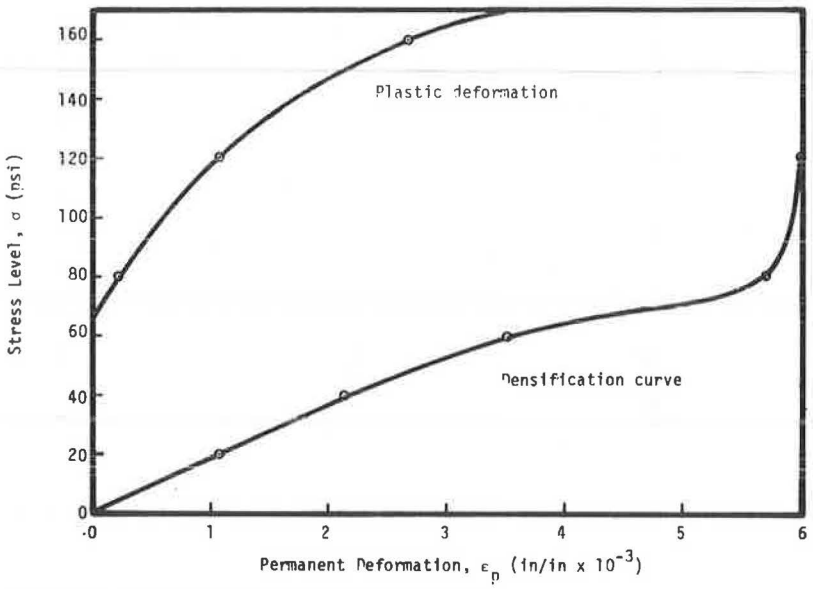

FIGURE 6 Permanent deformation versus stress level curve.

TABLE 4 Hardening Coefficient as a Function of Plastic Work Done

Stress level (psi)	20	40	60	80	120	160
H x 10^3 (psi)	--	--	--	45.59	29.72	16.09
W_p x 10^{-3} (psi)	--	--	--	16.06	98.06	327.66

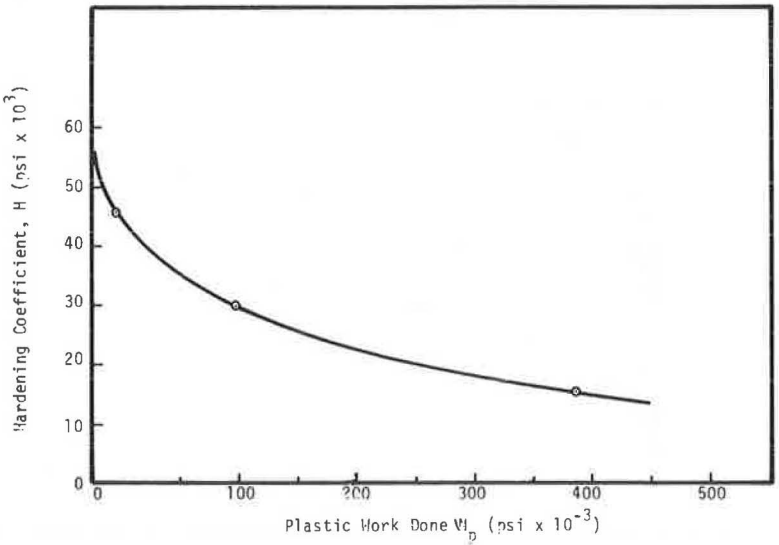

FIGURE 7 Hardening coefficient versus plastic work done curve.

where

$$H(W_p) = 49.38 - 0.243W_p + 0.00043W_p^2$$

$$n_1^2/H(W_p) = \begin{cases} 0 & \sigma_c < 75 \text{ and } \sigma_t < 3 \text{ psi} \\ 0.9117/H(W_p) & \sigma_t \geq 3 \text{ psi} \\ 0.00145/H(W_p) & \sigma_c \geq 75 \text{ psi} \end{cases}$$

RUTTING MODEL VERIFICATION

The rutting model requires determination of the permanent deformation versus number of cycles, in accordance with the dynamic series in VESYS II-M and the function $K_2(\sigma,t)$. The case of axial compression on 4 x 8-in. (diameter x height) samples is considered here. Test results are shown in Figure 8 on log-log scale, where the required relationship is found to be

$$\text{Log } \epsilon_p = 0.13 + 0.285 \log N \text{ in./in. x } 10^{-5} \quad (36)$$

from which the following is obtained:

$$\epsilon_p = 1.35N^{-0.715} \text{ in./in. x } 10^{-5} \quad (37)$$

Therefore, Equation 37 gives m = +0.715 and k_1 = 1.35 x 10^{-5} in./in.

The second step is to get $\epsilon(t)$ from monotonic testing or from creep test data (Table 3) at t = 100 sec: $\epsilon(t) = 10.445 \times 10^{-3}$ in./in.

The third step is to find the function $K_2(\sigma,t)$. This was done in the viscoelastic-plastic model with a yield surface model. The function is found to be

$$E' = 3.0656 \times 10^5 \text{ psi}$$

$$K_2(\sigma,t) = \{(1/E_{p_o}) + [1/(2.105 \times 10^8)]\, t + [0.00145/H(W_p)]\} \times 3.0656 \times 10^5$$

For σ = 80 psi representing the contact pressure of the design vehicle, $E_{p_o} = 5.7 \times 10^5$ psi (using Figure 6) and $H(W_p) = 45 \times 10^3$ psi (using Table 4). Therefore, $k_2(\sigma,t) = (0.53 + 0.145 + 0.01) = 0.693$. This indicates that 77.6 percent of the total permanent deformation is due to densification, 1.5 percent due to plastic deformation, and 20.9 percent due to viscous deformation. Then substitute Equation 28 to get

$$\epsilon_{P_{acc}} = 0.693\,[10.445 \times 10^{-3} - (1.35/10^5)N^{1-0.715}] \text{ in./in.}$$

For N = 840,000 cycles, $\epsilon_{P_{acc}}$ = 0.678 percent, and accordingly, a 10-in.-thick pavement, it is expected to accumulate 0.0678 in. permanent deformation due to direct compression on the surface after 840,000 load repetitions. Such a result is compatible with those obtained by using the VESYS III structural subsystem program given in Table 5. The laboratory densification phase includes sources of error factors such as seating and conditioning that do not occur or match those in the field, however.

CONCLUSIONS

1. A combo viscoelastic-plastic model has been developed to characterize asphalt mixes. The model parameters are easily found by simple adjustments, modifications, or extensions of existing routine testing schemes. Among the findings when developing this model were the following: (a) a true yield surface could be found and used instead of that of the Mohr-Coloumb failure surface, and (b) as a consequence of (a) and specific to the tested mix, yielding occurs at about 75 psi in compression and 3 psi in tension at 70°F. On this basis it is recommended that stress levels of less than 3 psi be used to find the MR. Further, plastic deformation should be accounted for in characterization because actual stress levels on pavement surfaces exceed 75 psi.

2. A Drucker-Prager true yield surface was identified and its parameters found experimentally.

3. A rutting model based on the viscoelastic-plastic characterization has been developed. The example illustrated the application of this model to predict rutting of laboratory-prepared asphalt mixes. Among the conclusions is that permanent deformation due to densification is better included in rut depth calculations based on laboratory and field measurement simulations. Further, densification permanent deformation could be represented by an elastic relaxing spring.

4. Test methods that use the incremental static series do not differentiate between densification and the rest of nonrecoverable deformation. However, a procedure was established in this work to accomplish that. Differentiating quantitatively between densification, viscous, and plastic deformation is

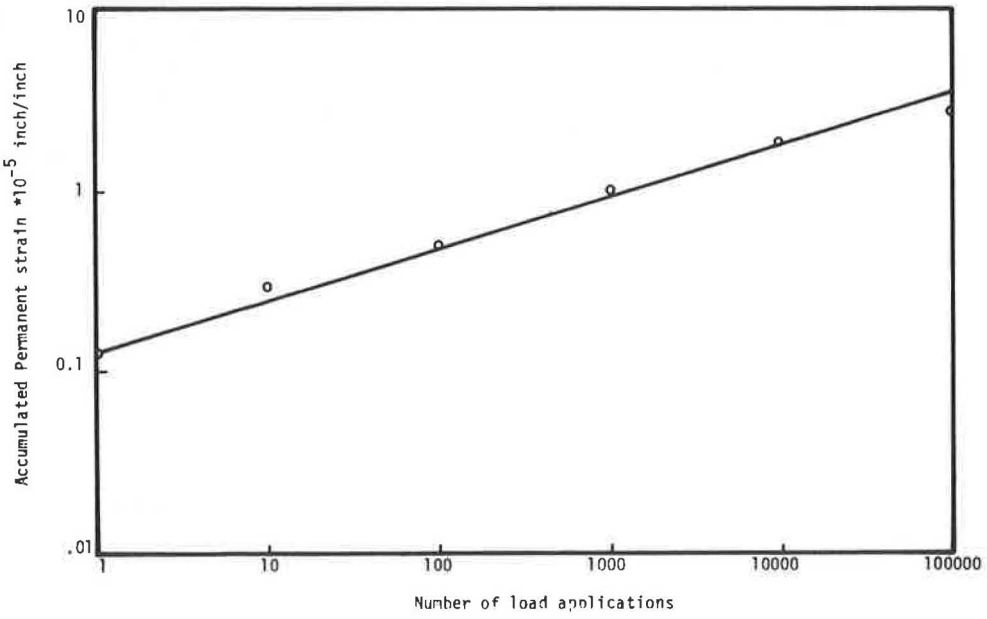

FIGURE 8 Rutting dynamic test series.

TABLE 5 Rut Depth in Inches, Using VESYS III

Traffic axle loads in 20 years	1.4 million			3.5 million	7 million		
Thickness(in) / No. of years	6	8	10	6	6	8	10
1/2	.036	.032	.029	.044	.051	.046	.042
2	.057	.056	.054	.071	.083	.08	.078
12	.086	.083	.082	.106	.124	.12	.118
20	.097	.094	.092	.119	.14	.135	.132

expected to rationalize decision alternatives for field problems, and hence, to implement asphaltic mix design.

REFERENCES

1. C.F. Rogers, H.D. Cashell, and P.E. Irick. Nationwide Survey of Pavement Terminal Serviceability. In Highway Research Record 42, HRB, National Research Council, Washington, D.C., 1963, pp. 26-40.
2. J. Morris et al. Permanent Deformation in Asphalt Pavements Can Be Predicted. Proc., Association of Asphalt Paving Technologists, Vol. 45, 1974.
3. K. Majidzadeh et al. Development and Field Verification of a Mechanistic Structural Design System in Ohio. Proc., 4th International Conference on Structural Design of Asphalt Pavements, Vol. 1, 1977.
4. K. Majidzadeh et al. Application of Fracture Mechanics for Improved Design of Bituminous Concrete. Report RF3736. Ohio State University, Columbus, 1976.
5. M. Karakouzian. A Simplified Method for Material Testing and Design of Pavement Systems. Ph.D. dissertation. Ohio State University, Columbus, 1978.
6. C.I. Monismith. Viscoelastic Behavior of Asphalt Concrete Pavements. Proc., International Conference on Structural Design of Asphalt Pavements, 1963.
7. H.S. Papazian. The Response of Linear Viscoelastic Materials in the Frequency Domain with Emphasis on Asphalt Cement. Proc., International Conference on Structural Design of Asphalt Pavements, 1965.
8. K.E. Secor and C.L. Monismith. Viscoelastic Response of Asphalt Paving Slabs Under Creep Loading. In Highway Research Record 67, HRB, National Research Council, Washington, D.C., 1965, pp. 84-97.
9. J.P. Elliot and F. Moavenzadeh. Moving Load on Viscoelastic Layered Systems: Phase II. Report 69-64. Department of Civil Engineering, Massachusetts Institute of Technology, Cambridge, 1969.
10. W.J. Kenis. Predictive Design Procedures, VESYS User's Manual: An Interim Design Method for Flexible Pavements Using the VESYS Structural Subsystem, Final Report. Report FHWA-RD-77-154. FHWA, U.S. Department of Transportation, 1978.
11. W.J. Kenis. Predictive Design Procedures: VESYS User's Manual. Report FHWA-RD-77-154. FHWA, U.S. Department of Transportation, Aug. 1980.
12. S.R. Bonder and Y. Partom. Constitutive Equations for Elastic-Viscoplastic Strain Hardening Materials. ASME, Journal of Applied Mechanics, Vol. 42, 1975, p. 385.
13. K.C. Valanis. A Theory of Viscoplasticity Without a Yield Surface--Part I: General Theory, Part II: Applications to Mechanical Behavior of Metals. Archiwum Mechaniki Stosowanej, Vol. 24, 1971.
14. D.R.J. Owen and E. Hinton. Finite Element in Plasticity: Theory and Practice. Pineridge Press Ltd., Swansea, England, 1980.
15. O.C. Zienkiewicz and I.C. Cormeau. Viscoplasticity, Plasticity, and Creep in Elastic Solids--A Unified Numerical Solution Approach. International Journal of Numerical Methods in Engineering, Vol. 8, 1974, pp. 821-824.
16. O.C. Zienkiewicz, V. Norris, and D.J. Naylor. Plasticity and Viscoplasticity in Soil Mechanics with Special Reference to Cyclic Loading Problems. Proc., International Conference on Finite Elements in Nonlinear Solid and Structural Mechanics, Aug. 1977, pp. 455-485.
17. R.D. Barksdale. Laboratory Evaluation of Rutting in Base Course Materials. Proc., 3rd International Conference on Structural Design of Asphalt Pavements, 1972.
18. M.R. El-Mitiny. Material Characterization for Studying Flexible Pavement Behavior in Fatigue and Permanent Deformation. Ph.D. dissertation. Ohio State University, Columbus, 1980.
19. K. Majidzadeh, F. Bayomy, and S. Khedr. Rutting Evaluation of Subgrade Soils in Ohio. In Transportation Research Record 671, TRB, National Research Council, Washington, D.C., 1978, pp. 75-84.
20. A. Phillips and G.J. Weng. An Analytical Study of Experimentally Verified Hardening Law. ASME, Journal of Applied Mechanics, Vol. 42, 1975.
21. W. Prager. An Introduction to Plasticity. Addison-Wesley, Reading, Mass., 1959.
22. A. Abdulshafi. Viscoelastic/Plastic Characterization, Rutting, and Fatigue of Flexible Pavements. Ph.D. dissertation. Ohio State University, Columbus, 1983.
23. M. Katona. Viscoelastic-Plastic Constitutive Model with a Finite Element Solution Methodology. Report TR-866. Civil Engineering Labora-

tory, Naval Construction Battalion Center, Port Hueneme, Calif., 1978.
24. O.C. Zienkiewicz. The Finite Element Method. McGraw-Hill, New York, 1972.
25. E.J. Yoder and M.W. Witczak. Principles of Pavement Design. Wiley, New York, 1975.
26. A.A. Abdulshafi. Rheological Behavior of Rejuvenated Aged Asphalt. M.S. thesis. Ohio State University, Columbus, 1981.

Publication of this paper sponsored by Committee on Characteristics of Bituminous Paving Mixtures to Meet Structural Requirements.

Evaluation of Tests for Characterizing the Stiffening Potential of Baghouse Dust in Asphalt Mixes

DAVID A. ANDERSON and STEVEN M. CHRISMER

ABSTRACT

Since the enactment of the 1970 Clean Air Act many asphalt plants have been forced to install baghouse dust collectors. Often this dust is added to asphalt concrete mixtures. The dust can stiffen mixes, thereby making them hard to compact, or it can act as an extender, thus causing bleeding and tenderness. There are no accepted specification tests for controlling the stiffening or the extending effects of baghouse dust. A variety of simple test procedures were evaluated for possible use for specification or quality control purposes to control stiffening. The customary physical properties of the dust, such as pH, shape, and gradation, do not predict stiffening. Two types of test procedures--fractional voids and consistency--were correlated with stiffening as measured by the increase in viscosity or softening point caused by the addition of dust to asphalt cement. Fractional voids in dust-asphalt mixtures were calculated from the bulk volume of dust compacted with impact and vibratory compaction and by consolidation in fluid media. Consistency tests included the kerosene, balling and crumbling, and bitumin number tests. The best correlation with stiffening ratio was obtained from the fractional voids as determined from the dry impact compaction. This test procedure is acceptable for process control and acceptance procedures; the other test procedures are not acceptable. The best means of determining the stiffening effect is to determine the stiffening directly with capillary viscometry. However, before either the fractional void test or the direct measure of stiffening is included as a specification criteria for stiffening, they must be determined through correlation with field performance.

Since the enactment of the 1970 Clean Air Act the operators of many asphalt concrete plants have found it necessary to install secondary dust-collection systems. These systems collect the fine dust that would otherwise be released from the exhaust gas to the atmosphere. Filter fabric dust collectors are the most commonly used secondary collection systems. They are usually referred to as baghouses, and the collected dust is called baghouse dust. Baghouse dust may be extremely fine (1 μm to 30 μm) or it may contain a wide range of particle sizes (1 μm to 300 μm), according to the configuration of the plant (1). Finer dust is produced when a cyclone or other type of primary collector is used in series with a baghouse. The cyclone collector effectively removes dust larger than 30 μm, thereby stripping the coarser fraction from the dust collected in the baghouse. Therefore, baghouse dust from different plants can vary widely in gradation.

Baghouse dust often presents a disposal problem, and in many plants it is common to add baghouse dust to the asphalt concrete. Some paving technologists are reluctant to do this because they believe that the dust can adversely affect the quality of the asphalt concrete. For example, baghouse dust can act as an asphalt extender, thus reducing the design asphalt content. If the addition of baghouse dust is not accounted for in the mix design, bleeding and tenderness can result (2,3).

Other problems that have been attributed to the improper use of baghouse dust include poor compaction and raveling resulting from excessive stiffening of the asphalt concrete (4-6). Concern about the stiffening effect of baghouse dust has led many highway agencies to restrict its use (7). Other agencies have adopted or are considering test procedures that are intended to control the use of baghouse dust (8). These test procedures are designed primarily to control mixture stiffening caused by baghouse dust.

The purpose of this paper is to report on a laboratory evaluation of several test procedures that measure the stiffening of asphalt cement that results from the addition of a fine mineral dust. The

stiffening effect produced by baghouse dust is not reflected in the usual Marshall mixture design parameters. A specification limit on the dust/asphalt ratio or dust content in a mixture is insufficient because of the widely varying stiffening effects caused by different dusts. Therefore, if control of stiffening is desired, an additional specification requirement or test procedure is warranted. The objective of this study was to evaluate test procedures that could be used at the plant as quality control and quality assurance or for source acceptance purposes.

In the past variability in the fineness or gradation of baghouse dust has also been cited as a problem. However, recent research has indicated that the gradation of baghouse dust is extremely uniform on a day-to-day and within-day basis (1). Improper plant operations or poorly designed dust handling systems may cause a problem of uniformity in the feed rate of baghouse dust to the pugmill. This problem is not addressed in this paper.

METHODOLOGY

First, a variety of different tests were used to characterize the physical properties of the dust. Second, the stiffening produced by the addition of baghouse dust to two different asphalt cements was determined directly by softening point and viscosity measurements on the dust-asphalt mixtures. Third, a number of different tests proposed as indirect measures of stiffening were conducted, and the results were compared with the actual stiffening measures in the viscosity tests.

Materials

As part of a larger study (NCHRP Project 10-19, Adding Dust Collector Fines to Asphalt Paving Mixtures), baghouse dust samples were collected from 26 asphalt concrete plants (1). The samples, collected in 12 states, represent the range of generic aggregate types in common use in the United States. Samples from 15 plants were selected for detailed study. A description of the samples is given in Table 1. Tests conducted on these samples included gradation, fineness modulus, pH, hygroscopic moisture, and Atterberg limits (1). The gradation data, including fineness modulus, are given in Table 2.

The properties of the two different asphalt cements used in the study are given in Table 3. The test results of the two asphalts were nearly identical, and therefore only the results for asphalt WB are presented in this paper.

Direct Measurement of Stiffening

Each of the dusts was added to the asphalt cement in two dust/asphalt ratios (0.20 and 0.40 by volume).

TABLE 1 Description of Dusts Used in Study

Plant No.	Aggregate Type	pH	Hygroscopic Moisture	Liquid Limit	Plastic Limit	Plasticity Index[a]
1	Dolomite	11.6	4.1	-	-	NP
2	Dolomite	11.2	0.6	-	-	NP
5	Traprock	9.8	1.9	39	37	2
6	Siliceous gravel	5.6	0.4	-	-	NP
7	Traprock	11.2	1.9	34	31	3
9	Limestone	12.1	0.6	-	-	NP
10	Limestone	10.9	0.4	-	-	NP
13	Gravel	12.1	1.5	34	32	2
14	Gravel	10.5	1.2	30	27	3
15	Limestone	12.2	1.2	32	29	3
20	Granite	8.3	0.7	35	35	NP
24	Granite	9.2	0.9	35	34	1
26	Granite	7.2	1.9	39	37	2
30	Traprock	6.4	0.8	32	31	1
33	Siliceous gravel	7.7	1.5	33	29	4

[a]NP = nonplastic.

TABLE 2 Grain-Size Distribution for Dusts Used in Study

Plant No.	Grain-Size Distribution (% passing)								Fineness Modulus[a]	Cu[b]
	No. 30 (600 μm)	No. 50 (300 μm)	No. 200 (75 μm)	50 μm	20 μm	10 μm	5 μm	1 μm		
1	99	96	60	54	18	7	2	1	2.43	27
2	99	89	64	61	43	27	14	3	2.21	4
5	100	100	100	99	95	73	41	7	1.21	2
6	99	94	43	40	23	12	4	0	2.55	10
7	100	100	100	99	91	63	35	7	1.40	3
9	100	94	47	44	27	17	9	3	2.42	5
10	95	88	35	34	22	15	9	3	2.65	4
13	100	100	96	94	80	61	40	12	1.33	2
14	100	99	83	81	72	61	47	12	1.47	2
15	100	100	98	97	92	73	44	8	1.14	2
20	100	100	93	92	75	52	27	4	1.59	3
24	100	100	99	97	83	52	29	7	1.44	3
26	100	100	100	100	95	78	49	12	1.10	2
30	100	99	94	92	71	45	23	5	1.59	4
33	100	99	73	69	47	35	25	7	1.90	3

[a]Based on percent retaining on 600, 300, 50, 10, 1 μm.
[b]Based on ratio of percent passing 50 μm divided by percent passing 5 μm.

TABLE 3 Physical Properties of Asphalt Cements

Property	Asphalt A	Asphalt WB
Viscosity (poises, 140°F)	2042	2208
Viscosity (cSt, 275°F)	404	438
Penetration, 77°F	73	100
Aging Index, 140 viscosity	2.26	3.00
Rostler-Sternburg composition (%)		
A	22.5	28.1
N	21.0	26.9
A_1	14.8	18.8
A_2	33.9	21.2
P	7.7	5.0
$(N + A_1)/(A_2 + P)$	0.86	1.74

The resulting dust-asphalt mixture was then tested for softening point (ASTM D 36) and viscosity (ASTM D 2171) at 60°C. The increase in softening point (Δ°F) greater than that of the neat asphalt cement was considered as one measure of stiffening. In addition, the stiffening ratio (SR) was calculated by dividing the viscosity of the dust-asphalt matrix by the viscosity of the neat asphalt cement. The results of these tests are given in Table 4. There

TABLE 4 Stiffening Ratios for Dust-Asphalt Mixtures

Plant No.	Dust-Asphalt Ratio: Asphalt A 0.2	Asphalt A 0.4	Asphalt WB 0.2	Asphalt WB 0.4	Aggregate Type	D_{80} (μm)	D_{50} (μm)	D_{20} (μm)
1	1.6	3.5	1.7	3.4	Dolomite	100	35	17
2	1.7	3.3	1.8	3.6	Dolomite	200	30	7
5	2.6	21.4	2.8	19.3	Traprock	10	7	3
6	1.8	3.8	2.4	4.2	Siliceous gravel	200	80	15
7	2.6	17.2	2.9	18.2	Traprock	15	7	3
9	1.7	2.8	1.6	3.1	Limestone	200	80	16
10	1.8	3.8	1.8	3.4	Limestone	260	100	12
13	2.4	12.0	2.6	11.7	Gravel	19	6	2
14	2.6	12.0	2.8	12.1	Gravel	50	6	2
15	2.3	8.7	2.4	8.4	Limestone	12	6	2
20	2.4	10.6	2.5	10.9	Granite	18	10	4
24	2.6	16.3	2.7	16.8	Granite	20	10	4
26	3.2	100.4	3.6	71.8	Granite	12	5	2
30	2.0	4.6	2.0	4.1	Traprock	27	10	5
33	2.1	5.2	2.2	5.5	Siliceous gravel	42	10	2

was a high degree of correlation between stiffening ratio and the increase in softening point temperature (Figure 1). This result agrees with the observations of other researchers (8); however, the relationship between the logarithm of stiffening and the softening point is nonlinear. Because of the strong correlation between stiffening ratio and softening point, only the stiffening ratio was considered further. Stiffening ratio was chosen because it is based on rational test measurements (viscosity versus softening point) and because the test procedure (ASTM D 2171) is readily performed in most asphalt testing laboratories. No difficulties were encountered in measuring the viscosity of the dust-asphalt mixtures.

Indirect Measurement of Stiffening

The test procedures used as indirect measures of stiffening can be divided into two categories: (a) measurements of the fractional voids in a compacted or consolidated bed of dust, and (b) measurements of the amount of liquid (asphalt cement, kerosene, or water) required to bring the dust-liquid mixture to a specified consistency.

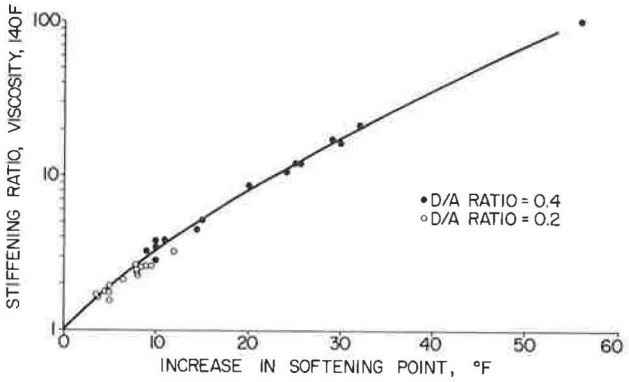

FIGURE 1 Change in softening point (°F) versus stiffening ratio, viscosity, 140°F.

Fractional Voids

Rigden (9) has proposed that the volume fraction of voids in a dry compacted bed of dust can be used as a measure or predictor of the stiffening potential of a mineral dust. In the fractional voids concept, the dust-asphalt mixture is composed of three volume fractions, as shown in Figure 2: the solid volume of the dust particles (V_{DS}) and the free (V_{AFR}) and fixed (V_{AFX}) volume of the asphalt cement. The fixed asphalt volume is defined as the volume of asphalt required to fill the volume between the solid dust particles, assuming that the dust is compacted or consolidated to some reference density. The free asphalt provides fluidity to the mixture and can be related to the viscosity of the mixture.

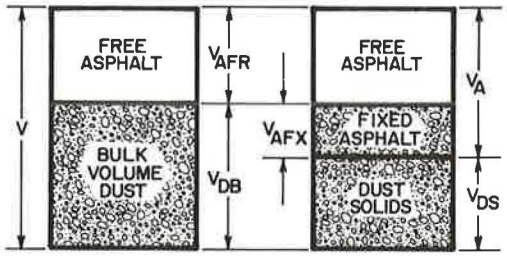

$$\%V_{AFR} = \frac{V_{AFR}}{V} \times 100\%$$

FIGURE 2 Schematic of fractional voids in dust-asphalt system.

At a given dust/asphalt ratio, the dust with the smaller bulk volume (V_{DB}) will yield more free asphalt volume. This will allow more asphalt to lubricate the mixture and will result in a lower viscosity.

Three methods were used to produce a compacted bed of dust so that the bulk volume of the dust could be measured. First, vibratory compaction of the dry dust was obtained by placing approximately 50 to 70 g of dust in a 100-mL graduated cylinder, which was fastened to a 16-gage steel base plate (Figure 3) (10). The base plate was vibrated until the level of the dust in the graduated cylinder reached equilibrium. The bulk volume of the dust was read from the graduations on the cylinder. Vibratory compaction, as described, produced highly repeatable results, much more so than manual tapping of the cylinder, as proposed by other researchers (8).

The bulk volume of the dust was also obtained by allowing 5 g of dust to settle in both polar (methyl-

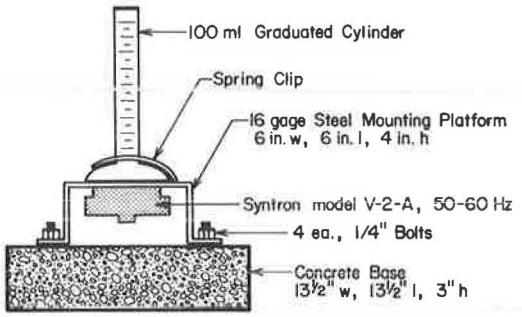

FIGURE 3 Schematic of dry vibration compaction procedure.

ethylketone) and nonpolar (toluene) liquids. In this paper bulk volume obtained in this manner is referred to as settled volume. A special 10-mL graduated test tube (Fisher No. 14-950A) was used and the settled volume was read directly from the graduations on the cylinder (10). It is important that the samples be de-aired before the settling process is initiated.

The third procedure was the dry impact compaction procedure described by Rigden (9). In this test a small drop hammer is used to compact the dust into a mold. The bulk volume was calculated on the basis of the area of the mold and the height of the compacted bed of dust. A 9.5-mm-diameter steel mold and a 100-g weight dropped 25 times through a 30-mm height of fall was used to compact the test samples. The most repeatable results are obtained when the height of the compacted bed approximates its diameter. Rigden also tested the compacted sample in a simple air permeability device to obtain the surface area and the average particle diameter of the dust (9).

Consistency Tests

Bitumen Number

This test, reported by van der Baan and Van Dijk (11) for mineral filler, does not involve bitumen; rather, water is added to the dust until it attains a specified consistency, as measured by a penetrometer. A standard penetrometer device (ASTM D 5) can be used for this test, although a modified penetrometer needle is required. The modified needle has a flat base that is 7.98 mm in diameter (10). The dust-water mixture is placed in a cylinder 30 mm in diameter by 30 mm deep. The volume of water required to bring the dust to a consistency corresponding to a penetration of 5 to 7 mm is reported as the bitumen number.

Kerosene Adsorption

In this test (12) 20 g of dust is placed, without any compaction, into a watch glass. Kerosene is then slowly dropped from a burette onto the surface of the dust. Capillary action causes the kerosene to saturate the dust. When the outer edge of the dust in the watch glass is saturated with kerosene, the flow is stopped and the volume of kerosene is recorded. The volume of adsorbed kerosene is a measure of the voids in the dust when the dust is in a loose condition.

Asphalt Mixing Test

In this test dust is added incrementally to 15 g of asphalt at 163°C. As the dust is added and mixed into the asphalt, two distinct changes in the consistency of the dust-asphalt mixture can be observed. These changes, in order of occurrence, are the balling point and crumbling point (8). The amount of dust that has been added (in grams) when balling or crumbling occurs is recorded.

DISCUSSION OF RESULTS

Physical Data

A considerable amount of physical test data, such as gradation, fineness modulus, pH, minerological content, and shape factors as determined from SEM photomicrographs, was obtained for each dust. None of these data explained the different levels of stiffening that were found for the different dusts. The test data (Table 2 and 4) indicate that the amount of stiffening is not directly related to the fineness or fineness modulus of the dust. Although in most cases a greater amount of stiffening was produced by the single-sized finer dusts, it is important to note that a dust can be extremely fine and still not produce a large stiffening effect. For example, the grain-size distribution of the dust from plant 15 was virtually the same as that for plant 26; however, the stiffness ratios were 8.65 and 100.4, respectively, for a dust/asphalt ratio of 0.4. Therefore, fineness alone, or measures of fineness, are not appropriate specification tests for baghouse dust.

Fractional Voids

The percentage of free asphalt in the dust-asphalt mixture ($\%V_{AFR}$), defined schematically in Figure 2, was calculated as follows:

$$\%V_{AFR} = \{(W_A G_{DS} \gamma_{DB} + W_{DS} G_A \gamma_{DB} - W_{DS} G_A G_{DS}) \div [\gamma_{DB}(W_A G_{DS} + W_{DS} G_A)]\} 100 \quad (1)$$

where

G_A = specific gravity of asphalt,
G_{DS} = specific gravity of dust solids,
W_A = weight of asphalt in dust-asphalt mixture (g),
W_{DS} = weight of dust solids in dust-asphalt mixture (g), and
γ_{DB} = bulk density of the compacted dust (g/cm³).

The bulk density of the dust (γ_{DB}) was obtained from the dry impact compaction, dry vibration, and settled volume tests. The bulk density is simply the weight of the dry dust divided by its bulk volume (V_{DB}). These values were used to calculate $\%V_{AFR}$ according to Equation 1. Regression equations for stiffening ratio versus $\%V_{AFR}$ were then obtained for each bulk volume test procedure. R^2 values for $\%V_{AFR}$ versus stiffening ratio for dry impact, nonpolar solution, dry vibratory, and polar solution were 0.94, 0.89, 0.88, and 0.80, respectively. Plots of stiffening ratio versus $\%V_{AFR}$ for dry impact and dry vibratory densification are shown in Figures 4 and 5. The relationship shown in Figure 4 is considerably better than that shown in a previous paper (13), where several methods of impact compaction were used to generate the data.

Another advantage of the original Rigden (9) procedure is that the compacted sample can also be used to monitor the fineness of the dust. By using air permeability theory (9), it is possible to calculate

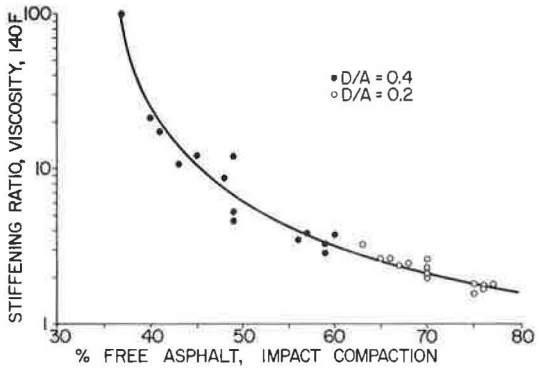

FIGURE 4 Percent free asphalt volume—drop hammer compaction versus stiffening ratio, viscosity, 140°F.

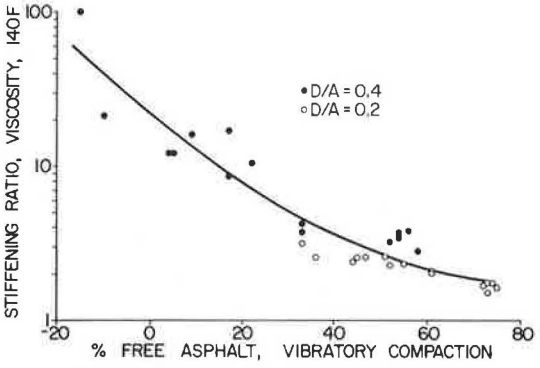

FIGURE 5 Percent free asphalt volume—vibratory compaction versus stiffening ratio, viscosity, 140°F.

the average hydraulic radius of the compacted dust and, in turn, calculate the average particle size of the dust. The results of these calculations are shown in Figure 6, where D_{10} [size corresponding to 10 percent passing (μm)] is plotted versus the average size as calculated from the hydraulic radius.

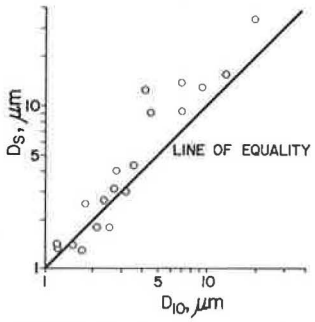

FIGURE 6 Average percent passing 10 μm versus average grain size from air permeability measurements.

Kandhal (8) has proposed that stiffening ratios greater than 10 can lead to unacceptable field performance. In Figure 4, which is based on dry impact compaction, it can be seen that the percentage of free asphalt must be greater than 45 percent if the stiffening ratio is to be less than 10. The curve plotted in Figure 4 was used to construct the isobars of $\%V_{AFR}$ that are shown in Figure 7, plotted

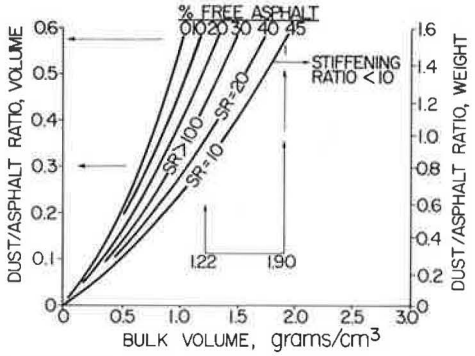

FIGURE 7 Proposed design chart for selecting dust/asphalt ratio and impact compaction.

on a graph of bulk volume versus dust/asphalt ratio. As long as the bulk volume and dust/asphalt ratio falls to the right of the V_{AFR} = 45 percent curve, the stiffening ratio will be less than 10 and thus result in an acceptable mixture. Dust/asphalt ratios that fall to the left of this curve would be acceptable only if the measured stiffening ratio is less than 10. In the example shown in Figure 7, a dust with a bulk volume of 1.90 would be acceptable as long as the dust/asphalt ratio is less than 0.60, but a dust with a bulk volume of 1.22 would require that the dust/asphalt ratio be less than 0.30.

Consistency Tests

The results of the consistency tests were correlated with the stiffening ratio to determine whether these tests, which can be performed with relative ease, can be used in lieu of a viscosity or softening point test.

A plot of stiffness ratio versus bitumen number is shown in Figure 8. Although a general relationship is indicated, the correlation coefficient is relatively low (R^2 = 0.83). Stiffening ratio increases asymptotically at the larger stiffening ratios, and therefore this test method cannot be recommended for specification purposes.

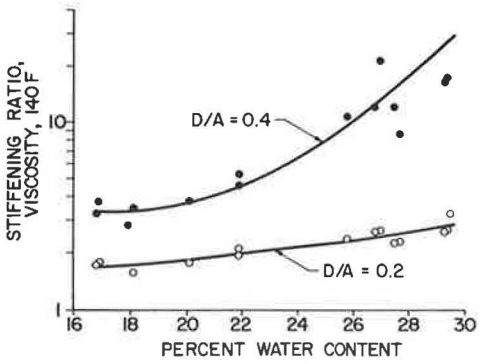

FIGURE 8 Bitumen number versus stiffening ratio, viscosity, 140°F.

The results of the asphalt mixing test are presented in Figure 9, where the balling and crumbling points are plotted versus stiffening ratio. The balling and crumbling points are highly related, as shown in Figure 10, and there is little to be gained by determining both points. Because the balling

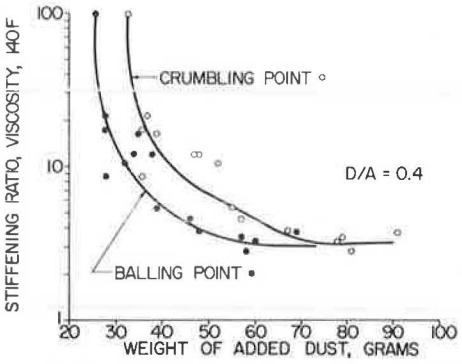

FIGURE 9 Stiffening ratio versus crumbling and balling points for dust-asphalt mixtures.

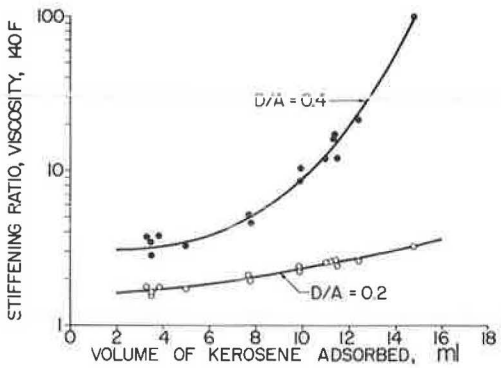

FIGURE 11 Volume of kerosene adsorbed versus stiffening ratio, viscosity, 140°F.

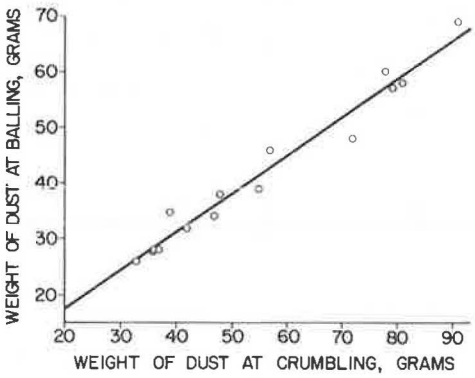

FIGURE 10 Crumbling point versus balling point.

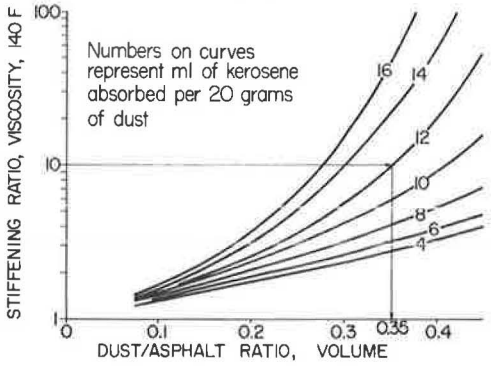

FIGURE 12 Proposed design chart for selecting dust/asphalt ratio based on kerosene adsorption.

point is easier to reproduce, this point is considered sufficient.

However, the test cannot be recommended for two reasons. First, the results cannot be conveniently related to stiffening ratio. Therefore, the test procedure is useful only in accepting or rejecting a dust and not in determining the maximum allowable dust/asphalt ratio. Second, neither the balling point nor the crumbling point is a good predictor of stiffening because the stiffening ratio increases asymptotically for the dusts that produce stiffer mixtures.

The stiffness ratio versus the volume of adsorbed kerosene is shown in Figure 11 for dust/asphalt ratios of 0.20 and 0.40. Excellent correlation between stiffness ratio and adsorbed kerosene volume was observed (R^2 = 0.98 for both dust/asphalt ratios). Because the relationships shown in Figure 11 are unique for each dust/asphalt ratio, the regression equations for each dust/asphalt ratio were used to construct the curves shown in Figure 12.

Such curves can be used for design purposes if the dust/asphalt ratio for a particular asphalt concrete mixture is known. The example in Figure 12 shows that, given a design dust/asphalt ratio of 0.35 and an adsorbed kerosene volume of 10 mL, the expected stiffening ratio is 12.0. The kerosene adsorption test is simple to perform and could also be used at a plant as a process control or quality assurance test to monitor changes in dust properties. Unfortunately, the repeatability of this test procedure between different operators has been found to be poor because of difficulties in determining the end point (saturation point).

SUMMARY AND CONCLUSIONS

The use of capillary viscosity (ASTM D 2171, 60°C), is the most direct method of measuring the stiffening effect of the fine mineral dust added to asphalt cement. Physical properties of the dust, such as particle shape, gradation, and pH, do not explain the difference in stiffening encountered in different dusts. Therefore, specification criteria based on gradation or physical properties, such as those described earlier, are not warranted as controls of stiffening.

Stiffening can be predicted from the fractional voids concept; however, the accuracy of the prediction depends on the method used to determine the bulk volume of the dust. The dry impact method of densifying the dust produced the best correlation and the highest level of densification. The test procedures that produced the closest packing of the dust appear to give the best correlation with stiffening. As the compactive energy increases, the tendency for fines to segregate according to size, or to form flocculated structures, is diminished. This segregation effect was noticeable in the liquid sedimentation tests and, to a lesser extent, in the vibrated density tests.

The asphalt mixing test (balling and crumbling points) and the bitumen number test procedure do not warrant further consideration as test procedures to control stiffening. Neither test is easily related to a dust/asphalt ratio, which makes it difficult to control that ratio in a mixture.

The fractional voids ($\%V_{AFR}$) and the kerosene adsorption test gave excellent correlations with

stiffening. Both tests could be used as source acceptance tests, for process control in the plant, and as a means to specify an upper limit on the dust/asphalt ratio in a mixture.

Further development of the kerosene adsorption test is required to refine the specific details of the test procedure before it can be accepted as a specification test. Accuracy and precision data must be developed for both the kerosene and the dry impact fractional voids procedure. Of even greater importance is the need to relate the stiffness of the dust-asphalt mixture to the rheology of the asphalt concrete mixture. This is required in order to set upper limits for allowable stiffening. Although an upper limit of 10 has been suggested for the stiffening ratio (8), this may be conservative (13); further research is needed to verify a tolerable limit for stiffening ratio.

The following conclusions are based on the research described in this paper.

1. Use of the volume percent free asphalt ($\%V_{AFR}$) as a predictor of stiffening is reliable, provided that a standard, repeatable method is used to obtain the measurement of bulk volume.
2. If a predicted stiffening ratio based on Rigden's fractional void concept is desired, the dry impact compaction procedure is the preferred method for obtaining bulk volume. The percent free asphalt volume from the dry impact compaction test provided the best correlation with stiffening ratio.
3. Data from the kerosene adsorption test provided the highest correlation with stiffening ratio. The test is not repeatable between operators and therefore there must be further development of this test before it can be recommended.
4. The bitumen number and the balling and crumbling point tests are not acceptable as specification tests to control stiffening.
5. Regardless of which test method is used to determine the stiffening characteristics of a dust, a chart such as the one shown in Figure 7 can be used for design purposes to select an allowable dust/asphalt ratio.
6. Dust gradation plays a limited role in determining asphalt stiffening and it should not be used by itself as a performance-related specification for dust.
7. The maximum dust/asphalt ratio for an asphalt concrete mixture varies from one dust to another. The maximum allowable ratio should be based on the stiffening of each individual dust and not set as an arbitrary value for all mixtures.

REFERENCES

1. D.A. Anderson and J.P. Tarris. Adding Dust Collector Fines to Asphalt Paving Mixtures. NCHRP Report 252. TRB, National Research Council, Washington, D.C., 1982, 90 pp.
2. T. Scrimsher. Baghouse Dust and Its Effect on Asphalt Mixtures. Res. Report CA-DOT-TL-3140-1-76-50. California Department of Transportation, Sacramento, 1976.
3. D.A. Anderson, J.P. Tarris, and J.D. Brock. Dust Collector Fines and Their Influence on Mixture Design. Proc., Association of Asphalt Paving Technologists, Vol. 51, 1982.
4. G.W. Maupin. Effect of Baghouse Fines on Compaction of Bituminous Concrete. Report VHTRC 81-R49. Virginia Highway and Transportation Research Council, Charlottesville, 1981.
5. J.H. Eick and J.F. Shook. The Effect of Baghouse Fines on Asphalt Mixtures. Res. Report 78-3. Asphalt Institute, College Park, Md., 1978.
6. R.H. Geitz. Mineral Fines Effect on Asphalt Viscosity. Report 164. Washington State Department of Transportation, Olympia, 1980.
7. D.A. Anderson and J.P. Tarris. Effect of Baghouse Fines on Mixture Design Properties. Quality Improvement Program 102. National Asphalt Pavement Association, Riverdale, Md., 1982.
8. P.S. Kandhal. Evaluation of Baghouse Fines in Bituminous Paving Mixtures. Proc., Association of Asphalt Paving Technologists, Vol. 50, 1981.
9. D.J. Rigden. The Rheology of Non-Aqueous Suspensions. Tech. Paper 28. Road Research Laboratory, Hammondsworth, England, 1954.
10. S.M. Chrismer. Evaluation of Tests for Characterization of Baghouse Dust Stiffening Potential in Asphalt. M.S. thesis. Pennsylvania State University, University Park, May 1983.
11. J. van der Baan and G. Van Dijk. Kennis van bouwstoffen v. Mortels en bitumineuze bouwstoffen (Mortars and Bituminous Building Materials). Denverter, 1952.
12. J.S. Miller and R.N. Traxler. Some of the Fundamental Physical Characteristics of Mineral Filler Intended for Asphalt Paving Mixtures. Proc., Association of Asphalt Paving Technologists, Vol. 46, 1977.
13. D.A. Anderson and J.P. Tarris. Characterization and Specification of Baghouse Fines. Proc., Association of Asphalt Paving Technologists, Vol. 52, 1983.

Publication of this paper sponsored by Committee on Characteristics of Bituminous Paving Mixtures to Meet Structural Requirements.

Thermal Properties of Some Asphaltic Concrete Mixes

WILLIAM H. HIGHTER and DOUGLAS J. WALL

ABSTRACT

To obtain an increased understanding of the energy transfer in asphaltic concrete recycling processes that use surface heat, laboratory tests were carried out on four asphaltic concrete mixes (three having limestone aggregate and one with expanded shale lightweight aggregate) to determine thermal properties. It was found that the thermal conductivity of the three limestone mixes depended on asphalt content and aggregate gradation, but that the conductivity of the lightweight aggregate mixes varied little as the asphalt content was increased from 3.5 to 6.5 percent. The specific heat and diffusivity of the mixes varied with mineralogy and gradation but changed little with asphalt content.

In the 1930s construction equipment was developed that would plane off the high surfaces of uneven, deteriorating asphaltic concrete pavements. It was found that, by first applying heat to the pavement surface to reduce the shearing resistance of the asphaltic concrete, the planing operation proceeded faster and easier and could be accomplished at less expense. These heater planers are still in use today and provide a cost-effective option for some types of pavement maintenance.

Heater scarifiers are also used in maintenance operations of asphaltic concrete pavements. These machines apply heat to the pavement surface to reduce the shear strength and then scarify or remove the degraded uppermost part of the pavement. This process allows new materials (or recycled materials), including aggregates, modifiers, and asphalt cement, to be thoroughly mixed into the scarified asphaltic concrete in situ or enables the spent pavement to be easily removed and hauled to a central location where additional materials are added. Recycling existing pavement materials can be an attractive alternative in pavement maintenance strategies because of the increased cost of asphaltic concrete in the past 10 years, which has been commensurate with the skyrocketing costs of petroleum products.

Although pavement heating techniques and equipment development have evolved over several decades, little research has been undertaken to provide an understanding of the heat transfer process in asphaltic concrete with a view toward optimizing the field procedure with respect to equipment costs and fuel consumed. Much of the research done in this field has been proprietary in nature and carried out by contractors on a trial-and-error basis. This work has been results-oriented, with success being the development of a method of pavement maintenance that is cost effective in competition with alternative nonheater methods.

Civilian and military airfield and highway pavement budgets have been and will continue to be heavily oriented toward maintenance of existing facilities rather than dedicated to new construction. Pavement recycling can be expected to play an increasingly important role in maintenance in the future, and, as the cost of the fuel used to heat pavements increases, the capability of predicting the temporal spatial-temperature field setup by a known heat source in an in-service pavement will be imperative in order for recycling methods using field heaters to remain competitive with recycling methods not using heat.

Accordingly, the subject of this paper is concerned with the first step leading to this goal: the measurement of the thermal properties of asphaltic concrete mixes that have different asphalt contents, aggregate densities, and aggregate gradations.

BACKGROUND INFORMATION

That some properties of asphaltic concrete vary with temperature has for many years fostered interest in the distribution of temperature within an in situ pavement. Interest in predicting frost penetration beneath pavements, minimum and maximum temperatures caused by ambient conditions, and the cooling rates of hot-laid asphaltic concrete has motivated research in heat transport through pavements.

Carlson and Kersten (1) applied heat transfer theory to the pavement and soil subgrade to develop a model used to predict frost penetration below asphaltic pavement. Input parameters included the thermal conductivity of the pavement (1.44 w/m°C), the latent heat of fusion of water, and the surface freezing index of the pavement. Aldrich (2) improved on Carlson and Kersten's approach of calculating frost penetration by including the effect of volumetric heat. Aldrich used a thermal conductivity value of 1.45 w/m°C in his analysis.

Barber (3) predicted in situ pavement temperatures by using the diffusion equation. Because the strength and stability of an asphaltic pavement are related to its temperature, research has been conducted to determine the minimum and maximum temperatures of pavement in natural field conditions. Southgate and Deen (4) analyzed the pavement temperatures recorded at various depths in a 0.3-m-thick asphaltic pavement. They found that a fourth-order polynomial fit the temperature as a function of depth data. No attempts were made to analyze the data by using heat transfer theory.

Rumney and Jimenez (5) recorded pavement temperatures with depth for a year in Arizona. Based on the observed data, they presented empirically derived curves whereby pavement temperature at depth could be estimated by knowing the maximum air temperature and average daily radiation rates.

Straub et al. (6) recorded pavement temperatures with depth for a 1-year period in 0.15- and 0.3-m-thick asphaltic concrete pavements and also measured corresponding air temperature and solar radiation. They found that the pavements had a substantial temperature gradient and no one temperature was representative of that of the pavement. They noted that changes in solar radiation have a larger effect on pavement temperatures than that caused by changes in air temperature. Straub et al. used a forward difference, one-dimensional transient heat flow program to predict pavement temperature with depth.

Dempsey and Thompson (7) used a model similar to that of Straub et al. to predict temperatures with depth in conjunction with highway frost studies. They reported that the accuracy of the temperatures predicted by the one-dimensional heat transfer model depended more on the quality of the input data than on the numerical method of calculation. They also pointed out the importance of accurately defining the boundary condition at the pavement surface because it is this input that is the major factor contributing to the heat transfer process.

Christison and Henderson (8) also used a finite difference approximation to predict temperatures in asphaltic concrete. They assumed a value of 1.45 w/m°C for the thermal conductivity of asphaltic concrete and stated that "the thermal conductivity (k) and heat capacity (c) of asphaltic concrete paving mixtures vary within narrow limits and for practical purposes can be considered independent." However, they did not indicate the basis for this statement or their source for the assumed thermal properties.

The references cited indicate that a numerical solution of the one-dimensional heat flow problem using a finite difference technique has excellent predictive capabilities for asphaltic concrete pavements under natural ambient conditions. However, the heat regime to which the pavement is subjected by a heater planer or heater scarifier is much different. The range of temperatures is greater, and the time scale is on the order of seconds, versus hours. Finally, the temperature level of the heat source and pavement surface is much different, which strongly affects the nature of the radiant heat exchange on the surface.

During paving operations a hot-laid asphaltic pavement must be sufficiently compacted before it cools below a specified temperature, which is about 90°C for most pavements. This temperature is required to achieve a specified density with a minimum amount of compactive effort. Compaction attempted when the pavement is too cool results in either a longer time period needed to reach a specified density or the inability to reach the specified density at all. Corlew and Dickson (9) used a one-dimensional transient flow of thermal energy equation to predict the temporal spatial-temperature field within a cooling layer of freshly placed hot-mix asphaltic concrete. By using a finite difference technique, they were able to predict temperatures in a 6-cm layer of asphaltic concrete within 7°C of measured temperatures in the range at which asphaltic concrete is compacted (greater than 90°C).

Frenzel et al. (10) developed a computer analysis to study the effect of preheating an existing asphaltic layer on the cooling of an overlay put down over the preheated base. They found, analytically, that preheating the base increased the cooling-down period in thin overlays sufficiently to allow a compaction window long enough to make paving in early spring and late fall feasible. Later, Corlew and Dickson (11) combined the base preheat model developed by Frenzel et al. and their previously described cooling model (9) to predict the temporal spatial-temperature field of an asphaltic concrete layer over a preheated base in a bench scale laboratory test. A sample with a 10-cm-diameter base was heated by a direct-fired propane heater. Agreement between predicted and measured temperatures was considered to be satisfactory. Assumed thermal properties of asphaltic concrete were used in the analysis. Another study of asphaltic pavement cooling rates was conducted by Wolfe and Colony (12). They developed a computer simulation method to predict cooling rates by using the same weather data and material property variables as Corlew and Dickson. The thermal properties of asphaltic pavement were taken from published values.

In-place surface recycling of asphaltic pavements involves reworking the surface to a depth of approximately 1 in. using a heater scarifier. This operation may involve the addition of new or recycled materials. The reworked material is then compacted, and sometimes a seal coat is applied. Typically, heater planers and heater scarifiers developed by contractors use propane as a fuel to fire a grid of torches. The grid is on the order of 3 m wide and 5 m or more long and is attached to a self-propelled machine. The torch grid is covered on the top and sides to diminish heat loss. Typically, the machine advances at the rate of about 4.5 m/min, giving a heat exposure time on the order of 1 min. To prevent combustion of the pavement, the temperature at the pavement surface should be limited to about 230°C. Contractors claim that, under these conditions, temperatures at a depth of about 2.5 cm in the asphaltic concrete are sufficiently high to allow easy scarification or removal of pavement to this depth. To increase the depth of influence of the heat source, a technique termed soaking is sometimes used. This method involves heating the surface as previously described and then insulating the pavement surface. This, in principle, allows the heat to soak in, thus producing greater heat penetration without exceeding the 230°C surface temperature requirement.

One of the few published studies undertaken on the subject of heat transfer in asphaltic concrete recycling appears to refute many of the contractor claims previously mentioned. Carmichael et al. (13) modeled an asphaltic concrete pavement as a semi-infinite solid and used a forward difference numerical method to solve the governing differential equation. They assumed that the thermal conductivity, density, and specific heat of asphaltic concrete were independent of temperature and did not vary from point to point. The authors, using realistic source and initial pavement temperatures along with realistic pavement parameters, found that even with an induced surface temperature of 540°C and a 30-sec exposure time, there was no increase in temperature of the pavement at a depth of 1.6 cm [see Figure 1 (13)].

It was also shown that for surface temperatures between 200° and 300°C, the temperature of the pavement at a depth of 1 cm hardly changed from its initial condition. This is illustrated in Figure 2 (13). Although it can be argued that the study by Carmichael et al. used restrictive assumptions, particularly with respect to the parameters used, and that the model had not been verified, it does indi-

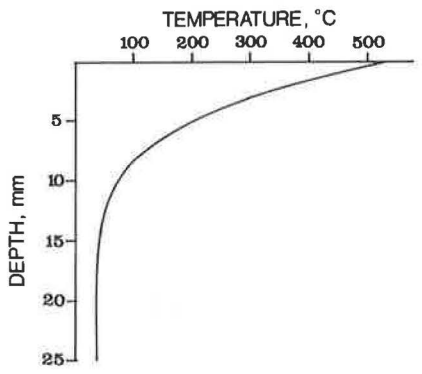

FIGURE 1 Pavement temperature versus depth for 1000°C source and 30-sec exposure time (13).

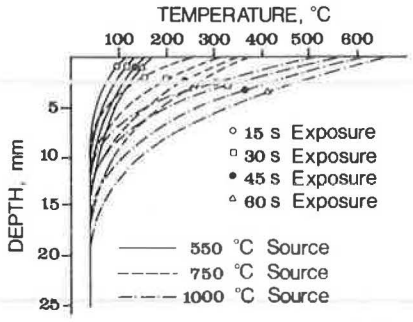

FIGURE 2 Pavement temperature versus depth as a function of source temperature and exposure time *(13).*

cate that the current development of pavement heating techniques and the current use of heater planer and heater scarifier equipment ignores some of the basic constraints of asphaltic concrete recycling: namely, that to obtain sufficient temperature increases at depth in a reasonable period of time, it appears that the surface must be heated to a temperature greatly in excess of that at which damage to the pavement can occur. Carmichael et al. pointed out that it is important that the full depth of pavement be properly heated before scarifying because "cold asphalts do not bond well and any attempt to force cold, asphalt coated aggregates together by force after scarifying them by tensile failure of the asphalt binder can only lead to future problems" (13).

Much of the literature already cited used assumed values of the thermal properties of asphaltic concrete. However, as the data in Tables 1 and 2 indicate, measured values of conductivity and specific heat of asphalt and asphaltic concrete as well as minerals and rocks commonly used as asphaltic concrete aggregate are available. Reported values of thermal conductivity range from 0.74 to 2.88 w/m°C for asphaltic concrete and from 0.14 to 0.17 w/m°C for pure asphalt. Diffusivity values ranging from $5.8 * 10^{-7}$ to $14.4 * 10^{-7}$ m^2/sec have been reported. The range of reported values of specific heat (c) is 879 to 963 J/Kg°C for asphaltic concrete.

The predominant component of asphaltic concrete is aggregate. The thermal properties of the particular aggregate used in a given asphaltic concrete can be expected to have an important effect on the properties of the mix. The literature indicates that common minerals and rocks used as aggregate can have conductivities that range from about 1 to 8 w/m°C (Table 2); the range of c can be expected to be on the order of 650 to 1000 J/Kg°C. Wolfe et al. (14) suggest 920 J/Kg°C as an average value based on their tests. Limited data on the diffusivity of the fine aggregate component indicate α is on the order of 2 to $9 * 10^{-7}$ m^2/sec.

Thermal properties of asphaltic concrete reported in the literature do not indicate the mineralogy, grain-size distribution, or density of the aggregate used in the mix. Nor has the fraction of asphalt or density of the mix been reported. Certainly these factors can be expected to influence the resulting thermal properties of asphaltic concrete and thus the transfer of heat from a field heater through an asphaltic concrete pavement.

DESCRIPTION OF EXPERIMENTS

Thermal Properties Required

The heat transfer process in a solid is described by the transient energy equation:

$$(\partial/\partial x)[k_x(\partial T/\partial x)] + (\partial/\partial y)[k_y(\partial T/\partial y)] + (\partial/\partial z)[k_z(\partial T/\partial z)] - \rho c(\partial T/\partial t) \quad (1)$$

where

x,y,z = spatial coordinates (m),
T = temperature (°C),
k = thermal conductivity (w/m°C),
ρ = density (Kg/m^3),
c = specific heat (J/Kg°C), and
t = time (sec).

Because the dimensions of field heaters are much greater than the thickness of a typical asphaltic concrete pavement, the heat transfer can be assumed to be one dimensional. Therefore, with the z dimension being vertical, $\partial T/\partial x \cong \partial T/\partial y \cong 0$, and Equation 1 becomes

$$k_z(\partial^2 T/\partial z^2) = \rho c(\partial T/\partial t) \quad (2)$$

Letting $\alpha = k/\rho c$ [diffusivity (m^2/sec)] and $k_z = k$, Equation 2 reduces to the familiar equation:

$$\alpha(\partial^2 T/\partial z^2) = \partial T/\partial t \quad (3)$$

Equation 3 can be written in finite difference form so that the temporal spatial-temperature field can be calculated for a pavement system that has

TABLE 1 Some Published Thermal Properties of Asphaltic Concrete

k(w/m°C)	α(m^2/sec)	ρc(J/m^3°C)[a]	Remarks	Reference
1.454		$1.41 * 10^6$		*16*
2.88	$14.4 * 10^{-7}$	$2.00 * 10^6$	18°C, dry	*17*
2.28	$11.5 * 10^{-7}$	$1.97 * 10^6$	38°C, dry	*17*
1.21	$5.75 * 10^{-7}$		Obtained from the Asphalt Institute	*13*
0.74-0.76			20°-56°C	*18*
0.167-0.172			Pure asphalt 20°-80°C	*19*
0.65-0.75			Asphalt used in street paving	*19*
1.37-1.75	$7-8 * 10^{-7}$	c = 879-963		*14*
0.80	$10 * 10^{-7}$			*20*
		c = 879	100°C	*19*
1.21		c = 920		*3*
1.2	$5.9 * 10^{-7}$	$2.07 * 10^6$	80°-149°C	*9,11*
		c = 921		
1.5				*2*
0.85-2.32				*21*
0.14-0.17		c = 1582-2561	Asphaltic bitumen free of paraffin wax 0°-300°C	*22*

[a] c in J/Kg°C

TABLE 2 Some Published Thermal Properties of Asphaltic Concrete Aggregate

Material	k(w/m°C)	α(m²/sec)	c(J/Kg°C)	Reference
Calcite				*23*
0°C			790	
200°C			1000	
Dolomite 60°C			930	*23*
Quartz				*23*
0°C			698	
200°C			969	
Limestone 58°C			1000	*23*
Limestone, mean of 3 at 50°C			680	*23*
Limestone, mean of 10 at 65°C			830	*23*
Quartzite				*23*
0°C			700	
200°C			970	
Granite				*23*
0°C			650	
200°C			950	
Basalt				*23*
0°C			850	
200°C			1040	
Sandstone 59°C			930	*23*
Diabase				*23*
0°C			700	
200°C			870	
Slate				*23*
0°C			710	
200°C			1000	
Avg value for sand and gravel	1.82			*24*
Calcite 100°C	2.86			*25*
Quartz 100°C	6.45			*25*
Granite 100°C	2.37			*25*
Basalt	1.8-2.2			*25*
Compact limestone	2.0-3.4			*25*
Porous limestone	1.1-2.2			*25*
Slate 100°C	1.8			*25*
Dolomite 100°C	3.99			*25*
Quartzite 100°C	5.2			*25*
Granite gneiss	1.8-2.8			*25*
Granite schist	2.7			*25*
Hard sandstone	2.6-4.5			*25*
Diabase 100°C	2.1			*25*
Quartz sand	1.1	$2 * 10^{-7}$		*25*
Sandy soil		$9 * 10^{-7}$		*25*

several layers, provided that the thermal properties ρ, c, and k (or α) are known for each layer. The mathematics and computer coding for predicting the temperature profile with time for a layered asphaltic concrete pavement system for a known heat input is routine, provided that the asphaltic concrete thermal properties are known.

Measurement of Properties

Determining the bulk density (ρ) of asphaltic concrete is routine. Typically, the as-placed density of asphaltic concrete is on the order of 2250 Kg/m³. Aggregate mineralogy and gradation, compaction effort, compaction temperature, and asphalt content will affect the density.

Numerous methods for measuring thermal properties have been proposed over the years. Most are for measuring a single thermal property at a time and usually use closed-form solutions for steady-state and transient cases. The method described here has some special advantages.

Beck and Al-Araji (15) developed a method of thermal property measurement capable of measuring the thermal conductivity, thermal diffusivity, and specific heat in a single test. The method requires the integration of some thermocouple signals, which can be accomplished by using available integrated circuits. The test procedure is quick and simple and requires minimal equipment.

To begin the test, a calorimeter (Figure 3) and a disk of asphaltic concrete (Figure 4) are placed in separate holders and insulated all around except for one face. The copper disk of the calorimeter is then heated to a uniform, elevated temperature (Figure 5) and brought into intimate contact with the asphaltic concrete sample (Figure 4). The differences in readings from thermocouples placed on the top (T_t) and bottom (T_b) of the sample are recorded at each time increment dt.

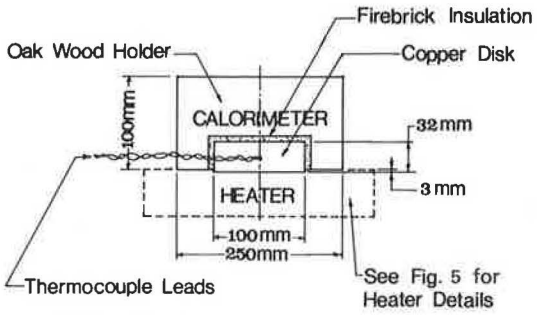

FIGURE 3 Calorimeter.

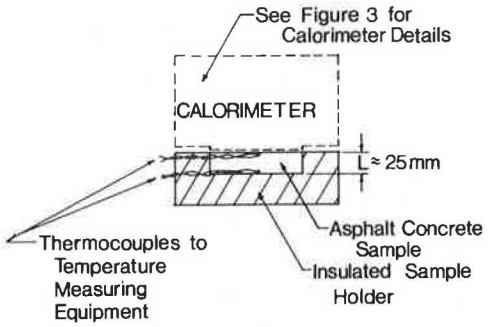

FIGURE 4 Calorimeter in contact with sample after being heated.

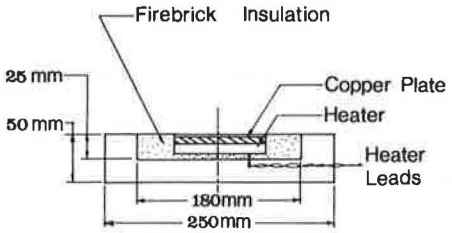

FIGURE 5 Calorimeter heater.

It has been found that, for a 30-mm-thick copper disk heated to a temperature of about 140°C and brought into contact with an asphaltic concrete disk about 25 mm thick at room temperature, the time required for T_b to equal T_t is about 30 min.

Beck and Al-Araji (15) showed that the thermal properties could be calculated from the following equations:

$$k = LQ/\left[2\int_0^\infty (T_t - T_b)dt\right] \quad (4)$$

$$\alpha = L^2(T_f - T_i)/\left[2\int_0^\infty (T_t - T_b)dt\right] \quad (5)$$

and

$$c = Q/[\rho L(T_f - T_i)] \quad (6)$$

where

Q = heat transferred from the copper disk to the asphaltic concrete sample (see Equation 7),
L = thickness of the asphaltic concrete disk,
T_f = final temperature of the asphaltic concrete sample (and the copper disk) when $T_t = T_b$,
T_i = initial temperature of the asphaltic concrete sample, and
ρ = previously measured density of the asphalt.

The integral in the denominators of Equations 4 and 5 are approximated by summing the temperature difference for each dt increment of time (dt = 15 sec was found to be appropriate) over the typical 30-min duration of the test and multiplying by dt. Because the surfaces are insulated, all the heat available in the copper disk is transferred to the asphaltic concrete sample, at which time both disks reach the same temperature. The heat-transferred Q can then be calculated from

$$Q = \rho_c L_c c_c (T_i - T_f)_c \quad (7)$$

where the subscript c refers to the copper disk.

Temperature Measuring System

The thermal property measuring device discussed in the previous section requires that temperatures be measured. Thermocouples were used to measure the temperatures. The TEMPSENSE Temperature Monitoring System (Interactive Microware, Inc.) in conjunction with an Apple II+ computer was used to calibrate the thermocouples and to select the frequency of sampling and the total duration of the test. The time of each measurement was displayed on the screen along with the temperature measured. The data were automatically stored on a disk for later analysis.

PRESENTATION AND DISCUSSION OF RESULTS

Asphaltic concrete samples were compacted as specified for the Marshall method of mix design (ASTM D 1559). Four different aggregate gradations were used: a base course, a dense-graded surface course, and an open-graded surface course, all using limestone aggregate; and a dense-graded surface course using lightweight aggregate (expanded shale). Samples of each mix were prepared at asphalt contents of 3.5, 5, and 6.5 percent. The 10.2-cm-diameter samples were cut into disks about 2.5 cm thick. Thermal properties of these disks were then obtained by the procedure described previously.

The particle-size distributions of the four asphaltic concrete mixes are shown in Figure 6. The base course and dense-graded surface course mixes were similar, except that the base course mix had particle sizes up to 38 mm, whereas the largest particles present in the dense-graded surface course were 12 mm. The open-graded surface course mix had the same range of particle sizes as the dense-graded surface course mix, but as shown in Figure 6 aggregate size is much more uniform.

The density-asphalt content relationship for each of the mixes is shown in Figure 7. Each point on the curves represents the average of the results of either four or five samples. Thermal properties of each mix were obtained from the disk samples, and

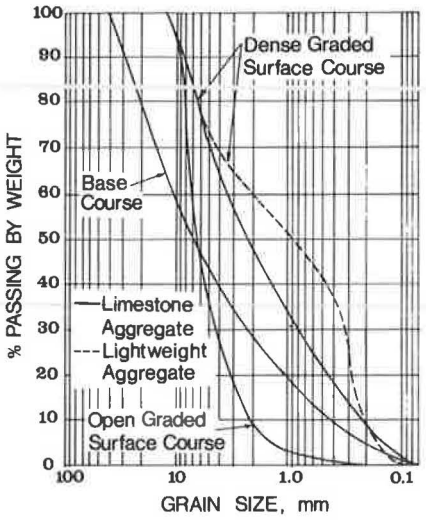

FIGURE 6 Grain-size distributions for the four aggregate mixes.

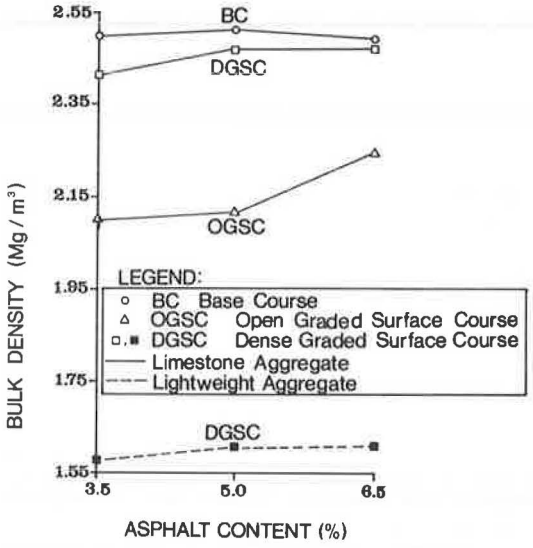

FIGURE 7 Bulk density as a function of asphalt content for the four aggregate mixes.

the results for thermal conductivity (k), specific heat (c), and diffusivity (α) are shown in Figures 8, 9, and 10, respectively. A comparison of Figures 7 and 8 indicates that thermal conductivity for the four mixes does not vary systematically with density or asphalt content.

For the dense-graded surface course mix with limestone aggregate, the thermal conductivity increased as the asphalt content increased from 3.5 to 5 percent. That the density of the mix increased as well (Figure 7) indicates that asphalt was replacing air in the mix voids. Because the thermal conductivity of asphalt is greater than air, the conductivity increased slightly (by about 4 percent). As the asphalt content of the mix was increased from 5 to 6.5 percent, the density remained essentially constant. This indicates that, in this range of asphalt content for this mix, asphalt had filled the voids and some of the mineral aggregate itself was being replaced by asphalt. Because the conductivity of asphalt is less than that of limestone (Tables 1 and 2), the thermal conductivity of the mix decreased, as shown in Figure 8.

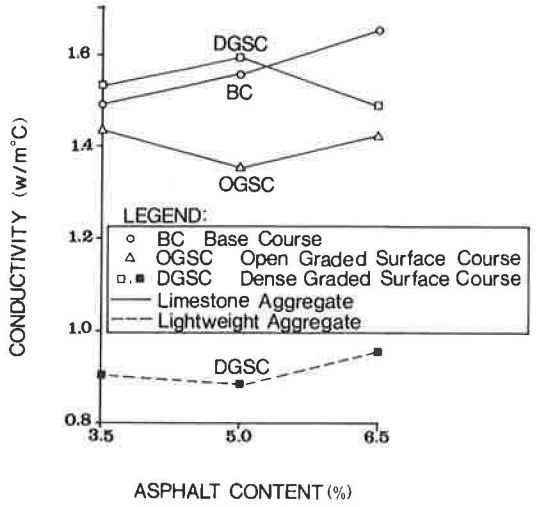

FIGURE 8 Thermal conductivity as a function of asphalt content for the four aggregate mixes.

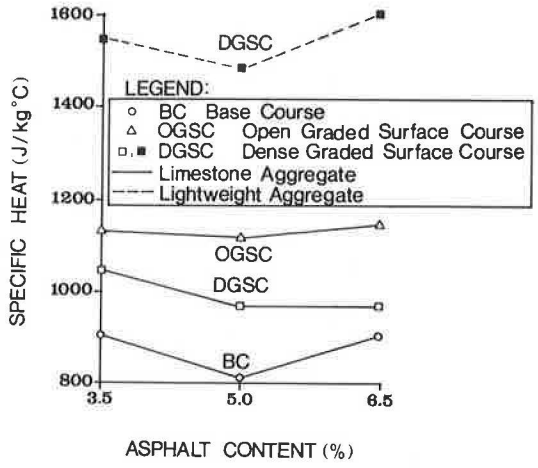

FIGURE 9 Specific heat as a function of asphalt content for the four aggregate mixes.

The thermal conductivity of the base course mix increased with asphalt content over the entire range of asphalt content (3.5 to 6.5 percent) at which samples were tested. This behavior was observed despite the fact that the density of the base course mix changed little with asphalt content. It is believed that this occurred because most of the heat transferred through this mix was through the larger aggregate (up to 38 mm), and that after the mineral aggregate voids were filled, the asphalt thickness around the larger particles was not increased substantially. The continuous increase in k with asphalt content may suggest a rearrangement of the mineral structure such that, although the mean distance between particles has increased (as suggested by a slight decrease in density), the nearest proximity points of individual aggregates may have decreased.

The open-graded surface course mix showed little change in conductivity with changing asphalt content. There are two opposing effects of adding asphalt to a uniform aggregate size. The first, as mentioned previously, is to replace air in the mineral aggregate voids with asphalt. This would tend to increase the conductivity of the mix. Working counter to this is the effect of increasing the asphalt coating around the particles as the asphalt

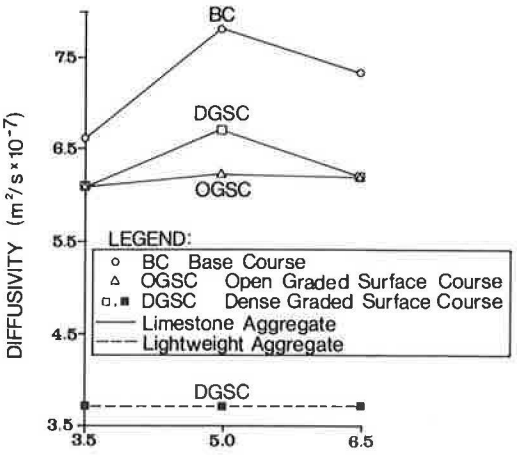

FIGURE 10 Thermal diffusivity as a function of asphalt content for the four aggregate mixes.

content is increased. This would reduce the conductivity of the mix. The increase in asphalt coating thickness as asphalt content increases would be greater on the open-graded surface course mix than on the other two limestone aggregate mixes studied because of the smaller specific surface of the open-graded mix.

The thermal conductivity of the dense-graded surface course mix with the lightweight aggregate was much less than that of the mixes that have limestone aggregates. This mix consisted (by weight) of 25 percent expanded shade (from 5 to 13 mm in size), 30 percent limestone aggregate and filler, and 45 percent river sand (quartz). The expanded shale controlled the conductivity of the mix and the asphalt content had little effect on the conductivity (Figure 8). It is postulated that the air trapped in the expanded shale is an important factor controlling the conductivity of this mix.

Because the specific heat of asphalt is much higher than air or limestone and shale (Tables 1 and 2), it was expected that, as the asphalt content of the mixes was increased from 3.5 to 6.5 percent, there would be a corresponding increase in the specific heat of the mixes. However, Figure 9 shows that the specific heat of the mixtures changed little with asphalt content and that specific heat of these mixes is more dependent on the aggregate gradation and mineralogy than the asphalt content. Based on these results, it appears that an average value of c for each mix could be used; the actual number used would depend on the mix. The average specific heat of the lightweight aggregate mixes was much higher than the limestone aggregate mixes. This is primarily due to the decrease in density of the expanded shale. The products ρc of the lightweight mixes and the surface course limestone mixes are nearly the same ($2.5 * 10^{-6}$ J/m³°C). This product for the base course mix is about 15 percent less.

The diffusivity (α) of the limestone aggregate mixes is shown as it varies with asphalt content in Figure 10. For the open-graded surface course mix, α is essentially independent of asphalt content; for the base course and dense-graded surface course mixes, the diffusivity varied about 10 percent over the range of asphalt contents used in the mixes. The values shown in Figure 10 for the limestone aggregate mixes are well within the range reported by other researchers (Table 1). The diffusivity of the dense-graded surface course that has lightweight ag-

gregate was much less than that of the limestone aggregate mixes and was found to be independent of asphalt content. Because the product ρc for the lightweight mixes is similar to that of the limestone mixes, the reduction in α is due to the smaller thermal conductivity of the lightweight mixes (Figure 8).

SUMMARY AND CONCLUSIONS

The conductivity (k) of the three limestone mixes of asphaltic concrete was found to vary as much as 20 percent over the range of asphalt contents (3.5 to 6.5 percent) used in this study. Two opposing mechanisms come into play that influence the thermal conductivity of an asphaltic concrete mix as the asphalt content is increased. On the one hand, the replacement of air in the voids in the mix by asphalt tends to increase the conductivity of asphaltic concrete because the conductivity of asphalt is much higher than that of air; on the other hand, the additional asphalt increases the thickness of the coating around aggregates, which tends to decrease the conductivity of the mix because the conductivity of asphalt is much less than that of the aggregate. The dominant mechanism depends on the asphalt content and the mix properties, such as the largest particle sizes present, the gradation, and the specific surface.

The conductivity of the lightweight aggregate mix was about 60 percent of that of similarly graded limestone aggregate mixes and varied little with asphalt content. It is believed that the conductivity of the lightweight mixes is controlled by air trapped in the expanded shale.

The specific heat (c) of the four mixes did not increase systematically with asphalt content, as was expected. The specific heat of the lightweight aggregate mixes was about 60 percent higher than that of the limestone aggregate mixes primarily because of the decrease in bulk density. The products ρc for similarly graded lightweight and limestone aggregate mixes were found to be similar.

The diffusivity (α) of each of the three limestone mixes varied less than 10 percent with asphalt content. The open- and dense-graded surface course mixes had similar diffusivities--the average was about $6.2 * 10^{-7}$ m^2/sec. The average α of the base course mix was about $7.3 * 10^{-7}$ m^2/sec. The diffusivity of the asphaltic concrete mixes that had lightweight aggregate was found to be essentially independent of asphalt content. The reduction in α from limestone to lightweight aggregate dense-graded surface course mixes was nearly the same in magnitude as the corresponding reduction in thermal conductivity.

Based on the results of this study, it appears that in analyzing heat transfer in asphaltic concrete having limestone aggregate, an average value of specific heat and an average value of diffusivity can be used that are independent of asphalt content but depend on the aggregate gradation. The conductivity used in analysis must reflect the asphalt content as well as the gradation of the aggregate. It appears that average values of diffusivity and specific heat can be used for lightweight aggregate mixes similar to that investigated, and it appears that little accuracy would be lost if an average value of conductivity, independent of asphalt content, were used.

ACKNOWLEDGMENT

The research in this paper was sponsored by the Air Force Office of Scientific Research, Air Force Systems Command, U.S. Air Force, and by the Engineering Services Laboratory of the Air Force Engineering and Services Center. The U.S. government is authorized to reproduce and distribute reprints for governmental purposes, notwithstanding any copyright notation thereon. The contents of this paper were originally presented at the AIAA/ASCE/TRB/ATRIF/CASI International Air Transportation Conference in Montreal in June 1983. The authors would like to acknowledge the contributions of Alexander B. Moore to this research.

REFERENCES

1. H. Carlson and M.S. Kersten. Calculation of Depth of Freezing and Thawing Under Pavements. Bull. 71. HRB, National Research Council, Washington, D.C., 1953, pp. 81-98.
2. H.P. Aldrich, Jr. Frost Penetration Below Highway and Airport Pavements. Bull. 135. HRB, National Research Council, Washington, D.C., 1956, pp. 124-149.
3. E.S. Barber. Calculation of Maximum Pavement Temperature from Weather Reports. Bull. 168. HRB, National Research Council, Washington, D.C., 1957, pp. 1-8.
4. H.F. Southgate and R.C. Deen. Temperature Distribution Within Asphalt Pavement and Its Relationship to Pavement Deflection. In Highway Research Record 291, HRB, National Research Council, Washington, D.C., 1969, pp. 116-131.
5. T.N. Rumney and R.A. Jimenez. Pavement Temperatures in the Southwest. In Highway Research Record 361, HRB, National Research Council, Washington, D.C., 1971, pp. 1-13.
6. A.L. Straub, H.L. Schenck, Jr., and F.E. Przybycien. Bituminous Pavement Temperature Related to Climate. In Highway Research Record 256, HRB, National Research Council, Washington, D.C., 1968, pp. 53-77.
7. B.J. Dempsey and M.R. Thompson. A Heat Transfer Model for Evaluating Frost Action and Temperature-Related Effects in Multilayered Pavement Systems. In Highway Research Record 342, HRB, National Research Council, Washington, D.C., 1970, pp. 39-56.
8. J.T. Christison and K.O. Henderson. Response of Asphalt Pavements to Low Temperature Climatic Environments. Proc., 3rd International Conference on the Structural Design of Asphalt Pavements, Vol. 1, Sept. 1972, pp. 41-52.
9. J.S. Corlew and P.F. Dickson. Methods for Calculating Temperature Profiles of Hot-Mix Asphalt Concrete as Related to the Construction of Asphalt Pavements. Proc., Association of Asphalt Paving Technologists, Vol. 37, 1968, pp. 101-140.
10. B.G. Frenzel, P.F. Dickson, and J.S. Corlew. Computer Analysis for Modification of Base Environmental Conditions to Permit Cold Weather Paving. Proc., Association of Asphalt Paving Technologists, Vol. 40, 1971.
11. J.S. Corlew and P.F. Dickson. Cold-Weather Paving of Thin Lifts of Hot-Mixed Asphalt on Preheated Asphalt Base. In Highway Research Record 385, HRB, National Research Council, Washington, D.C., 1972, pp. 1-6.
12. R.K. Wolfe and D.C. Colony. Asphalt Cooling Rates: A Computer Simulation Study. Report OHIO-DOT-07-06. Ohio Department of Transportation, Columbus, Oct. 1976, 91 pp.
13. T. Carmichael, R.E. Boyer, and L.D. Hokanson. Modeling Heater Techniques for In-Place Recycling of Asphalt Pavements. Proc., Association

of Asphalt Paving Technologists, Vol. 46, 1977, pp. 526-540.
14. R.K. Wolfe, G.L. Heath, and D.C. Colony. University of Toledo Time Temperature Model Laboratory and Field Validation. Report FHWA/OH-80/006. Ohio Department of Transportation, Columbus, April 1980, 56 pp.
15. J.V. Beck and S. Al-Araji. Investigation of a New Simple Transient Method of Thermal Property Measurement. ASME, Journal of Heat Transfer, Feb. 1974, pp. 59-64.
16. E.J. Yoder and M.W. Witczak. Principles of Pavement Design, 2nd ed. Wiley, New York, 1975, 711 pp.
17. A. Kavianipour and J.V. Beck. Thermal Property Estimation Utilizing the LaPlace Transform with Application to Asphaltic Pavement. International Journal of Heat and Mass Transfer, Vol. 20, No. 3, March 1977, pp. 259-266.
18. A.I. Brown and S.M. Marco. Introduction to Heat Transfer, 3rd ed. McGraw-Hill, New York, 1958, 332 pp.
19. C.S. Cragoe. Thermal Properties of Petroleum Products. Misc. Publ. 97. U.S. National Bureau of Standards, Nov. 9, 1929, 48 pp.
20. M. Spall. Developing a Thermal Model for Asphaltic Concrete. M.S. thesis. Department of Mechanical and Industrial Engineering, Clarkson College of Technology, Potsdam, N.Y., 1982, 68 pp.
21. J.D. O'Blenis. Thermal Properties of West Virginia Highway Materials. M.S. thesis. Civil Engineering Department, West Virginia University, Morgantown, 1982.
22. R.N.J. Saal. Physical Properties of Asphaltic Bitumen: Surface Phenomena, Thermal and Electrical Properties, Etc. In The Properties of Asphaltic Bitumen (J.Ph. Pfeiffer, ed.), Elsevier, New York, 1950, Chapter III.
23. R.W. Goranson. Heat Capacity: Heat of Fusion. In Handbook of Physical Constants (F. Birch, J.F. Schairer, and H.C. Spicer, eds.), Geological Society of America, Special Papers 36, 1942, Section 16, pp. 223-242.
24. B. Gebhart. Heat Transfer, 2nd ed. McGraw-Hill, New York, 1971, 596 pp.
25. F. Birch. Thermal Conductivity and Diffusivity. In Handbook of Physical Constants (F. Birch, J.F. Schairer, and H.C. Spicer, eds.), Geological Society of America, Special Papers 36, 1942, Section 17, pp. 243-265.

Publication of this paper sponsored by Committee on Characteristics of Bituminous Paving Mixtures to Meet Structural Requirements.

Evaluating Moisture Susceptibility of Asphalt Mixtures Using the Texas Boiling Test

THOMAS W. KENNEDY, FREDDY L. ROBERTS, and KANG W. LEE

ABSTRACT

A description of the development and use of the Texas boiling test to evaluate stripping of materials susceptible to moisture damage is presented. Based on a review and comparison of boiling tests currently in use by several agencies and a limited test evaluation program, a tentative test procedure was prepared and used for all subsequent testing. Tests were performed on eight mixtures, of which five had stripped in the field and three had not. Each mixture and its individual aggregate components were tested to determine if the results could be used to differentiate between stripping and nonstripping mixtures. Because antistripping additives are commonly used in stripping-prone mixtures, a few additives and aggregate combinations were tested to determine if test results were affected by the presence of these additives. Test results indicate that valuable information is provided by the Texas boiling test. The test is simple and easy to perform; it can be performed either in the laboratory during mixture design or on field-mixed mixtures. Evaluation of known aggregates and various antistripping additives indicates that the Texas boiling test generally can be used to detect moisture-susceptible mixtures.

Water-induced damage of asphalt mixtures has produced serious distress, reduced performance, and increased maintenance for pavements in Texas as well as in other regions of the United States. Moisture-induced damage produces several forms of distress, including localized bleeding, rutting, shoving, and ultimately complete failure because of permanent deformations and cracking. This damage occurs because of stripping of asphalt from aggregate and in some cases possibly because of softening of the asphalt matrix.

Stripping, which is of primary concern, is the physical separation of the asphalt cement and aggregate produced by the loss of adhesion between the asphalt cement and the aggregate surface primarily due to the action of water or water vapor. Stripping is accentuated by the presence of aggregate surface coatings and by smooth surface-textured aggregates. Softening is a general loss of stability of a mixture that is caused by a reduction in cohesion due to the action of moisture within the asphalt matrix.

Field and laboratory experience to date (1-10) indicates that stripping is primarily an aggregate problem, but the type of asphalt is also important. Thus it is important to evaluate both the asphalt and the aggregate that is proposed for use. In addition, attempts to reduce the magnitude of the problem often have centered on introducing various antistripping additives to asphalt mixtures. Unfortunately, there has been no generally accepted, reliable way to evaluate proposed aggregate-asphalt combinations to determine their water susceptibility.

In response to this problem, the Center for Transportation Research and the Texas State Department of Highways and Public Transportation, through their cooperative research program, initiated a research project to study water-induced damage to asphalt mixtures in Texas. This study included an evaluation of proposed test methods for ascertaining the water susceptibility of asphalt mixtures and the effectiveness of antistripping agents.

As a result of the study, three tests were identified and were found to provide significant information with respect to distinguishing between stripping and nonstripping mixtures. These tests are the Texas freeze-thaw pedestal test, the Texas boiling test, and the wet-dry indirect tensile test.

The Texas boiling test is a rapid method to evaluate the moisture susceptibility of an aggregate-asphalt mixture before using the mixture in the field. The Texas freeze-thaw pedestal test is described elsewhere (2,3,8,10), and the wet-dry indirect tensile test is described by Kennedy and Anagnos (9). In this paper the development of the Texas boiling test procedure and the findings of studies to evaluate its effectiveness are summarized.

TEXAS BOILING TEST AND EVALUATION

The Texas boiling test is a rapid method to evaluate the moisture susceptibility, or stripping, of aggregate-asphalt mixtures, with and without antistripping agents, and is a composite of procedures that are described in other publications (11-14). In this test a visual observation is made of the extent of stripping of the asphalt from aggregate surfaces after the mixture has been subjected to the action of boiling water for a specified time. After reviewing the various test methods and performing a preliminary evaluation, the best features of each procedure were synthesized to produce a test procedure that would minimize potential field problems while minimizing the difficulty and cost of performing these laboratory tests. The standard procedure used in this study was designed for evaluating both the potential stripping mixtures and the effect of adding antistripping additives. The standard procedure is included in the Appendix and is summarized in the following sections.

Aggregate

Aggregate mixtures can contain several materials that are blended naturally or by the contractor to satisfy grading requirements. These individual materials and the total mixture vary in size, shape, surface texture, and chemical composition. The test method allows the individual materials and the total mixture to be evaluated.

Individual Aggregates

When an individual aggregate is to be evaluated, the proposed Texas boiling test permits testing of individual component materials in a range of sizes such as

1. Passing 3/8-in. retained on No. 4,
2. Passing No. 4 retained on No. 10,
3. Passing No. 10 retained on No. 40, and
4. Passing No. 40 retained on No. 80.

Additional size ranges can also be tested if needed.

Total Aggregate Mixture

When evaluating the total mixture, the sample should have the same gradation as proposed for construction; aggregates greater than 7/8 in. are normally eliminated. Care should be taken in the evaluation to ensure that a proper determination is made of the amount of asphalt retained on the aggregate because the fine aggregates have a significant effect on the visual appearance of the mixture.

Asphalt Cement

Both the type and amount of asphalt cement influence stripping and test results.

Type and Source

The asphalt cement should be the same as that proposed for use during construction. It is recommended that the asphalt-aggregate mixture be retested if the source or type of asphalt changes.

Asphalt Content

To evaluate the total aggregate mixture, the aggregates should be blended according to the specified project gradation, and the ashalt content should be that determined by Tex-204-F (15) or other design procedures. When the individual components of the mix are evaluated, a constant asphalt content can produce different film thicknesses because the design asphalt content varies with the size, shape, absorption, and surface area (16) of the aggregate being tested. To produce an asphalt film thickness for an individual aggregate that approximates the film thickness for the total mixture, the asphalt content should be increased or decreased until the proper film thickness, as determined visually, is secured. This can be done by visually ensuring that all particles are coated and that excess asphalt is not left in the mixing pan. Future refinements should consider the surface area of the individual aggregates in order to produce uniform film thicknesses.

Mixture Preparation

The asphalt cement, with or without an antistripping agent, is heated at 325° ± 5°F for 24 to 26 hr, which allows the heat stability of the additive to be considered. For the evaluation of the total ag-

gregate mixture, 300 g of aggregate should be used; for the evaluation of an individual aggregate component, 100 g of material should be used. The dry aggregate is heated at 325° ± 5°F for 1 to 1.5 hr. The asphalt cement is added to the aggregate and mixed manually on a hot table. The mixture is allowed to cool at room temperature for at least 2 hr before testing.

Test Procedure

A 1000-mL beaker or other suitable container is filled one-half full (approximately 500 cc) with distilled water and heated to boiling. The prepared aggregate-asphalt mixture is added to the boiling water, which will temporarily lower the temperature below the boiling point. The heat should be increased so that the water reboils in approximately 2 to 3 min. The water should be maintained at a medium boil for 10 min, stirring with a glass rod at 3-min intervals. During and after boiling the stripped asphalt should be skimmed away from the surface of the water with a paper towel to prevent recoating of the aggregate. The mixture is then allowed to cool to room temperature while still in the beaker. After cooling, the water is drained from the beaker and the wet mixture is emptied onto a paper towel and allowed to dry.

Evaluation and Reporting

The amount of stripping is determined by a visual rating, expressed in terms of the percentage of asphalt retained (scale 0 to 100 percent retained). Such a rating is subjective and will vary with time and for different operators. To standardize the evaluation, a standard rating board (Figure 1) has been developed with 10 intervals from 0 to 100 percent retained. This scale is constructed by using a set of specimens that have been selected to provide visual examples of varying degrees of stripping that can be compared with the test specimen to obtain a test value. A photograph should not be used because of textural differences. The mixture should not be evaluated until air-dried because laboratory results have demonstrated that stripping of the fines in some mixtures is not as apparent if the mixture is wet.

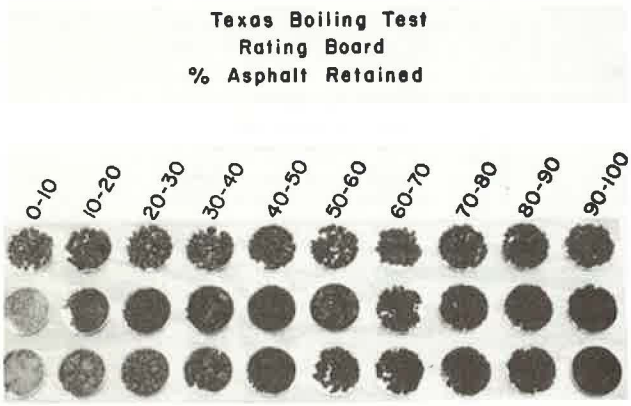

FIGURE 1 Texas boiling test rating board.

Analysis of Critical Test Variables

Initial laboratory evaluation of the test method indicated that test results were sensitive to three test variables: the number of times the asphalt and aggregate were mixed, the temperature to which the aggregate was heated before mixing, and the type of water used to boil the mixture. Thus these variables were evaluated to determine their effects, and the results were used to establish the test procedure.

Number of Times Mixed

Results of the boiling test indicated that reheating and remixing the asphalt-aggregate mixtures dramatically increased the amount of asphalt retained (Figure 2). A set of specimens, prepared from seven individual aggregates and one mixture, was prepared by mixing the aggregates and asphalt once; a second set of specimens was prepared where the specimens were mixed, reheated, and mixed again; and a third set of specimens was prepared where the specimens were

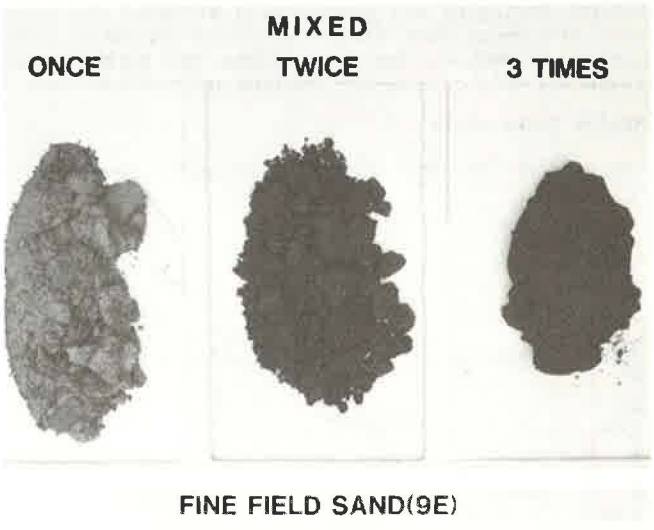

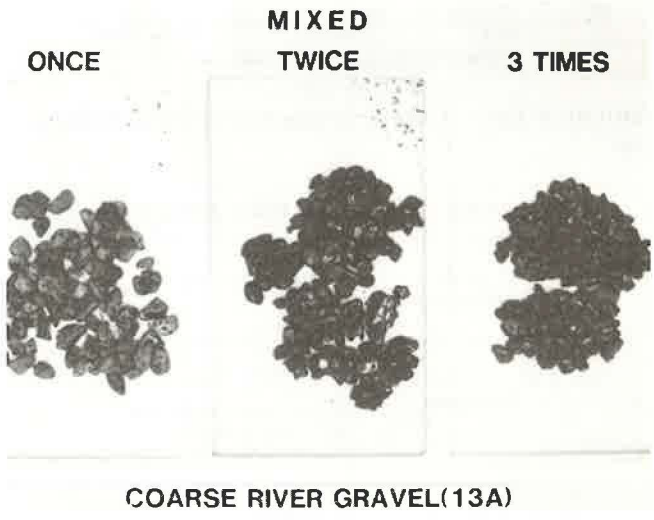

FIGURE 2 Effect of number of times mixed on Texas boiling test.

TABLE 1 Summary of Effect of Number of Times Mixed

Field Performance	Individual Aggregates and Mixture	Aggregate Size	Asphalt Content %	Asphalt Retained, %		
				Mix Once	Mix Twice	Mix 3 Times
Stripping	River gravel, 9D	-3/8 + 4	2.3	45	65	95
	Washed sand, 9F	-10 + 40	6.3	15	35	85
	Field sand, 9E	-40 + 80	6.3	15	75	95
	Coarse river gravel, 13A	-3/8 + 4	3.0	5	75	75
	Coarse field sand, 13C	-10 + 40	7.0	15	75	75
	Combined mixture, 13A & C		6.0	35	65	85
Nonstripping	Coarse crushed limestone, 14I	-3/8 + 4	3.4	75	75	85
	Limestone screening, 14K	-4 + 10	3.4	75	85	95

mixed three times. The results are summarized in Table 1 and Figure 3. As shown, the amount of retained asphalt was greater for mixtures that were reheated and remixed. In addition, the separation between stripping and nonstripping mixtures was best when specimens were mixed once. The standard procedure, therefore, involves mixing the asphalt and aggregate only once before cooling and boiling.

Mixing Temperature

The effect of the initial aggregate temperature (mixing temperature) was also evaluated. A series of boiling test specimens were prepared with aggregates heated to either 200°, 250°, or 325°F and then mixed with asphalt cement at 325°F. After mixing and cooling, each mixture was boiled and the amount of asphalt retained was determined. The results indicated that a greater amount of asphalt was retained when the aggregate and resulting mixing temperatures were higher (Table 2 and Figures 4 and 5). Therefore, in the standard boiling test procedure both the aggregates and the asphalt cement are heated to 325°F before mixing.

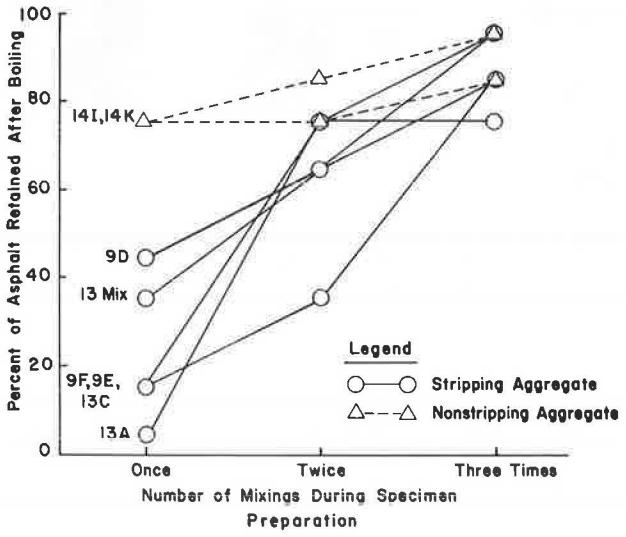

FIGURE 3 Effect of number of times mixed on Texas boiling test.

Water for Boiling

A comparison of test results obtained by using distilled water and tap water indicated that dramatically different results can be obtained and that the type of water also produces effects (Figure 6). Similar effects were also reported by personnel of the Alabama Department of Transportation. Thus the standard procedure uses distilled water.

TEXAS BOILING TEST TO EVALUATE MATERIALS

A series of tests on mixtures with and without antistripping additives was conducted to evaluate the ability to distinguish between known stripping and nonstripping mixtures and to evaluate the effect of antistripping additives.

Materials

Eight mixtures from actual projects were selected for use in this study. Of these eight mixtures, five previously exhibited stripping in the field and

TABLE 2 Summary of Effect of Initial Aggregate Temperature

Field Performance	Individual Aggregate	Aggregate Size	Asphalt Content %	Asphalt Retained, %		
				200°F	250°F	325°F
Stripping	Field sand, 9E	-40 + 80	6.3	15	15	55
	Coarse field sand, 13C	-10 + 40	7	25	25	65
	Gem sand, 13M	-3/8 + 4	3	5	5	26
	Coarse sand, 13N	-10 + 40	7	15	25	65
Nonstripping	Sandstone, 13L	-3/8 + 4	3	35	35	85
	Field sand, 13D	-40 + 80	7	85	65	85

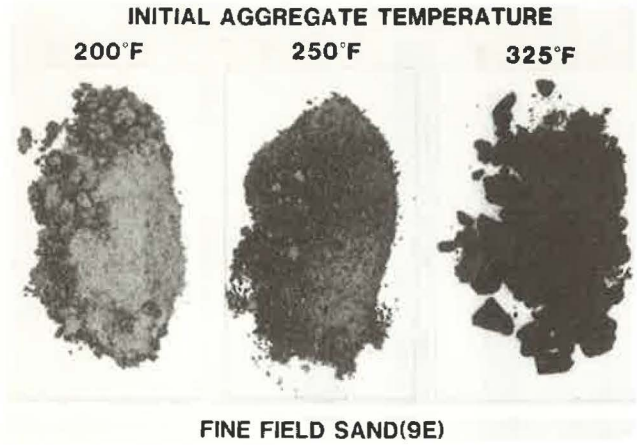

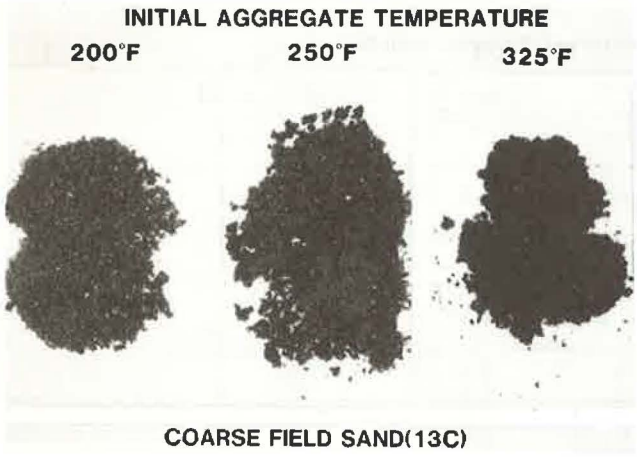

FIGURE 4 Effect of initial aggregate temperatures on Texas boiling test.

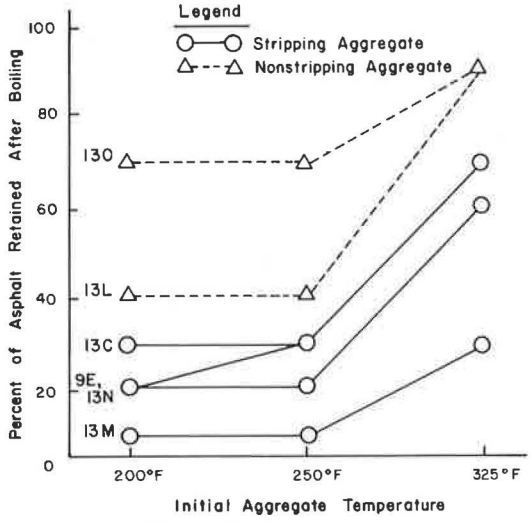

FIGURE 5 Effects of initial aggregate temperatures on Texas boiling test.

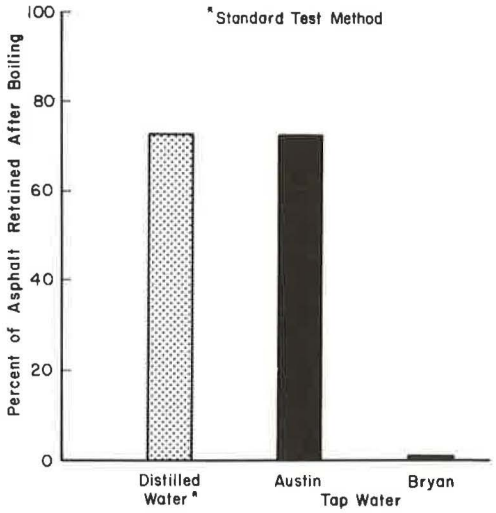

FIGURE 6 Effects of type of water on the Texas boiling test.

three did not. The major components of these stripping mixtures were silicious river gravel and sand. The major components of the nonstripping mixtures were crushed limestone, caliche, or slag. The composition of each mixture by aggregate type and percentage is reported elsewhere (6).

The gradations of aggregates used for the boiling test were the same as those used in construction. Two materials met the requirements of grade 1 flexible base item 238 (processed gravel) and item 232 (caliche), respectively (17). Gradations of the other six materials met the requirements of type D surface course paving mixtures.

The asphalt cements included in the testing program were the same as those used in pavement constructions.

Evaluation of Mixtures

Results for each of the eight mixtures are shown in Figure 7. All mixtures that experienced stripping in the field retained less than approximately 60 percent asphalt after boiling. The nonstripping mixtures retained more than 75 percent.

By using these data as well as other test results as a base, it is currently recommended that 70 percent of asphalt retained after boiling be the division between stripping and nonstripping mixtures. Based on this study and other experience, aggregates that retain more than 85 percent are judged to be moisture resistant. Those between 70 and 85 percent are borderline and would benefit from treatment. Thus the Texas boiling test offers a quick method of detecting asphalt-aggregate mixtures that are susceptible to stripping and moisture in the field. Because this test can be performed quickly in either the laboratory or the field, and because the results provide a satisfactory indication of stripping, it is recommended for use in evaluating mixtures during both design and construction.

Evaluation of Individual Aggregates

The boiling test has also been used to evaluate the individual components of these aggregate mixtures to determine their water susceptibility. Test results for each of the individual aggregates included in the eight project mixtures are given in Tables 3 and

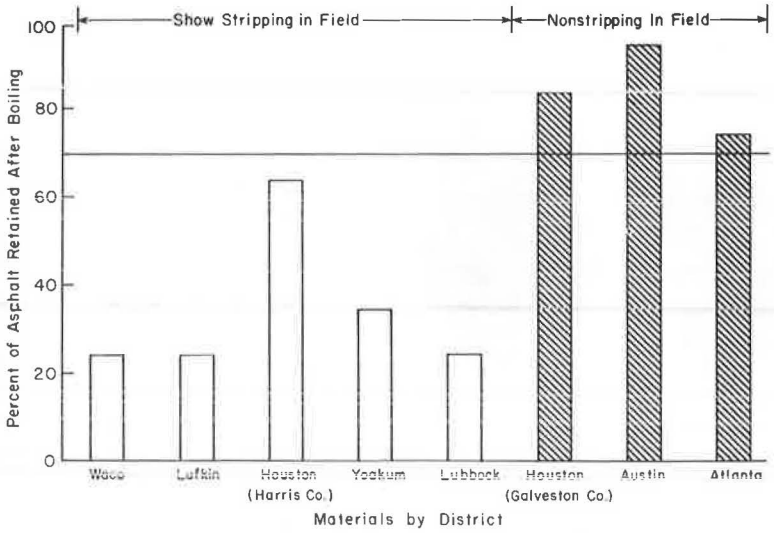

FIGURE 7 Texas boiling test results for stripping and nonstripping mixtures.

TABLE 3 Texas Boiling Test Results for Individual Aggregates and Stripping Design Mixtures

District	Individual Aggregate and Design Mixture	Aggregate Size Tested	Asphalt Content, %	Percent of Asphalt Retained After Boiling
5 Lubbock	Crushed caliche (5A)	all gradation	9.0	25
9 Waco	Coarse gravel (9D)	-3/8 + 4	2.3	45
	Washed sand (9F)	-10 + 40	6.3	15
	Field sand (9E)	-40 + 80	6.3	15
	Design mixture	all gradation	4.3	25
11 Lufkin	Crushed limestone (11C)	-3/8 + 4	5.0	35
	Pea gravel (11D)	-3/8 + 4	3.0	35
	Coarse field sand (11E)	-3/8 + 4	7.0	15
	Local field sand (11F)	-40 + 80	7.0	15
	Design mixture	all gradation	5.0	25
12 Houston (Harris Co.)	Gravel screenings (12B)	-3/8 + 4	2.3	35
	Crushed limestone (12A)	-3/8 + 4	4.3	85
	Local field sand (12C)	-40 + 80	6.3	95
	Design mixture	all gradation	4.3	65
13 Yoakum	Coarse river gravel (13A)	-3/8 + 4	3.0	5
	Fine river gravel (13B)	-3/8 + 4	5.0	25
	Coarse field sand (13C)	-10 + 40	7.0	15
	Fine field sand (13D)	-40 + 80	8.0	85
	Design mixture	all gradation	5.0	35

4. In general, when a major component of the mixture retains less than 50 percent asphalt, the mixture itself strips significantly. However, there were anomalies that occurred between results for individual aggregates and for mixtures of the aggregates.

Evaluation of Antistripping Additives

Several techniques have been proposed in the technical literature or have been demonstrated in the field to limit the water damage to asphalt concrete mixtures. These include pretreatment or elimination of stripping-prone aggregates, design control, and construction control. However, the most commonly used procedure is to treat the aggregate or asphalt with an antistripping additive. To evaluate the effectiveness of these additives in reducing moisture susceptibility, a limited study was performed.

Antistripping Additives

During recent years various antistripping additives have been incorporated into asphalt mixtures to reduce the magnitude of the stripping problem. The most common categories of additives that have been used and judgments of their effectiveness have been summarized by Majidzadeh and Brovald (18). These additives are either mixed with the binder or applied to the aggregate surfaces. Some test results indicate that the effectiveness of the additives may be better when applied directly on the aggregate than when added to the binder (19,20). However, blending the additive with the binder is easier, more economical, and is the current practice with liquid chemical additives. These chemical antistripping additives are usually added at a rate of 0.5 to 1.0 percent by weight of the asphalt (21).

Hydrated lime has been used quite successfuly in

TABLE 4 Texas Boiling Test Results for Individual Aggregates and Nonstripping Design Mixtures Materials

District	Individual Aggregate and Design Mixture	Aggregate Size Tested	Asphalt Content, %	Percent of Asphalt Retained After Boiling
12 Houston (Galveston Co.)	Crushed limestone (12E)	-3/8 + 4	5.0	85
	Limestone screenings (12F)	-10 + 40	5.0	85
	Field sand (12G)	-40 + 80	7.0	55
	Design mixture	all gradation	6.0	85
14 Austin	Crushed limestone (14 I&J)	-3/8 + 4	3.4	95
	Limestone screenings (14K)	-4 + 10	4.4	75
	Local field sand (14L)	-40 + 80	7.4	75
	Design mixture	all gradation	5.4	95
19 Atlanta	Coarse slag (19A&B)	-3/8 + 4	5.5	95
	Field sand (19C)	-40 + 80	7.5	85
	Local field sand (19D)	-10 + 80	6.5	65
	Design mixture	all gradation	7.5	75

the past as an antistripping additive (2-7,10). Usually, 1 to 2 percent hydrated lime is applied directly to the aggregate in slurry form (10). However, it has also been added to the asphalt and to the aggregate in dry form, but test results have not been as dramatic as those from slurry applications.

Effectiveness of Antistripping Additives

A limited laboratory study was designed to evaluate the effectiveness of several antistripping additives using results from the Texas boiling test. Two groups of specimens were prepared with antistripping additives for the purposes of

1. Evaluating the effectiveness of adding antistripping additives to the stripping materials, and
2. Detecting any adverse effect of antistripping additives in the nonstripping materials.

Eleven different liquid chemical antistripping additives, representing five antistripping categories and a lime slurry, were used as additives in specimens prepared for this study. The lime slurry was added directly to the aggregate while the liquid antistripping additives were added to the asphalt before mixing. The amount of liquid agents was 1 percent by weight of asphalt. The lime slurry was prepared with 1 percent hydrated lime and 3 percent water by weight of the aggregate. After applying the selected treatment, the asphalt mixture was prepared, the mixture boiled, and the amount of stripping estimated after cooling.

The three individual aggregates selected for use in this investigation were a coarse aggregate river gravel, rhyolite from west Texas, and crushed limestone. The coarse river gravel was a silicious aggregate with crushed faces and is a stripping-prone aggregate. The rhyolite was a gray, rough, subangular material that has exhibited severe moisture-related problems in both asphalt mixtures and seal coats. The crushed limestone was a rough, subangular, porous material; it is a nonstripping aggregate. Two asphalt cements from different Texas refineries were selected.

Test results are summarized in Figure 8 for the silicious river gravel. The antistripping additives were grouped by classification as obtained from each

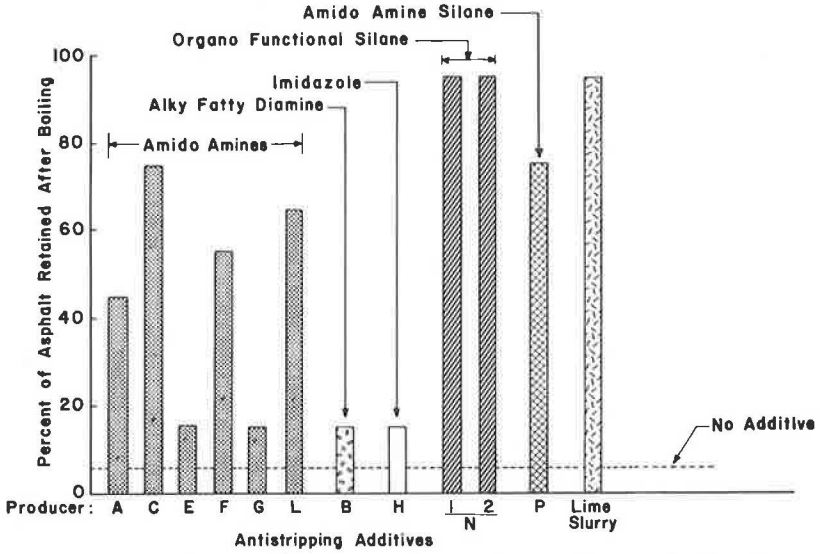

FIGURE 8 Texas boiling test results on mixtures of coarse river gravel with various antistripping additives.

producer. In general, the results from the Texas boiling test indicated positive benefits for lime slurry and selected chemical antistripping additives, depending on the aggregate. Other unreported test results suggest that some of these additives are more effective when sprayed directly on the aggregate rather than being added to the asphalt.

It was observed that there is significant interaction between additives, asphalt, and aggregate (i.e., the magnitude of test results may be affected if any one of these three factors is changed). Thus each combination of asphalt, aggregate, and antistripping additive must be evaluated to determine whether the combination provides increased resistance to stripping.

For the nonstripping aggregates, no differences between test results were detected when the antistripping additives were used and when they were not used. This indicates that no adverse effects occurred due to the presence of the various antistripping additives for the quantities used and for the aggregates included in this test program.

Because the effectiveness of antistripping agents is dependent on the aggregate and asphalt used, evaluation should be conducted on the actual asphalt cement-aggregate combination to be used in the field. Consideration should also be given to treating the aggregates with chemical additives in a water-soluble form rather than adding the additive directly to the asphalt.

CONCLUSIONS

Results from the Texas boiling test provide valuable information that can differentiate between asphalt mixtures that are known to strip in the field and those that do not strip. Specific conclusions are as follows.

1. The number of mixing times affects the test results significantly. The best differentiation between stripping and nonstripping mixtures occurred when the specimen was mixed only once. Therefore, in the standard procedure the specimen is prepared by mixing once.
2. The mixing temperature produced a significant effect on test results: the higher initial aggregate temperature produced less stripping. Test results, however, indicated that when aggregates were heated to 325°F, the results more consistently differentiated between stripping and nonstripping mixtures. Therefore, 325°F was incorporated in the standard boiling test procedure.
3. Aggregates that retain less than 70 percent asphalt are tentatively judged to be moisture susceptible; aggregates that retain more than 85 percent are believed to be moisture resistant. Those between 70 and 85 percent are probably borderline and would benefit from treatment.
4. A rating board (Figure 1) should be used to make the visual estimates of the amount of asphalt retained to ensure uniformity of results. A photograph should not be used.
5. Based on a limited evaluation, the results of the Texas boiling test appeared to be useful in evaluating the effectiveness of antistripping additives. Based on these test results, the lime slurry and silanes appeared to be the most effective.

RECOMMENDATIONS

Results from this study indicate that the Texas boiling test can detect asphalt mixtures that exhibit stripping tendencies in the field. The test is rapid and can be conducted with a minimum amount of special equipment. Thus the test offers a method for the field control of aggregates and asphalts to ensure moisture-resistant asphalt mixtures and a means to evaluate proposed antistripping additives.

Because of the potential offered by this test, the following recommendations are offered.

1. The Texas boiling test should begin to be used to evaluate the moisture susceptibility of asphalt-aggregate mixtures proposed for use in construction and as a quality control test.
2. In the event that a stripping mixture is detected, the proposed antistripping additive can be tested by using the Texas boiling test to evaluate its effectiveness in improving the adhesion between the asphalt cement and each aggregate in the mixture.
3. If any component of a mixture is changed, the mixture should be reevaluated because stripping is dependent on the asphalt as well as on the aggregate and because the effectiveness of some antistripping agents appears to be aggregate and asphalt dependent.
4. Other tests such as the Texas freeze-thaw pedestal test and the wet-dry indirect tensile test should also be conducted if time allows.
5. Consideration should be given to evaluating chemical additives in their water-soluble form as aggregate pretreating agents.

ACKNOWLEDGMENT

The research described in this paper was carried out by the Center for Transportation Research, Bureau of Engineering Research, University of Texas at Austin. The authors are grateful for the support of the Texas State Department of Highways and Public Transportation and that of the FHWA, U.S. Department of Transportation.

REFERENCES

1. R.B. McGennis, R.B. Machemehl, and T.W. Kennedy. Stripping and Moisture Damage in Asphalt Mixtures. Res. Report 253-1. Center for Transportation Research, Bureau of Engineering Research, University of Texas, Austin, Dec. 1981.
2. T.W. Kennedy, F.L. Roberts, K.W. Lee, and J.N. Anagnos. Texas Freeze-Thaw Pedestal Test for Evaluating Moisture Susceptibility for Asphalt Mixtures. Res. Report 253-3. Center for Transportation Research, Bureau of Engineering Research, University of Texas, Austin, Feb. 1982.
3. T.W. Kennedy. Lime Treatment of Asphalt Mixtures. Res. Report 253-4. Center for Transportation Research, Bureau of Engineering Research, University of Texas, Austin, May 1983.
4. T.W. Kennedy, F.L. Roberts, and K.W. Lee. Prediction and Evaluation of Moisture Effects on Asphalt Concrete Mixtures in Pavement Systems. Presented at Korean Society of Engineers in America Symposium, Seoul, Korea, July 1982.
5. T.W. Kennedy, F.L. Roberts, and K.W. Lee. Evaluation of Moisture Susceptibility of Asphalt Mixtures Using the Texas Freeze-Thaw Pedestal Test. Proc., Association of Asphalt Paving Technologists, Vol. 51, 1982, pp. 327-341.
6. T.W. Kennedy, F.L. Roberts, and J.N. Anagnos. Texas Boiling Test for Evaluating Moisture Susceptibility for Asphalt Mixtures. Res. Report 253-5. Center for Transportation Research, Bureau of Engineering Research, University of Texas, Austin, May 1983.
7. T.W. Kennedy, J.W. Button, J.A. Epps, and N. Turnham. Field Study Using Lime as an Anti-

stripping Additive for Asphalt Pavement. Res. Report THM-1F. Center for Transportation Research, Bureau of Engineering Research, University of Texas, Austin, 1983.
8. T.W. Kennedy and J.N. Anagnos. Modified Texas Freeze-Thaw Pedestal Test Procedure. Res. Report. Center for Transportation Research, Bureau of Engineering Research, University of Texas, Austin (in preparation).
9. T.W. Kennedy and J.N. Anagnos. Indirect Tensile Test for Evaluating Moisture Susceptibility of Asphalt Mixtures. Res. Report. Center for Transportation Research, Bureau of Engineering Research, University of Texas, Austin (in preparation).
10. T.W. Kennedy. Hydrated Lime in Asphalt Paving. Bull. 325. National Hot Lime Association, 1984.
11. S.C. Shah. Antistripping Additives in Lieu of Mineral Fillers in Asphaltic Concrete Mixtures. Res. Report 88, Res. Project 72-3B(B), Louisiana HPR 1(12). Louisiana Department of Transportation and Development, Baton Rouge, April 1975.
12. Procedure for Evaluating Stripping of Asphalt in HMAC. Report to D-9 from District 11, Lufkin. Texas State Department of Highways and Public Transportation, Austin. 1980.
13. Virginia Test Method for Heat Stable Additives. Designation VTM-13. Virginia Department of Highways and Transportation, Richmond, 1978.
14. Qualifications of Antistripping Additives. DOTD Designation TR 317-77. Louisiana Department of Transportation and Development, Baton Rouge, Feb. 1977.
15. Manual of Testing Procedures. Bituminous Section, 200-F Series. Texas State Department of Highways and Public Transportation, Austin, 1978.
16. Mix Design Methods for Asphalt Concrete and Other Hot Mix Types. Report MS-2. Asphalt Institute, College Park, Md., July 1978.
17. Standard Specifications for Construction of Highways, Streets, and Bridges. Texas State Department of Highways and Public Transportation, Austin, 1972.
18. K. Majidzadeh and F.N. Brovald. State of the Art: Effect of Water on Bitumen-Aggregate Mixtures. HRB Special Report 98, HRB, National Research Council, Washington, D.C., 1968, 77 pp.
19. J.C. Peterson, H. Plancher, E.K. Ensley, R.L. Venable, and G. Miyake. Chemistry of Asphalt-Aggregate Interaction: Relationship with Pavement Moisture-Damage Prediction Test. In Transportation Research Record 843, TRB, National Research Council, Washington, D.C., 1982, pp. 95-104.
20. J.N. Dybalski. Cationic Surfactants in Asphalt Adhesions. Proc., Association of Asphalt Paving Technologists, Vol. 51, 1982, pp. 293-297.
21. Asphalt Antistripping Agents. Special Specification, Item 3181. Texas State Department of Highways and Public Transportation, Austin, April 1984.

APPENDIX: TEXAS BOILING TEST--STANDARD TEST PROCEDURE

Scope

The method is used as a screening device to evaluate the moisture susceptibility of an asphalt concrete mixture by visually estimating the degree of stripping after boiling in distilled water. The procedure can also be used to evaluate the effectiveness of antistripping additives added to moisture-susceptible mixtures.

Apparatus

1. Oven--an electric oven capable of maintaining a temperature of 163° ± 2.8°C (325° ± 5°F) to heat the asphalts and to heat or dry the aggregates;
2. Sample mixing apparatus--suitable equipment for hand mixing the aggregate and asphalt; includes round mixing pans of various sizes, small masonry pointed trowels, and spatulas;
3. Balance--a balance with a capacity of 5 kg that is sensitive to at least 0.1 g;
4. Hot table--an electric hot table capable of maintaining a temperature during mixing;
5. Beaker--a 1,000-mL beaker capable of being heated;
6. Source of heat--a heat source that consists of a burner or an electric heater, with beaker support or an oil bath with an internal chamber capable of holding 500 cc of distilled water and the sample; and
7. Miscellaneous apparatus--stop watches, scoops, glass rods, gloves, paper towels, and aluminum foil.

Preparation of Specimen Mixture

1. Selection of asphalt content: Determine the optimum asphalt content for the asphalt-aggregate mixture according to test method Tex-204-F (15) or other design method. For individual aggregates, a trial mixture of asphalt and aggregate should be prepared. If some of the aggregate is not coated well or if the mixture appears rich, increase or decrease the asphalt cement content, respectively, until a satisfactory mixture is secured (i.e., all aggregates are coated and no excess asphalt is left on the mixing bowl). Future refinements should consider surface area in order to ensure a relatively uniform film thickness.
2. Preparation of aggregates: If a mixture is to be evaluated, the mixture must have components representative of each of the aggregate sources and sizes. All materials should be combined in the specimen mixture in the same gradation that they occur in the field mixture. If an individual aggregate is being evaluated, use the fraction passing the 9.52 mm (3/8 in.) and retained on the 4.76 mm (No. 4) sieves. If the predominance of the material is smaller than the No. 4 sieve, a finer fraction can be tested.
3. Adding antistripping additives: If an antistripping additive is to be evaluated, it must be either blended with the asphalt or placed on the aggregate before final mixing. In case of blending with the asphalt, the asphalt needs to be preheated at 135° to 149°C (275° to 300°F). Pour 100 g of asphalt into a 6-ounce can. Add the desired amount of antistripping additives as a weight percent of the asphalt. Immediately stir the two materials with a small spatula for approximately 2 min.
4. Preparation of mixtures: Weigh out 300 g of the aggregates mixture or 100 g of an individual aggregate. Heat the asphalt cement or asphalt cement plus chemical additive at 163° ± 2.8°C (325° ± 5°F) for 24 to 26 hr, and heat the aggregate at 163° ± 2.8°C for 1 to 1.5 hr. After both materials are at 163 ± 2.8°C, pour the required asphalt cement into the preweighed aggregate, which is in a metal container on the hot table. Mix the aggregate and asphalt by hand as thoroughly and rapidly as possi-

ble. Transfer the mixture to a piece of aluminum foil and allow to cool at room temperature for 2 hr.

Test Procedure

1. Boiling mixture in water: Fill a 1000-mL beaker one-half full (500 cc) with distilled water and heat to boiling. Add the mixture to the boiling water. Addition of the mixture will temporarily cool the water below the boiling point. Apply heat at a rate such that the water will reboil in not less than 2 or more than 3 min after addition of the mixture. Maintain the water at a medium boil for 10 min, stirring with a glass rod three times during boiling, then remove the beaker from the heat. During and after boiling dip a paper towel into the beaker to skim any stripping asphalt from the surface of the water. Cool to room temperature, drain the water from the beaker, and empty the wet mix onto a paper towel and allow to dry.
2. Visual observation: Visually estimate the percentage of cement retained after boiling by comparing the specimen with a standard rating scale (Figure 1). A photograph should not be used. The mixture should also be examined on the following day after it has been allowed to dry because stripping of the fines is not as apparent when the mixture is still wet.

[Note: The standard rating scale (Figure 1) consists of samples that represent various degrees of stripping selected to provide examples at 10 percent intervals ranging from 0 percent to 100 percent retained asphalt cement.]

Report

The percentage of asphalt retained after boiling should be based on a comparison with the standard scale, not a photograph. Select the specimen nearest in appearance to the test specimen and report that as the test result.

Publication of this paper sponsored by Committee on Characteristics of Bituminous Paving Mixtures to Meet Structural Requirements.

Analysis of Asphalt Concrete Test Road Sections in the Province of Quebec, Canada

JOSEPH HODE KEYSER and BYRON E. RUTH

ABSTRACT

Data were collected from test road sections in the Province of Quebec, Canada, for the purpose of evaluating the effects of materials and in situ conditions on the performance of asphalt concrete pavements. These pavements were tested in 1980 to determine rutting, ride, and deflection characteristics. In situ conditions were determined by sampling and test measurements. Asphalt concrete cores were obtained for indirect tensile strength tests and for recovery of asphalt for conventional consistency tests (penetration, viscosity, and softening point). These data were compiled along with information contained in the original construction records and pavement crack surveys. Statistical analyses were conducted and various relationships were developed that relate to factors that influence asphalt binder properties, tensile strength, and transverse cracking. The most significant findings include (a) a verification of greater age hardening when in-service asphalt concrete pavements have air voids in excess of 4.0 percent, (b) a tentative test method that incorporates the work of Goode and Lufsey to evaluate the age hardening of binders, and (c) mathematical relationships developed from statistical analyses by using recovered asphalt penetration and traffic level for the prediction of transverse cracking. Results of other analyses are presented that define those variables that have an effect on consistency parameters, mix tensile strength, rutting, and ride quality. Dynaflect deflection basins were analyzed by using an elastic layer computer program, which resulted in the development of relationships between subgrade moduli and the fifth-sensor deflection.

Data were collected from 3-km-long test road sections for evaluation of the effects materials and in situ conditions have on pavement performance. Analyses were conducted to develop relationships (a) between asphalt consistency measurements, (b) for in situ differences in asphalt and mix properties, and (c) for differences in pavement performance. Twenty-three test sections were used as the data base. These sections were located throughout the Province of Quebec, including areas in Montreal, Sherbrooke, Trois Rivieres, Rimouski, and Lake St. Jean.

The data base contained 44 variables that were initially evaluated by using a variety of statistical methods. The data included in situ measurements of rutting, cracking, pavement response (deflections), and ride (Mays meter). In 1980 core samples were obtained from the test sections to determine the properties of the asphalt mixtures and recovered bitumens. Penetration and viscosity data for the original bitumens were also included in the data base. Parameters defining environmental conditions, drainage, soil type and moisture content, layer thicknesses, and properties of foundations and pavement materials were documented. Numerical rating systems were used to quantify variables such as traffic, drainage conditions, and type of soil.

A comprehensive series of statistical methods were used to determine which variables had a high degree of interaction and to what degree of significance the variables were related to a specific material, performance, or response parameter. Analysis of variance (ANOVA) and clustering techniques were used to assess the significance of numerous variables and their interdependency. The results derived from these analyses were used as the basis for development of relationships (mathematical models) between the most promising combinations of variables.

Single independent variable and multivariable regression analyses were conducted by using these combinations. Initially, only linear-regression analyses were conducted. Consequently, few regression equations had correlation coefficients (R^2) in excess of 0.36. Subsequently, a considerable amount of effort was expended in plotting data to select potentially suitable transformations and performing additional regression analyses.

Some of the results obtained from these analyses are discussed in detail in the ensuing segments of this paper. Emphasis is placed on both the positive and negative aspects of the mathematical models. Although these models define the effects of variables, they should not be used indiscriminately. There are many pitfalls that may be encountered in using empirical models as an analytical tool or for adaptation to the design and evaluation of asphalt concrete pavement systems.

GENERAL DESCRIPTION OF TEST ROADS

In Table 1 the basic data that describe the general characteristics of the different test sections are presented. Most of the test sections were in service for 7 to 9 years under medium traffic conditions (levels 3 and 4). Freezing index values ranged between 1,500 and 3,000 degree days. Granular base thickness varied considerably, as might be expected when considering the diversity of soil types and climatic conditions.

A typical section for pavements in the Province of Quebec is shown in Figure 1.

ASPHALT CONSISTENCY RELATIONSHIPS

Initial results from the cluster analysis indicated that penetration, viscosity, and softening point for recovered asphalts were related. Various transformations were used to develop suitable mathematical models. In Table 2 the eight best regression equations, and also Equation 9, which was mathematically derived from Equations 6 and 7, are listed.

TABLE 1 Basic Data for Test Sections

	Age	Traffic [a]	Freezing	Layer thickness, inches		Subgrade	
Section	Years	Level	Index, °days	Asphalt Conc.	Granular Base [b]	Soil Type [c]	/w%
1	9	5	1800	2.5	15	6/7	
2	9	6	1933	3.3	28	5/11	
3	9	4	2000	4.4	18	4/10	
4	8	3.5	1800	4.4	48	1/24	
5	8	5	1500	3.5	21	1/5	
6	8	2	1850	4.0	41	1/6	
8	7	2	2000	4.0	45	3/-	
9	8	4.5	2000	3.8	30	1/31	
10	7	1	2000	3.7	42	6/7	
11	9	1	2000	5.5	42	3/-	
12	7	1	2000	5.5	39	2/13	
14	7	3	1873	3.9	39	2/11	
15	7	3	1500	4.3	30	2/-	
104	8	3	2800	3.0	41	1/18	
107	7	3	3000	4.0	42	6/8	
108	7	3.5	3000	3.0	36	2/8	
109	8	4	3000	4.0	54	6/3	
110	8	4	3000	3.5	42	6/8	
111	7	3	2250	3.0	25	6/6	
114	7	4	2250	4.0	30	4/8	
116	6	3	2000	4.0	15	4/-	
120	5	4	3000	3.0	24	6/4	
121	6	4	3000	3.0	28	1/-	

[a] Traffic ranges from high (e.g., 1, Auto routes) to low (e.g., 5, rural highway, or 6, local streets).
[b] Included all granular material above subgrade that generally contains base, subbase, and sand (frost) layers.
[c] 1 = clay, 2 = clayey silt, 3 = sandy silt, 4 = silty sand, 5 = clayey sand, and 6 = sand.

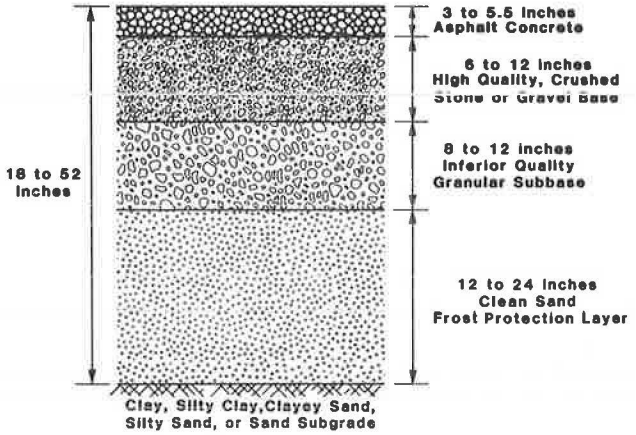

FIGURE 1 Typical pavement sections in the Province of Quebec.

Figures 2-4 illustrate the data and the developed viscosity-penetration, softening point-penetration, and viscosity-softening point relationships, respectively. It is obvious that excellent correlations were obtained between these variables.

The results suggest there is little need for more than one consistency measurement, provided the developed relationships apply to original as well as to recovered asphalts throughout the diverse range of bitumens used by the paving industry. However, it is a known fact that penetration-viscosity relationships for original asphalts can be considerably different. This difference has been used in Canada as an indicator of temperature susceptibility and to establish asphalt specifications to minimize thermal cracking at low temperatures (1,2).

Data generated and reported by Lefebvre (3) were analyzed to establish a softening point-penetration relationship for a variety of original asphalts with penetrations up to 265. Regression analysis of 24 different asphalts yielded the following equation with an $R^2 = 0.77$:

$$SP = 95.026(450/Pen)^{0.1232}$$

Comparison of this equation with Equation 7 indicates little difference between the constants and coefficients. Plots were prepared that demonstrated satisfactory agreement, except that the Lefebvre data tended to give lower softening point values when the penetration was 80 or less. Although these results are not conclusive, they imply that parameters generated by using both penetration and softening point, such as penetration index (PI), are of questionable value.

The Quebec Ministry of Transport specifications for asphalt cements include a requirement for retained penetration using the residue from the thin-film oven test. Figure 5 shows the comparison between original and recovered penetration with respect to the percent retained penetration specifications. Seven of the 15 test road binders

TABLE 2 Relationships Between Consistency Parameters

Eqn. No.	Regression Equations for Different Consistency Parameters[a]	R^2
1(a)	$Log(PEN) = 2.947 - 734.0E\text{-}7(SP)^2$	0.947
	or:	
1(b)	$(SP)^2 = 38969 - 12896\ Log(PEN)$	
2(a)	$Log(PEN) = -0.96543 + 345.48(\frac{1}{SP})$	0.958
	or:	
2(b)	$\frac{1}{SP} = 0.00299 + 0.00278\ Log(PEN)$	
3(a)	$Log(PEN) = 4.0438 - 0.8692\ Log(VIS)$	0.671
	or:	
3(b)	$Log(VIS) = 4.0355 - 0.77183\ Log(PEN)$	
4(a)	$\frac{1}{PEN} = 0.001122 + 378.0E\text{-}7(VIS)$	0.815
	or:	
4(b)	$VIS = 94.282 + 21602(\frac{1}{PEN})$	
5(a)	$VIS = -2544.7 + 23.828(SP)$	0.848
	or:	
5(b)	$SP = 110.89 + 0.03559(VIS)$	
6	$VIS = 13.053(\frac{6000}{PEN})^{0.7835}$	0.940
7	$SP = 91.812(\frac{450}{PEN})^{0.1579}$	0.956
8	$VIS = 105.66(\frac{SP}{91.812})^{4.7843}$	0.937
9	$VIS = 99.337\ (\frac{SP}{91.812})^{4.9621}$ (derived from 6&7)	

Note: Presented in this table are mathematical models developed by statistical regression analyses to define the relationships between penetration at 25°C, viscosity at 275°F, and the ring and ball softening point temperature for bitumens recovered from cores in 1980.

[a]PEN = penetration at 25°C (77°F); VIS = viscosity, centistokes at 135°C (275°F); and SP = softening point temperature (°F).

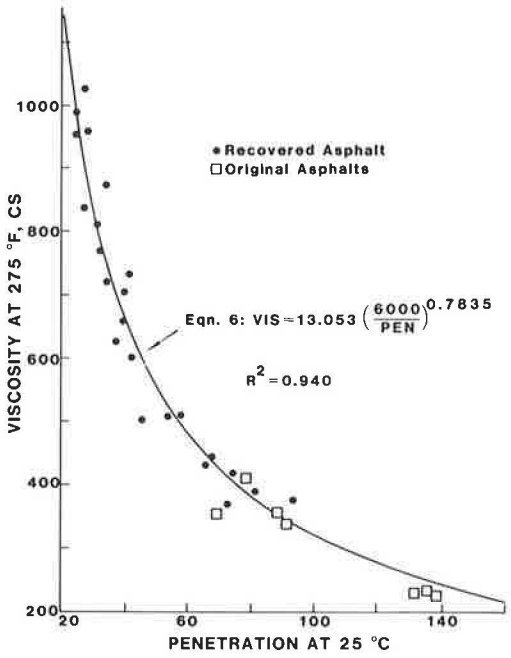

FIGURE 2 Viscosity-penetration relationship.

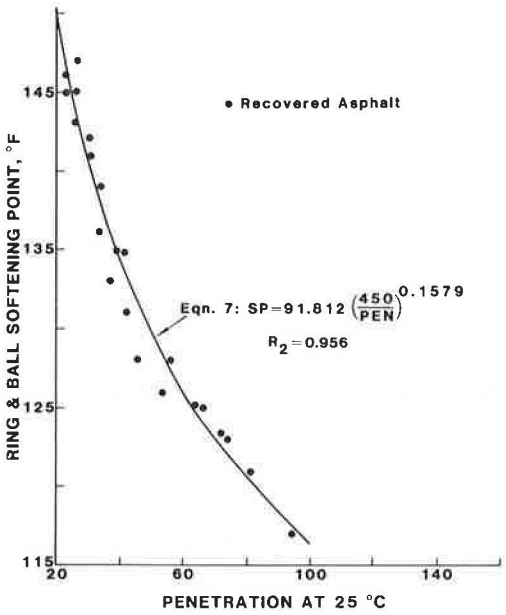

FIGURE 3 Ring and ball softening point-penetration relationship.

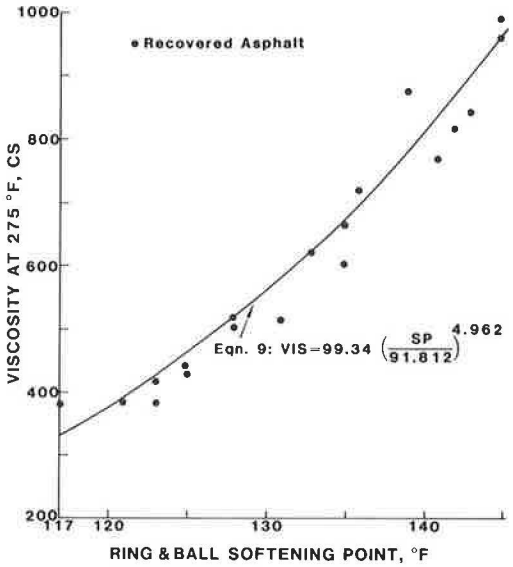

FIGURE 4 Viscosity-ring and ball softening point relationship.

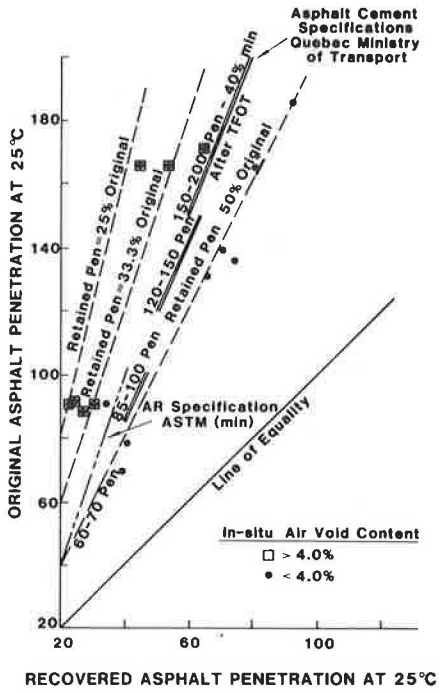

FIGURE 5 Retained penetration comparison.

had a retained penetration greater than 49 percent, which is considerably greater than the current Ministry of Transport specifications. The remaining eight binders had a lower retained penetration than either the ASTM asphalt residue (AR) or the Ministry of Transport specifications.

Although these specifications do not apply to recovered asphalts, it is an indication that excessive hardening has occurred. The exact cause of the high degree of age hardening was not identified, although it was observed that the in-service air void content was greater than 4.0 percent in seven of the test sections. These sections had the lowest retained penetration, which suggests that inadequate compaction was achieved during construction, the bitumen was damaged because of overheating, or the composition of the bitumen promoted rapid age hardening.

RELATIONSHIPS BETWEEN ASPHALT CONSISTENCY AND MIX PARAMETERS

A review of the results from clustering and initial regression analyses indicated that (a) asphalt consistency values were affected by the air void content of the mix and (b) both parameters influenced the tensile strength of cores obtained from the test section. Additional statistical analyses were performed, which resulted in the development of the regression equations given in Table 3.

TABLE 3 Relationship for Air Void Effects and Tensile Strength

Eqn. No.	Regression Equations for Different Parameters[a]	R^2
9	$VIS = 531.74\ (VV)^{0.2904}$ (sections 1 to 15)	0.762
10	$VIS = 295.87\ (VV)^{0.3295}$ (sections 104 to 121)	0.692
11	$PEN = \frac{50.43}{(VV)^{0.3237}}$ (sections 1 to 15)	0.714
12	$PEN = \frac{144.34}{(VV)^{0.6384}}$ (sections 104 to 121)	0.910
13	$\Delta VIS = 203.61\ (VV)^{0.5716}$ (sections 1 to 15)	0.692
14	$\Delta VIS = 84.37\ (VV)^{0.7068}$ (sections 104 to 121)	0.707
15	$\Delta PEN = 35.30\ (VV)^{0.300}$ (sections 1 to 15)	0.488
16	$\Delta PEN = 55.46\ (VV)^{0.357}$ (sections 104 to 121)	0.255
17	$ITS = 134.01 + 0.2461\ (VIS) - 15.4203\ (VV)$	0.567
18	$\text{Log } ITS = 0.6694 + 0.6531 \text{ Log } (VIS) - 0.2479 \text{ Log } (VV)$	0.567
19	$\text{Log } ITS = 3.31015 - 0.48905 \text{ Log } (PEN) - 0.2842 \text{ Log } (VV)$	0.471
	or: $ITS = \frac{2042.44}{(PEN)^{0.48905}\ (VV)^{0.2842}}$	

Note: Presented in this table are mathematical models developed by statistical regression analyses to define the relationships between tensile strength, air void content, and asphalt consistency parameters from cores in 1980.

[a]VIS = viscosity @ 135°C, cs; PEN = penetration @ 25°C; VV = percent air void content; ITS = indirect tensile strength @ 0°C (32°F); 0.05 in./min rate of loading.

Asphalt Consistency

Equations 9 and 10 (Table 3) indicate that viscosity at 275°F (135°C) would increase between 20 to 60 centistokes for each 1.0 percent increase in air void content for pavements that are about 7 to 9 years old. A similar effect was obtained from Equations 11 and 12, which predict a decrease in penetration of between 1 to 20 for each 1.0 percent increase in air void content. Figures 6 and 7 show these relationships and the plotted data for viscosity and penetration of the Abson recovered asphalts versus the in-service air void contents. The trends illustrated in these figures suggest that the 275°F (135°C) viscosity and the 77°F (25°C) penetration for recovered asphalts are primarily dependent on the grade of the original asphalt cement and the air void content. Obviously, high air void contents after 7 to 8 years of traffic were the result of inadequate compaction and insufficient densification due to traffic. Four of the 23 test sections had air void contents in excess of 6.4 percent. These sections were constructed with 60-100 penetration asphalt cements and were among the nine sections exhibiting the most cracking.

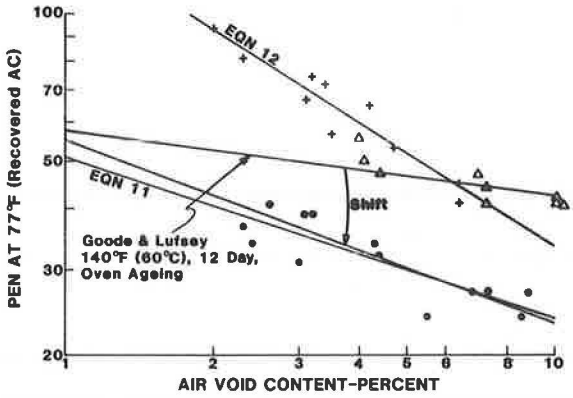

FIGURE 7 Recovered asphalt penetration-air void content relationship.

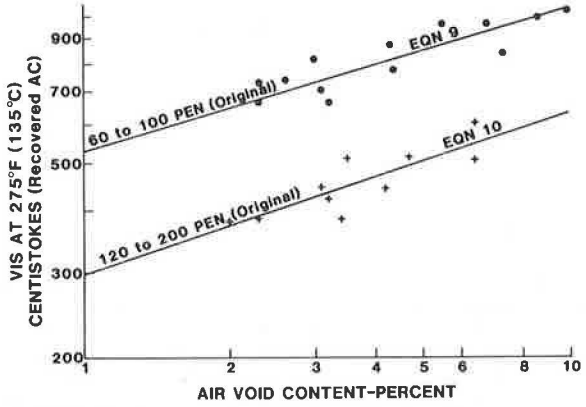

FIGURE 6 Recovered asphalt viscosity-air void content relationship.

Relationships were developed for the actual change from original to recovered consistency values with respect to in-service air void content. Figure 8 shows the data and resulting trend from regression Equations 13 and 14. Regression analyses were also performed to evaluate the change in penetration as a function of air void content. Equations 15 and 16 define the change in penetration. Correlation coefficients for these equations were extremely low. However, the exponents in both equations are almost identical. This suggests that the effect of air void content on hardening is logarithmically linear for any grade of asphalt cement, and the constant in the

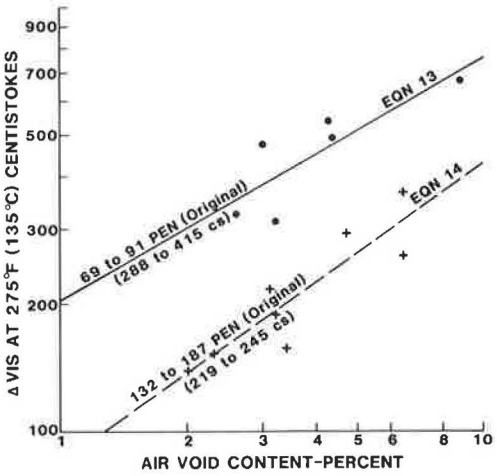

FIGURE 8 Effect of in-service air void content on asphalt hardening.

equation denotes the shift factor to accommodate different grades.

Air void and penetration data from an asphalt hardening study by Goode and Lufsey (4) were used to predict the oven age hardening effects. Their aging procedure used mixtures prepared with a 91 penetration asphalt cement at different air void contents and processed for 12 and 63 days in a 140°F (60°C) oven. The penetration was obtained on asphalts recovered from specimens with and without oven aging. The average penetration of the nonaged specimens was 65.4. The difference between this value and the 12-day oven-cured specimens was used to establish the following equation:

$$\Delta PEN = 9.66\ (VV)^{0.372}$$

where

ΔPEN = 65.4 - PEN at 12 days,
VV = air void content (%), and
R^2 = 0.704.

By using the following expression,

$$RPEN = 65.4 - S(\Delta PEN)$$

where RPEN is the penetration of asphalt recovered from test road samples, and S is the shift factor to predict penetration of approximately 8-year-old pavements with 85-100 penetration grade asphalt.

The shift factor obtained to predict the in-service penetration from the 12-day oven-aging data was 1.85. The shifted relationship is illustrated in Figure 7. The relatively good approximation provided by this procedure suggests that the methods used by Goode and Lufsey (4) could be used to estimate the age hardening of asphalts and the resulting indirect tensile strength. This, of course, depends on the amount of hardening that occurs in mixing either in the laboratory or at the plant, as well as the difference in climatic effects and composition of the asphalt. Additional experimentation will be required to determine if this procedure is valid or can be modified to accommodate different grades of asphalt cement and the effects of time exposure and hardening rate.

Mix Tensile Strength

Indirect tensile tests were conducted on cores at 0°C (32°F) by using a 0.05 in./min (1.27 mm/min) rate of loading. The influence of asphalt viscosity and air void content on the tensile strength of these cores is defined in Table 3 by Equations 17 and 18. Figure 9 illustrates the relationship provided by Equation 17. The relatively low R^2 values for both equations appeared to be caused primarily by excessive variation in tensile strength or air void content values or both.

According to Equation 17, an increase in viscosity of 100 centistokes would increase the tensile strength at 0°C by 25 psi. Similarly, a 1.0 percent increase in air void content would reduce the tensile strength by 15 psi. This reduction is approximately equivalent to a 5 to 10 percent reduction in tensile strength. Other limited indirect tensile strength data from cores provided a 12 percent change per percent voids for air void contents between 5.5 and 8.7 percent. Results by other investigators indicate that the dynamic modulus of asphalt concrete pavements is reduced by about 11.5 percent for each 1.0 percent increase in air void content (5).

The substantial difference between test temperatures for viscosity and indirect tensile tests may have a significant effect on the interpretation of these results. The viscosity and shear susceptibility of these recovered asphalts at lower temperatures (e.g., 0°C) could possibly provide more realistic and meaningful relationships. Unfortunately, only penetration values were available for analysis

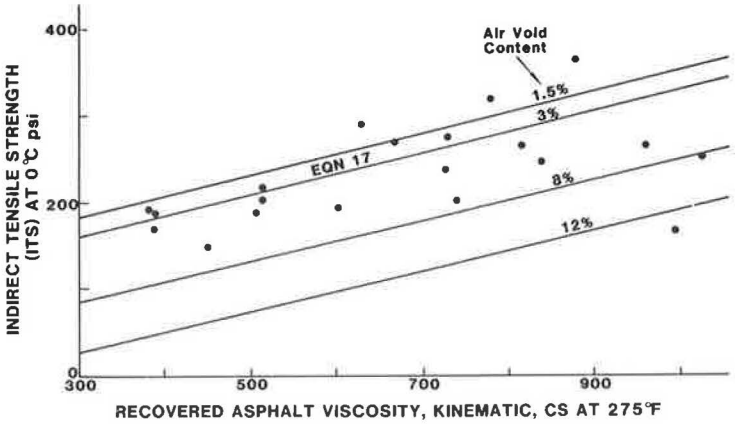

FIGURE 9 Effect of viscosity and air void content on indirect tensile strength.

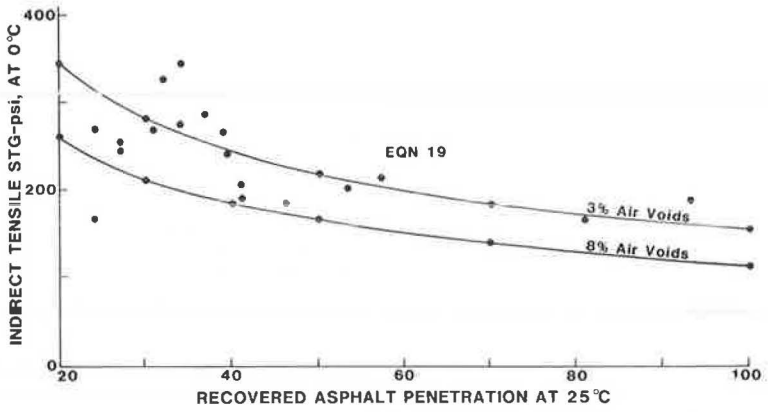

FIGURE 10 Effect of penetration and air void content on indirect tensile strength.

at these lower temperatures. These values and corresponding air void content values were used in a regression analysis that yielded Equation 19 and is shown with the plotted data in Figure 10. Although the correlation coefficient is low, it is obvious that the effect of air voids on tensile strength is almost identical for both Equations 18 and 19.

The Schweyer constant stress rheometer was used to obtain low temperature viscosity data for asphalts recovered from five test sections. The regression equation developed by using the 0°C viscosities is

$$ITS = 0.6164\ (VC)^{0.2815} - 15.42\ (VV)$$

where

ITS = indirect tensile strength at 0°C (psi),
VC = constant power viscosity (J = 100 w/m³) at 0°C (Pa.s),
VV = air void content (%), and
R^2 = 0.851.

This equation predicts the indirect tensile strength within about 10 percent of the measured values. In this equation, a 1.0 percent change in air void content would decrease the indirect tensile strength 6 to 8 percent within the 180- to 280-psi range.

The results of analyses for consistency and tensile strength indicate the need to attain a reasonably low air void content in the compacted mix that will minimize age hardening and the potential for low-temperature cracking. In general, pavements with air voids in excess of 4 or 5 percent after 1 or 2 years of service are likely to harden sufficiently to prevent any further traffic densification. This in turn can promote additional hardening of asphalt binders and eventually result in cracking.

MIX PARAMETERS RELATED TO PAVEMENT CRACKING

Longitudinal pavement cracking was classified according to the lineal feet of simple or multiple and polygonal longitudinal cracks in the 3-km-long test sections. The amount of longitudinal cracking was insignificant and generally less than 100 lineal feet. Only four pavement sections exhibited longitudinal cracking in excess of 50 lineal feet. Two of these sections had extremely low penetration and the other two had exceptionally high pavement deflection values.

Transverse cracks were classified as the number of simple or multiple and polygonal transverse cracks in a test section. Also, the severity of transverse cracking was rated according to the class of cracking (class 1, 2, or 3). Except for sections 5 and 15, the amount of class 1 cracking exceeded 58 percent of the total transverse cracking. Twelve of the 23 test sections had less than 35 transverse cracks (1.2 cracks per 100 m). Cracking in the other sections increased to a maximum of 176 transverse cracks (5.9 cracks per 100 m) for section 10.

Efforts to develop correlations between longitudinal cracking and other parameters were unsuccessful primarily because of the lack of longitudinal cracking. Analysis of the transverse cracking data resulted in the development of single and multiple variable relationships. Some of the regression equations that were obtained from analyses of the transverse cracking data are given in Table 4. Equations 20-22 have extremely low correlation coefficients, but suggest that penetration, traffic, and air void content affect the degree of pavement cracking.

When plotted, transverse cracking and penetration data indicated that the data should be segregated according to traffic levels 3 to 6 (medium to light) and 1 to 3 (heavy to medium). The results of regression analyses for each category of traffic yielded excellent results. Figure 11 shows the trends for regression Equations 23 and 24 and the corresponding data points.

Sections 1 and 6 were excluded from the analysis because they did not conform to the trends of other test sections. The thickness of the asphalt concrete in section 1 was only 2.5 in. (64 mm), which was less than any of the other pavements. Section 6 had extremely low Dynaflect deflections and an extremely high subgrade modulus, which apparently produced considerably less cracking, even though the recovered asphalt penetration was 31.

Multivariable regression analyses were performed in an attempt to improve the correlation by using combinations of those parameters considered to have a significant effect on pavement cracking. Equation 25 defines transverse cracking (TC) on the basis of penetration and traffic. This equation format plus the interaction of the thickness and traffic gave Equation 26 (see Table 4). Although the correlation is mediocre ($R^2 \approx 0.68$), the effects of penetration, thickness, and traffic appear to be generally reasonable. Figure 12 illustrates the effects of these variables. If traffic is lighter than levels 1 to 3, the amount of cracking is minimal, particularly if the in situ binder penetration is greater than 40, as shown in Figure 11. Increasing pavement thickness from 3 to 6 in. (76 to 154 mm) when the penetration is greater than 40 reduces the amount of

TABLE 4 Relationships for Transverse Cracking

Eqn. No.	Regression Equations for Different Parameters[a]	Std. Error	R^2
	Single Variable Correlations:		
20	$TC = 25.326 + 0.396(\frac{120}{PEN})^{3.3}$	37.8	0.311
21	$TC = -131.251 + 247.84(TRA)^{-0.3}$	33.8	0.449
22	$TC = 4.8471 + 10.035\ (VV)$	40.4	0.213
23	$TC = 5.15 + 0.235(\frac{120}{PEN})^{3.3}$	----	0.933
	(Light to medium traffic, Levels 6 to 3)		
24	$TC = 21.58(\frac{120}{PEN})^{1.206}$	----	0.855
	(Medium to heavy traffic, Levels 3 to 1)		
	Multiple Variable Correlations		
25	$TC = -129.37 + 0.323(\frac{120}{PEN})^{3.3} + 218.57(TRA)^{-0.3}$	27.6	0.650
26	$TC = -239.91 + 0.321(\frac{120}{PEN})^{3.3} + 407.54(TRA)^{-0.3} - \frac{17.05\ THICK}{(TRA)^{-0.3}}$	27.2	0.679
27	$TC = -97.619 + 0.0682(VIS) + 263.96(TRA)^{-0.3} - 0.0228(FI) - 0.0426\ (THICK)(ITS)$	27.9	0.682

Note: Presented in this table are mathematical models developed by statistical regression analyses to define the relationships between different parameters and transverse cracking.

[a]TC = total simple, multiple, and transverse cracks; PEN = penetration @ 25°C; TRA = traffic (1 = heavy, 6 = light); THICK = thickness of asphalt concrete pavement (in.); FI = freezing index (° days); ITS = indirect tensile strength at 0°C.

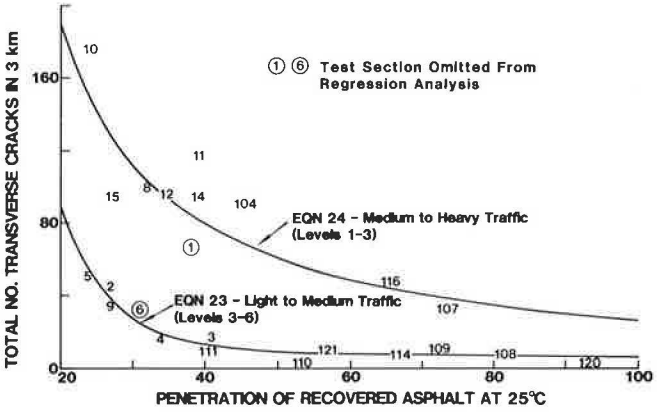

FIGURE 11 Effect of binder penetration and traffic on transverse cracking.

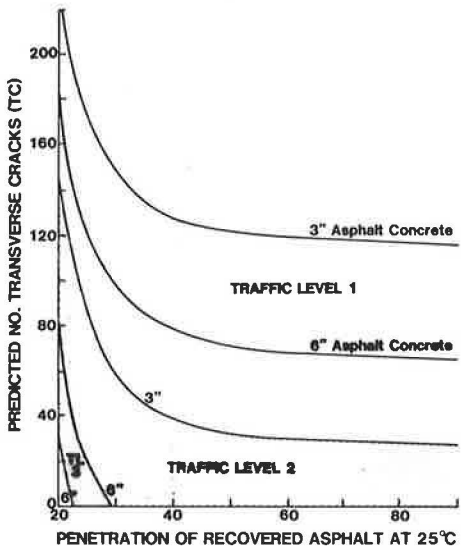

FIGURE 12 Effect of variables on transverse cracking.

cracking by about 40 percent for heavy traffic conditions (level 1). Furthermore, these results indicate that 3 in. of asphalt concrete with a binder penetration of 50 to 60 is essentially equivalent to 6 in. of asphalt pavement with a 25 penetration asphalt binder.

Asphalt viscosity, traffic, freezing index, thickness, and indirect tensile strength parameters were evaluated to determine their effects on transverse cracking. The results of these analyses did not indicate any improvement over those expressions containing penetration as the asphalt consistency measurement. Equation 27 defines the best multiple variable correlation obtained using the viscosity. This equation indicates that cracking increases with viscosity and traffic, decreases with an increase in freezing index, and decreases with increasing thickness and tensile strength. The effect of these variables on cracking is logical, but the effects of variables other than viscosity and traffic are relatively insignificant.

The most important aspects of the transverse cracking analyses are the effects of traffic level and asphalt binder consistency. It is apparent that traffic contributes to the severity of transverse thermal cracking. Equally important is the extremely

significant effect of penetration, as shown in Figure 11, which suggests that pavement cracking would be substantially reduced if in situ penetration was never less than about 40.

PREDICTION OF TRANSVERSE CRACKING

Two models were selected for evaluation and use in the prediction of transverse cracking and cracking temperatures. The Haas model (6) is intended for use in calculating a cracking index. The Asphalt Institute procedure (7) determines a critical temperature that may be compared with the minimum temperature in the winter to evaluate the potential for thermal cracking. The following discussion presents the results and demonstrates that neither method appears suitable for transverse cracking predictions for highways in Quebec.

A method for designing asphalt pavements to minimize low-temperature shrinkage cracking was proposed by Haas (6). This method was empirically derived by using stiffness of the asphalt concrete pavement, a winter design temperature, and type of soil to predict a cracking index (I). The cracking index is the number of transverse cracks per 500 ft of two-lane highway pavement. Transverse cracks that do not extend across one lane are not counted.

A computer program was written to facilitate computation of the cracking index. Data for the recovered asphalt were used instead of data for the original asphalt because of incomplete data. This produced computed stiffness and cracking index values much greater than those that would have been obtained by using original asphalt properties. The effect of age was evaluated by using the difference between cracking index values for in-service age in years and zero years ($I_n - I_o$). This assumes that the in-service asphalt stiffness for input into the model does not change over the age of the pavement.

The results of cracking index computations for the different test sections are given in Table 5. The predicted amount of cracking ranged from 394 to 847 transverse cracks in a 3-km section as compared with 1 to 176 in the test road sections. Figure 13 shows that the amount of predicted cracking is not related to the number of simple transverse cracks observed in 1980. It is obvious that the cracking index is not suitable for Quebec conditions. The extremely high degree of predicted cracking may be due to using the recovered asphalt properties. However, even the soft residues (e.g., 93 penetration) gave exceedingly high values of cracking (e.g., 394 per 3 km).

The Asphalt Institute has compiled the results of various researchers into design procedures to minimize low-temperature transverse cracking (7). Critical temperatures (T_c) for cracking were computed for each section by using these procedures. The difference between T_c and the minimum winter temperature (T_{min}) was used to compare the amount of transverse cracking in the test sections. The data in Table 6 present values of T_c, T_{min}, and $T_c - T_{min}$. Figure 14 illustrates that there was

TABLE 5 Cracking Index Values (Haas method)

Section No.	Io @ 0 yrs[a]	I_n @ Age in yrs[a]	19.69 (I_n-I_o) No. Cracks in 3km	No. of Transverse Cracks		
				simple	polygonal & multiple	Total
1	1016	1054	748	38	25	63
2	1870	1913	847	34	11	45
3	825	861	704	7	11	18
4	749	784	689	9	9	18
5	999	1037	748	27	23	50
6	750	785	689	11	21	32
8	1471	1450	650	17	83	100
9	1321	1360	768	32	3	35
10	2303	2337	669	107	69	176
11	894	933	768	91	4	95
12	923	953	591	28	59	87
14	684	712	551	64	30	94
15	934	965	610	59	38	97
104	1626	1665	768	49	42	91
107	1251	1281	591	23	9	32
108	931	960	571	3	5	8
109	1757	1794	729	4	6	10
110	2391	2430	768	1	0	1
111	1910	1942	630	7	4	11
114	851	879	551	7	1	8
116	825	850	473	35	12	47
120	916	936	394	1	1	2
121	956	983	532	3	7	10
$\bar{x}$			654			49.1
Std. Dev.			111			44.6

[a]Predicted number of transverse cracks in 500 ft.

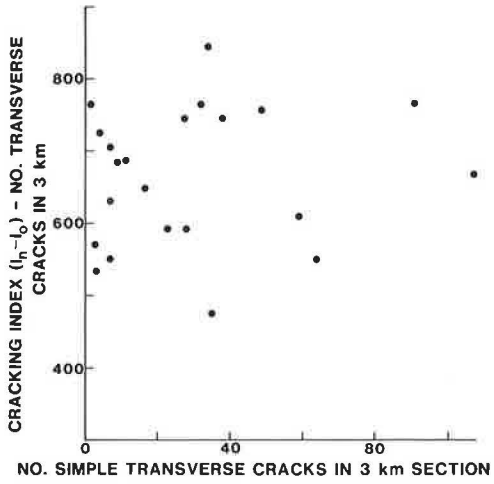

FIGURE 13 Comparison of predicted to measured transverse cracks.

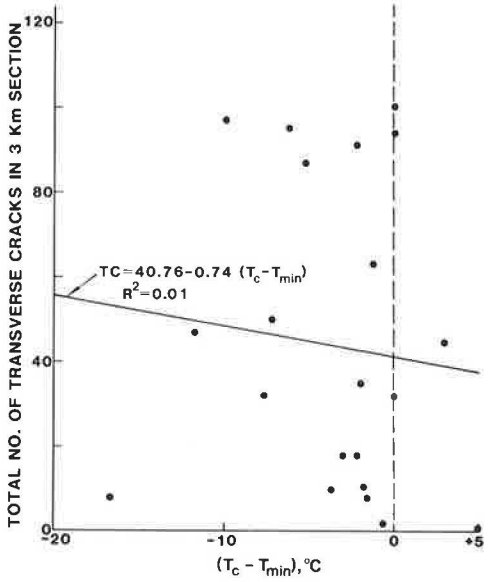

FIGURE 14 Comparison of transverse cracking to predicted differential cracking temperature.

TABLE 6 Predicted Cracking Temperatures (Asphalt Institute method)

Section	Predicted Cracking Temp. (T_c), °C	Winter minimum Temp., °C	T_c - T_{min}
1	-33	-31.7	-1.3
2	-32	-35.0	+3.0
3	-33	-30.0	-3.0
4	-34	-31.7	-2.3
5	-35	-27.8	-7.2
6	-37.5	-37.2	0
8	-37	-37.2	0
9	-32	-30.0	-2.0
11	-38	-31.7	-6.3
12	-37	-31.7	-5.3
14	-33	-32.8	0
15	-40	-30	-10.0
104	-39	-36.7	-2.3
107	-47	-39.4	-7.6
108	-41	-39.4	-1.6
109	-43	-39.4	-3.6
110	-39	-43.9	+4.9
111	-39	-37.2	-1.8
114	-44	-27.2	-16.8
116	-39	-27.2	-11.8
120	-40	-39.4	-0.6
121	-41	-39.4	-1.6

essentially no correlation between the number of transverse cracks and the predicted differential cracking temperature. These poor results may be due to insufficient range in data, inadequate methodology for computation of critical temperatures, or poor definition of minimum temperatures over the time period that the pavements have been in service.

EVALUATION OF RIDE QUALITY

The Mays meter is used extensively for evaluation of the ride quality of pavements. Measurements were obtained on the test road sections during the summer and winter. Inspection of the Mays meter and transverse cracking values indicated that ride quality was not generally degraded by cracking. Little difference was observed between summer and winter measurements.

Regression analyses were performed to evaluate variables that had a significant effect on ride quality. Only three of the various combinations of variables were sufficiently significant to warrant further investigation. These three regression equations are given in Table 7.

The equations indicate that ride quality decreases as the soil becomes more sandy and increases with freezing index, percent fill, depth of drainage ditches, and the amount of transverse cracking. Close inspection of plots of these parameters versus Mays meter values indicated that the bias created by the limited range and interaction of variables produced a meaningless relationship. Only the percent fill has any basis for rational interpretation when considering trends of the plotted data. Improved ride in fill sections may be the result of better quality control and drainage conditions than encountered in cut sections. The indication that better riding quality occurs with greater cracking is probably related to the design and quality control on major highway pavements that are subjected to heavy traffic. However, in some instances traffic can produce definite improvement in ride over that obtained immediately after construction.

RUT DEPTH OBSERVATIONS

Attempts to develop rational relationships to predict rut depth from the available data were totally unsuccessful. This may be partly caused by the insufficient range in rutting depth values. Only 5 of the 23 test sections exhibited rutting in excess of 0.5 in., and 10 sections had nonmeasurable, insignificant rutting. Therefore, it can be concluded that rutting is not a problem when similar asphalt mixtures and pavement designs are used for new construction in comparable climatic regions.

TABLE 7 Relationship Between Mays Meter (ride quality) and Other Parameters

Equation No.	Regression Equations for Different Parameters [a]	R^2
28	MMW = 3.093 - 0.0049 (FI) - 0.0041 (PF) - 0.0862 (DDD) - 0.0046 (TC)	0.510
29	MMW = 3.131 - 0.0059 (FI) - 0.0044 (PF) - 0.0910 (DDD) - 0.0047 (TC) + 0.063 (TYSOL)	0.585
30	MMS = 2.541 - 0.0037 (FI) - 0.0029 (PF) - 0.075 (DDD) - 0.0043 (TC) + 0.079 (TYSOL)	0.608

[a]MMW = Mays meter (winter), MMS = Mays meter (summer), FI = freezing index, degreee-days), PF = percent fill, DDD = depth of drainage ditches (ft), TC = total number of transverse cracks, TYSOL = type of soil: clay = 1.0, clayey silt = 2.0, sandy silt = 3.0, silty sand = 4.0, clayey sand = 5.0, and sand = 6.0.

DYNAFLECT DEFLECTIONS AND SUBGRADE MODULI

Dynaflect deflections were used to estimate the moduli of the pavement and subgrade. These subgrade modulus values were plotted versus the Dynaflect fifth-sensor (S-5) deflections, as shown in Figure 15. These data were evaluated by using regression analysis, and the results were compared to the relationship established by Majidzadeh (8). Figure 15 shows that the estimated moduli are less than those obtained by Majidzadeh for equivalent deflections. The slope of the line established by the regression equation indicates a greater difference between the Majidzadeh and estimated modulus values at low deflections (high modulus). This may be attributed to the differences in pavement systems or to calibration and accuracy of the Dynaflect deflections.

An analysis was performed to tune the layer moduli and deflection basins for five of the test sections that were selected to encompass a large range in recovered penetration and Dynaflect deflections values. Low-temperature viscosities were determined for recovered asphalts by using the Schweyer constant stress rheometer. The dynamic modulus of the asphalt concrete pavement was obtained by using these viscosities and a correlation between viscosity and dynamic modulus (9). The computed asphalt concrete moduli and the estimated base and subgrade moduli with their appropriate Poisson's ratio were used in a multilayer elastic stress analysis program. The predicted deflection basins were compared with Dynaflect measured basins. The base and subgrade moduli were adjusted slightly until the predicted deflection response was essentially equal to the mean measured response.

The subgrade moduli obtained from this analysis were plotted against the predicted deflection (S-5), as illustrated in Figure 15. The slope of the line is parallel to the Majidzadeh relationship and suggests that this trend may provide an excellent relationship for the prediction of subgrade moduli. Regression analysis of these data yielded the following equation:

$$E_S = 5.3966(S_5)^{-1.0006}$$

where

E_S = subgrade modulus (psi),
S_5 = Dynaflect fifth-sensor deflection (in.), and
R^2 = 0.997.

Other analyses were conducted in an attempt to relate deflections to transverse cracking. In general, the deflection data were stratified according to the hardness of the binder (penetration). Therefore, no improvement was obtained over the previously presented transverse cracking predictions. There was a definite indication that pavement stresses were related to the degree of cracking.

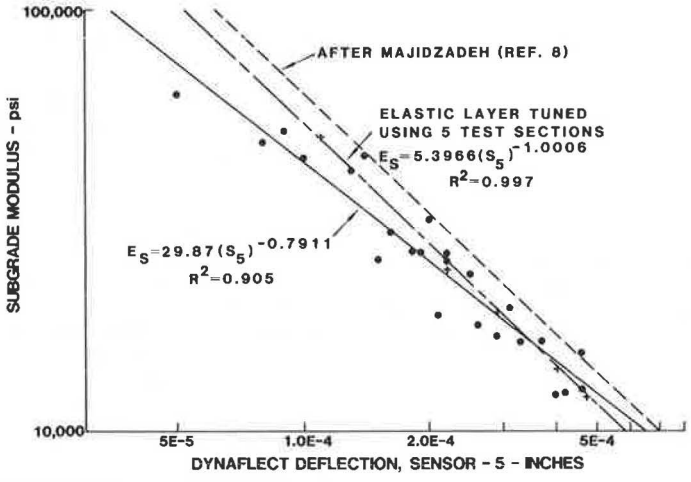

FIGURE 15 Subgrade modulus-Dynaflect deflection relationships.

However, this is also masked by the thermal stresses that were not evaluated because pavement cooling curves were not available.

SUMMARY

The results of analyses performed on data collected from 23 test road sections in the Province of Quebec, Canada, provided information on the effect that certain parameters have on the properties and performance of asphalt concrete. The most significant finding was that consistency of recovered asphalts and traffic level defined to a high degree of significance the amount of transverse cracking on 6- to 9-year-old pavements.

The effects of air void content on asphalt hardening and indirect tensile strength at 0°C (32°F) were identified. Relationships were developed by using the results of the Goode and Lufsey (4) investigations, which compared voids and penetration by using the 60°C (140°F) oven aging test. A tentative procedure for prediction of in-service hardening of bitumens has been suggested for use in determining the effects of air void content and age on the indirect tensile strength and consistency (penetration or viscosity) of the asphalt binder.

Relationships developed between penetration, viscosity, and ring and ball softening point of recovered asphalts demonstrate that these consistency measurements are related to such a high degree of significance that only one of these consistency parameters is needed to characterize the asphalt. However, viscosity-penetration relationships for original asphalts are not uniquely related and form the basis for selection of asphalts to minimize low-temperature cracking potential.

Several existing models were used to predict transverse cracking and cracking temperature. Analysis of these values and the actual number of observed transverse cracks provided absolutely no correlation between predicted and actual cracking. The use of two categories of traffic level and the penetration (25°C) of recovered asphalt provided an excellent relationship with the number of transverse cracks.

The depth of rutting was insignificant, except for five sections that had ruts in excess of 0.5 in. No relationships were found to define the amount of rutting.

Analysis of ride quality using the Mays meter indicated that fill sections provide a better ride than do cut sections. The amount of transverse cracking had little effect on ride quality. Other variables were considered in the analysis, but their effect on ride quality was marginal or not significant.

A relationship was developed between subgrade moduli and Dynaflect fifth-sensor deflections. Data from five sections that had substantially different characteristics were used and adjusted in a multilayer elastic stress analysis program until the predicted deflection basin conformed to the mean or typical Dynaflect basin. The developed relationship compares favorably with the data generated to estimate subgrade moduli for the other test sections.

REFERENCES

1. N.W. McLeod. A 4-Year Survey of Low Temperature Transverse Pavement Cracking on Three Ontario Test Roads. Proc., Association of Asphalt Paving Technologists, Vol. 41, 1972.
2. L.M. Lefebvre, A. Dion, R. Langlois, D. Champagne, and N.W. McLeod. Paving the 385-Mile Jones Bay Access Road with 300/400 Penetration Asphalt Cement. Proc., Association of Asphalt Paving Technologists, Vol. 47, 1978.
3. L.M. Lefebvre. A Modified Penetration Index for Canadian Asphalts. Proc., Association of Asphalt Paving Technologists, Vol. 39, 1970.
4. J.F. Goode and L.A. Lufsey. Voids, Permeability, Film Thickness vs. Asphalt Hardening. Proc., Association of Asphalt Paving Technologists, Vol. 34, 1965.
5. B.E. Ruth, K.W. Kokomoor, A.E. Veitia, and J.D. Rumble. Importance and Cost Effectiveness of Testing Procedures Related to Highway Construction. Final Report, Project 245-U39. Department of Civil Engineering, University of Florida, Gainesville, 1982.
6. A Method for Designing Asphalt Pavements to Minimize Low Temperature Shrinkage Cracking. Res. Report 73-1. Asphalt Institute, College Park, Md., 1973.
7. Design Techniques to Minimize Low-Temperature Asphalt Pavement Transverse Cracking. Res. Report 81-1. Asphalt Institute, College Park, Md., 1981.
8. K. Majidzadeh. An Overview of Deflection Parameters for Performance Analysis. Proc., International Symposium on Bearing Capacity of Roads and Airfields, Vol. 2, 1982.
9. B.E. Ruth, L.A.K. Bloy, and A.A. Avital. Prediction of Pavement Cracking at Low Temperatures. Proc., Association of Asphalt Paving Technologists, Vol. 51, 1982.

Publication of this paper sponsored by Committee on Characteristics of Bituminous Paving Mixtures to Meet Structural Requirements.

Laboratory Study of the Effects of Recycling Modifiers on Aged Asphalt Cement

DAVID E. NEWCOMB, BETTY J. NUSSER, BADRU M. KIGGUNDU, and DENNIS M. ZALLEN

ABSTRACT

An on-going research program to study the effects of recycling modifiers on aged asphalt cement is described. So far nine modifiers and one aged asphalt have been investigated. Blends of the modifiers and asphalt were tested chemically and physically in both an unaged condition and after aging in a rolling thin-film oven. Chemical characterization included clay-gel compositional analysis, solubility testing, and high pressure gel permeation chromatography. Physical testing included penetration, viscosity, and ductility testing. The results indicate that the influence of the polar to saturate ratio (P/S) on consistency may diminish with higher levels of aromatic fractions in the modifiers. Higher levels of P/S in the modifiers were also responsible for better properties on aging of the blends. Clay-gel results revealed that the compositional effects of modifiers are not additive in the blends. On aging, the blends increased in asphaltene content and decreased in polar content. Solubility test results revealed that the effects of different modifiers on aged asphalt can be detected. Solubility trends were also observed after aging of the blends. Blends with low aging indices were also found to have an increase in state of peptization after aging.

Since the mid-1970s recycling of asphalt pavements has been a popular concept in the paving industry. As described by Epps et al. (1), recycling can be accomplished either in-place or in a central plant and can be either a hot or cold process. In any case, it almost always involves the use of some type of petroleum product to restore the asphalt binder to some acceptable level of consistency. These petroleum products may be soft asphalts, high polar content oils, or highly aromatic oils. Modifiers are added to the aged binders to

1. Restore the recycled asphalt to a suitable consistency for construction,
2. Restore optimal chemical characteristics to the aged asphalt,
3. Provide sufficient additional binder to coat any new aggregate, and
4. Provide sufficient binder content to satisfy mixture design requirements.

The engineer must have a means of specifying the type and amount of modifier to be used for a particular recycling project. The study presented in this paper was undertaken with this goal in mind for hot, central plant operations.

Organizations such as ASTM and the West Coast User-Producer Group have recognized the need for recycling agent specifications and are currently taking action to develop these specifications. It is widely acknowledged that modifiers should change the consistency of the recycled binder to an acceptable level and increase the life expectancy of recycled mixtures (2-4). Kari et al. (4) have also stated that modifiers should disperse readily in recycled mixtures and produce uniform mixture properties from batch to batch. With respect to chemistry, Davidson et al. (2) have concluded that modifiers should be compatible with the aged asphalts so that syneresis does not occur. Dunning and Mendenhall (3) suggest that the modifiers should also serve to redisperse asphaltenes in the aged binders.

Some of the more commonly used tests to chemically characterize modifiers include the Rostler-Sternberg analysis (2,5-8), clay-gel adsorption chromatography (3), and refractive index (5). Recommended procedures for physical characterization include viscosity measurements at different temperatures (2-5), flash point (2-6), and rolling thin-film oven (RTFO) parameters (3).

The purpose of this research project was to identify useful chemical and physical parameters by which to evaluate modifiers and blends of modifiers and aged asphalt binders. Further research will be conducted on laboratory recycled mixtures.

The experiments in this study were based on clay-gel compositional analysis of the modifiers. The parameters used were the ratios of polar to saturate fractions (P/S) and the percent aromatics in the modifiers. Figure 1 shows the test matrix. The levels of high, medium, and low for both parameters were selected arbitrarily according to the materials on hand.

PHYSICAL CHARACTERIZATION

Modifier Tests

The modifiers were initially tested for flash point

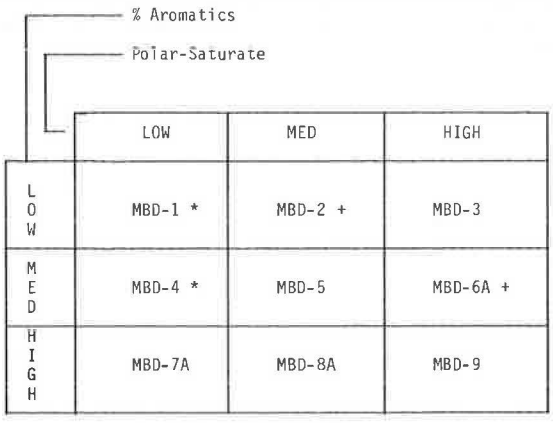

FIGURE 1 Test matrix.

and consistency at different temperatures. The flash point test was performed as a safety precaution for the laboratory. Viscosities were run at 100°, 140°, and 212°F to investigate the temperature susceptibility of these products. The viscosity at 140°F was also used to calculate the percentage of modifiers to be incorporated into the blends.

Tests on Blends

Different percentages of each modifier were blended with the aged asphalt and tested for viscosity at 140°F to determine the final blend percentages for viscosities between 3,000 and 4,000 poises. Consistencies of the final blends were tested over a wide range of temperatures. Penetration values were obtained at 39.2° and 77°F in accordance with ASTM D 5 (9). A temperature-penetration index (TPI) was established according to the following formula:

$$TPI = (\text{Pen at } 77°F)/(\text{Pen at } 39.2°F) \quad (1)$$

Thus the greater the value of TPI, the more temperature susceptible was the material at low temperature.

Likewise, viscosity was measured at 39.2° and 77°F in a constant pressure (Schweyer) rheometer. The principle and operation of this device have been described by Schweyer et al. (10). The information from this test can be used to compute the viscosity of a material over a range of shear rates. High temperature viscosities were measured at 140° and 275°F in accordance with ASTM D 2171 and D 2170, respectively. The viscosities at 275°F were used to evaluate the differences in high temperature behavior of the materials.

The blends were subjected to conditioning in the RTFO as per ASTM D 2872 (9). After this treatment they were tested for penetration at 39.2° and 77°F, viscosity at 140°F, and ductility at 77°F. The penetration values were also expressed as percentages of the unaged penetration values. The aging index for the viscosity at 140°F was calculated according to the following formula:

$$\text{Aging index} = (\text{Viscosity at } 140°F \text{ after RTFO}) \div (\text{Viscosity at } 140°F \text{ before RTFO}) \quad (2)$$

CHEMICAL CHARACTERIZATION

Clay-Gel Composition

The clay-gel compositional analysis ASTM D 2007 (11) was used in this study. Basically, this procedure involves separation of the asphalt into the four generic fractions of asphaltenes, saturates, aromatics, and polars. Several modifications have been implemented in order to apply this procedure to a variety of asphaltic materials. These modifications are as follows:

1. Stripping the silica column with 70 percent toluene/30 percent methanol (vol. %),
2. Discarding the factor 0.88 in the calculations for polar compounds,
3. Solvent amount to separate asphaltenes,
4. Sample size,
5. Solvent percentages to strip the polar fraction,
6. Discarding use of separatory funnel and calcium chloride,
7. Stripping the polar fraction with additional polar solvent, and
8. Alternate solvent evaporation.

Repeatability is a question that has been raised with regard to the clay-gel compositional analysis. By using the modifications outlined, excellent repeatability has been obtained on a variety of asphaltic materials. With the exception of asphaltenes, the clay-gel procedure has produced results within ASTM limits. The ASTM procedure was originally developed for extender oils, which are very low in asphaltenes. The modifications outlined here have produced results within 0.6 percent in the asphaltene fraction.

Solution Properties

Heithaus (12) defined the solution properties of an asphalt system in terms of asphaltene peptizability (P_a), Maltene peptizing power (P_o), and the state of peptization (P). The properties defined by Heithaus are considered important in describing the mutual solubility of asphalt fractions. Waxman et al. (13) have correlated solubility parameters for asphaltic materials to solubility parameters of various solvents. They also observed that removing resins from an asphalt reduced the solubility characteristics of the asphalt.

Venable and Peterson (14) evaluated a series of fresh and aged asphalts as well as recycling agents by using Heithaus parameters. They found that variations in these parameters were dependent on the type of material and the conditions of the test. Venable and Peterson observed that asphaltene peptizability was inversely related to the polar functionality content of the asphalt system.

The solubility evaluation technique used in this study was designated the Heithaus/Waxman approach. This technique was chosen because the test procedures are similar, except for the following items.

1. The data handling and interpretation are different.
2. The nonpolar solvent used for titration is different. Heithaus used n-heptane and Waxman used n-dodecane. In this study n-dodecane was used.
3. The microscope magnification is 400X in the Heithaus procedure and 88X in the Waxman procedure. Observations in this study were made at 100 to 150X.

The Heithaus/Waxman procedure was generally the same as that used by Venable and Peterson (14) with some additional modifications. These modifications included reducing the sample size to 1.00 ± 0.05 g for five data points, weighing the samples to ±1 mg, and maintaining constant polar solvent (toluene) volumes throughout the test program. A finite and consistent wait time was instituted before testing. All testing was conducted at 77° ± 5°F. The modifications to the procedure by Venable and Peterson were made in order to conserve asphalt, reagents, and time without reducing the reliability of the results.

The Heithaus parameters are obtained from the following relationships (14):

$$\text{Flocculation ratio (FR)} = (\text{Volume of toluene}) \div [\text{Volume (toluene + n-dodecane)}] \quad (3)$$

$$\text{Dilution ratio (X)} = [\text{Volume (toluene + n-dodecane)}] \div (\text{Weight of asphalt}) \quad (4)$$

The calculations from these equations are presented graphically as FR versus 1/X. The extension of this plot leads to FR_{max} and $1/X_{min}$ as the ordinate and abscissa intercepts, respectively. These values are used to compute the Heithaus parameters:

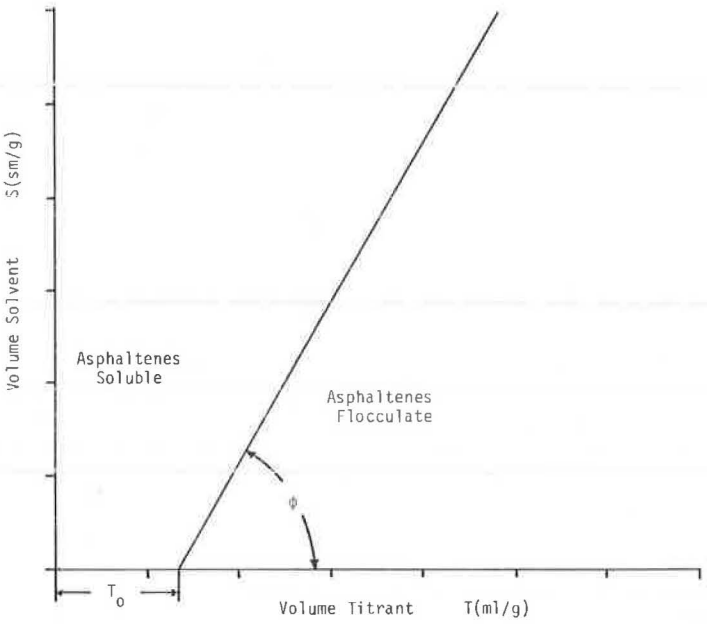

FIGURE 2 Schematic showing Waxman parameters.

$$P_a = 1.0 - FR_{max} \quad (5)$$

$$P_o = FR_{max}(1 + X_{min}) \quad (6)$$

$$P_a = P_o/(1 - P_a) = 1 + X_{min} \quad (7)$$

The Waxman parameters are shown in Figure 2. The cotangent of the angle ϕ is defined as:

$$\text{Cot } \phi = (T - T_o)/S \quad (8)$$

where

T = volume of titrant (mL) per gram of material,
T_o = volume of titrant per gram of material required for precipitation of the least soluble asphaltenes, and
S = volume of solvent per gram of material.

The value of T_o is considered to be a measure of the stability of the complex collodial micellar asphaltenes in the asphalt. It has the same function as the X_{min} term in the Heithaus procedure.

High Pressure Gel Permeation Chromatography

The high pressure gel permeation chromatography (HP-GPC) technique separates components of a sample based on molecular size. P.W. Jennings at Montana State University is currently involved in a 17-state project investigating this technique as a possible

TABLE 1 Modifier Properties

Modifier Designation	Clay-Gel Compositional Analysis, percent				P/S	Viscosity at 100°F, poises	Viscosity at 140°F, poises	Viscosity at 212°F, poises	Flash Point COC, °F
	Asphaltenes	Saturates	Aromatics	Polars					
MBD-1	0.25	84.34	12.68	2.74	0.03	0.77	0.25	0.07	420
MBD-2	20.35	20.78	23.19	35.48	1.72	15,300	490	14	555
MBD-3	9.78	15.96	24.34	49.87	3.12	20,000	540	9.7	535
MBD-4	0.73	50.49	43.95	4.97	0.10	0.19	0.08	0.03	325
MBD-5	0.20	23.46	49.02	27.73	1.18	16	2.8	0.25	435
MBD-6A	23.79	15.22	26.37	34.63	2.28	5,400	300	9.8	460
MBD-7A	0.24	22.17	62.40	15.55	0.70	6.2	1.0	0.15	445
MBD-8A	0.30	17.78	60.20	21.98	1.24	9.9	1.8	0.24	480
MBD-9	0.12	6.44	64.50	29.07	4.51	27	2.3	0.19	420

TABLE 2 Pope AFB Recovered Asphalt Properties

Property	Value
Penetration at 39.2°F, 200 g, 60 sec, 0.1 mm	11
Penetration at 77°F, 100 g, 5 sec, 0.1 mm	22
Viscosity at 39.2°F, 0.05 sec^{-1} (poises)	1.2×10^9
Shear susceptibility (c) at 39.2°F	0.71
Viscosity at 77°F, 0.05 sec^{-1} (poises)	2.4×10^7
c at 77°F	0.61
Viscosity at 140°F (poises)	56,800
Viscosity at 275°F (cSt)	1,413
Clay-gel composition (%)	
Asphaltenes	43.57
Saturates	10.79
Aromatics	12.78
Polars	32.82

tool in the evaluation of asphaltic materials. The samples in this study were sent to Jennings for analysis.

The results of the initial work by Jennings et al. (15) suggest that molecular size distribution is characteristic of each asphalt and may be a valuable tool in designing pavement recycling projects, as well as defining excellent to poor pavements. Jennings suggests that HP-GPC analysis along with physical tests and additional chemical tests such as compositional analysis may lead to a reasonable explanation for the performance of pavements.

The HP-GPC chromatograms are divided into three regions: large molecular size (LMS), medium molecular size (MMS), and small molecular size (SMS). The calculated areas are based on elution time and a standard asphalt sample. Jennings has stated that the LMS region along with the asphaltene content is significant in predicting pavement performance. This was based only on data from the Montana study.

MATERIALS

Materials used in this study included nine compositionally different modifiers and one field-sampled aged asphalt. Figure 1 shows that two highly paraffinic oils and two soft asphalts were included along with five commercially available recycling agents. The compositions and physical characteristics of the selected modifiers are given in Table 1. The level of aromatics ranged from 12.7 percent for MBD-1 to 64.5 percent for MBD-9. MBD-1 also had the lowest P/S value (0.03). MBD-9 had the highest P/S level (4.51). Although MBD-3 is marketed as a recycling agent, it exhibits viscosities comparable to the soft asphalts included in the study.

The aged asphalt used in this study was extracted from pavement samples obtained at Pope Air Force Base (AFB), North Carolina. The pavement feature was a taxiway that had been constructed in 1941. The taxiway was so severely fatigued that it was recycled immediately after sampling. The aged paving mixture had the characteristics of high void content and a large amount of fine material in the gradation. The properties of the extracted asphalt are given in Table 2.

RESULTS AND DISCUSSION

Physical Properties of Asphalt-Modifier Blends

The physical properties of the unaged blends are given in Table 3. Some of these data are shown in Figures 3-5 with respect to the P/S in the modifiers. This parameter appeared to have more of an influence on the physical behavior of the blends than did the level of aromaticity in the modifiers.

Figure 3 shows the effect of modifier P/S on the temperature-penetration index of the blends. The effect of modifier P/S is greatest at the low level of aromatic fractions ranging from 1.40 at a P/S of 0.03 to 3.05 at a modifier P/S of 3.12. Modifiers in the medium level of aromaticity (<50 percent) showed a less dramatic increase in blend TPI. Blends made with high aromatic modifiers (>50 percent) showed no difference in TPI according to the modifier P/S. Therefore, at modifier aromatic contents of less than 50 percent, the low-temperature susceptibility of the blends increased with the increasing P/S's of the modifiers.

Shear susceptibility of the blends at 39.2°F, in general, decreased with an increasing P/S, as shown

TABLE 3 Physical Properties of Unaged Blends

Blend	% Modifier	Pen at 39.2°F 200 gm, 60 sec, 0.1 mm	Pen at 77°F 100 gm, 5 sec, 0.1 mm	η at 39.2°F, 0.05 sec^{-1} x 10^7 poises	"c" at 39.2°F	η at 77°F, 0.05 sec^{-1} x 10^6 poises	"c" at 77°F	η at 140°F, poises	η at 275°F, cSt
MBD-1	16	50	70	3.3	0.43	3.3	0.53	3,970	277
MBD-2	65	35	65	11	0.62	3.6	0.53	3,340	414
MBD-3	36	19	58	68	0.96	3.7	0.86	3,470	426
MBD-4	10	37	63	5.8	0.52	3.0	0.64	3,500	350
MBD-5	13	37	68	13	0.66	3.2	0.73	3,990	405
MBD-6A	43	34	73	8.9	0.65	2.3	0.76	3,420	497
MBD-7A	13	37	71	10	0.68	2.7	0.72	3,260	350
MBD-8A	16	36	68	13	0.68	2.6	0.75	3,760	405
MBD-9	12	36	74	16	0.79	2.4	0.80	3,500	424
Control	0	11	22	120	0.71	24	0.61	56,800	1413

η = Viscosity

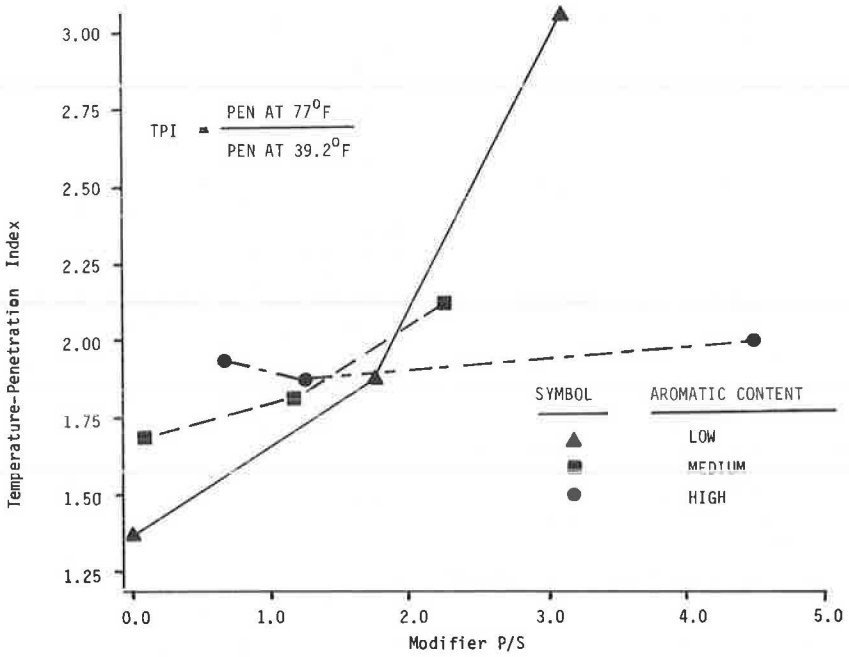

FIGURE 3 Effect of modifier P/S on temperature-penetration index.

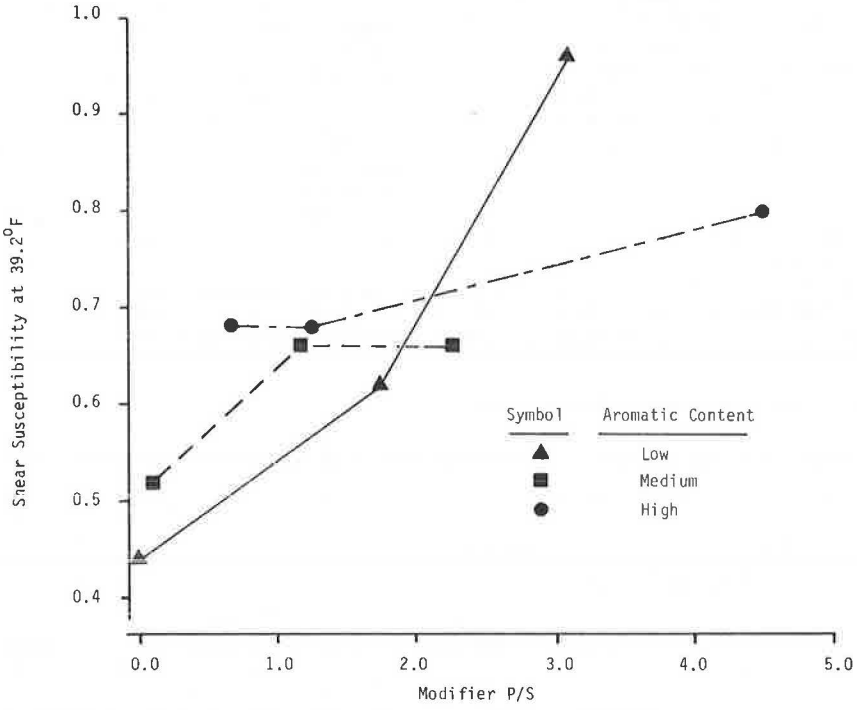

FIGURE 4 Effect of modifier P/S on shear susceptibility at 39.2°F.

in Figure 4. As the value of c approaches 1, the flow becomes more Newtonian. As c decreases from 1, the nature of the material is more psuedoplastic (shear susceptible). Again, those blends that have modifiers low in percent aromatics showed the most dramatic differences, ranging from a c value of 0.43 at a low P/S level to 0.96 at a high P/S. These same trends were noted for the shear susceptibility values at 77°F.

Figure 5 shows that the viscosities at 275°F for blends made with low P/S modifiers all had values less than 400 cSt. Increasing P/S's in the modifiers led to increased viscosities at 275°F.

The properties of the blends after conditioning in the RTFO are given in Table 4. Some of these data are presented in Figures 6-8. The P/S's of the modifiers had even greater effects on the aged blends than on the unaged blends.

The percent of penetration retained after the RTFO increased with increasing modifier P/S at 77°F, as can be seen in Figure 6. In this test the level of aromaticity in the modifiers did not have the dampening effect on the modifier P/S as noticed for the unaged blends. At 77°F the percentage of retained penetration ranged from a low of 24 percent for MBD-4 to 57 percent for MBD-2 and MBD-3.

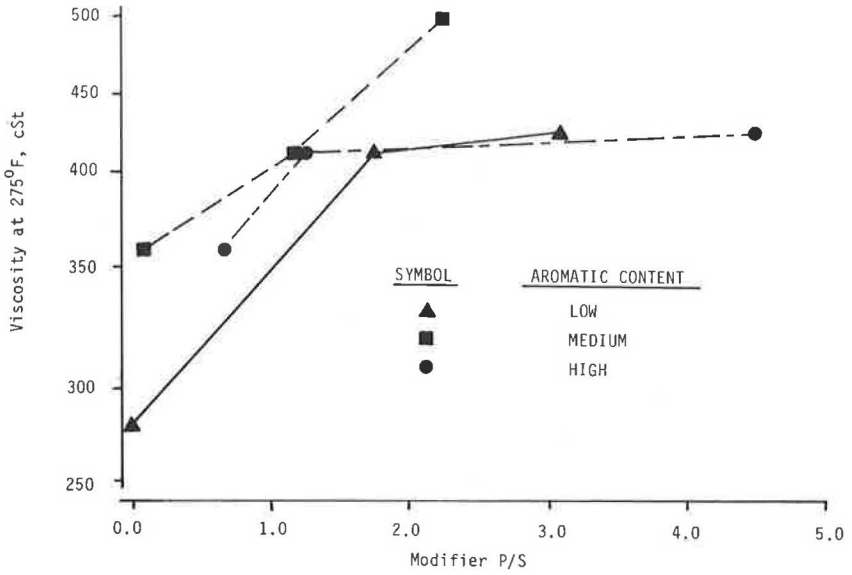

FIGURE 5 Effect of modifier P/S on viscosity at 275°F.

TABLE 4 Physical Properties of Blends After RTFO

Blend	Pen at 39.2°F, 200 gm, 60 sec		Pen at 77°F, 100gm, 5 sec		Viscosity at 140°F		Ductility at 77°F,
	0.1 mm	Percent of Unaged	0.1 mm	Percent of Unaged	Poises	Aging Index	cm/min, cm
MBD-1	19	38	28	40	118,700	29.9	4
MBD-2	17	48	37	57	23,620	7.1	10
MBD-3	14	74	33	57	10,220	2.9	100+
MBD-4	5	14	15	24	222,000	63.4	4
MBD-5	8	22	20	29	57,470	14.4	8
MBD-6A	20	59	38	52	13,520	4.0	100+
MBD-7A	9	24	21	31	43,020	13.2	9
MBD-8A	21	58	39	53	14,040	3.7	59
MBD-9	18	50	37	51	12,420	3.5	100+
Control	3	27	8	36	534,000	9.4	4

Figure 7 shows that as the P/S of the modifiers increased, the aging index decreased in a logarithmic fashion. The aging index was highest for the blend made with MBD-4 at 63 and lowest for the MBD-3 blend at 3. This appears to be a useful parameter for evaluating recycled blends, as does the ductility after RTFO, as shown in Figure 8. It is shown that blends with high P/S modifiers all exceeded 100 cm in the ductility test at 77°F. Blends made with low and medium P/S modifiers had ductilities considerably less than 100 cm.

Clay-Gell Analysis and Solution Properties

Based on the percent modifier added to the aged asphalt to prepare the blends used in this study, the respective percentages of asphaltenes, saturates, aromatics, and polars were calculated to see if the effect of the modifier was additive. Without exception, the actual percent asphaltenes was lower and the polar percentage was higher. This indicates that the effects of the modifiers were not additive. The modifiers increased the solubility of the maltene phase and redispersed the asphaltenes into the maltene phase. The data in Table 5 give three examples that illustrate this phenomenon. On RTFO aging, there was an increase in the asphaltene content and a decrease in the polar content. The saturate and aromatic fractions remained essentially the same. The clay-gel data for each blend unaged and aged are

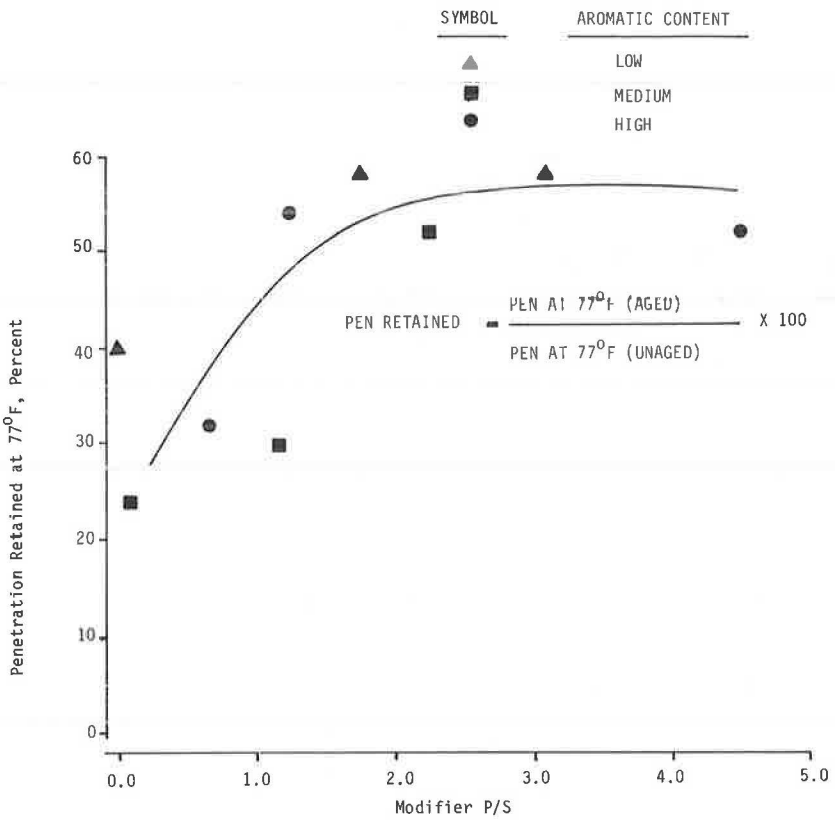

FIGURE 6 Effect of modifier P/S on percent penetration retained at 77°F after RTFO.

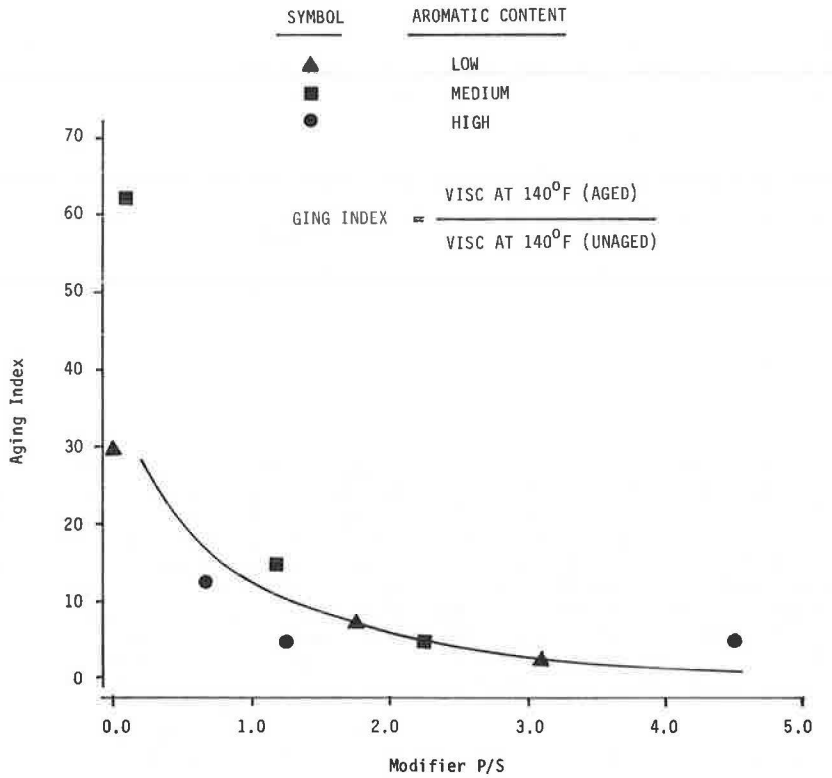

FIGURE 7 Effect of modifier P/S on aging index.

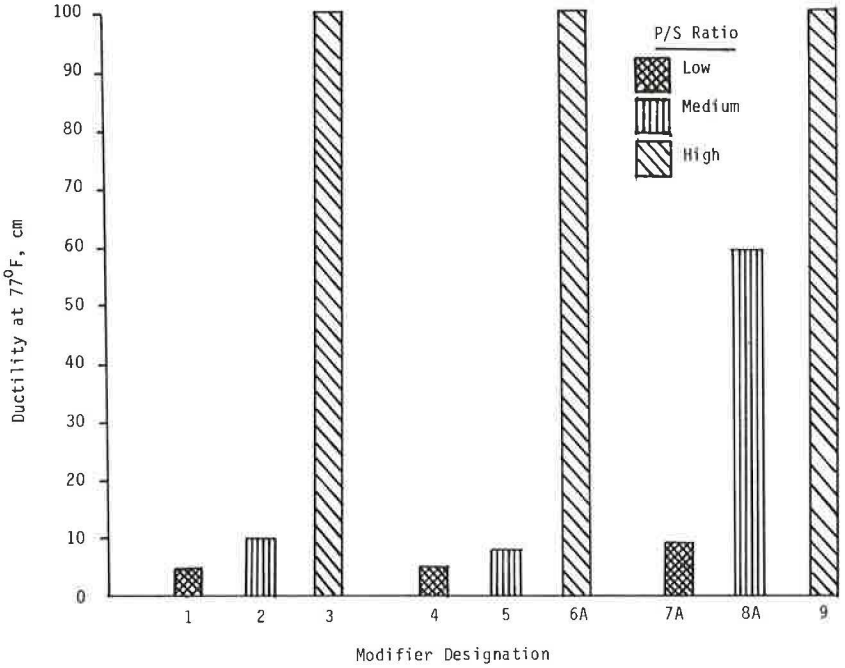

FIGURE 8 Ductility of blends after RTFO.

given in Table 6. The trends seen in the clay-gel analysis of the blends completed so far in this project correlate well with physical data obtained on aging.

The data in Tables 7 and 8 present the solubility data of the aged and unaged blends, respectively. The results for one of the blends, MBD-3, are shown in Figures 9 and 10. These figures show the curves for the control asphalt (Pope AFB), the unaged blend, and the RTFO-aged blend. Figure 9 is a Heithaus plot and Figure 10 is a plot of the Waxman data.

The results given in Table 7 reveal a decrease in asphaltene peptizability and cot ϕ values from the control sample in all blends except MBD-6A. According to Venable and Peterson (14), MBD-6A may have a lower polar functionality and a more homogenous molecular system than the other unaged blends. The general trend noted in these results was also observed by Venable and Peterson, even when modifiers were added to fresh asphalts. The state of asphaltene peptization and the maltene peptizing power were improved through the addition of the modifiers. This is further evidenced by the value of T_o and

TABLE 5 Examples of Compositional Effects of Modifiers on Aged Asphalt

	ASPHALTENES	SATURATES	AROMATICS	POLARS
POPE WHOLE AGED ASPHALT	43.57	10.79	12.78	32.82
MBD-1 16%	0.25	84.34	12.68	2.74
CALCULATED	36.64	22.56	12.76	28.01
ACTUAL	32.90	20.94	15.14	29.74
MBD-6A 43%	21.47	15.07	33.56	29.44
CALCULATED	33.71	12.80	22.33	31.45
ACTUAL	30.32	11.09	15.86	42.59
MBD-9 12.5%	0.12	6.44	64.50	29.07
CALCULATED	38.15	10.27	19.56	32.49
ACTUAL	32.68	10.09	17.00	39.90

TABLE 6 Clay-Gel Analysis of Blends

Blend	Asphaltenes		Saturates		Aromatics		Polars	
	Unaged	Aged	Unaged	Aged	Unaged	Aged	Unaged	Aged
MBD-1	32.90	34.24	20.94	22.51	15.14	13.39	29.74	29.86
MBD-2	26.56	28.01	14.79	15.55	16.82	15.53	41.53	40.53
MBD-3	26.12	30.92	11.39	14.34	14.26	15.24	48.15	39.50
MBD-4	35.86	39.10	13.29	12.79	17.60	18.75	33.38	29.36
MBD-5	33.76	35.95	12.27	13.16	16.99	16.98	36.79	33.54
MBD-6A	30.32	33.15	11.09	12.38	15.86	16.06	42.59	38.41
MBD-7A	31.98	34.95	11.93	11.24	21.33	20.40	34.76	33.41
MBD-8A	30.81	33.69	10.60	11.56	22.31	23.86	36.28	30.90
MBD-9	32.68	33.20	10.09	11.42	17.00	18.65	39.90	36.68
Control	37.70	40.34	11.75	12.31	15.72	12.72	36.25	34.63

TABLE 7 Solubility Test Results (unaged)

Material Type	Heithaus Parameters				Waxman Parameters	
	P_a	P_o	P	X_{min}	T_o	Cot ø
MBD-1	0.204	1.750	2.199	1.199	1.252	0.224
MBD-2	0.313	1.678	2.441	1.441	1.117	0.596
MBD-3	0.259	2.085	2.816	1.816	1.798	0.358
MBD-4	0.207	1.884	2.374	1.374	1.465	0.208
MBD-5	0.237	1.800	2.358	1.358	1.355	0.302
MBD-6A	0.370	1.673	2.655	1.655	1.274	0.760
MBD-7A	0.338	1.476	2.230	1.230	1.411	0.420
MBD-8A	0.290	2.179	2.691	1.691	1.757	0.191
MBD-9	0.419	1.070	1.842	0.842	0.911	0.713
CONTROL[a]	0.356	1.316	2.044	1.044	0.901	0.623

Note: Unaged = RTFC aging.

[a]Aged recovered asphalt treated in the same manner as the blends.

TABLE 8 Solubility Test Results (aged)

Material Type	Heithaus Parameters				Waxman Parameters	
	P_a	P_o	P	X_{min}	T_o	Cot ø
MBD-1	0.193	1.636	2.026	1.026	1.068	0.207
MBD-2	0.267	1.892	2.580	1.580	1.497	0.397
MBD-3	0.308	1.995	2.882	1.882	1.887	0.438
MBD-4	0.161	2.113	2.518	1.518	1.546	0.178
MBD-5	0.119	2.074	2.355	1.355	1.250	0.165
MBD-6A	0.215	2.197	2.797	1.797	1.814	0.264
MBD-7A	0.153	1.868	2.206	1.206	1.140	0.216
MBD-8A	0.392	1.019	1.676	0.676	1.438	0.318
MBD-9	0.193	2.213	2.742	1.742	1.711	0.248
CONTROL[a]	0.224	1.942	2.503	1.503	1.586	0.243

Note: Aged = RTFC aging.

[a]Aged recovered asphalt treated in the same manner as the blends.

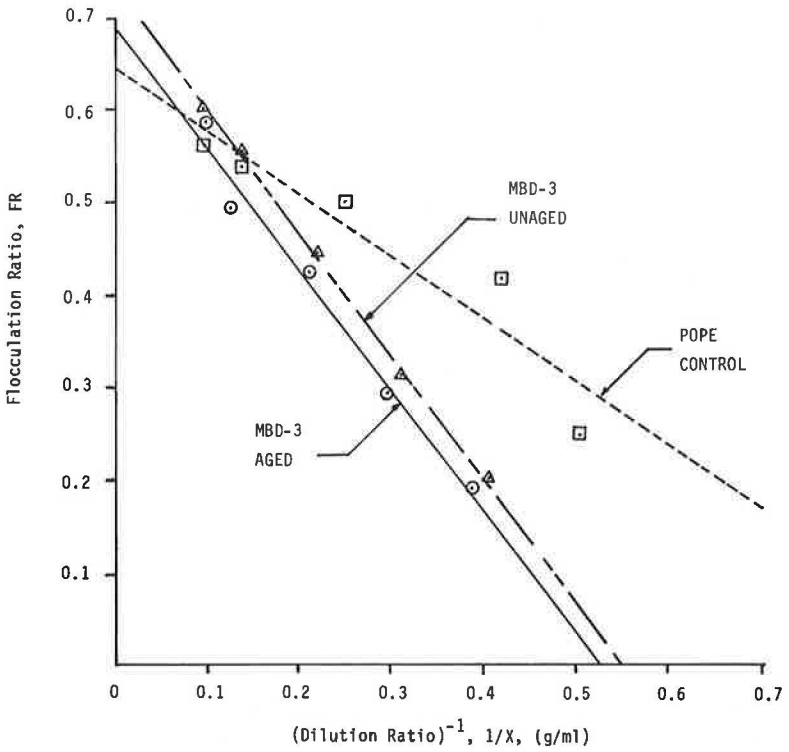

FIGURE 9 Heithaus solubility test results.

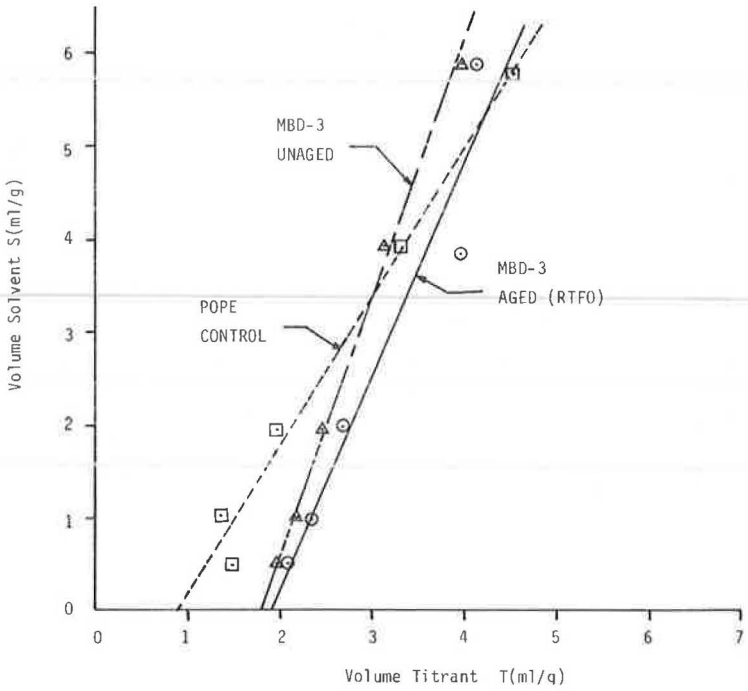

FIGURE 10 Waxman plot of S versus T.

the rightward shift of the curve for MBD-3 in Figure 10. The leftward shift of the curve for MBD-3 in Figure 9 further confirms this observation.

The solubility test results given in Table 8 reveal a decrease in asphaltene peptizability except for MBD-3 and MBD-8A. A similar trend may be noted in the cot ϕ values. According to Venable and Peterson (14), an increase in asphaltene peptizability after an oxidation process implies that the peptizing components from the maltenes are being converted to asphaltenes. This also implies that the maltene peptizing power decreases.

The result of T_o for MBD-3 indicates an overall improvement in the solvency characteristics after RTFO aging. It is interesting to note that MBD-3 also had the lowest aging index, the highest retained penetration, and a ductility value greater than 100 cm after aging. This blend also showed a large gain in its aromatic fraction and a lower P/S after aging.

Blend MBD-8A showed decreases in X_{min} and T_o on RTFO conditioning. This may indicate a degradation of the blend. The drastic decreases in X_{min} for MBD-8A is evidenced by a sharp decrease in the peptizing power of the maltenes.

HP-GPC Analysis

Jennings et al. (15) report that there are five features to examine in the HP-GPC chromatograms for interpretation:

1. Elution time of the largest molecules,
2. Height of the curve in the LMS region,
3. Elution time of the curve maximum,
4. Height of curve maximum relative to height in LMS and SMS regions, and
5. Height of the curve in the SMS region.

Figure 11 illustrates three overlayed chromatograms. The three curves represent Pope AFB whole asphalt, the modifier MBD-3, and the MBD-3 blend. It can be seen that the Pope AFB whole asphalt has a

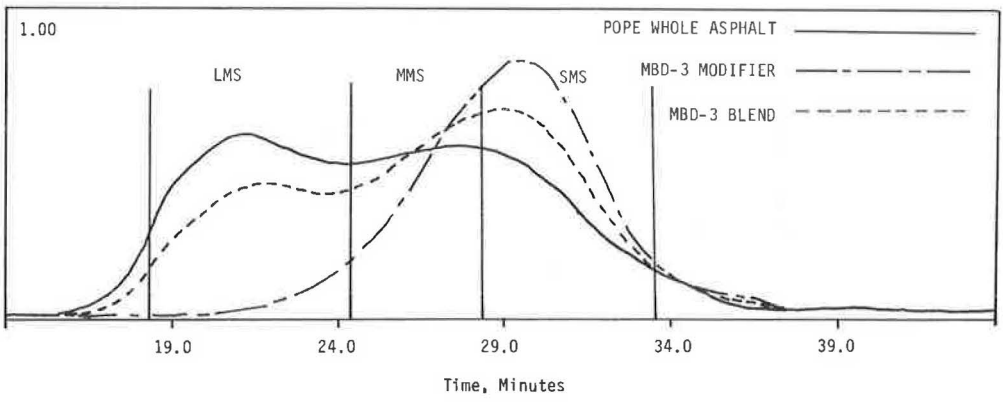

FIGURE 11 Effect of modifier on molecular size distribution of blend.

large amount of LMS material, whereas the modifier has little LMS. When the modifier is added to the whole asphalt, it reduces the area of the curve in the LMS region, which is a desirable effect. It is speculated that the modifier is breaking the aggregation of molecules that add to the LMS region and that separate as asphaltenes in the compositional analysis. This same trend is also evident in the compositional analysis. Currently, only a trend can be seen in the HP-GPC data, and that is a reduction of the LMS region when a modifier is added.

CONCLUSIONS

From the nine modifiers and one aged asphalt used in this study, the following conclusions are made.

1. As the modifier P/S increased at the low and medium levels of modifier percent aromatic content, the low-temperature susceptibility of the blends increased. However, as the level of aromatic content increased, P/S had less influence on the low-temperature susceptibility.
2. As the modifier P/S increased, less shear susceptibility was exhibited by the modified blends at 39.2° and 77°F.
3. As the modifier P/S increased, so did the blend viscosity at 275°F.
4. The penetration of the blends retained after RTFO increased and the aging index of the blends decreased with increasing modifier P/S. The ductility of the blends after RTFO increased with increasing modifier P/S.
5. Modifiers do not have a compositionally additive effect to aged asphalt fractions.
6. On RTFO aging of the blends, there were increases in the asphaltene contents and decreases in the polar fractions. The saturate and aromatic fractions did not change markedly.
7. Solution properties as determined by the Heithaus/Waxman procedure can be used to characterize the effects of modifiers on aged asphalts. The results of this test can be used to infer variations in polar functionality.
8. The most sensitive physical parameters with regard to the effects of modifiers on the aged asphalt cement were the aging index and ductility at 77°F after RTFO conditioning.

ACKNOWLEDGMENT

The authors wish to express their thanks for the technical efforts and contributions of Jon Epps, J.C. Peterson, R.L. Venable, D. Anderson, P.W. Jennings, R.L. Dunning, H. Plancher, and the Chevron Research Company.

This research was performed under contract to the U.S. Air Force Engineering and Service Center, Tyndall AFB, Florida. The project officer was James G. Murfee.

The authors also express their sincere appreciation for the superior efforts of the technicians: Thomas Escobedo, Ginger Kiscaden, Mark Rohrscheib, Mary Searles, and Brenda Wiuff.

REFERENCES

1. J.A. Epps, D.N. Little, R.J. Holmgreen, and R.L. Terrel. Guidelines for Recycling Pavement Materials. NCHRP Report 224. TRB, National Research Council, Washington, D.C., Sept. 1980, 137 pp.
2. D.D. Davidson, W. Canessa, and S.J. Escobar. Practical Aspects of Reconstituting Deteriorated Bituminous Pavements. In Recycling of Bituminous Pavements (L.E. Wood, ed.), Publ. STP 662, ASTM, Philadelphia, Nov. 1978, pp. 16-34.
3. R.L. Dunning and R.L. Mendenhall. Design of Recycled Asphalt Pavements and Selection of Modifiers. In Recycling of Bituminous Pavements (L.E. Wood, ed.), Publ. STP 662, ASTM, Philadelphia, Nov. 1978, pp. 35-46.
4. W.J. Kari, L.E. Santucci, and L.D. Coyne. Hot Mix Recycling of Asphalt Pavements. Proc., Association of Asphalt Paving Technologists, Vol. 48, Feb. 1979.
5. D.I. Anderson, D.E. Peterson, M.L. Wiley, and W.B. Betenson. Evaluation of Selected Agents Used in Flexible Pavement Recycling. Report FHWA-TS-79-204. FHWA, U.S. Department of Transportation, April 1978.
6. R.B. Brownie and M.C. Hironaka. Recycling of Asphalt Concrete Airfield Pavements. Report FAA-RD-78-58. Naval Civil Engineering Laboratory, Port Hueneme, Calif., April 1978.
7. S.J. Escobar and D.D. Davidson. Role of Recycling Agents in the Restoration of Aged Asphalt Cements. Proc., Association of Asphalt Paving Technologists, Vol. 48, Feb. 1979.
8. R.J. Holmgreen, J.A. Epps, D.N. Little, and J.W. Button. Recycling Agents for Recycled Bituminous Binders. Report FHWA-IRD-82/010. FHWA, U.S. Department of Transportation, Dec. 1980.
9. Annual Book of ASTM Standards. ASTM, Philadelphia, 1983, Part 04.03.
10. H.E. Schweyer, L.L. Smith, and F.W. Fish. A Constant Stress Rheometer for Asphalt Cements. Proc., Association of Asphalt Paving Technologists, Vol. 45, Feb. 1976.
11. Annual Book of ASTM Standards. ASTM, Philadelphia, 1979, Part 37.
12. J.J. Heithaus. Measurement and Significance of Asphaltene Peptization. Presented at Symposium on Fundamental Nature of Asphalt, Division of Petroleum Chemistry, American Chemical Society, New York, Sept. 1960.
13. M.H. Waxman, C.T. Deeds, and P.J. Closmann. Thermal Alterations of Asphaltenes in Peace River Tars. Report SPE 9510. Society of Petroleum Engineers of AIME, Dallas, Sept. 1980, pp. 1-20.
14. R.L. Venable and J.C. Peterson. Investigation of Factors Affecting Asphalt Pavement Recycling and Binder Compatibility, Parts I and II. Draft Final Report. U.S. Department of Energy, June 1982.
15. P.W. Jennings, J.A. Pribanic, W. Campbell, K.R. Dawson, and R.B. Taylor. High Pressure Liquid Chromatography as a Method of Measuring Asphalt Composition. Report FHWA M7-7930. FHWA, U.S. Department of Transportation, March 1980.

Publication of this paper sponsored by Committee on Characteristics of Bituminous Paving Mixtures to Meet Structural Requirements.

Evaluation of Recycled Mixtures Using Foamed Asphalt

FREDDY L. ROBERTS, JOHANN C. ENGELBRECHT, and THOMAS W. KENNEDY

ABSTRACT

The economic pressure from higher fuel, asphalt, and material prices, along with the growing use of milling equipment for smoothing pavement profiles and the problems of bridge clearances, have worked together to provide an abundance of salvaged roadway materials that are available for recycling. This material availability and the appearance of some performance problems with recycled materials on heavily traveled roadways have led to the consideration of using these salvaged roadway materials on low-volume roads. The laboratory study reported in this paper evaluated the feasibility of using foamed asphalt to recycle asphalt mixtures and compared the properties of foamed mixtures with those of conventional cold mixtures. The study involved an initial evaluation of the foamed process using two field sands. Additional tests were conducted by using salvaged pavement materials mixed with a foamed asphalt cement (AC-5) and with a cutback (MC-800) and two emulsions (EA-11M and AES-300). Specimens were prepared, cured, and tested under both dry and wet conditions. The wet strengths were less than approximately one-half the dry strengths, but in almost all cases the foamed AC-5 produced strength values equal to or higher than those using either the cutback or emulsions. In addition, the asphalt content for the foamed asphalt specimens was lower than for the cutback or emulsions. Overall, the foamed asphalt materials appear to offer a possible option for use in cold recycled asphalt mixtures for low-volume roadways.

Because of the continued price escalation for both energy and asphalt cement there is a continuing interest in producing asphalt mixtures by using cold mixing techniques, especially for lower volume roads. In addition, substantial volumes of surface material from the growing use of cold milling as well as the use of salvaged materials from existing roadways represent high-quality materials that can be recycled with the proper technology. Because there have been conflicting reports on the performance of foamed asphalt mixtures, a laboratory evaluation was conducted to determine the properties of foamed asphalt mixtures and to compare these properties with those of cutback and emulsion mixtures. Properties evaluated were indirect tensile strengths, static moduli of elasticity, and Hveem stabilities.

FOAMED ASPHALT PROCESS

In 1957 Csanyi (1) of Iowa State University demonstrated the effectiveness of preparing low-cost mixes by stabilizing ungraded local aggregates such as gravel, sand, and loess with foamed asphalt. Controlled foam was produced by introducing saturated steam into heated asphalt through a specially designed nozzle. The reduced viscosity, increased volume (±2,000 percent), and reduced surface energy in the foamed asphalt allowed intimate coating when mixed with the cold, wet aggregates. Foamed asphalt allowed materials normally considered unsuitable for hot plant-mixed applications to be used in stabilized bases and surface mixtures for low-volume roads.

In 1968 the patent rights for the Csanyi process were acquired by Mobil of Australia (1). Mobil modified the steam production process by blending 1 to 2 percent cold water with the hot asphalt before mixing with cold, mineral aggregate.

MATERIALS SUITABLE FOR USE

Aggregates

Bowering and Martin (2) tested foamed asphalt mixtures comprised of materials ranging from a sandy clay to a well-graded gravel. Test results indicated that the low-plasticity materials with a relatively large percentage of fines (-200 sieve) were best because the asphalt tends to coat the fines and partly coat the larger particles (3). Acott (4) suggested adding fines to increase low stabilities of foamed asphalt mixtures made with both clean and dirty sands. Fine material must be present to enhance the ability of the foam to produce uniform, thin coatings on a large surface area. Soils that benefit the most from the addition of foamed asphalt also show significant strength loss when tested wet.

In addition to using natural aggregates, foamed asphalt mixtures have been prepared with salvaged asphalt materials. Lee (5) prepared foamed asphalt mixtures by using two recycled materials. The reclaimed materials were blended with virgin aggregates of the type and amount normally specified in Iowa for hot recycled mixtures.

Brennan et al. (6) produced a foamed recycled asphalt mixture by using salvaged material from a state road near Wabash, Indiana, that had an asphalt content of 5.4 percent and a penetration of 20. The material was crushed, graded, separated into four sizes, and recombined to produce a 100 percent recycled mixture.

These studies (5,6) demonstrate the feasibility of using salvaged material to produce a foamed, recycled mixture with or without virgin material. Generally, the mixture properties were reported to have improved when fines were added to the salvaged material.

Asphalt

The percent asphalt included in a foamed asphalt mixture is a function of the soil type and moisture content and the desired mixture properties. Generally, foamed asphalt mixtures can be prepared at lower asphalt contents and can obtain about the same properties as conventional cold mixtures at higher asphalt contents (1,3). Typical asphalt contents for foamed mixtures range from 3 to 6 percent. When the films are too thick, the asphalt simply lubricates the aggregate particles. When the films are too thin, there may not be enough asphalt for coating,

with a resulting decrease in mixture stability and high strength loss when tested wet.

Brennan et al. (6) reported excellent Marshall stabilities by adding 0.5 and 1.0 percent asphalt by total weight to salvaged material with stabilities peaking at 1 percent asphalt. The amount of water absorption and the effect of water on stability decreased with increasing asphalt content.

Most asphalt cement (7) can be foamed, but Abel (3) reported that the lower viscosity asphalts foamed better than higher viscosity asphalts, but the higher viscosity asphalts produce better aggregate coating.

Shackel et al. (8) reported that mixtures made from higher penetration asphalt (lower viscosity) experienced lower strains under repeated loading, but also had lower resilient moduli.

CONSTRUCTION CONSIDERATIONS

Prewetting Aggregate

Brennan et al. (6) reported that it is necessary to add a small amount of water to the aggregate before mixing so that the foamed asphalt would thoroughly coat and adhere to the particles. Best mixing occurred at the fluff point; that is, the point at which the loose material occupies the maximum volume.

The amount of moisture was reported to be fairly critical because the proper amount of water aids in the distribution of the asphalt, whereas insufficient water results in a mixture that cannot be laid (9). Too much water increases curing times and reduces both density and strength of the compacted mixtures.

Anderson et al. (7) reported different optimum water contents for strength, density, minimum moisture absorption, and minimum expansion. Anderson et al. concluded that because mixing generally controls the construction process, the selected optimum moisture content should be controlled by that value. Lee (5) recommended that 65 to 85 percent of the AASHTO optimum moisture content be used for mixing and stressed that the moisture content before mixing was the most important design factor that affected the construction of foamed asphalt mixtures.

Construction and Curing

Most foamed asphalt mixtures have been mixed in a conventional pugmill, fitted with a special spray bar for mixing the water and asphalt to produce foam (10). After mixing, the material can be placed and compacted with conventional equipment and traffic may be allowed on the pavement shortly after compaction. Brennan et al. (6) indicated that most of the mixing water had to evaporate before best compaction could be achieved. Curing of foamed asphalt mixtures occurs as the water evaporates (3,7) and is considerably longer than that for emulsion mixtures. During the curing period the mixture can be reworked and relaid with no apparent detrimental effects (9). Laboratory test results indicate that the method of curing and length of the curing period significantly affect the properties of the foamed mixture. Bowering (11) stressed the importance of curing and reported that laboratory specimens developed full strength only after a large percentage of the mixing water was lost.

LABORATORY STUDIES

A preliminary laboratory study was conducted first to evaluate the effects on tensile strength and Hveem stability produced by curing methods, moisture content, and asphalt content. Subsequently, the main laboratory study to evaluate the characteristics of foamed recycled mixtures was conducted.

Specimens were prepared with both the field sands and the salvaged asphalt material by using a cutback and two emulsions in order to compare properties of foamed specimens with those prepared by using traditional cold-mixed procedures. The asphalts used in the laboratory study are given in Table 1, along with the properties of the recycled asphalt.

All mixtures were tested to obtain indirect tensile strengths and moduli of elasticity and Hveem stabilities.

TABLE 1 Asphalt Used in Laboratory Study

Asphalt Used	Value
Tests on residual asphalt	
Recycled project	
Penetration (77°F)	37
Ductility (cm)	141
Viscosity at 140°F (Stokes)	5,592; 5,549
Tests on new asphalt	
No. 399, cutback MC-800 (producer: Cosden Oil & Chemical Co.)	
Penetration (77°F)	208
Kinematic viscosity (140°F)	1,266
No. 395, AES-300 (producer: Texas Emulsions, Inc.)	
Furol viscosity (77°F)	180
Penetration (77°F)	300
No. 398, EA-11M (producer: Texas Emulsions, Inc.)	
Furol viscosity (sec @ 77°F)	74
Penetration (77°F)	134
No. 274, AC-5 (producer: Dorchester)	
Penetration (77°F)	208

Preliminary Laboratory Study

The sand consisted of a fine white sand and a coarser sand that were blended in equal parts to produce a gradation with 100 percent passing the No. 10 sieve, 73 percent passing the No. 40 sieve, 31 percent passing the No. 80 sieve, and 10 percent passing the No. 200 sieve.

The curing cycle consisted of oven curing for 4 days at 140°F followed by either the wet or dry 3-day cure at 75°F. The wet cure consisted of 2 hr of 26-in. vacuum saturation followed by 3 days of soaking at 75°F. Bowering (11) previously concluded that the moisture content of the specimen reaches equilibrium after 3 days of curing at 140°F.

Specimens prepared at different asphalt and initial water contents and tested in the Hveem stabilimeter at 140°F and indirect tensile test at 75°F (10) gave the following results.

1. There was a significant increase in tensile strengths as curing temperatures increased from 75° to 140°F.
2. Specimens tested after wet curing had less than 50 percent of the strength of those tested after dry curing.
3. Stabilities of all specimens were low, which is typical of sand-asphalt mixtures, and the stability decreased with increased asphalt content.
4. Stabilities of foamed asphalt-sand specimens were higher than those of sand mixtures mixed with MC-800 cutback and AES-300 and EA-11M emulsions.
5. Tensile strengths for the foamed sand asphalt were substantially higher than those for either the cutback or the emulsions.

Details of this preliminary analysis can be found in Roberts et al. (12).

Laboratory Study of Salvaged Pavement Material

A laboratory study was conducted to evaluate the characteristics of salvaged materials recycled using foamed asphalt. The purposes of the study were to evaluate the properties of foamed recycled materials and to compare those properties with the properties of more traditional cold mixtures prepared with the same salvaged material using the two emulsions and a cutback.

Specimen Preparation

The salvaged material was sieved into two sizes and recombined with 40 percent of material passing the No. 4 sieve and with 60 percent material retained on the No. 4 sieve; material larger than 3/4 in. was discarded. This gradation is shown in Figure 1. In preparing the foamed asphalt materials, the mixing water varied from zero to approximately 2 percent by weight of aggregate.

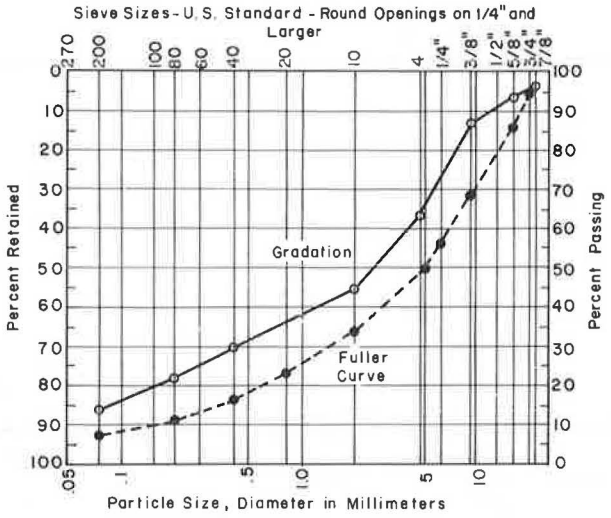

FIGURE 1 Gradation of salvaged pavement materials from TSDHPT District 13.

Experimental Program

The first series of tests was performed on specimens prepared from salvaged materials that had no water added before mixing. These specimens were cured for 7 days, including 4 days at 140°F with 3 additional days at 75°F either dry or submerged in water (wet).

A second series of tests was conducted to evaluate the effect of mixing water content and curing temperature on the strengths of the foamed, recycled asphalt mixtures. The water content before mixing varied from zero to 2 percent. The curing temperatures ranged from 140° to 75°F for the initial 4-day cure and the final 3 days of curing was at 75°F either dry or submerged in water (wet).

A third series of tests involved using the salvaged material to prepare specimens with two emulsified asphalts and one cutback asphalt. Test results from these specimens were used to compare the properties of foamed, recycled specimens with those of specimens prepared by using traditional cold-mixed processes. To ensure accurate comparisons, curing conditions for all specimens were kept constant.

Specimens were tested by using the indirect tensile and Hveem stability tests. In addition to engineering properties, various other standard tests were conducted on specimens to determine specific gravity, density, air void content, asphalt content, and gradations to evaluate the characteristics of foamed, recycled asphalt specimens and to compare those results with specimens prepared by using other techniques or materials.

Series 1: Test Results–No Mixing Water

Specimens were prepared at asphalt contents varying from zero to 2 percent and tested at 75°F after the dry and wet curing periods. Because of the foaming process, the amount of water in the mix varied from about 0.5 to 1.0 percent, averaging about 0.8 percent at the time of compaction.

Figure 2 shows tensile strength results for dry- and wet-cured specimens. The dry-cured specimens show a definite optimum at 0.5 percent foamed asphalt, whereas the wet-cured specimens achieved a maximum tensile strength at about 1 percent. In general, the strengths of the wet-cured specimens were less than 50 percent of the strengths of the dry-cured specimens. Strength losses of this magnitude are fairly typical for specimens of foamed asphalt mixtures tested wet (6,11).

Hveem stabilities for dry-cured specimens are shown in Figure 3 along with the stabilities for specimens of salvaged material heated and compacted at 320°F without the addition of new asphalt.

These data indicate that only specimens with around 0.5 percent foamed asphalt would meet the Texas State Department of Highways and Public Trans-

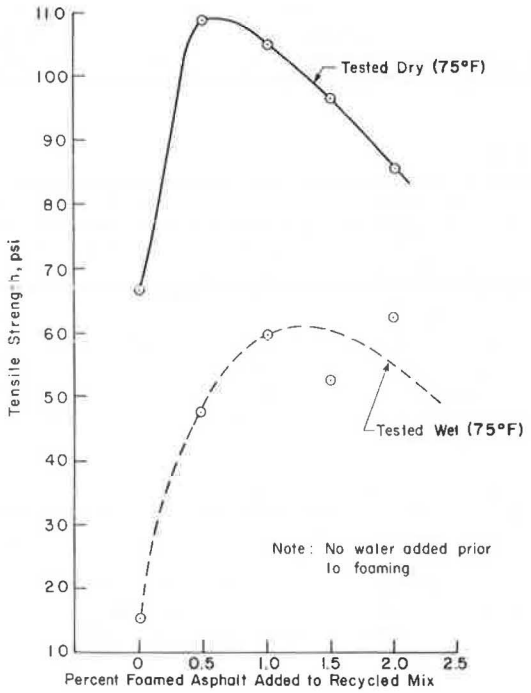

FIGURE 2 Comparison of tensile strength at various percentages of foamed asphalt with no water in mix before foaming.

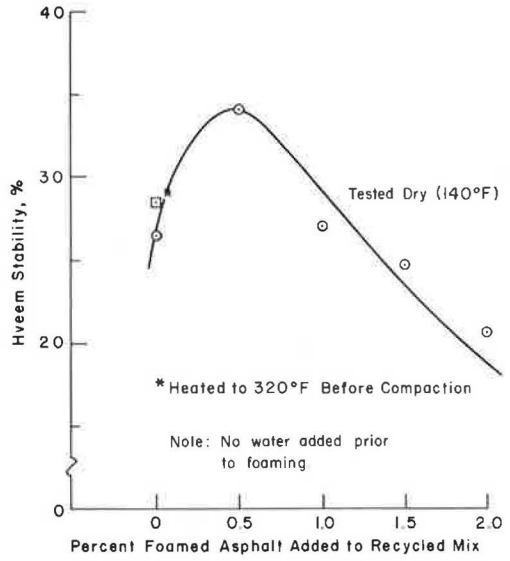

FIGURE 3 Comparison of Hveem stability to percentages of foamed asphalt with no water added before foaming.

portation (TSDHPT) Type B stability requirement of 30. However, it should be noted that the stabilities of the foamed specimens compare favorably with those of the salvaged material that was only heated and compacted. Because stability tests are performed immediately after curing and because no soaking is prescribed in the procedure, stability tests were performed only on the dry-cured foamed asphalt specimens.

The static moduli of elasticity of both dry- and wet-cured foamed, recycled asphalt specimens and of recycled mixtures that were heated to 320°F before compaction and testing are shown in Figure 4. The static moduli were fairly constant for both dry- and wet-cured foamed asphalt specimens for asphalt contents between 0.5 and 1.5 percent. The static moduli decreased significantly at values greater than and less than this range. In the asphalt content range between 0.5 and 1.5 percent the static moduli for the dry-cured specimens were at least 3 times the moduli for the wet-cured specimens, indicating again the significant effect of moisture on the engineering properties of foamed asphalt mixtures. The static moduli for the recycled mixtures that were only heated before compaction and testing were higher than those for the foamed asphalt specimens and the strength loss was much less for the wet specimens.

Figure 5 shows the relationship between foamed asphalt content and density for both the wet- and dry-cured specimens. The optimum asphalt content for both sets of data indicates that about the same density was achieved between 0.5 and 1.5 percent asphalt. The percentages of theoretical maximum density achieved for the dry-cured specimens ranged from about 93 to 95 percent for added asphalt contents ranging from 0.5 to 1.5 percent. The density for the recycled mixtures that were only heated before compaction and testing was significantly higher than that for the foamed, dry-cured specimens.

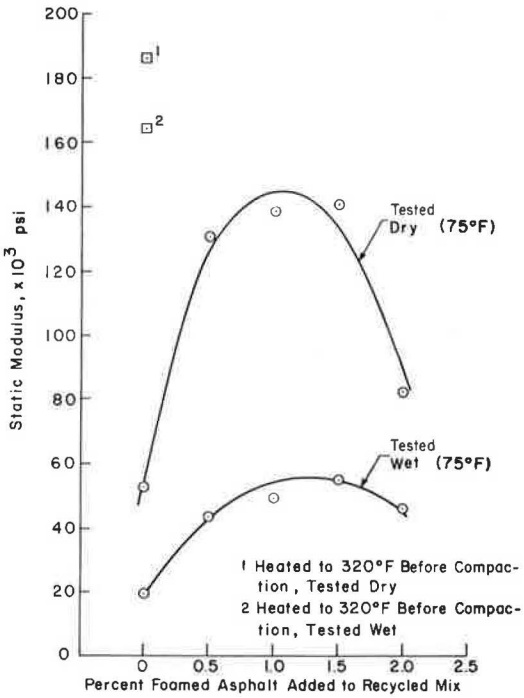

FIGURE 4 Comparison of modulus values to percentage of foamed asphalt with no water added before foaming.

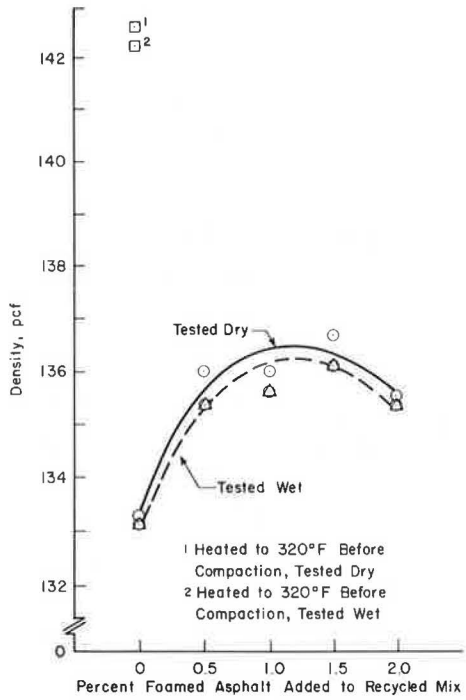

FIGURE 5 Relationship between density and percentage of foamed asphalt with no water added before foaming.

Series 2: Test Results–Effect of Mixing Water on Properties

Specimens were prepared at 0.5 and 1.0 percent asphalt with the water content at compaction varying from zero to slightly greater than 2 percent. Both the foaming process and the premixing water contributed to the total water in the material at compaction; therefore, water contents were determined from the weights of specimens immediately after compaction and after curing 4 days at ±40°F.

The effect of mixing water content and asphalt content on tensile strength is shown in Figure 6. For both those specimens tested wet and those tested dry the total liquids at optimum were about the same (i.e., the percent water in the specimens with 1.0 percent asphalt is about 0.5 percent less than for the specimens with 0.5 percent asphalt). In addition, the loss of tensile strength between the dry and wet specimens is consistent with that previously shown in Figure 2 and in the preliminary testing.

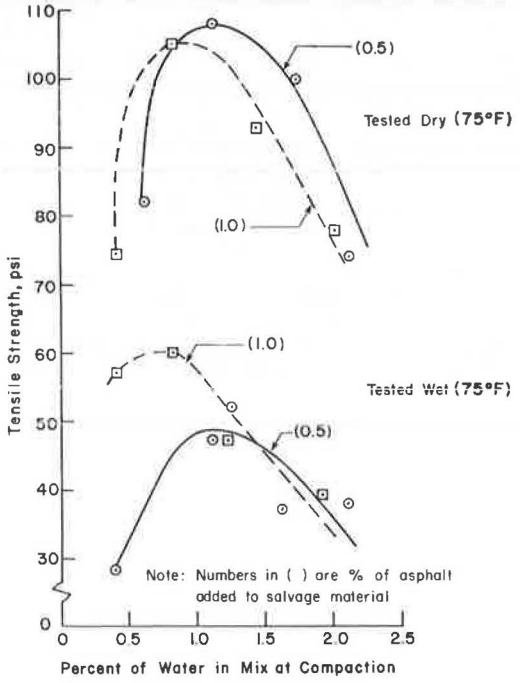

FIGURE 6 Comparison of results of foamed specimens at different mixing water and asphalt contents.

There was no significant difference in density for the wet specimens at either 1.0 or 0.5 percent asphalt. The increased wet tensile strength at 1.0 percent asphalt is probably caused by the protection provided by the extra asphalt.

Figure 7 shows the effect of both asphalt content and moisture content at compaction on Hveem stability. As expected, the stabilities are lower for specimens prepared with 1.0 percent foamed asphalt because at the same water content the total volume of liquids is larger than for 0.5 percent asphalt, producing additional lubrication and hence lower stability. The optimum moisture content appears to be slightly lower for the 1.0 percent asphalt curve than for the 0.5 percent asphalt, although the latter is not well defined. The optimum stability for both curves may well occur at about the same total liquids content.

The effect of temperature during the initial 4-day curing period on the tensile strength of specimens tested dry and wet is shown in Figure 8. These specimens were compacted from a different mixture. Because of variations in asphalt concrete (AC) content of the salvaged material, the results are different from those obtained in series 1 (Figure 2). The foamed asphalt content varied from zero to 1.0 percent. For the specimens tested dry, the optimum foamed asphalt content was 0.5 percent. However, for the specimens tested wet, the tensile strength continued to increase as the asphalt content increased.

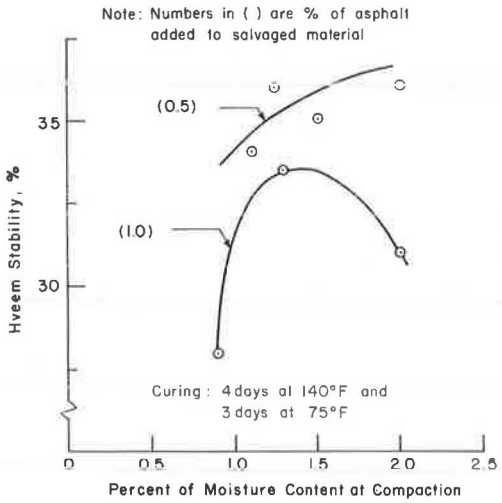

FIGURE 7 Effect of moisture content at compaction on the Hveem stability of foamed specimens.

For the specimens tested wet, however, the effect of curing temperature was much more significant than the effect of asphalt content, indicating the tremendous impact of curing conditions on the properties of this type of pavement material. These results indicate that the higher the initial curing temperature, the less the effect of moisture for the wet tests and the lower the strength loss due to wetting. For the specimens tested dry, the effect of asphalt content was much less than for those tested wet; however, a well-defined optimum asphalt content occurred at 0.5 percent.

The effects of temperature and length of the curing period on tensile strengths were also investigated and the results from specimens tested wet after curing are shown in Figure 9. These specimens were prepared from a different mixture. Because of

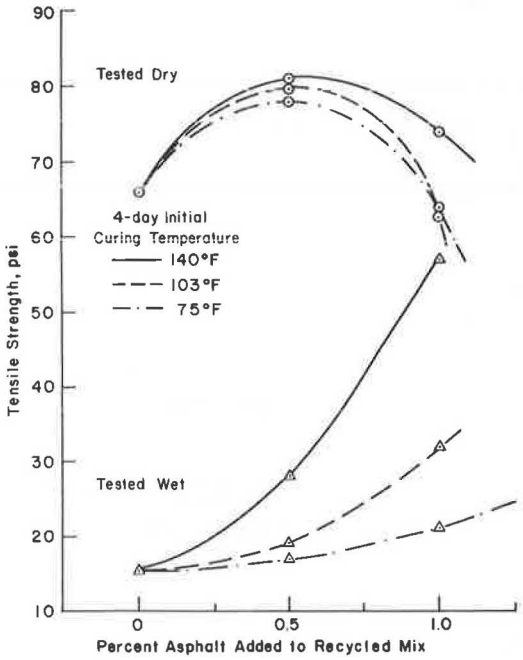

FIGURE 8 Effect of curing on tensile strength with dry mixing of foamed specimens.

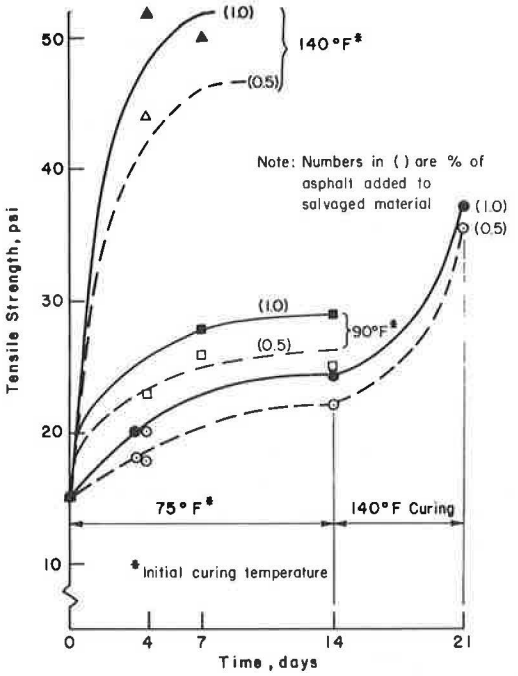

FIGURE 9 Effect of curing temperature and length of curing period on tensile strength of specimens tested after soaking.

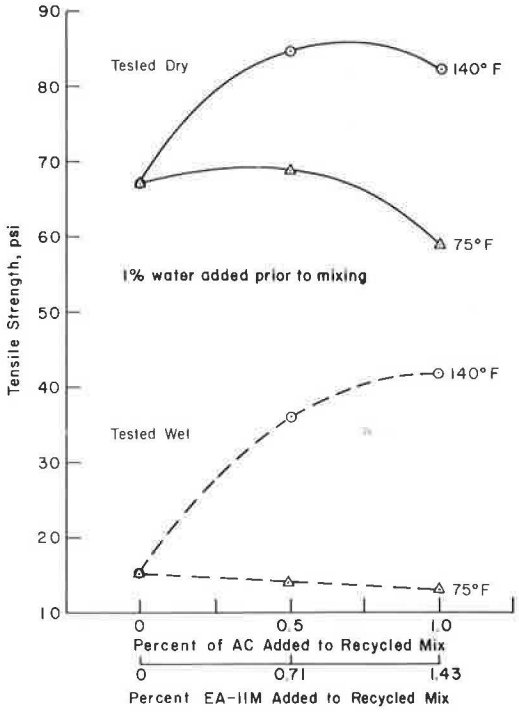

FIGURE 10 Comparison of tensile strengths at various percentages of emulsion EA-11M (70/30).

variability of AC content of salvaged material, results are somewhat different from those of Figure 8. These results indicate that the higher the temperature during curing, the higher the tensile strength, but that about 75 percent of the strength was developed after 4 days of curing for all curing temperatures. After curing begins, if the curing temperature is increased to 140°F, the tensile strength also increased, but at a lower rate than for specimens that began curing at 140°F.

Series 3: Test Results–Comparison with Emulsions and Cutbacks

To evaluate the engineering properties of foamed asphalt specimens, a series of comparison tests was conducted on cold-mixed specimens prepared by using selected emulsions and a cutback asphalt. The foaming process caused a moisture content of ±1 percent at compaction. Premixing water of 1 percent was added to the emulsion mixes for consistency. Specimens were prepared and cured in the same manner as for the foamed asphalt specimens: one set at 140°F for 4 days followed by 3 days of either wet or dry curing at 75°F, and a second set at 75°F for 4 days and then either wet or dry cured for 3 days at 75°F. The specimens were then tested immediately after curing at 75°F; those that were tested after dry curing were designated as tested dry, whereas those tested after wet curing were designated as tested wet.

Test results for the specimens prepared with EA-11M and AES-300 emulsions are shown in Figures 10 and 11, and the results for specimens prepared with the MC-800 cutback are shown in Figure 12. The same basic trends as for the foamed, recycled asphalt are evident in these relationships. The tensile strength of the dry specimens cured at 140°F for 4 days exhibited a fairly well-defined optimum asphalt content of 0.5 percent for both the dry-tested specimens and the wet-tested specimens cured at 140°F. Generally, the strengths of the specimens prepared with emulsions and cutbacks compared favorably with those of similar specimens prepared with foamed asphalt. However, as shown in Figure 13, the tensile strengths for the specimens prepared with foamed asphalt were consistently higher than those for specimens prepared with either of the other asphalt materials; the differences were as significant for the specimens cured at 75°F for 4 days, wet cured (soaked) at 75°F for 3 days, and then tested.

Hveem stabilities from specimens prepared with

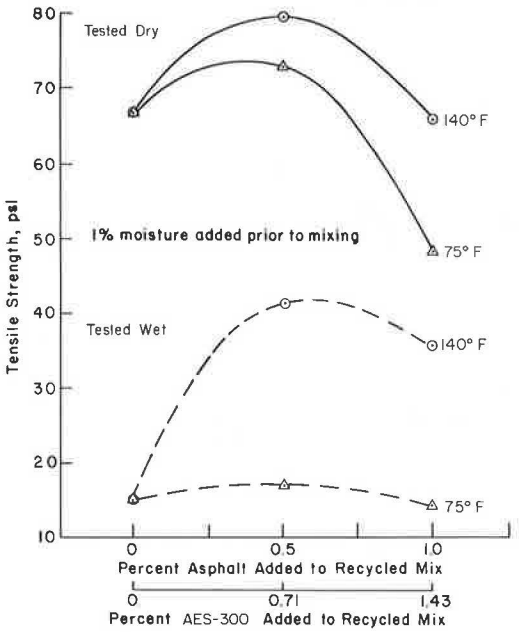

FIGURE 11 Comparison of tensile strength at various percentages of emulsion AC and curing effects AES-300 (70/30).

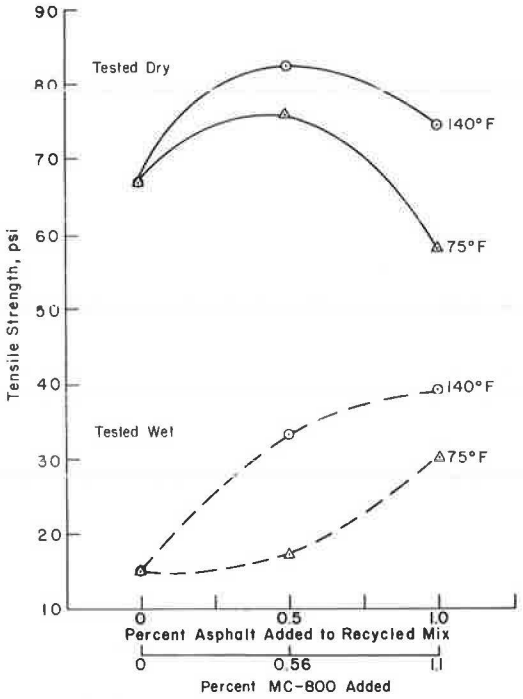

FIGURE 12 Comparison of tensile strengths at various percentages of cutback MC-800.

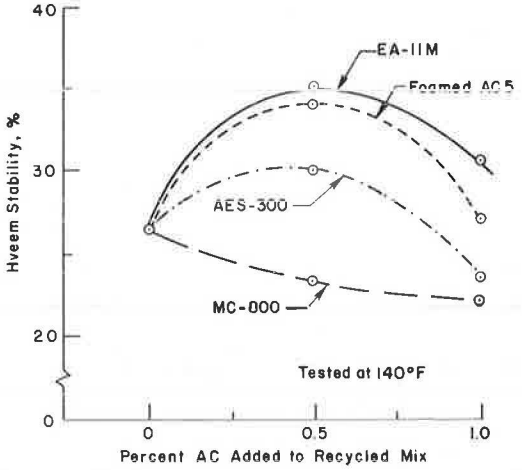

FIGURE 14 Hveem stability in relation to emulsions, cutbacks, and foamed specimens at various percentages of asphalt.

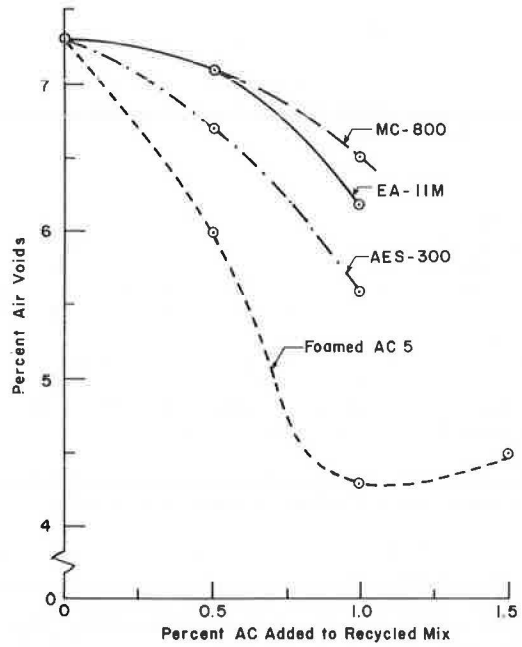

FIGURE 15 Air void contents for mixture prepared by using different asphalts.

foamed AC-5, EA-11M, AES-300, and MC-800 and then dry cured are shown in Figure 14. Specimens prepared by using the foamed AC-5 and EA-11M asphalts showed higher stabilities than those prepared by using AES-300 and MC-800. Except for the MC-800 specimens, the optimum asphalt content for stability occurred at 0.5 percent. Stabilities were low at both zero and 1.0 percent added asphalt. When no new asphalt was added, the air void content was around 7 percent; at an asphalt content of 1.0 percent, the voids ranged from about 4.3 to 6.5 percent, as shown in Figure 15. It is obvious that the foamed asphalt specimens were compacted to a higher density than were specimens prepared with either the emulsions or the cutback. This ease of compaction could have resulted from better distribution of the asphalt because of the thinner films produced by the foaming process and from the lubricating effects of extra water introduced into the foamed materials from the cold water that produced the foaming of the asphalt.

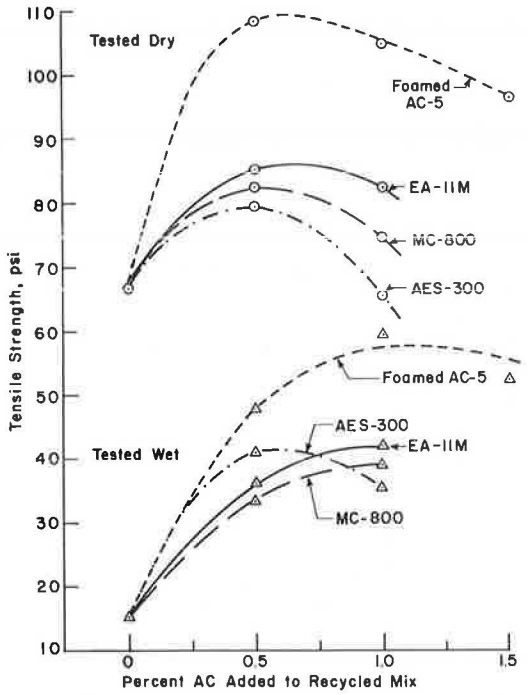

FIGURE 13 Comparison of tensile strength results for foamed, emulsions, and cutback specimens.

CONCLUSIONS AND RECOMMENDATIONS

Based on the data collected in this limited laboratory study using one salvaged pavement material, one

blend of field sands, an AC-5 asphalt cement, two emulsions, and one cutback, the following tentative conclusions and recommendations were prepared.

Conclusions

1. Curing temperature, length, and moisture conditions dramatically affected the strength of foamed asphalt mixtures prepared by using both the sand and the salvaged pavement materials.
2. The stabilities of dry-cured foamed asphalt and sand mixtures were equivalent to that of a hot sand-asphalt prepared by using the same sand and asphalt cement. However, when the foamed asphalt-sand mixtures were tested wet, the strengths were reduced to less than 50 percent; however, all specimens lost at least 50 percent of their strength when tested wet as compared with the strengths when tested dry.
3. The foamed asphalt specimens prepared from both the salvaged pavement materials and the sand exhibited equivalent or superior engineering properties to specimens prepared by using either the emulsions or the cutback.
4. The engineering properties of the foamed salvaged asphalt specimens were substantially less than the properties of mixtures prepared by heating the salvaged materials before compaction; however, specimens prepared from the heated materials were compacted to much higher densities than were achieved for any of the cold-mixed materials.
5. Within the range of values investigated, increases in asphalt content for specimens of foamed asphalt-recycled materials increased the strength of the specimens tested wet but decreased the strength of the specimens tested dry.
6. Hveem stabilities were significantly affected by the total volume of liquids added to the salvaged materials, with these changes being more pronounced at higher asphalt contents.

Recommendations

1. In those situations where cold-mixed materials are being considered for use in bases or subbases, foamed asphalt may be a feasible alternative, especially if available materials include silty sands and gravels that are otherwise considered marginal.
2. The foamed asphalt process probably can be used with salvaged pavement materials to produce base courses and paved shoulder surfaces. However, at this time the use of these materials as a permanent surface on any road is not recommended.
3. Field experience should be well documented because, to date, reports on the performance of foamed asphalt mixtures have been conflicting.

ACKNOWLEDGMENT

The research described in this paper was carried out in the Center for Transportation Research, Bureau of Engineering Research, University of Texas at Austin. The authors are grateful for the support of the TSDHPT and that of the FHWA, U.S. Department of Transportation.

REFERENCES

1. L.H. Csanyi. Foamed Asphalt in Bituminous Paving Mixtures. Bull. 160. HRB, National Research Council, Washington, D.C., 1957, pp. 108-122.
2. R.H. Bowering and C.L. Martin. Foamed Bitumen Production and Application of Mixtures Evaluation and Performance of Pavements. Proc., Association of Asphalt Paving Technologists, Vol. 45, 1976, pp. 453-477.
3. F. Abel. Foamed Asphalt Base Stabilization. Presented at 6th Asphalt Paving Seminar, Colorado State University, Fort Collins, Dec. 1978.
4. S.M. Acott. Sand Stabilization: Using Foamed Bitumen. Proc., Conference on Asphalt Pavements for South Africa, Sept. 1979, pp. 155-167.
5. D.Y. Lee. Treating Iowa's Marginal Aggregates and Soils by Foamix Process. Final Report. Iowa State University, Ames, May 1980.
6. M. Brennen, M. Tia, A. Altschaeffl, and L.E. Wood. Laboratory Investigation on the Use of Foamed Asphalt for Recycled Bituminous Pavements. In Transportation Research Record 911, TRB, National Research Council, Washington, D.C., 1983, pp. 80-87.
7. K.O. Anderson, R.C.G. Haas, and A.D. LaPlante. Triaxial Shear Strength Characteristics on Some Sand-Asphalt Mixtures. In Highway Research Record 91, HRB, National Research Council, Washington, D.C., 1965, pp. 1-12.
8. B. Shackel, K. Makuichi, and J.R. Derbyshire. The Response for a Foamed Bitumen Stabilized Soil to Repeated Triaxial Loading. Proc., 7th Australian Road Research Board Conference, Adelaide, Australia, 1974.
9. E.V. Petersen. Foamed Asphalt Wins Job. Construction Canada, Vol. 1, No. 6, July 1964, pp. 16-27.
10. J.N. Anagnos and T.W. Kennedy. Practical Method for Conducting the Indirect Tensile Test. Res. Report 98-10. Center for Highway Research, University of Texas, Austin, Aug. 1972.
11. R.H. Bowering. Properties and Behavior of Foamed Bitumen Mixtures for Road Building. Proc., 5th Australian Road Research Board Conference, Canberra, Australia, 1970, pp. 38-57.
12. F.L. Roberts, J.C. Engelbrecht, and T.W. Kennedy. Use of Foamed Asphalt for Cold, Recycled Mixtures. Res. Report 252-3. Center for Transportation Research, University of Texas, Austin, Aug. 1983.

Publication of this paper sponsored by Committee on Characteristics of Bituminous Paving Mixtures to Meet Structural Requirements.

Effect of Mix Conditioning on Properties of Asphaltic Mixtures

OK-KEE KIM, C. A. BELL, and R. G. HICKS

ABSTRACT

The serviceability of asphalt pavements is controlled by many factors, such as expected load, mixture, and environmental variables. In order to provide satisfactory serviceability, an asphalt mixture must have several characteristics: stiffness, tensile strength, resistance to fatigue, permanent deformation, and resistance to water damage. Recently, water-induced damage of asphalt mixtures has caused serious distress, reduced performance, and increased maintenance for pavements in Oregon. The information from tests performed at Oregon State University concerning three projects built between 1978 and 1980 was used to determine relationships between asphalt concrete pavement performance as indicated by resilient modulus, indirect tensile strength, fatigue life, and mix level of compaction for both as-compacted and conditioned samples. It was found that the rate of water-induced damage of asphalt mixtures was strongly related to aggregate quality and air void content of the mixture--the higher the air void content and the poorer the aggregate, the larger the loss of strength.

The performance of asphalt pavement materials is affected by many factors, including type of mixture, degree of compaction, stress level, rate of loading, and environmental factors. Currently, the effects of the environment under which pavements serve, including both climatic and loading factors, are receiving increased notice. For example, several studies have recently been performed to investigate the effect of water on asphalt pavement performance, including the effect of additives to reduce moisture damage (1-5). The loss of adhesion between the asphalt cement and aggregate surface, which affects the asphalt mixture properties, is primarily due to the action of water. Decreases in strength and modulus because of moisture reduce the performance of the asphaltic mixtures and, consequently, should be considered in pavement and mixture design practice.

The purpose of this paper is to (a) summarize the test results for three recent projects in Oregon, (b) obtain a better understanding of the causes of the pavement problems with respect to moisture, and (c) develop relationships between mixture performance (resilient modulus, fatigue life, and indirect tensile strength) and the different mix variables for as-compacted and conditioned samples.

PROJECTS EVALUATED

The projects studied were North Oakland-Sutherlin (NO-S), Castle Rock-Cedar Creek (CR-CC), and Warren-Scappoose (W-S). These three projects were constructed between 1978 and 1980 in Oregon, and each project used an Oregon class B mix (Table 1). The construction reports of top lift and base lift of the pavement indicated that several mix variables were ranging within a very wide band, which indicated quality control problems during mixing (asphalt content, gradation) and during compaction (air void content) (6-8). The pavement cross sections are illustrated in Figure 1.

TABLE 1 Aggregate Gradation for Oregon Class B Mix for Each Project

		Job Mix Tolerance		
Sieve Size	Opening (mm)	NO-S	CR-CC	W-S
1 in.	25		100	100
3/4 in.	19	95-100	95-100	92-100
1/2 in.	12.5	80-92	81-93	82-94
3/8 in.	9.5			73-85
1/4 in.	6.25	54-66	57-69	54-66
No. 4	4.75			46-56
No. 10	2.00	21-29	22-30	26-34
No. 40	0.425	8-16	8-16	8-16
No. 200	0.075	3-7	3-7	2.6-6.6

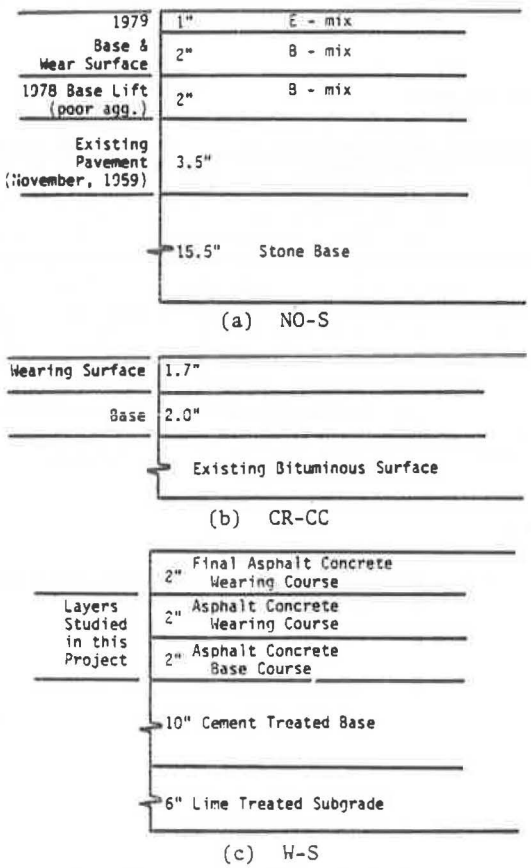

FIGURE 1 Cross sections of projects studied.

North Oakland-Sutherlin Project

The North Oakland-Sutherlin (NO-S) project is a section of Interstate 5 located approximately 12 miles (19 km) north of Roseburg. Its overall length is 3.21 miles (5.14 km). The recommended asphalt content was 6.9 percent of an AR 8000 asphalt cement treated with 0.85 percent "pavebond" (an antistrip agent). The asphalt concrete base on this project was paved in October through December 1978 and showed problems of raveling and potholing shortly thereafter. An investigation performed by the Oregon Department of Transportation (ODOT) indicated that the reduced quality of the paving was basically the result of using varying amounts of unsound and nondurable aggregate in the mix. The aggregate used in this project was a submarine basalt that contained seams of sulfate compounds of calcium, sodium, and magnesium. Soundness test results for produced aggregate used in the paving ranged from 4.16 to 38.94 percent loss for coarse aggregate and 11.56 to 48.23 percent loss for fine aggregate (6).

Castle Rock-Cedar Creek Project

The Castle Rock-Cedar Creek (CR-CC) project, built in 1979, is a section of the Hebo-Valley Junction Highway located in Tillamook and Yamhill counties. The overall length is 11.7 miles (18.7 km). Asphalt contents of 6.1 percent for wearing surface and 6.7 percent for the base course were recommended. The average for the as-constructed thickness is 2.0 in. (5.1 cm) for the base course and 1.7 in. (4.3 cm) for the wearing surface. The asphalt grade recommended was an AR 4000. Progressive pavement raveling and potholing was noticed during the months following construction of this project. In this case the ODOT investigation indicated that the reduction in pavement life resulted from excess variability in aggregate gradation, inadequate asphalt coating of aggregate, and high air void content (7).

Warren-Scappoose Project

The Warren-Scappoose (W-S) project is a section of the Columbia River Highway located in Columbia County. The overall length is 5.05 miles (8.13 km). The base course was constructed in 1979 and the wearing surface was constructed in 1980. The recommended asphalt content was 5.1 percent for the wearing surface and 5.7 percent for the base course. The asphalt grade recommended was an AR 4000. Progressive pavement raveling and potholing were noticed in the base course during the months following construction. The core data obtained for this project indicated that the reduction in pavement life resulted from high air void content and variability in aggregate gradation (8).

SAMPLE PREPARATION AND TEST METHODS

Laboratory samples were prepared at Oregon State University to determine the resilient modulus, tensile strength, fatigue life, and permanent deformation of the asphaltic mixtures. For each project the percent passing the No. 200 sieve material was 6 percent and the asphalt contents were as follows: NO-S = 6.0 percent, CR-CC = 6.0 percent, and W-S = 5.5 percent.

For each project samples were prepared at the range of compaction levels given in Table 2. All tests were run on standard laboratory samples by using the repeated load indirect tensile test.

TABLE 2 Range of Compaction Levels Considered

Extent of Laboratory Compaction	Percent of Maximum Compaction		
	NO-S	CR-CC	W-S
2nd compaction[a]	100	100	100
1st compaction[a]	96	97	97
95 blows at 100 psi, 500 psi leveling load	92	92	93
30 blows at 100 psi, 300 psi leveling load	91	90	90

[a]See Laboratory Manual of Test Procedures (9).

Sample Preparation

Following the standard ODOT procedure (9), 4-in.-diameter (100 mm) by 2.5-in.-high (63 mm) samples were fabricated for each project by using the same materials (asphalt and aggregate) employed during construction. Sixteen samples were prepared for each mix condition. Eight samples were tested as compacted and eight samples were tested after moisture and freeze-thaw conditioning (Figure 2). All samples were tested in the diametral mode for elastic modulus, fatigue life, and permanent deformation. MTS equipment was used for measurement of indirect tensile strength. The results of permanent deformation tests are not included in this paper.

Test Method

Dynamic diametral tests were run to obtain the data of modulus, fatigue life, and permanent deformation. The dynamic load duration was fixed at 0.1 sec and the load frequency at 60 cycles per minute. All tests were carried out at room temperature [22° ± 2°C (71.6 ± 3.6°F)]. The Lottman conditioning procedure (3) was used to evaluate the influence of moisture and freeze-thaw conditioning. The main steps of this conditioning procedure are as follows:

1. Determine the resilient modulus of the as-compacted samples;
2. Vacuum saturate [26 in. (66 cm Hg)] the samples for 2 hr;
3. Place the saturated samples in a freezer at -18°C (0°F) for 15 hr;
4. Place the frozen, saturated specimen in a warm water [60° ± 2°C (140° ± 3.6°F)] bath for 24 hr;
5. Place the specimen in a water bath at room temperature [22.8° ± 1°C (73° ± 1.8°F)] for 3 hr; and
6. Rerun the modulus test along the same sample axis as the as-compacted modulus was measured (step 1) [22.8° ± 1°C (73° ± 1.8°F)].

RESULTS

All tests were run at horizontal tensile strains ranging between 50 and 150 microstrain. The bulk specific gravity and air void content corresponding to each level of compaction for the three projects are given in Table 3.

Resilient Modulus

The following equation was used to determine the modulus (10):

$$M_R = [P/(\Delta H \times h)](0.2692 + 0.9974\nu) \quad (1)$$

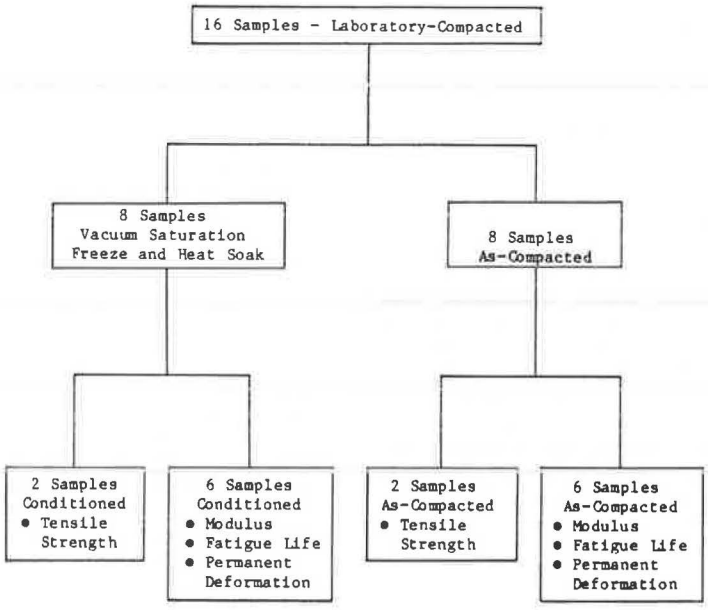

FIGURE 2 Test program.

TABLE 3 Bulk Specific Gravity and Air Void Content

Degree of Compaction (%)	Bulk Specific Gravity			Air Void Content (%)		
	NO-S	CR-CC	W-S	NO-S	CR-CC	W-S
100	2.41	2.30	2.45	3.3	5.3	1.6
97	2.31	2.23	2.38	7.3	8.2	4.4
92	2.22	2.11	2.29	10.9	13.2	8.0
90	2.19	2.08	2.20	12.0	14.4	11.6

where

M_R = resilient modulus (psi),
P = dynamic load (lb),
ΔH = horizontal elastic tensile deformation (in.),
h = sample thickness (in.), and
ν = Poisson's ratio.

Poisson's ratio was assumed constant and equal to 0.35, which simplifies Equation 1 to

$$M_R = (P \times 0.6183)/(\Delta H \times h) \quad (2)$$

Moduli values of as-compacted and conditioned samples from all projects are given in Table 4. In order to determine the effect of conditioning on mixture performance, two parameters--RCL_{mod} and $R100_{mod}$--were computed for each level of compaction; they are also given in Table 4. These parameters are defined as follows: RCL_{mod} is the ratio of retained stiffness at the same compaction level [(Modulus of conditioned sample) ÷ (Modulus of as-compacted sample)], and $R100_{mod}$ is the ratio of retained stiffness compared to the modulus at 100 percent compaction of as-compacted samples [(Modulus of conditioned sample) ÷ (Modulus of as-compacted sample at 100 percent compaction)]. The moduli of as-compacted and conditioned samples and the values of RCL_{mod} for the North Oakland-Sutherlin project were the lowest, whereas those for the Warren-Scappoose project for each compaction level were the highest. The Warren-Scappoose project also exhibited higher bulk specific gravities or lower air void content than the others (Table 3) and had lower asphalt content.

Figure 3 shows the variation of resilient modulus with air void content. As indicated for both as-compacted (Figure 3a) and conditioned samples (Figure 3b), the diametral modulus has a strong linear relationship to the air void content. The coefficients of determination of each project are around 1.0. In general, as the air void content decreased from 10 to 4 percent, the moduli increased about twofold for both as-compacted and conditioned samples.

Values for $R100_{mod}$ increase as the air void content decreases (Figure 4). As would be expected, $R100_{mod}$ has a strong linear relationship with air void content. Values for RCL_{mod} are given in Figure 5. As indicated, most of the RCL_{mod} for the North Oakland-Sutherlin project are less than 70 percent, whereas those for the others are greater than 70 percent. The RCL_{mod} less than 70 percent for the North Oakland-Sutherlin project is a result

TABLE 4 Resilient Modulus and Retained Resilient Modulus Ratio

Degree of Compaction (%)	Resilient Modulus ($x10^3$, psi)						RCL_{mod}			$R100_{mod}$		
	As-Compacted			Conditioned								
	NO-S	CR-CC	W-S	NO-S	CR-CC	W-S	NO-S	CR-CC	W-S	NO-S	CR-CC	W-S
100	488	710	1,082	435	638	1,008	0.89	0.90	0.93	0.89	0.90	0.93
97	389	466	887	214	357	688	0.55	0.77	0.78	0.44	0.50	0.64
92	220	238	736	126	147	610	0.57	0.62	0.83	0.26	0.21	0.56
90	191	163	265	109	139	312	0.57	0.85	1.18	0.22	0.20	0.29

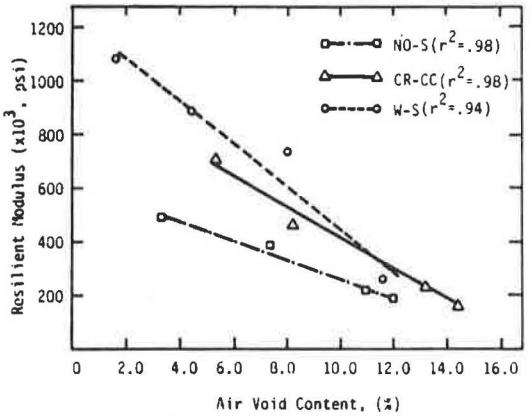

(a) As - Compacted

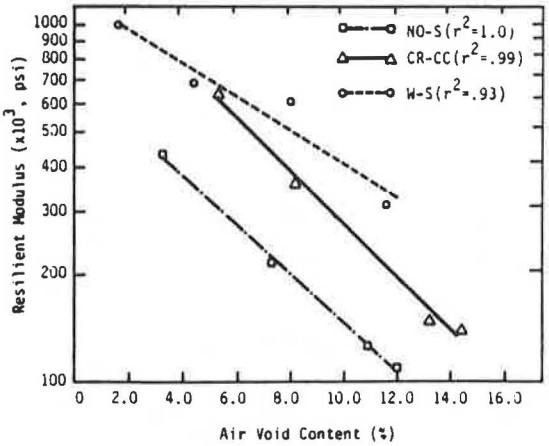

(b) Conditioned

FIGURE 3 Influence of air void content on resilient modulus for each project.

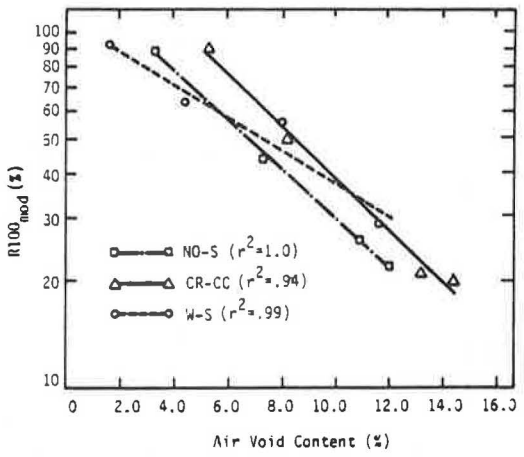

FIGURE 4 Influence of air void content on $R100_{mod}$ for each project.

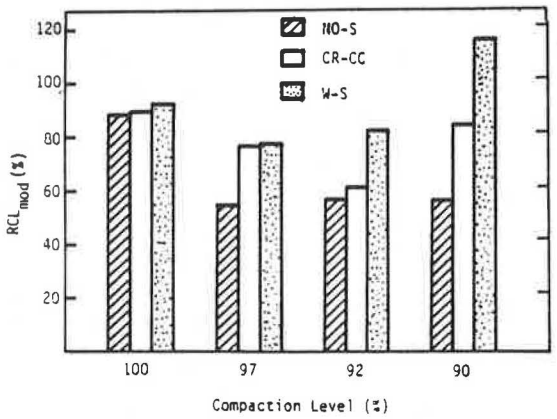

FIGURE 5 RCL_{mod} for each project at four compaction levels.

of using poor quality aggregate. Hence the parameter RCL_{mod} demonstrates clearly that with poor quality aggregate there is a rapid loss of performance if satisfactory compaction is not maintained. The parameter $R100_{mod}$ shows the importance of mixture compaction more strongly than RCL_{mod}, but it does not indicate the influence of aggregate quality. In summary, the effect of moisture conditioning on the stiffness of the three projects is significantly affected by the quality of aggregate used and has a linear relationship to air void content.

Indirect Tensile Strength

Values for indirect tensile strength of as-compacted and conditioned samples of each project are given in Table 5 together with their ratios of retained indirect tensile strength (i.e., $R100_{ts}$ and RCL_{ts}). For the North Oakland-Sutherlin project, the indirect tensile strength of as-compacted and conditioned samples are generally lower than the other two projects. Also, RCL_{ts} and $R100_{ts}$ for the North Oakland-Sutherlin project are lower at all compaction levels. The Warren-Scappoose project again exhibits the highest strength and $R100_{ts}$ value, particularly at high levels of compaction. Figure 6 shows that indirect tensile strength of both as-compacted and conditioned samples have strong linear relationships

TABLE 5 Indirect Tensile Strength and Retained Indirect Tensile Strength Ratio

Degree of Compaction (%)	Indirect Tensile Strength (psi)						RCL_{ts}[a]			$R100_{ts}$[b]		
	As-Compacted			Conditioned								
	NO-S	CR-CC	W-S	NO-S	CR-CC	W-S	NO-S	CR-CC	W-S	NO-S	CR-CC	W-S
100	199	230	362	109	227	371	0.55	0.99	1.02	0.55	0.99	1.02
97	123	142	273	84	170	321	0.68	1.20	1.18	0.42	0.74	0.89
92	113	67	108	50	105	105	0.44	1.57	0.97	0.25	0.46	0.29
90	95	71	65	27	84	75	0.28	1.18	1.15	0.14	0.37	0.21

[a] RCL_{ts} = retained indirect tensile strength ratio at same compaction level = (Tensile strength of conditioned sample) ÷ (Tensile strength of as-compacted sample).

[b] $R100_{ts}$ = retained indirect tensile strength ratio compared to 100 percent of as-compacted samples = (Tensile strength of conditioned sample) ÷ (Tensile strength of as-compacted sample at 100 percent compaction).

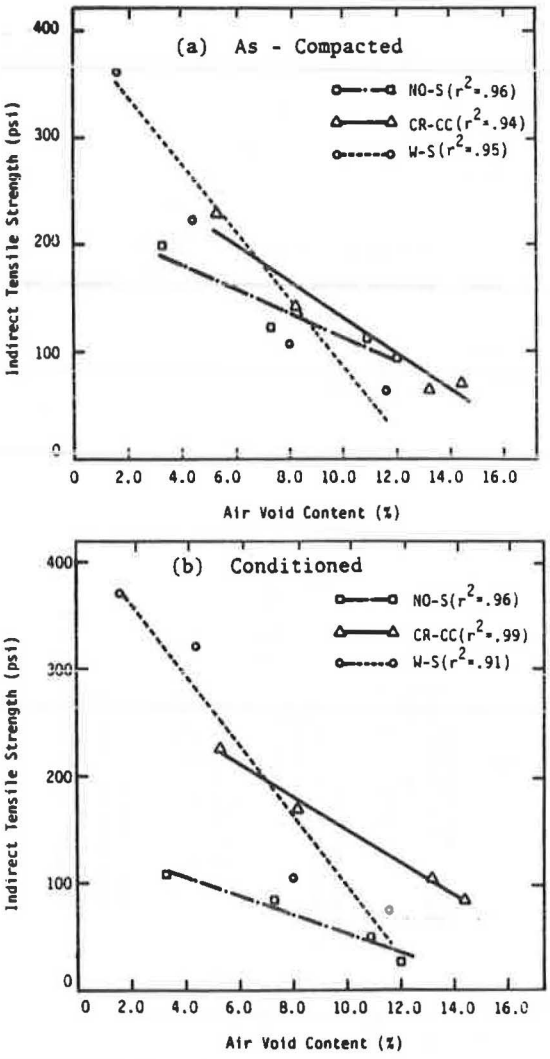

FIGURE 6 Influence of air void content on indirect tensile strength for each project.

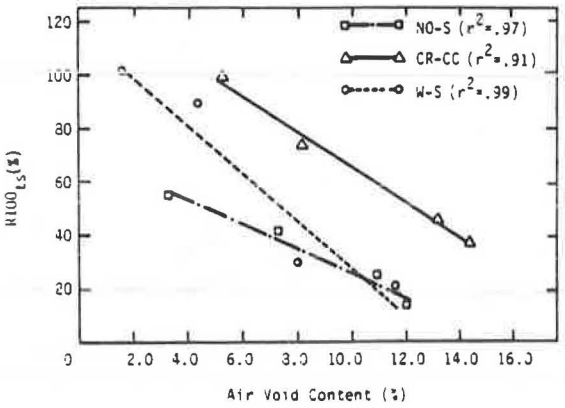

FIGURE 7 Influence of air void content on $R100_{ts}$ for each project.

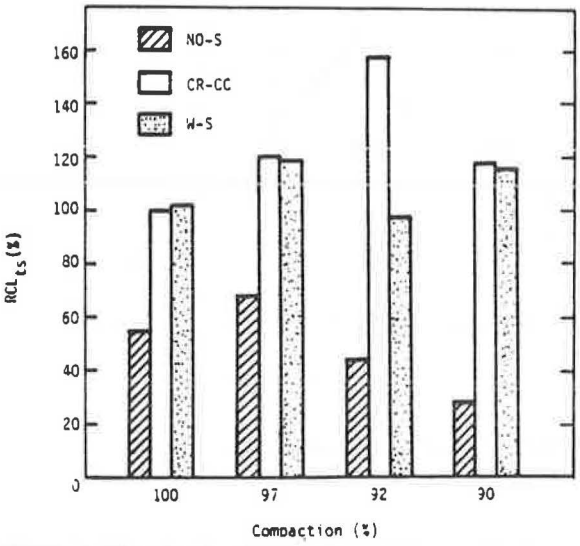

FIGURE 8 RCL_{ts} for each project at four compaction levels.

with air void content. Like $R100_{mod}$, there is a strong linear relationship between $R100_{ts}$ and the air void content (Figure 7). In general, as the air void content decreases from 12 to 4 percent, the indirect tensile strength increases about twofold in both as-compacted and conditioned samples. Figure 8 shows RCL_{ts} of each project at all compaction levels tested. Again note that values of RCL_{ts} for the North Oakland-Sutherlin project remain less than 70 percent, whereas those of the other projects rise greater than 100 percent; that is, the retained indirect tensile strengths of conditioned samples are greater than those of as-compacted samples in the test of the Castle Rock-Cedar Creek and Warren-Scappoose project for each compaction level.

The data in Figure 9 indicate that indirect tensile strengths of as-compacted and conditioned samples also have fairly linear relationships with resilient modulus at the corresponding air void content. In summary, the results of the indirect tensile strength of each project are similar to those of resilient modulus; that is, the effect of aggregate quality on RCL_{ts} is similar to RCL_{mod}. For poor quality aggregate, RCL_{ts} is consistently less than 70 percent, whereas for good quality aggregate RCL_{ts} is greater than 70 percent.

Fatigue Life

Fatigue life is characterized by the number of load applications required to cause failure of the sample. Attempts to relate the number of load applications to the state of stress or strain have shown that the best correlation exists between the tensile strain and the number of load applications, as follows:

$$N_f = K(1/\varepsilon_t)^m \quad (3)$$

where

N_f = number of load repetitions to failure,
ε_t = initial elastic tensile strain, and
K,m = regression constants.

The fatigue life of a specific mix is, therefore, defined by the constants K and m. Both K and m are affected by the mix variables. The horizontal tensile strain for the diametral test specimen is calculated from the following equation (10):

$$\varepsilon_t = H \times [(0.03896 + 0.1185\nu)/(0.0673 + 0.2494\nu)] \quad (4)$$

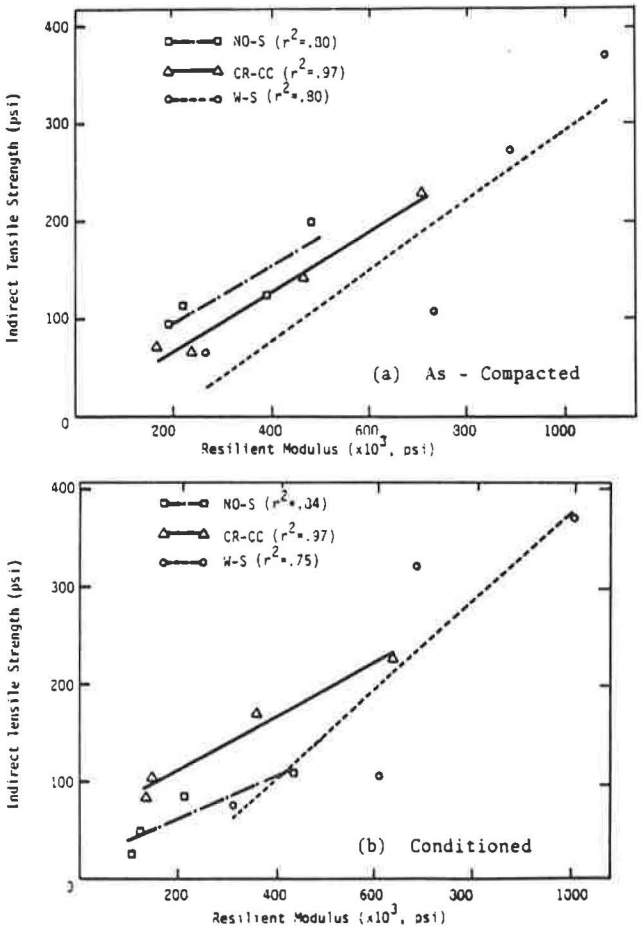

FIGURE 9 Relationship between indirect tensile strength and resilient modulus for each project.

Assuming that the Poisson's ratio is constant and equal to 0.35, Equation 4 becomes

$$\varepsilon_t = H \times 0.5203 \quad (5)$$

Horizontal tensile strains versus number of load repetitions to failure of each project are shown in Figures 10-12, together with the level of compaction. The results for both as-compacted and conditioned specimens show a substantial decrease in fatigue life when the level of compaction drops. For the North Oakland-Sutherlin project, the fatigue relationship is affected significantly at a low level of compaction and is not affected greatly at a high level of compaction. This may be due in part to the low quality aggregate used on this project. For the Castle Rock-Cedar Creek and Warren-Scappoose projects, good quality aggregates were used. The fatigue life after conditioning generally increased compared with that of the as-compacted samples. This is due in part to the fact that the load applied for conditioned samples, in order to maintain the initial strain, was lower than that for the as-compacted samples. The samples from the Warren-Scappoose project had the highest moduli and generally the shortest fatigue life for both compaction levels. Although the North Oakland-Sutherlin project gave lowest moduli at a compaction level of 96 percent, the fatigue life was shorter than that for the Castle Rock-Cedar Creek project. In addition, the fatigue life for the North Oakland-Sutherlin project at 50 microstrain and compaction

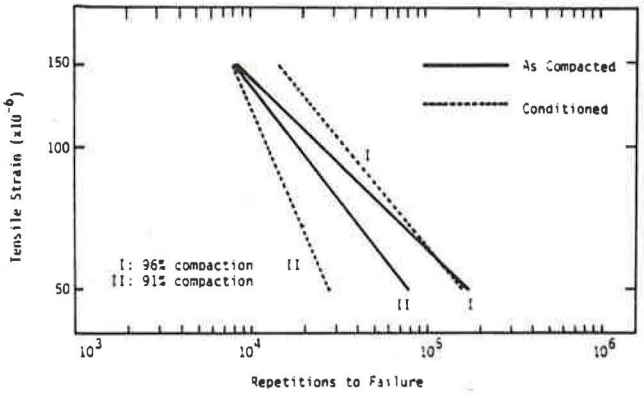

FIGURE 10 Horizontal tensile strain versus number of load repetitions: North Oakland-Sutherlin.

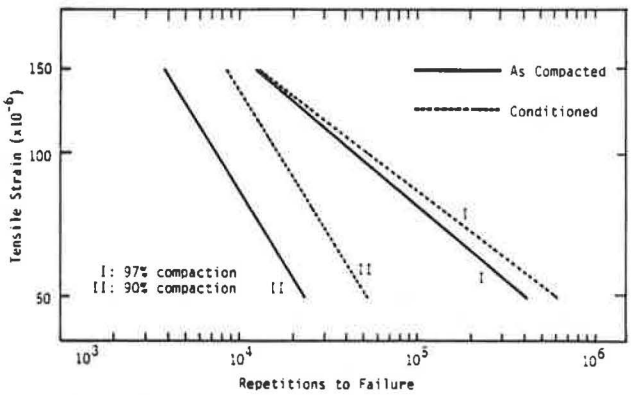

FIGURE 11 Horizontal tensile strain versus number of load repetitions: Castle Rock-Ceder Creek.

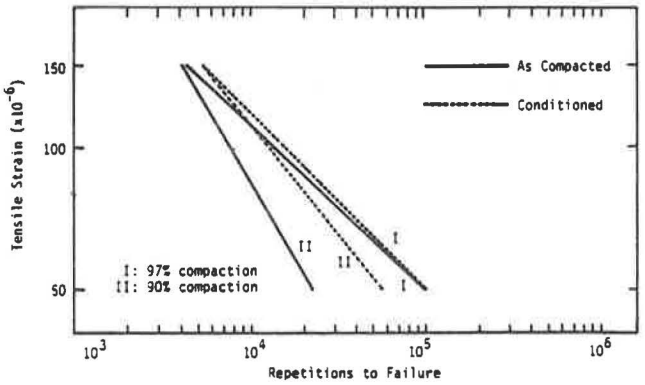

FIGURE 12 Horizontal tensile strain versus number of load repetitions: Warren-Scappoose.

level of 96 percent decreased slightly after conditioning, but at a low compaction level it decreased drastically at all strain levels even though the conditioned samples had lower moduli than as-compacted ones. This result is due principally to the quality of aggregate used.

The initial tensile strain, air void content, and aggregate quality are predominant factors to the fatigue life. This result indicates that the durability of asphalt pavement is dependent on the quality of aggregate, the load applied and the level of compaction, or the air void content.

DISCUSSION OF RESULTS

The results of tests on mixtures from the three projects indicate that damage to the pavement is increased with the low values of tensile strength and resilient modulus, or with relatively large drops in strength after conditioning the sample. The data from the tests demonstrate that values of modulus and indirect tensile strength for the North Oakland-Sutherlin project are considerably lower than those for the Castle Rock-Cedar Creek and Warren-Scappoose projects. The fatigue life for each project generally increased after conditioning for each compaction level and initial tensile strain. The exception was the North Oakland-Sutherlin project, for which the fatigue resistance decreased especially at a low compaction level.

Fatigue life is expressed as a function of modulus, initial tensile strain, and air void content. Thus fatigue life can be used as a valuable mix characteristic to evaluate the effect of conditioning. One possible parameter is the conditioning effectiveness factor (CEF). CEF represents the effects of material used and conditioning in reducing the modulus and prolonging the mixture life. When good quality aggregate was used (Castle Rock-Cedar Creek and Warren-Scappoose projects), the modulus after conditioning decreased and the fatigue life increased at the same initial tensile strain used for measuring modulus before conditioning. When poor quality aggregate was used, the fatigue life as well as the modulus of conditioning samples decreased, compared to as-compacted samples, as occurred in the North Oakland-Sutherlin project. A high value of CEF, therefore, represents poor materials and a low value represents good materials, and are less susceptible to conditioning. From the results of the test, the CEF for the North Oakland-Sutherlin project is 1.61, whereas the CEF for the Castle Rock-Cedar Creek and Warren-Scappoose project is 0.37 and 0.43, respectively (Table 6). The CEF clearly shows the effect of the quality of aggregate with conditioning.

TABLE 6 CEF at 90 Percent Compaction and 50 Microstrain

Project	RCL_{mod}	Fatigue Life		CEF[a]
		As-Compacted	Conditioned	
NO-S	0.57	79,142	28,006	1.61
CR-CC	0.85	23,084	52,851	0.37
W-S	1.18	20,684	57,331	0.43

[a]CEF = conditioning effectiveness factor = $RCL_{mod} \div (N_f$, conditioned/N_f, as-compacted).

CONCLUSIONS

Performance of as-compacted and conditioned mixtures used in the construction of three Oregon State projects was evaluated by using dynamic testing of laboratory-compacted samples. Mix resilient modulus, indirect tensile strength, and fatigue life of as-compacted and conditioned samples were determined for samples prepared within the following range of variables:

1. Mix level of compaction: 100, 97, 92, and 90 percent;
2. Asphalt content: 6 percent; and
3. Percent passing No. 200 sieve: 6 percent.

The following major conclusions are drawn from the findings of this study:

1. There is a strong linear relationship between air void content and the properties of the conditioned as well as the as-compacted samples;
2. At low air void content as-compacted and conditioned samples of each project have high values of resilient modulus, indirect tensile strength, and fatigue life;
3. The resilient modulus, indirect tensile strength, and fatigue life of conditioned samples are affected by the quality of aggregate used and the air void content;
4. The results of this study indicate the importance of obtaining good quality aggregate and a low level of air void content in mixture through a high level of compaction; and
5. The CEF is used for evaluating the quality of aggregate and the effectiveness of conditioning; a high CEF represents a mixture more susceptible to moisture damage.

REFERENCES

1. H.J. Fromm. The Mechanism of Asphalt Stripping from Aggregate Surfaces. Proc., Association of Asphalt Paving Technologists, Vol. 43, 1974, pp. 191-223.
2. I. Ishai and J. Craus. Effect of the Filler on Aggregate-Bitumen Adhesion Properties in Bituminous Mixtures. Proc., Association of Asphalt Paving Technologists, Vol. 46, 1977, pp. 228-258.
3. R.P. Lottman. Predicting Moisture-Induced Damage to Asphaltic Concrete. NCHRP Report 246. TRB, National Research Council, Washington, D.C., May 1982, 50 pp.
4. R.S. Dalter and D.W. Gilmore. A Comparison of Effects of Water on Bonding Strengths of Compacted Mixtures of Treated Versus Untreated Asphalt. Proc., Association of Asphalt Paving Technologists, Vol. 51, 1982, pp. 317-326.
5. T.W. Kennedy, F.L. Roberts, and K.W. Lee. Evaluation of Moisture Susceptibility of Asphalt Mixtures Using the Texas Freeze-Thaw Pedestal Test. Proc., Association of Asphalt Paving Technologists, Vol. 51, 1982, pp. 327-341.
6. J.L. Walter et al. Impact of Variation in Material Properties on Asphalt Pavement Life: North Oakland-Sutherlin Project. Interim Report FHWA-OR-81-4. Oregon Department of Transportation, Salem, Nov. 1981.
7. J.L. Walter et al. Impact of Variation in Material Properties on Asphalt Pavement Life: Castle Rock-Cedar Creek Project. Interim Report FHWA-OR-81-6. Oregon Department of Transportation, Salem, Dec. 1981.
8. J.L. Walter et al. Impact of Variation in Material Properties on Asphalt Pavement Life: Warren-Scappoose Project. Interim Report FHWA-OR-81-7. Oregon Department of Transportation, Salem, Dec. 1981.
9. Laboratory Manual of Test Procedures. In Laboratory Manual, Volume 1, Material and Research Section, Highway Division, Oregon Department of Transportation, Salem, March 1978.
10. T.W. Kennedy. Characterization of Asphalt Pavement Materials Using the Indirect Tensile Test. Proc., Association of Asphalt Paving Technologists, Vol. 46, 1977, pp. 132-150.

Publication of this paper sponsored by Committee on Characteristics of Bituminous Paving Mixtures to Meet Structural Requirements.